ITALIAN JOURNAL OF FOOD SCIENCE

Rivista italiana di scienza degli alimenti
(www.itjfs.com)

Volume XXXIV
Number 2
(2022)

ITALIAN JOURNAL OF FOOD SCIENCE

(RIVISTA ITALIANA DI SCIENZA DEGLI ALIMENTI) 2nd series

Founded By Paolo Fantozzi under the aegis of the University of Perugia
Official Journal of the Italian Society of Food Science and Technology
Società Italiana di Scienze e Tecnologie Alimentari (S.I.S.T.Al)
Initially supported in part by the Italian Research Council (CNR) -Rome -Italy
Recognised as a "Journal of High Cultural Level"
by the Ministry of Cultural Heritage -Rome -Italy
(www.itjfs.com))

Editor-in-Chief:
Paolo Fantozzi-Dipartimento di Scienze Agrarie, Alimentari ed Ambientali, Università di PerugiaVia S. Costanzo, I-06126 Perugia, Italy -Tel. +39 075 5857910 -Telefax +39 075 5857939-5857943
e-mail: paolo.fantozzi@ijfs.eu

Co-Editors:
FOOD SCIENCE
(Members of S.I.S.T.Al - Italian Society of Food Science and Technology)
Alessandra Del Caro -Università degli Studi di Sassari -e-mail: delcaro@uniss.it
Alyssa Hildago -Università degli Studi di Milano, e-mail: alyssa.hidalgovidal@unimi.it
Monica Rosa Loizzo -Università della Calabria, e-mail. monìcarosa.Ioizzoéàunical.it
Kalliopi Rantsiou -Università di Torino, e-mail: kalliopi.rantsiou@unito.it
Massimiliano Rinaldi -Università di Parma, e-mail: massimiliano.rinaldi@unipr.it
Valeria Sileoni - Universitas Mercatorum, e-mail: valeria.sileoni@unimercatorum.it
Simone Vincenzi -Università degli Studi di Padova, e-mail: simone.vincenzi@unipd.it
Elena Giovanna Vittadini -Università di Camerino, e-mail: elenagiovanna.vittadini@unicam.it
Giuseppe Zeppa -Università di Torino, e-mail: giuseppe.zeppa@unito.it

FOOD ENGINEERING, FOOD NUTRITION, FOOD CLINICAL PATHOLOGY
(Under the Aeges of Depts of Engineering and Pharmaceutical Sciences, University of Perugia)
Elisabetta Albi - Università degli Studi di Perugia, e-mail: elisabetta.albi@unipg.it
(Member of ISBB - Italian Society for Space Biomedicine and Biotechnology)
Tommaso Beccari - Università degli Studi di Perugia, e-mail: tommaso.beccari@unipg.it
(Member of SIMMESN - Italian Society of Metabolic Diseases and Neonatal Screening)
Francesco Fantozzi - Università degli Studi di Perugia, e-mail: francesco.fantozzi@unipg.it
(Member of ASME - American Society of Mechanical Engineers)

Publisher:
Codon Publications: email: admin@codonpublications.com, URL: www.codonpublications.com.

Aim:

The Italian Journal of Food Science is an international journal publishing original, basic and applied papers, reviews, short communications, surveys and opinions on food science and technology with specific reference to the Mediterranean Region. Its expanded scope includes food production, food engineering, food management, food quality, shelf-life, consumer acceptance of food stuffs. Food safety and nutrition, and environmental aspects of food processing. Reviews and surveys on specific topics relevant to the advance of the Mediterranean food industry are particularly welcome.

Upon request and free of charge, announcements of congresses, presentations of research institutes, books and proceedings may also be published in a special "News" section.

Review Policy:

The Co-Editors with the Editor-in-Chief will select submitted manuscripts in relationship to their innovative and original content. Referees will be selected from the Advisory Board and/or qualified Italian or foreign scientists. Acceptance of a paper rests with the referees.

Frequency:

Quarterly -One volume in four issues. Guide for Authors is published in each number and annual indices are published in number 4 of each volume.

Impact Factor:

0.875 published in 2020 Journal of Citation Reports, Scopus CiteScore 2020: 1.5. IJFS is abstracted/indexed in: Chemical Abstracts Service (USA); Foods Adlibra Publ. (USA); Gialine – Ensia (F); Institut Information Sci. Acad. Sciences (Russia); Institute for Scientific Information; CurrentContents®/AB&ES; SciSearch® (USA-GB); Int. Food Information Service - IFIS (D); Int. Food Information Service – IFIS (UK); UDL-Edge Citations Index (Malaysia); EBSCO Publishing; Index Copernicus Journal Master List (PL).

IJFS has a publication charge of USD 1100 each article.
Subscription Rate: IJFS is now an Open Access Journal and can be read and downloaded free of charge.

VOLUME XXXIV IJFS No. 2, 2022

CONTENTS

Italian Journal of Food Science, 2022; 34 (2): 1–8

A novel cascade approach to extract bioactive compounds from officinal herbs

Yubin Ding[1], Ksenia Morozova[1], Matteo Scampicchio[1]*, Angelo Morini[2], Massimiliano Ferrari[2]

[1]*Faculty of Science and Technology, Free University of Bozen-Bolzano, Bolzano, Italy;* [2]*Naturalsalus srl., Bolzano, Italy*

***Corresponding Author:** Matteo Scampicchio, Faculty of Science and Technology, Free University of Bozen-Bolzano, Piazza Università 1, 39100 Bolzano, Italy. Email: matteo.scampicchio@unibz.it

Received: 5 October 2021; Accepted: 20 January 2022; Published: 1 April 2022
© 2022 Codon Publications

OPEN ACCESS

PAPER

Abstract

This research aims to compare a novel cascade extraction method with a conventional solid–liquid extraction method, both assisted by ultrasounds. The cascade extraction method consists of a sequential series of extractions performed with the same hydroalcoholic solvent, which is reused from one herb to the other. In practice, a hydroalcoholic solution is firstly used to extract one botanical herb. The resulting extract is then reused for the extraction of a second herb. The process is repeated as many times as the number of herbs composing the final formulation. The main advantage of this approach is firstly the lower need of solvents compared with the individual extraction procedures, where a fresh solvent is needed on each extraction step. Furthermore, extracts of the two methods (solid liquid vs cascade extraction) were characterized with several antioxidant assays (DPPH, ORAC, and FRAP) and total phenolic content (TPC). The results show that the solid–liquid extraction method achieves similar yields to total phenols and similar TAC in comparison to the extracts obtained by the cascade extraction method. Also, the HPLC analysis of the extracts showed that both methods lead to similar chromatographic profiles either when analyzed by an electrochemical detector (CoulArray) or by a spectrometric diode array detector (DAD). However, our findings support the idea that the cascade extraction method obtains extracts richer of minor peaks, showing a more complex bioactive profile. Such results could be explained considering that the solvent used during the series of cascade extractions was enriched not only by antioxidants but also by plant surfactants, like saponins, which increase the solvent solubility. Overall, this research shows that the cascade extraction method can not only provide officinal herb extracts with similar phenolic yield and antioxidant capacity than conventional solid–liquid extraction but also with a more complex bioactive profile compared to traditional solid–liquid extraction and with a minor consumption of solvents.

Keywords: antioxidant ability; cascade extraction; herbal tincture; HPLC

Introduction

Herbal extracts are hydroalcoholic preparations typically obtained by maceration or percolation (Karioti *et al.*, 2011). After extraction with a hydroalcoholic solution, the resulting extracts contain a complex profile of bioactives that can be used as supplements for human health. Several studies report the beneficial effect of extracts obtained from botanicals. For example, according to Dos Reis *et al.*, the extract of *Ptychopetalum olacoides*, which contains tannins, flavonoids, and terpenoids, is used as a remedy for problems concerning the central nervous system (Dos Reis and Mendes, 2018). Also, the extract prepared with *Turnera diffusa* has anxiolytic and antidepressant effects (Ana María *et al.*, 2019). However, the composition in bioactives depends on a proper extraction technique.

The most traditional way to prepare extracts is the classical maceration of dry herbs with a hydroalcoholic solution, in a solid-to-liquid ratio of 1:–5 or 1:–10. With slight modifications, other parent techniques have been developed, like percolation, hydro-distillation, boiling with reflux, and Soxhlet (Alara *et al*., 2018). Unfortunately, such techniques consume large amounts of organic solvents with high purity, and have limited extraction yields and low selectivity. Moreover, they need long extraction times, which may cause the thermal degradation of some sensitive bioactives (Rostagno *et al*., 2010).

Recently, the efficiency of the process has been greatly improved by implementing innovative technologies, such as ultrasound-assisted extraction (UAE), supercritical fluid extraction (SFE), and microwave-assisted extraction (MAE) (Reverchon and De Marco, 2006; Valachovic *et al*., 2001; Xia *et al*., 2011). When traditional extraction is assisted with such techniques, the duration of the extraction process is greatly reduced (i.e., a few hours), maximizing the yield of the extracted bioactives and limiting thermal degradation problems (Valachovic *et al*., 2001; Vinatoru *et al*., 2017).

Despite such improvements, the extraction process still has some limitations. The most evident is that many lipophilic bioactives present in herbs (like carotenoids or terpenes) are scarcely soluble in hydroalcoholic solvents. This clearly limits the potential quality, potency, and effectiveness of the resulting extracts. For this purpose, some recent researches have tried to overcome the low solvation capacity of pure hydroalcoholic solvents by the addition of ionic liquids (Han *et al*., 2011), lime juice (Cheok *et al*., 2013), diethylamines (Choi *et al*., 2000), and saponins. Through the careful use of some additives, important solvent properties like viscosity, pH, or polarity can be fine-tuned as required. This, ultimately, could increase the extraction yield of bioactive compounds.

A further important limitation on the current use of traditional extraction techniques is the high solvent consumption. Generally, for each volume of dry herbs, 5–10 volumes of fresh hydroalcoholic solvent are needed (Council of Europe, 2019). Although such high solvent to sample ratio is intended to maximize the yield of extractable compounds, it represents a relevant manufacturing cost, a high energy demand, and an environmental concern (Abubakar *et al*., 2015).

Accordingly, this work aims to propose a simple but ingenious cascade extraction protocol, which reuses the same initial hydroalcoholic solvent in a series of extraction cycles. In practice, the procedure starts with a hydroalcoholic solvent, which is used for the first extraction of one selected botanical herb. Then, the resulting extract is recycled for the extraction of a second selected botanical herb. The procedure continues in a series of extractions, where the extract of each step becomes the solvent for the subsequent step. Thanks to such an innovative extraction procedure, during the reutilizations of the solvent, and through the wise selection of the herbal sequences, the hydroalcoholic solvent is progressively enriched not only with the main characteristic bioactives from each botanical herb but also with natural modifiers, which fine-tune the viscosity, pH, and polarity of the initial hydroalcoholic solvent. This, ultimately, will enhance its solvation capacity, leading to final extracts with richer bioactives profile, higher yields, and less solvent consumption.

Thus, in this work, the extraction efficiency of a traditional solid–liquid extraction method is compared with the proposed cascade extraction approach. Total phenolic content (TPC) together with total antioxidant capacity (DPPH, FRAP, and ORAC) of both approaches were compared. High performance liquid chromatography (HPLC) coupled with diode array detector (DAD) and coulometric array detector (CoulArray) were used to analyze the bioactive compounds extracted with both approaches.

Material and Methods

Reagents

Ethanol, Folin–Ciocalteau reagent, sodium carbonate, gallic acid, 2,5,7,8-tetramethylchromane-2-carboxylic acid (Trolox), 2,2-Diphenyl-1-picrylhydrazyl (DPPH), sodium acetate, acetic acid, ferric chloride, hydrochloric acid, disodium phosphate, monosodium phosphate, sodium hydroxide, fluorescein, 2,2'-Azobis(2-amidinopropane) dihydrochloride (AAPH), HPLC grade ammonium formate, formic acid, and acetonitrile were obtained from Sigma-Aldrich (USA). 2,4,6-Tris(2-pyridyl)-s-triazine (98%) was purchased from Alfa Aesar (USA). The Milli-Q water was purified by Sartorius arium® mini (Germany).

Samples

Four varieties of officinal herbs, namely, *Ptychopetalum Olacoides Benth. (stem)*, *Turnera Aphrodisiaca Willd. (leaf)*, *Schisandra Chinensis baill. (fruit)*, and *Poligonum Multiflorum Thunb. (root),* were kindly provided by Naturalsalus® and preprocessed based on their standardized protocols. In brief, the dried herbs were grounded with a laboratory mill (PerkinElmer, Laboratory Mill 3100, Germany) and sieved (Retsch, AS 200, Germen) to reach a uniform size (<250 μm). The powder was then preserved at ambient temperature before extraction.

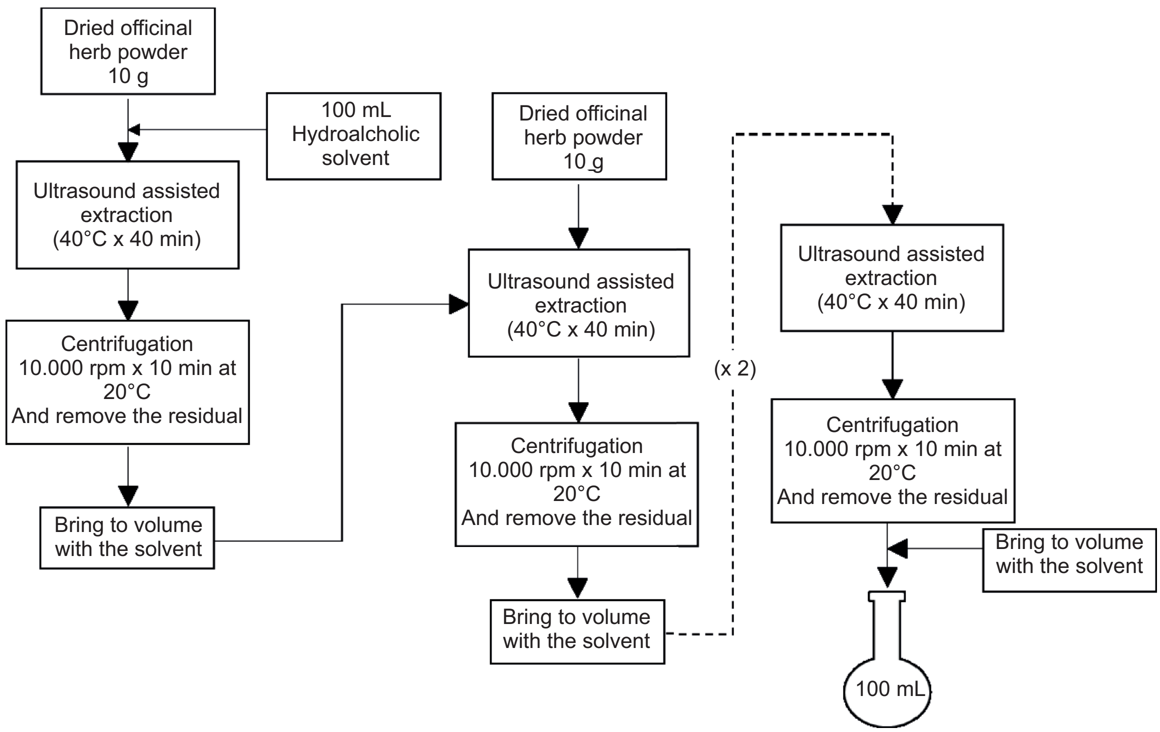

Figure 1. The process of cascade extraction used in the current research.

Extraction

Extractions were performed with an ultrasound reactor (STEEL®, digital ultrasonic generator, Italy). Briefly, 10 g of dry herbal powder was mixed with 100 mL of solvent (water: ethanol = 1:1, *v/v*) and extracted for 40 min at 40°C. Ultrasound power was set to 60% (345 W, 38 kHz). After extraction, the resulting solution was filtered (PTFE 0.45 μm, Pall Corporation, USA) and centrifuged (10,000 rpm for 10 min at 20°C, SL 16R Centrifuge, Thermo Scientific, USA). The resultant supernatant was collected and stored at −80°C.

Cascade extraction consists of using the extract (obtained from an extraction step) as the solvent for the next step. During each step, fresh hydroalcoholic solvent (typically less than 10% of the initial volume) could be added to replace the solvent evaporated and trapped in the herb matrix during the operation, and maintain a fixed initial sample to solvent ratio (1:10). The experimental conditions of solid–liquid ratio, extraction time, temperature, and ultrasound power were applied equally to each extraction step modified from the previous officinal herb extraction conducted by Rodríguez-Pérez *et al.* in 2015 (see Figure 1). The optimized sequence used in this work is the following: *Ptychopetalum*, *Turnera*, *Schisandra*, and *Poligonum*. For comparison, individual extraction was also performed, similar to cascade extraction, which compensated for the lost solution (100 mL) before performing the analysis.

Total phenol content

The TPC analysis was based on Margraf *et al.* with small modifications (Margraf *et al.*, 2015). Briefly, 110 μL of distilled water, 10 μL of sample or gallic acid standard, 10 μL of Folin–Ciocalteu reagent, and 10 μL of saturated sodium carbonate solution were added to a 96-well microplate. The microplate was incubated for 120 min at 25°C. Finally, the absorbance of each well was measured at λ = 765 nm (Tecan, Infinite M Nano⁺, Switzerland). From the absorbance measurements, the total phenol content was expressed as gallic acid equivalent (GAE) based on a calibration curve, built with a series of gallic acid standards.

Antioxidant assays

DPPH assay

The free radical scavenging activity was measured with 2,2-diphenyl-1-picrylhydrazyl stable radical ($DPPH^{\cdot\cdot}$). 160 μL of DPPH working solution (125 μM) was added to 40 μL of Trolox standards or herbal extracts into a 96-well microplate. The mixture was left to stand for 30 min in the dark at room temperature. The absorbance was measured at 515 nm and the result was expressed based on the Trolox equivalent (Mishra *et al.*, 2012).

FRAP assay

The ferric reducing antioxidant power (FRAP) assay was conducted based on previous research by Benzie and Strain with modifications (Benzie and Strain, 1996). 180 µL of FRAP reagent (pH = 3.6 acetate buffer, 20 mM ferric chloride, 40 mM TPTZ in 40 mM hydrochloric acid in 10:1:1 ratio) was added to 20 µL of Trolox standard or herbal extracts. After incubation for 1 h at 25°C, the absorbance at 593 nm was recorded and the result was expressed as µmol TE/g DW.

ORAC assay

The oxygen radical absorbance capacity (ORAC) assay was performed using the method modified from Prior *et al.* (2003). Phosphate buffer (75 mM, pH 7.0) was used to dilute all the solutions, including fluorescein (3.19 µM), AAPH solution (111 mM), Trolox, and herbal extracts. 30 µL of sample or Trolox standard was premixed with 75 µL of fluorescein and incubated at 37°C for 5 min before adding freshly prepared 75 µL of AAPH in a 96-well microplate. The fluorescence signal was monitored every minute, during 2 h reaction time with excitation wavelength at 485 nm and emission wavelength at 535 nm. The antioxidant capacity was calculated based on the area under the fluorescence decay curve and expressed as µmol TE/g DW.

HPLC analysis

The sample extracts were analyzed with Agilent 1260 Infinity HPLC system with a binary pump, an autosampler with the temperature control system, a DAD (Agilent Technology, USA), and a 16 channel CoulArray detector (ThermoFisher scientific, USA). A Kinetex Biphenyl column (100 × 2.1 mm, 2.6 µm particle size with a precolumn, Phenomenex, USA) was applied for the separation of compounds at constant 30°C. The separation was conducted with 6.5 mM ammonium formate in Milli-Q water with 0.1% formic acid as phase A, and 6.5 mM ammonium formate in acetonitrile with 0.1% formic acid as phase B. 5 µL of the sample was injected with a constant flow rate of 0.3 mL·min^{-1}. All the samples were previously loaded into the autosampler and kept at 5°C before analysis. The elution gradient was 98% of phase A from 0–8 min, then down to 40% at 20 min, to 5% A at 27 min, kept constant for 2 min, and the final equilibration was 98% A at 31 min. The DAD detector was set at 280 nm and the CoulArray was set from 50 to 800 mV, with 50mV increment through the 16 electrodes (vs. Pd electrode).

Results

The total phenolic content

Table 1 presents the TOC of the extracts obtained by using the traditional maceration process, either of individual herbs (obtained under the same sample to solvent ratio) or their mix in comparison with the proposed cascade method. Among the individual herbs, the *Poligonum* (10 g in 100 mL of fresh solvent) showed the highest TPC (27.3 ± 3.3 mM), while the *Ptychopetalum* (10 g in 100 mL of fresh solvent) showed the lowest (3.49 ± 0.20 mM). The combination of the herb extracts (each obtained with a sample to solvent ratio of 1:10) resulted in a total phenol content of 59.1 ± 7.3 mM of gallic acid equivalent.

Concerning the extracts obtained with the proposed cascade extraction, the TPC was 57.0 ± 1.7 mM. Such a result is not significantly different from the mix of individual extracts (t-test, $P < 0.05$). Furthermore, it is important to highlight that, although the cascade extraction used the same amount of dry herbs as the traditional maceration method (10 g of each botanical), the volume of hydroalcoholic solvent needed was about one fourth. These findings suggest that the cascade extraction method is able to extract similar amount of phenolic compounds than the maceration method, but with less solvents.

The antioxidant assays

The results of antioxidant assays, including DPPH, FRAP, and ORAC, are presented in Table 1. In general, those individual sample extracts that showed higher TPC also had higher antioxidant capacity. In detail, the *Turnera* and *Poligonum* showed the highest antioxidant capacity in all the antioxidant assays. On the contrary, the *Ptychopetalum* and *Schisandra* had lower antioxidant capacity. What is striking here is that the extracts obtained with the cascade extraction method have ORAC, FRAP, and DPPH assay values that are not significantly different ($P < 0.05$) from those obtained by mixing the individual extracts. Overall, these results confirm those obtained by total phenol content (*vide supra*).

The HPLC-CoulArray analysis

Figure 2 shows the chromatogram obtained by HPLC coupled with an electrochemical array detector (CoulArray) of the extracts. The electrochemical detector is useful for providing quantitative and qualitative information of each compound eluted from the chromatographic column (Haque *et al*., 2021). First, the analysis of the peak current values obtained at different applied potentials can be used to determine the redox potential of each eluted species. Furthermore, the peak heights obtained at very high oxidative potentials (i.e., +800 mV vs ref. electrode) can also be used to express the total amount of antioxidant present in the sample, i.e., the total antioxidant capacity (Hicks *et al*., 2017). From Figure 2, the herbs *Poligonum* and *Turnera* showed higher peak heights than *Schisandra* and *Ptychopetalum*.

Table 1. The TPC, DPPH, FRAP, and ORAC results of individual herb sample extracts and those from cascade extraction.

	TPC (mM GAE)	DPPH (mM TE)	FRAP (mM TE)	ORAC (mM TE)
(1) Ptychopetalum	3.49 ± 0.20	0.37 ± 0.08	1.48 ± 0.20	12.01 ± 0.80
(2) Turnera	22.2 ± 3.4	13.44 ± 0.58	11.98 ± 0.86	51.7 ± 1.2
(3) Schisandra	6.02 ± 0.41	3.00 ± 0.78	5.10 ± 0.58	22.2 ± 2.1
(4) Poligonum	27.3 ± 3.3	13.8 ± 1.2	11.43 ± 0.04	36.57 ± 0.51
Mix of individuals[a]	59.1 ± 7.3	30.6 ± 2.6	30.0 ± 1.7	122.5 ± 4.6
Cascade extraction	57.0 ± 1.7	28.5 ± 3.9	30.5 ± 5.0	123.0 ± 1.7

[a]The accumulation of four individual herb sample extracts.

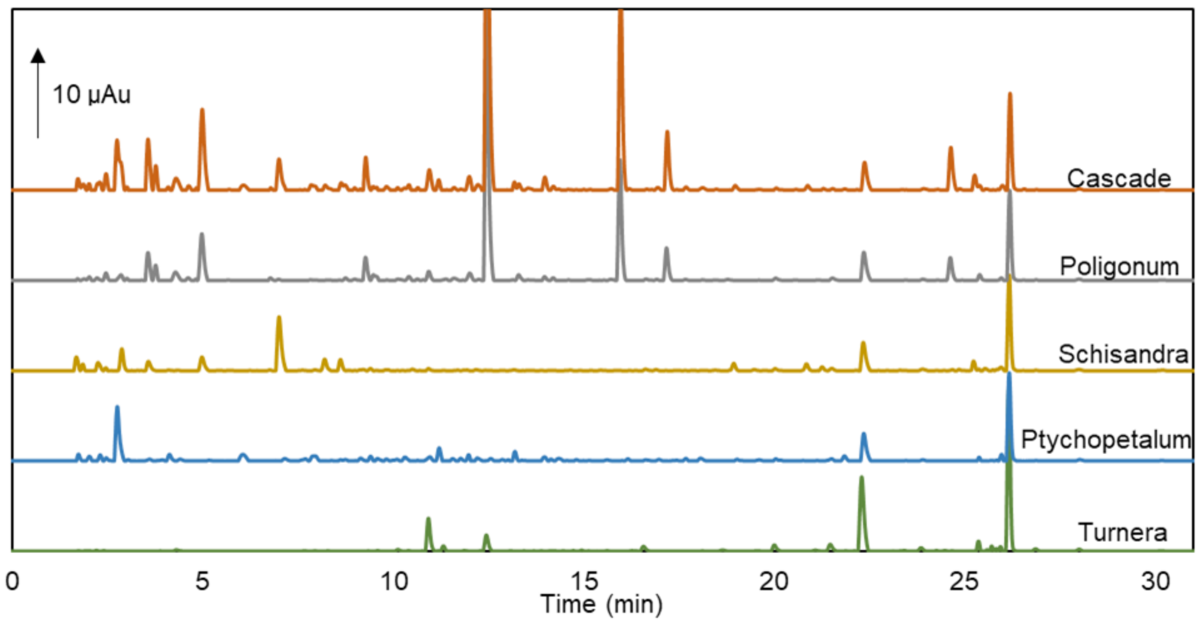

Figure 2. The HPLC-CoulArray result of the individual and cascade sample extracts (potential poised at +800 mV versus Palladium electrode).

This finding correlated with the values of total phenol content and total antioxidant capacity determined previously. Meanwhile, the chromatograms confirmed that the cascade extraction was able to extract all the main redox compounds present in the individual herbs, although with less solvents.

HPLC-DAD analysis

The HPLC-DAD analysis was performed to compare the bioactive compound profile of individual and cascade extraction at 280 nm. Figure 3 shows the chromatograms of all individual herbs and that of the extract obtained by cascade extraction. The results show that the sum of the main peaks observed in the individual herbs is also present in the cascade extraction. This finding confirms the results obtained by the HPLC-CoulArray and supports the conclusion that both extraction methods, i.e., traditional maceration versus cascade extraction, provide extracts with similar composition.

However, through a more detailed analysis of the HPLC-DAD chromatogram, it is possible to observe that the extracts obtained from the cascade method present a more complex profile. With such extracts, several minor compounds (see Figure 4) were observed as small peaks along the chromatographic trace. It is important to highlight that such peaks were not present in the HPLC-DAD of the individual extracts. For instance, the peaks observed at a retention time of around 8.5 min (peaks A, B, and C) and at 13.5 min (peak D) were only present in the extracts obtained by the cascade method, while they were absent in the chromatograms of the individual

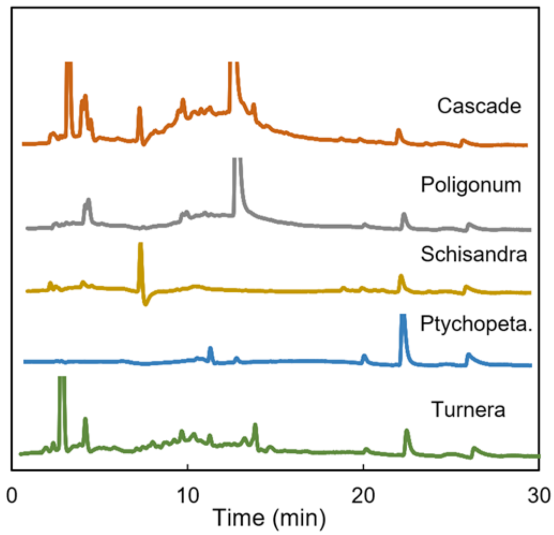

Figure 3. The HPLC-DAD analysis of individual and cascade extraction at 280 nm.

herbs. This finding suggests that the cascade extraction was able to increase the recovery of more minor bioactives than the maceration method of individual herbs.

Meanwhile, Figure 3 shows that the sample extract obtained by the cascade extraction method results in a chromatogram with a lower content of some peaks, if compared with the samples obtained from the single extraction methods. This is clearly observable in the chromatogram of the first herb, *Ptychopetalum*. Such loss of certain phenolic compounds can be explained with their adsorption to the solid retentate, which occurs between one extraction and the other. However, Figure 3 also shows that some other peaks are bigger in the cascade extract than in the individual extracts. This observation may also be explained considering that the cascade extraction generates solvents that are progressively richer not only of phenols but also of natural modifiers, which modify the solvating power of the solvent.

For this purpose, several studies have shown that the botanicals used in this study are naturally rich of surfactants, like saponins, which act as solvent modifiers and could be useful to increase the extraction of certain bioactive compounds (Peng *et al.*, 2018; Walthelm *et al.*, 2001). In particular, one of the main benefits of using a solvent naturally enriched by saponins is that the solvent viscosity is reduced, the surface tension is lowered, and micelles are generated. Overall, such effects may explain the enhanced solvating power of a solvent enriched by natural saponins (Vinarov *et al.*, 2018).

Several extraction methods have been developed focusing on solvent saving during the extraction process. The most traditional and widely applied method is Soxhlet extraction. This method continuously recycles the solvent by a series of evaporation/condensation cycles, while accumulating the extracted bioactives in a boiling flask (Patel *et al.*, 2019). In recent years, other continuous and batch extraction techniques have been developed (Poirot *et al.*, 2007). Among other methods, accelerated solvent extraction (Richter *et al.*, 1996) and Randall extraction (Thiex *et al.*, 2003) are very promising for their solvent

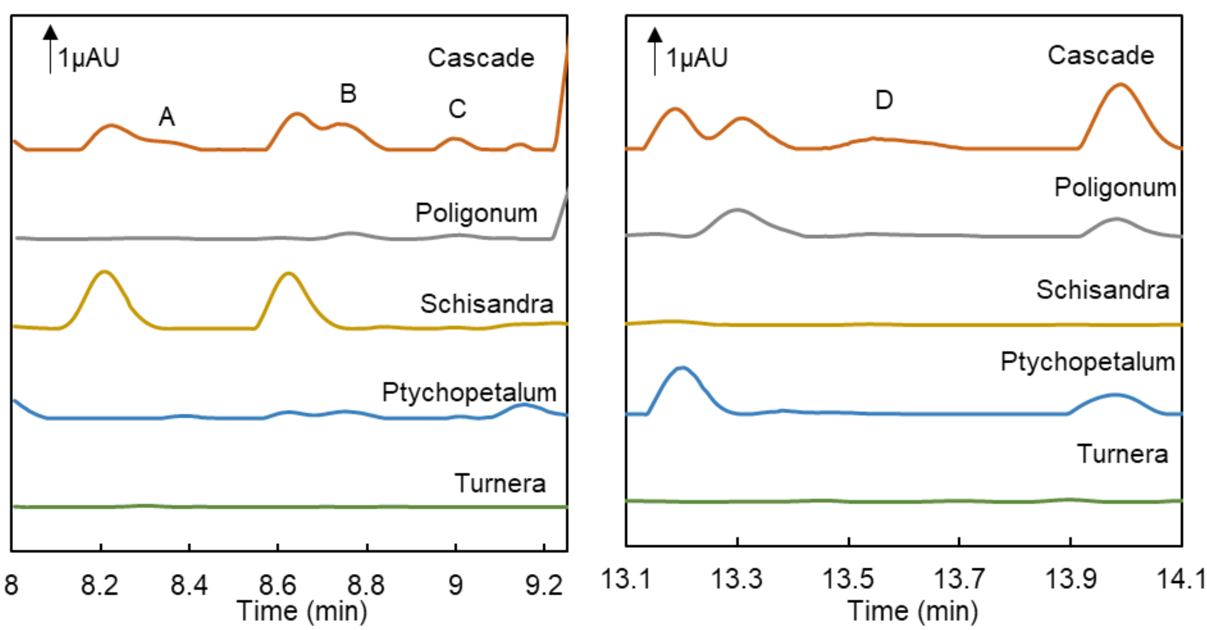

Figure 4. The HPLC-DAD analysis of individual and cascade extraction at certain time 8–9.2 min and 13.1 to 14.1 min.

saving attributes. However, in comparison with the above-mentioned extraction technologies, the cascade extraction approach proposed in this research is still more advantageous. For instance, to prepare an extract composed of four individual botanicals, the single extraction method needs a total of 400 mL of solvent for the extraction of 40 g of herbs. On the contrary, the cascade extraction needs only 140 mL of solvent in total. Such solvent reduction is a unique feature of the cascade extraction approach that cannot be simply achieved with other techniques.

Conclusion

This research proposes an innovative extraction method, called cascade extraction, that presents some advantages compared to the traditional solid–liquid extraction (i.e., maceration), especially when the final desired extract is a mixture of several botanical herbs. Although the overall extraction efficiency (determined by TPC, DPPH, FRAP, and ORAC assays, and HPLC analysis coupled with the electrochemical detector) of the proposed cascade extraction procedure is not significantly different from that achieved by the mixture of individual herbal extracts, HPLC-DAD showed that the extracts obtained by the cascade extraction procedure were richer in minor compounds. This means that the resulting extract with the proposed method has a more complex profile of bioactives. Furthermore, it is important to highlight that this result was achieved with less solvents. Indeed, the cascade extraction reuses the same initial solvent during the series of extraction steps, resulting in a simple and more sustainable extract. Moreover, it provides extracts with a richer bioactive profile than the traditional maceration of individual herbs and can be further applied in the food or pharmaceutical industries for the extraction of certain compounds from food or herbal materials.

References

Abubakar, U.I., Chua, L.S. and Aziz, R., 2015. Kinetics of green solid-liquid extraction of andrographolide from andrographis paniculata: effects of particle size and solid-liquid ratio. Green Processing and Synthesis 4(5): 399–410. https://doi.org/10.1515/gps-2015-0018

Alara, O.R., Abdurahman, N.H. and Ukaegbu, C.I., 2018. Soxhlet extraction of phenolic compounds from vernonia cinerea leaves and its antioxidant activity. Journal of Applied Research on Medicinal and Aromatic Plants 11 (June): 12–17. https://doi.org/10.1016/j.jarmap.2018.07.003

Ana María, D.B., María, V.V.S., Lilian, M.N., Lucía, M.M., Oscar, G.P. and Rosa, E.R., 2019. Neurobehavioral and toxicological effects of an aqueous extract of turnera diffusa willd (turneraceae) in mice. Journal of Ethnopharmacology 236 (December 2018): 50–62. https://doi.org/10.1016/j.jep.2019.02.036

Benzie, I.F.F. and Strain, J.J., 1996. The ferric reducing ability of plasma (FRAP) as a measure of "antioxidant power": the FRAP assay. Analytical Biochemistry 239(1): 70–76. https://doi.org/10.1006/abio.1996.0292

Cheok, C.Y., Chin, N.L., Yusof, Y.A., Talib, R.A. and Law, C.L., 2013. Anthocyanin recovery from mangosteen (Garcinia Mangostana l.) hull using lime juice acidified aqueous methanol solvent extraction. Food Science and Technology Research 19(6): 971–978. https://doi.org/10.3136/fstr.19.971

Choi, Y.H., Kim, J., Kim, J.Y., Joung, S.N., Yoo, K.P. and Chang, Y.S., 2000. Modifier effects on supercritical CO2 extraction efficiency of cephalotaxine from cephalotaxus wilsoniana leaves. Archives of Pharmacal Research 23(2): 163–166. https://doi.org/10.1007/BF02975507

Council of Europe, 2019. European pharmacopoeia 10.0.

Dos Reis, L.F. and Mendes, F.R., 2018. Ptychopetalum olacoides benth. pp. 401–411. https://doi.org/10.1007/978-94-024-1552-0_36

Han, D., Zhu, T. and Row, K.H., 2011. Ultrasonic extraction of phenolic compounds from laminaria japonica aresch using ionic liquid as extraction solvent. Bulletin of the Korean Chemical Society 32(7): 2212–2216. https://doi.org/10.5012/bkcs.2011.32.7.2212

Haque, M.A., Morozova, K., Ferrentino, G. and Scampicchio, M., 2021. Electrochemical methods to evaluate the antioxidant activity and capacity of foods: a review. Electroanalysis 33(6): 1419–1435. https://doi.org/10.1002/elan.202060600

Hicks, M.B., Salituro, L., Mangion, I., Schafer, W., Xiang, R., Gong, X. and Welch, C.J., 2017. Assessment of coulometric array electrochemical detection coupled with HPLC-UV for the absolute quantitation of pharmaceuticals. The Analyst 142(3): 525–536. https://doi.org/10.1039/C6AN02432G

Karioti, A., Fani, E., Vincieri, F.F. and Bilia, A.R., 2011. Analysis and stability of the constituents of curcuma longa and harpagophytum procumbens tinctures by HPLC-DAD and HPLC-ESI-MS. Journal of Pharmaceutical and Biomedical Analysis 55(3): 479–486. https://doi.org/10.1016/j.jpba.2011.02.029

Margraf, T., Karnopp, A.R., Rosso, N.D. and Granato, D., 2015. Comparison between folin-ciocalteu and prussian blue assays to estimate the total phenolic content of juices and teas using 96-well microplates. Journal of Food Science 80(11): C2397–C2403. https://doi.org/10.1111/1750-3841.13077

Mishra, K., Ojha, H. and Chaudhury, N.K., 2012. Estimation of antiradical properties of antioxidants using DPPH- assay: a critical review and results. Food Chemistry 130(4): 1036–1043. https://doi.org/10.1016/j.foodchem.2011.07.127

Patel, K., Panchal, N. and Ingle, P., 2019. Review of extraction techniques extraction methods: microwave, ultrasonic, pressurized fluid, soxhlet extraction, etc. International Journal of Advanced Research in Chemical Science 6(3): 6–21. https://doi.org/10.20431/2349-0403.0603002

Peng, S., Li, Z., Zou, L., Liu, W., Liu, C. and McClements, D.J., 2018. Improving curcumin solubility and bioavailability by encapsulation in saponin-coated curcumin nanoparticles prepared using a simple PH-driven loading method. Food and Function 9(3): 1829–1839. https://doi.org/10.1039/c7fo01814b

Poirot, R., Prat, L., Gourdon, C., Diard, C. and Autret, J.M., 2007. Optimization of batch to continuous transposition: solid-liquid extraction from plant in an industrial contactor. Proceedings of European Congress of Chemical Engineering (ECCE-6), Copenhagen, September 16–20, 2007.

Prior, R.L., Hoang, H., Gu, L., Wu, X., Bacchiocca, M., Howard, L., Hampsch-Woodill, M., Huang, D., Ou, B. and Jacob, R., 2003. Assays for hydrophilic and lipophilic antioxidant capacity (oxygen radical absorbance capacity (ORACFL)) of plasma and other biological and food samples. Journal of Agricultural and Food Chemistry 51(11): 3273–3279. https://doi.org/10.1021/jf0262256

Reverchon, E. and De Marco, I., 2006. Supercritical fluid extraction and fractionation of natural matter. Journal of Supercritical Fluids 38(2): 146–166. https://doi.org/10.1016/j.supflu.2006.03.020

Richter, B.E., Jones, B.A., Ezzell, J.L., Porter, N.L., Avdalovic, N. and Pohl, C., 1996. Accelerated solvent extraction: a technique for sample preparation. Analytical Chemistry 68(6): 1033–1039. https://doi.org/10.1021/ac9508199

Rodríguez-Pérez, C., Quirantes-Piné, R., Fernández-Gutiérrez, A. and Segura-Carretero, A., 2015. Optimization of extraction method to obtain a phenolic compounds-rich extract from moringa oleifera lam leaves. Industrial Crops and Products 66: 246–254. https://doi.org/10.1016/j.indcrop.2015.01.002

Rostagno, M.A., D'Arrigo, M., Martínez, J.A. and Martínez, J.A., 2010. Combinatory and hyphenated sample preparation for the determination of bioactive compounds in foods. TrAC – Trends in Analytical Chemistry 29(6): 553–561. https://doi.org/10.1016/j.trac.2010.02.015

Thiex, N.J., Anderson, S. and Gildemeister, B., 2003. Crude fat, diethyl ether extraction. In: Feed, cereal grain, and forage (Randall/Soxtec/Submersion method): collaborative study. Journal of AOAC International 86(5): 888–898. https://doi.org/10.1093/jaoac/86.5.888

Valachovic, P., Pechova, A. and Mason, T.J., 2001. Towards the industrial production of medicinal tincture by ultrasound assisted extraction. Ultrasonics Sonochemistry 8(2): 111–117. https://doi.org/10.1016/S1350-4177(00)00066-3

Vinarov, Z., Radeva, D., Katev, V., Tcholakova, S. and Denkov, N., 2018. Solubilisation of hydrophobic drugs by saponins. Indian Journal of Pharmaceutical Sciences 80(4): 709–718. https://doi.org/10.4172/pharmaceutical-sciences.1000411

Vinatoru, M., Mason, T.J. and Calinescu, I., 2017. Ultrasonically assisted extraction (UAE) and microwave assisted extraction (MAE) of functional compounds from plant materials. TrAC – Trends in Analytical Chemistry 97: 159–178. https://doi.org/10.1016/j.trac.2017.09.002

Walthelm, U., Dittrich, K., Gelbrich, G. and Schöpke, T., 2001. Effects of saponins on the water solubility of different model compounds. Planta Medica 67(1): 49–54. https://doi.org/10.1055/s-2001-10876

Xia, E.Q., Wang, B.W., Xu, X.R., Zhu, L., Song, Y. and Li, H.B., 2011. Microwave-assisted extraction of oleanolic acid and ursolic acid from ligustrum lucidum ait. International Journal of Molecular Sciences 12(8): 5319–5329. https://doi.org/10.3390/ijms12085319

Italian Journal of Food Science, 2022; 34 (2): 9–20

Effect of high-moisture extrusion on soy meat analog: study on its morphological and physiochemical properties

Monirul Islam[1,2], Yatao Huang[1], Md. Serajul Islam[3], Ningyu Lei[1], Lei Shan[1], Bei Fan[1], Litao Tong[1], Fengzhong Wang[1]*

[1]Institute of Food Science and Technology, Chinese Academy of Agricultural Sciences/Key Laboratory of Agro-Products Processing, Ministry of Agriculture and Rural Affairs, Beijing, People's Republic of China; [2]Rural Development Academy (RDA), Bogura, Bangladesh; [3]State Key Laboratory of Food Science and Technology, Jiangnan University, Wuxi, People's Republic of China

***Corresponding Author:** Fengzhong Wang, Institute of Food Science and Technology, Chinese Academy of Agricultural Sciences, Beijing, 100193, People's Republic of China. Email: wangfengzhong@sina.com

Received: 10 October 2021; Accepted: 7 December 2021; Published: 2 April 2022
© 2022 Codon Publications

OPEN ACCESS CC BY NC SA

PAPER

Abstract

There has been a growing interest in meat analog, microstructure characteristics, and anti-nutritional content obtained from soybean. High-moisture extrusion parameters are the input extruder of moisture content (>40%) that get the advantages of lower energy input. Thermo-mechanical treatment has a considerable influence on structural properties of soy-based meat analog. Texturized soy proteins can substitute meat products while providing a high-protein food ingredient which can be consumed directly as meat analogs. Therefore, this review aims to the effect on soybean of micro-structural and physicochemical properties of meat analogs by high-moisture extrusion. Thus, further studies are required concerning a large-scale meat products with purify protein structure.

Keywords: soy meat analog; high-moisture extrusion; allergenic protein; anti-nutritional factors; textural properties

Introduction

Soybean (*Glycine max*), which has its origin in East Asia (especially in China and Japan), belongs to the legume family (Kader *et al*., 2017). It is an excellent alternative source of proteins, complex carbohydrates, polyunsaturated fatty acids, soluble fibers, and isoflavones. Nowadays, it's grown worldwide as an edible bean (Peluso *et al*., 2014). Wang *et al*. (2020) reported that 60 varieties were used for the product development by 2018; 398 million tons of soybeans were produced worldwide, with 61% for oilseed production. In addition, Salgado and Donado-Pestana (2011) found that 90% of the total soybean production in the world is from the United States of America (USA), Brazil, South America, and Northwestern Europe. Moreover, Jooyandeh (2011) reported soybean oil composition that is 15% saturated, 61% polyunsaturated, and 24% monounsaturated fats. Furthermore, Fiala (2008) described that by 2030, the increase in the population, industrialization, and urbanization will also increase the plant meat demand by about 72%.

Golbitz and Jordan (2006) found that soybeans typically contain 35–40% proteins with well-balanced amino acid composition, 30% carbohydrate, 15–20% fat, 10–30% moisture content as well as fiber, calcium (Ca), iron (Fe), zinc (Zn), and vitamin B complex. The nutritional composition of soybean/legume is presented in Table 1. In addition, soybean contains some minor compounds, such as lecithin, isoflavones, bio-peptides, and others, that are effective against chronic cancer, cardiovascular diseases, and type II diabetes (Dixit *et al*., 2011; Singh, 2010; Singh *et al*., 2008). Soybean protein is suitable for people, who lack plant protein, for nutritional value and

Table 1. Nutritional composition of plant based protein, Quorn protein and microbial proteins legume.

Protein source	Protein content	Mineral content	References
Legume protein	Legume seed (20–30%)	–	(Riascos *et al*., 2010)
	–	Soy protein (concentrate): Potassium (2.4%), Phosphorus (0.9%), Calcium (0.4%), Magnesium (0.3), Iron (0.02%), Zinc (0.005%)	(Singh *et al*., 2008)
Oilseed protein	Safflower seed (13–17%)	–	(Asgar *et al*., 2010)
	Cottonseed (23%)	–	
	Rapeseed (25%)	–	
	Gourd seed	Calcium (0.055%), Magnesium (0.720%), Potassium (0.965%), Iron (0.021%), Zinc (0.016%)	(Olaofe *et al*., 1994)
	Pumpkin seed	Calcium (0.072%), Magnesium (0.778%), Potassium (1.127%), Iron (0.027%), Zinc (0.017%)	(Olaofe *et al*., 1994)
Cereal protein	Maize (8.8–11.9%)	–	(Orcutt *et al*., 2006; Riaz, 2004)
	Wheat (8–17.5%)	–	
	Oats (8.7–16%)	–	
	Rice (7–10%)	–	
	Barley (7–14.6%)	–	
	Rye (7–14%)	–	
Quorn protein	Mycoprotein 11%	Sodium (mg) 5.0 Cholesterol (g) 0 Iron (mg) 0.5 Zinc (mg) 9.0 Selenium (μg) 20	(Finnigan *et al*., 2019)
Bacterial protein	*Bacillus cereus* (Ram horn) 68% *Bacillus licheniformis* (Potato starch processing waste) 38% *Corynobacterium ammoniagenes* (Glucose + fructose) 61% *Escherichia coli* (Ram horn) 66% *Corynobacterium ammoniagenes* (Glucose + fructose) 61% *Cupriavidus necator* (Synthetic growth medium) 40–46%	–	(Ritala *et al*., 2017)

good health effects on calcium metabolism and lowering cholesterol (Shih *et al*., 2016). Moreover, soy products, such as soy flour, soy milk/powder, soy protein isolate (SPI), soy protein hydrolysates (Guo *et al*., 2018; He *et al*., 2019; Simmons *et al*., 2012), could be used as food additives and nutraceutical ingredients.

Meat alternatives could be classified as plant-based (soy, gluten, pea, etc.), cell-based (vitro or cultured meat), and fermentation-based (mycoproteins) (Sha & Xiong, 2020). In recent years, plant-based meat has been developed for meeting consumer demands, exponentially grown market, and the sustainability of future food supply (Sha & Xiong, 2020). The plant-based meat market's expansion is predicted to increase from $4.6 billion in 2018 to $85 billion in 2030, and as a milestone by 2026, it would achieve $30.9 billion (Sha & Xiong, 2020). Among the several mechanistic techniques for the texturization of plant-based meat, extrusion is the most often applied one (Dekkers *et al*., 2018).

Plant proteins represent a safe, sustainable, and practical non-pharmacological approach for lowering cholesterol. Recently, the most famous attributes of plant-based protein, that is soybean protein, is their health benefits linked to the prevention and treatment of many chronic diseases. Regular consumption of soy products reduces one's risk for chronic diseases such as cancer, heart disease, and stroke (Jooyandeh, 2011). Moreover, plant-based meat analog consumption is also beneficial in protecting against heart disease, lowering blood cholesterol; reducing the risk of cancer, and increasing bone mass (Joshi & Kumar, 2015). Furthermore, recent studies have well established that the plant-based food and beverage help in the improvement or management of immune system, have potential antimicrobial effects, helps in reducing risk of cardiovascular and gastro-intestinal diseases with improved physiological functions, decreases risk of low bone mass as well as very high levels of antioxidant activity (Paul *et al*., 2019).

In addition, high-moisture extrusion (HME), over 40% of moisture contents during processing, has the enormous advantage of lesser energy input, lower waste discharge, higher efficiency, and more excellent value of texturized products. Therefore, it is lately considered as the better choice for developing plant protein-based meat substitutes (Zhang *et al*., 2019). For texture optimization, exogenous polysaccharides are one of the functional primary additives used in food industries. At the time when proteins are denatured during the extrusion process, the dormant reactive sites of the interior proteins would become available, and the structure proteins would become flexible, which permits the protein-polysaccharide interactions. Polysaccharides could be used as cross-linker to alter the conformation of proteins, interact with proteins by cross-linking to protein side chains through Maillard reaction, and form a complex structure of protein (Caillard *et al*., 2010).

Plant-based meat analogs

Meat analog is also called meat substitute, faux meat, mock meat, or imitation meat. Analog can be defined as the compound of the same structure, such as texture, but slightly different in composition. There are two stages in the production of conventional meat analogs: preparation of emulsion and formation of its chunk. Typically, the emulsion is primed by mixing, chopping, and emulsifying proteins, fats, salts, and other inclusions to form a protein matrix. Meat analogs can be produced at low moisture (<35%) using a single screw extruder or at high moisture (>50%) using a twin-screw extruder (Lin *et al*., 2000). Moreover, Riaz (2004) described that meat analog could be formed into strips, sheets, patties, disks, and other shapes. It can absorb water at least three times its weight when cooked in boiling water for at least 15 min. The fibrous, anisotropic structure of meat analog products contributes to the meat-like feel and sensory view (Elzerman *et al*., 2013). Table 2 presents summaries of the comparison between the plant-based and animal-based alternatives to meat. Meat analogs look like textured meat and are healthy (cholesterol-free) and low-cost. In addition, mycoprotein meat analog, originated from fungus, is used as a healthy food alternative for its high-protein

Table 2. A comparison among cultured meat, plant-based meat, and animal-based meat.

	Dimension	Cultured meat	Plant-based meat	Animal-based meat	References
Background information	Origins, history, and technical operation	Idea articulated around 1930. Since 2000s, research into animal-cell culturing to produce meat.	Available in the market for several decades, made from concentrated protein- soy, wheat, pea by extrusion or coagulation.	Traditional in China, Japan, research on cell cultures for various production purposes since early 2000s.	(Bryant & Barnett, 2018; Sharma *et al*., 2015; Smetana *et al*., 2015)
	Nutritional value	Identical of regular meat.	Amino-acid profile nutritionally to meat.	Rich in protein but extraction needed due to indigestible walls.	
	Consumption and production rates and patterns	Not available in the market (optimists predict market introduction by 2019).	Established. Modest, relatively stable market share, increase since by 2010.	Products from extracted protein.	
	Position as meat alternative	Plant meats are more sustainable and animal friendly than animal-based meat.	Functional equivalent to meat.	Potentially protein-rich source for human consumption. Products rising.	
Current practice and situation	Technological	Proof of principle in 2013. Ongoing research and development.	Use of purified ingredients, increased efforts to improve meat similarity.	Growing and processing under research, have many challenges.	(Berghout *et al*., 2015; Dekkers *et al*., 2018; Osen *et al*., 2014; van der Weele *et al*., 2019)
	Lifestyle and Consumption	Proper meat produced without animal suffering.	Established as vegan alternatives replacing meat.	Novel: green product color and market profile.	
	Supporters and opposition	Attracts venture capitalists and entrepreneurs in Silicon Valley, animal welfare organizations, and other innovators. Emerging interest from meat industry.	Mix of alternative retail sector, experiments with hybrids of meat also startups and meat companies.	Pioneer companies and scientists, no consolidated coalition.	(Aiking, 2011; Aiking *et al*., 2006; Alexandratos & Bruinsma, 2012)

and low-fat content, and quality texture. The primary function of meat analogs is to replace the animal meat in the human diet. The consumers of soybean-based meat analogs include not only vegetarians but also the non-vegetarians who want to reduce their meat consumption for health reasons. For example, soybean meat analogs contain protein (50 to 95%, dry matter), and soy protein is primarily used as the protein ingredient (Chen *et al.*, 2010). Samard *et al.* (2019) demonstrated the high-moisture meat analogs are coupled with a higher integrity index and they have the stability of springiness as well as cutting strength than low-moisture meat substitute which is produced using the similar formula and screw-speed. The mechanical approaches summarized to make plant-based meat analogs are displayed in Table 3.

High-moisture extrusion of soy meat

The HME approach can be used to impart a specific texture to proteins such as soy-proteins, whey-proteins, pea-protein, or wheat-gluten (Pietsch *et al.*, 2017; Wolz *et al.*, 2016). HME is a crucial technology for transforming plant-based protein into palatable meat-like products. During the HME process, the input extruder of moisture content is more than 40%, which results in the advantages of lower energy input and higher quality of the texturized products (Zhang *et al.*, 2019). Chen *et al.* (2010) described that when moisture content of soy meat is increased from 28 to 60% (wet base), the indicator residence time and specific mechanical energy (SME) are significantly decreased. In addition, when cooking temperature is increased from 140 to 150°C, the in-line viscosity at die and SME reduced considerably, particularly at lower moisture contents (LMC). Most studies found the effects of processing parameters were done for low to moderate moisture processing. Still, these parameters can significantly affect protein structure during high-moisture processing (Palanisamy *et al.*, 2019). Due to its desirable texture and nutritional value, soy protein can be used to make soy protein products by the extrusion process (Wu *et al.*, 2019). For the traditional extrusion methods, extrusion at higher moisture conditions would reduce viscous dissipation at the lower extrusion temperature. Still, these changes would be expected during high-moisture extrusion conditions (MacDonald *et al.*, 2009). Zahari *et al.* (2020) reported the chosen parameters including concentration (0, 20, 40, 60%) of hemp protein concentrate (HPC), target moisture content (65, 70, 75%), temperature (40–120°C), and screw speed (300–800 rpm), whereas, SPI was extruded with 500 rpm at 70 and 75% of target moisture content. To summarize some literature, extrusion parameters and selected formulations of high-moisture meat analogs are shown in Table 4. MacDonald *et al.* (2009) also reported that high-moisture extrusion was useful to generate high-quality protein foods. Mechanical treatment is more effective during the high-moisture extrusion process for other plant proteins when compared with wheat gluten. Therefore, the influence of HME processing on the change of protein-protein interactions is used to form the anisotropic structures of SPIs (Chen *et al.*, 2011; Fang *et al.*, 2014).

Die-cutting

Die-cutting is a critical technology used to bring out the indentation of die-cutting of the surface to retouch the processing equipment, where this technique is a complex core unit. The die-cutting indentation position must be precise to cause simultaneously, and the complete platform stress must assure that the place of two active faces in contacts top and bottom to be mutually parallel. Shen *et al.* (2012) reported the speed of 7000 RH-1, travelling schedule 61 mm, cap board located 80°, the cam midpoint distance was 279 mm in a stand die-cutting machine. For instance, "the follower maximum pivot angle is 20°, main cam swing follower 240-mm long, roller radius 15 mm, vice-cam swing follower 240-mm long, roller radius 15 mm, the base circle initial radius is 60 mm. Moreover, the cam angle for outer dwell is 110°, the cam angle for inner dwell is 10°, work travel angle of follower is 150°, return travel angle of follower is 90°, allowed pressure angle of actuating travel is 35° allowed pressure angle of return travel is 60°, and allowable curvature radius of the real contour line of cam is 3 mm in a platform die-cutting machine (Shen *et al.*, 2012).

Table 3. Overview of mechanistic techniques to make plant-based meat analogs.

Technique	Starting material	Equipment type	Product	Process	Key technology	References
Bottom-up strategy	–	–	Structure/ structural element	–	Length scale anisotropy	(Post, 2012)
Wet spinning	Protein isolate, coagulation bath	Wet spinning setup: barrel, spinning nozzle, water bath, winding device	Fibers	–	Micrometer	(Post, 2012)

Table 4. Extrusion-parameters involved for screening and selected formulations of high-moisture meat analogs (HMMA).

Formulation	Speed of screw	Targeted moisture content (%)	Temperature (°C) (Zone 1–2–3–4)	Visual appearance color	References
0% HPC and 100% soy SPI	500	70	40–60–80–100	Light color, compact	Zahari *et al*. (2020)
	500	75		Light color, compact	
20% HPC and 80% soy SPI	800	65	40–60–80–100	Compact	Zahari *et al*. (2020)
	800	70		Compact	
	800	75		Less compact	
	600	75		Less compact	
	600	80		–	
	400	75		Less compact	
	300	75		Less compact	
40% HPC and 60% soy SPI	800	65	40–60–80–100	Compact, dark spot	Zahari *et al*. (2020)
	800	70		Compact	
	800	75		Pale, less compact	
60% HPC and 40% soy SPI	800	60	40–60–80–100	–	Zahari *et al*. (2020)
	800	62.5		–	
	800	65		Less compact	
	800	70		Less compact	
	800	75		Came out foamy	
	800	65	60–80–100–120	Less compact	

HPC: hemp protein concentrate; SPI: soy protein isolate.

Die pressure

The viscosity of the molten blend may be attributed to the decrease in pressure with the increase in temperature. The growth in feed moisture and die temperature then affects the mass thickness over the extruder and decreases the die-pressure value. Zhang *et al.* (2020a) found that the coefficient variation of the die pressure and die temperature was 26.71 and 1.74%. In addition, the measured die pressure in extrusion cooking of apple meat blend ranged from 9 to 16 MPa. The negative coefficient of the first-order term of temperature, screw speed, and moisture content indicated that die pressure increased with temperature decrease (Singha & Muthukumarappan, 2017).

High-pressure homogenization

High-pressure homogenization (HPH) is an applicable unit operation based on cavitation to improve processed soybean materials' extraction yields. Debruyne (2006) demonstrated that homogenization could cause a negative effect on separation efficiency. In addition, investigations may require evaluating the scalability of this promising result obtained by using a lab-scale homogenizer. Denaturation of the lipoxygenase occurred of enzyme high-temperature treatment may also catalyze the oxidation of polyunsaturated fatty acids, and also may also be responsible for turning into volatile off-flavors.

Characteristics of soy meat

Microstructure

Scanning electron microscopy (SEM), light microscopy (LM), Fourier transform infrared spectroscopy (FT-IR), as well as differential scanning calorimeter (DSC) are usually used to obtain more detailed information on the protein network microstructure of the meat analog. The micro-extraction technique is an environment-friendly procedure due to the reduction of polluting solvents and sample volume. For instance, the micro-extraction approach increases the extraction yield and diminishes the sample equilibrium time (Barzegar *et al.*, 2019). Micro-extraction includes several performances such as single drop micro-extraction (SDME), dispersive-liquid–liquid micro-extraction (DLLME) and hollow-fiber micro-extraction (HFLPME). Preece *et al.* (2017) reported "the cotyledon-cells protein bodies found in size range from 2.4 to 13.5 μm when used SEM approach without sample-hydration." Lakemond *et al.* (2000) described two significant storage proteins that compose 60–80% of the total soybean protein: the β-conglycinin and glycinin. Soybean protein is a complex mixture containing various proteins, and each of them has unusual denaturation temperatures. Glycinin and β-conglycinin are two main storage proteins, and their denaturation temperatures were 68 and 86°C, correspondingly (Peng *et al.*, 2016). Throughout the low moisture extrusion, the ingredients can undergo structural changes caused by high temperature and shear. It can also affect the product's characteristics, such as microstructure and expansion (Beck *et al.*, 2018).

DSC, TG and DTG measurements

The differential scanning calorimetry (DSC) analysis can be conducted with Thermal-Analysis-Systems Model Q-200. Non-isothermal degradation can be measured by using thermogravimetric/differential-thermal-analysis (TG/DTA). The thermal analysis techniques such as thermo-gravimetric-analysis (TGA) can provide information on thermal stability, including thermal-degradation of protein films. Zhang *et al.* (2020b) observed that the mixtures pass through extruder from the mixing-zone to the melting-zone for peanut protein/exogenous polysaccharide mixture, the endothermic-peaks of arachin and conarachin were both prominently reduced due to the denaturation of protein-molecules.

In the mixing zone, 2% WS (wheat starch) could cause a significant decrease in the thermal transition peak temperature (*Tp*) value and a significant increase in the enthalpy changes (ΔH) value of the conarachin. As a result, it indicated that 2% WS accelerated the thermal transition of conarachin and the energy required to open the increased molecule. Guo *et al.* (2012) described that exogenous polysaccharides had no significant effect on the ΔH value of arachin, due to the relatively tight structure of arachin. In addition, Zhang *et al.* (2020b) found that the exogenous polysaccharides had enhanced the protein-lipid interaction, when 0.1% CA or 2% WS was added. Moreover, the exogenous polysaccharides could decrease, particularly when 2% WS was added, and the value significantly reduced from 310 to 302°C.

Textural properties

There are two textural properties as the transverse (T) and directions cutting force in longitudinal (L) are positively correlated with the carrageenan (ICGN) concentration in the meat analog sample. The cutting force can also be interpreted as an indirect indicator of texturization and hardness (Palanisamy *et al.*, 2018). The elasticity differences between the raw samples containing 0.75, 1.5, and 3% ICGN were not significant, while no significant differences between all ICGN added cooked samples could be detected. Shahiri Tabarestani and Mazaheri Tehrani (2014) found that adding soy-flour, flour of split-pea, and wheat-starch could improve low-fat hamburger's texture properties by reducing shrinkage. For example, Smith *et al.* (1976) proved that the presence of textured soy protein was associated with the substantial reduction of shrinkage in the blended ground. The transversal cutting strength of texturized vegetable protein (TVP) and meat samples was slightly higher than their longitudinal cutting strength. It is stated that the cutting strength in parallel and vertical directions of extrudates could indicate the texturization degree or fibrous-structure formation (Fang *et al.*, 2014; Gu & Ryu, 2017). When SME is decreased, there is an increase in instrumental chewiness and hardness. As a result, instrumental chewiness and hardness of meat analogs increased with decreasing SPC-WG ratio (Fiorentini *et al.*, 2020). Additionally, Fang *et al.* (2014) reported that the instrumental hardness and chewiness of texturized soybean proteins increased more than 22 and 17%, respectively. Day and Swanson (2013) described that high chewiness in meat analogs corresponded with low SME values, indicative of low-melt viscosity. To summarize the literature, common soy meat analogs available in the market are presented in Table 5, which were both prominently reduced due to the denaturation of protein molecules.

Anti-nutritional factors

A wide variety of anti-nutritional substances are available in most of the potential and alternative plant-derived nutrient sources. Metabolic products arising in living systems may be defined as anti-nutrient substances that affect health or food production by themselves or through their food utilization. Anti-nutritional substances could be usually divided into four groups: (1) factors that affect mineral utilization, including gossypol pigments, phytates (Hexa-phosphates of Myo-inositol), oxalates and glucosinolates, (2) factors that affect protein utilization and digestion, including lectins, protease inhibitors and tannins, (3) Anti-vitamins, (4) Miscellaneous substances for example, mycotoxins, cyanogens, mimosine, alkaloids, nitrate, phytoestrogens, photosensitizing agents, and saponins.

Besides, Ma *et al.* (2020) recounted those anti-nutritional compounds that reduced the bio-availability of the essential nutrients or energy in the diet. Reducing the content of the anti-nutritional factors (ANFs) can efficiently improve the use of soy nutrients. Based on protein content, products from soy-protein are divided into three broad categories: (1) soy flour and grits (50% protein on a moisture-free basis); (2) soy protein concentrates (70% protein), and (3) isolated soy proteins (90% protein) reported by Singh *et al.* (2008). In addition, Thadavathi *et al.* (2019) reported that the high protein vegetable-based foods were used as an alternative for meat products which was enormously advantageous for the increasing human population in the world, and it could address the environmental concerns as well as the health considerations from meat consumption. Moreover, Aijie *et al.* (2014) reported that the ANFs decreased during germination, which was attributed to the activation of several enzymes in the seed. The summarized literature on anti-nutrients and ANFs of soybean are presented in Table 6.

Allergenic protein

There are many kinds of allergenic compounds and ANF's present in soybean. According to the report of food allergens, almost 2% of adults and 5–8% of children have food allergic reactions associated with the consumption of soybean or soybean derived food products (John *et al.*, 2017). Additionally, Gagnon *et al.* (2010) reported that food allergies are a big concern for health in most countries. In addition, allergic reactions to food affect 4–6% of children and 1.5% of adults (Uguz *et al.*, 2005). There are different allergenic proteins present in soybeans. However, soybean proteins allergic reactions are mostly transient and non-life-threatening and are usually outgrown after 3 years of age. It seems to be tolerant within 2–5 years after the initial diagnosis. Soybean allergenic proteins can be detecting to soybean allergens. In recent years, researches about allergenic soybean proteins detection have been rapidly expanded. Currently using two most approaches

Table 5. Common soybean meat analogs existing in market.

Name of product	Introduction/first reported	Main ingredients/origin	Characteristics/remarks	References
Tofu	China	Pressed soy curd prepared from coagulated soy.	Most widely recognized meat alternatives, blind taste, can impart flavor by smoking/marinating.	(Sadler, 2004)
Tivall	1997	Soy-based fibrous vegetable protein.	Simulate meat muscle, provide a different eating textures to other soy formats.	(Sadler, 2004)
Tempeh	1851 in Indonesia	Fermented soy-based cake.	Controlled fermentation of soy leads, similar shape to burger patties.	(Kumar *et al*., 2017; Malav *et al*., 2015)
Grillers original burgers		Extruded vegetable protein burgers.	Veggie goodness, soy protein concentrate, water for hydration.	(Kyriakopoulou *et al*., 2019)
Schnitze		Rehydrated soy protein products.	–	(Kyriakopoulou *et al*., 2019)

Table 6. Comparison of the soybean and other grains substitute of anti-nutritional factors and fractions.

Plant substitutes	Anti-nutritional factors				References
Soybean meal	Protease inhibitors, saponins, anti-vitamins , phytic acid, lectins, phytoestrogens and allergens.				(Francis *et al*., 2001)
Rapeseed meal	Rapeseed meal, protease-inhibitors, phytic acid glucosinolates and tannins.				
Pea seed meal	Pea seed protease-inhibitors, tannins, lectins, cyanogens and phytic acid.				
Sesame meal	Sesame phytic acid and protease inhibitors.				
Cottonseed meal	Cottonseed meal phytic-acid, phyto-estrogens, gossypol and anti-vitamins.				
Various grains	**Grains fractions**	**Arabinoxylans**	**β-Glucans**	**Cellulose**	
Soybean	Soluble	–	–	–	(Choct, 1997)
	Insoluble	–	–	4.4%	
Wheat	Soluble	1.8%	0.4%	–	
	Insoluble	6.3%	0.4%	2%	
Barley	Soluble	0.8%	3.6%	–	
	Insoluble	7.1%	0.7%	3.9%	
Maize	Soluble	0.1%	–	–	
	Insoluble	5.1%	–	2%	
Sorghum	Soluble	0.1%	0.1%	–	
	Insoluble	2%	0.1%	2.2%	

like Enzyme linked immunosorbent assays (ELISA) and Immunoblotting, also using by Radio allegro-sorbent test inhibition, Enzyme allego-sorbent test, Polymerase chain reaction, Mass spectrometry, High-performance liquid chromatography (Wang *et al*., 2014). ELISA is a powerful tool for detecting proteins, ELISA such as Sandwich ELISA, Competitive ELISA and Indirect ELISA are widely used to determine soybean proteins in food products (Wang *et al*., 2014). Immunoblotting is a powerful research tool which can indicate molecular mass and immunoreactivity of allergenic proteins. Beardslee (2000) found soybean allergenic proteins glycinin G1 acidic chain and a 22 kDa G2 glycinin by using immunoblotting.

Sensory evaluation

The mouthfeel and fibrousness are the same as meat, which are the primary sensory properties to consider when consuming the meat alternatives. The addition of IoT-carrageenan (ICGN) concentration is essential to increase the fibrousness of the product because of its denser structure. Palanisamy *et al.* (2018) observed extra 2.25 to 3% ICGN can increase elasticity which could be detected significantly with the overall scores' acceptance ranged from 1.73 to 2.49%. The ICGN concentration was positively correlated with the fibrousness; the hardness could also be influenced by the preference (Palanisamy *et al*., 2018). Cheftel *et al.* (1992) reported that texturization with HME is entirely different from other protein texturization processes such as manufacturing cheese curds, sausages, tofu, in which fiber was formed by extrusion cooking or by spinning. In addition, proteins would be plasticized in the heating chamber during the extrusion process of texturizing a long cooling die at the end. The process could be optimized by varying the temperature, moisture, pressure, and shear.

Health characteristics of soybean

Regular consumption of soy products can reduce the risk of chronic diseases such as cancer, stroke, heart disease, and type 2 diabetes (Jooyandeh, 2011). Soy-based foods also provide beneficial health compounds, including vitamins, minerals, fiber, and flavonoids. In addition, various clinical trials have investigated the potential of soybean and soybean products to protect against the risk of chronic diseases. Furthermore, Scheiber *et al.* (2001) described soybean consumption as reducing the risk of cardiovascular disease. Recently, pea protein is used as an alternative ingredient in high-moisture meat analogs because of its functional characteristics and low potentiality for allergic responses (Osen *et al*., 2014). Akdogan (1999) reported that protein and other food additives, such as starch or lipid, probably have a positive or negative effect on forming the desired texture. Furthermore, Asgar *et al.* (2010) reported that other types of legumes and oilseeds could also be used as protein-rich materials to develop a variety of high-moisture meat analogs, which could contribute to alternative protein sources.

Market potential alternate plant proteins

In contemporary years, plant-based proteins have received increasing attention as good substitutes for animal-based proteins. The important reasons for the increasing acceptability of plant-based protein are the low cost and fibrous texture (Echeverria-Jaramillo *et al*., 2021). Plant-based protein's growing trend is setting out to increase the number of vegetarians or meat avoiders (Aschemann-Witzel *et al*., 2021). Proteins, in particular, plant-based proteins are more important in the face of future challenges, ensuing from unceasing population growth and the unevenness between malnutrition and overweight/obesity (Mittermeier-Kleßinger *et al*., 2021). Time trends for the development of alternative protein ingredients are demonstrated in Table 7. The key drivers of market growth include: (1) consumers concern over food safety in relation to animal products; (2) growth in the number of vegetarians, meat avoiders, and meat reducers; (3) meat eaters seeking more variety in their diet; (4) growing interest in healthy eating which includes incorporating more plant-based foods into the diet.

Conclusion

This review concluded that high-pressure extrusion is an effective technology that can potentially be used to produce natural food products in which heat treatment will be reduced. This enhances the hydrophobic interactions and increases the visible viscosity to stabilize the newly formed conformation of the texturized effects. Plant proteins have some physiologically active components such as protease phytosterols, inhibitors saponins, and isoflavones. The thermo-mechanical treatment affects the microstructural changes and the rheological properties in SPC during high-moisture extrusion processing. Therefore, the importance of soybean meat analog products as an alternative soy meat source that should be explored along with studies to clarify the underlying effects of the quality and increasing acceptability of plant-based protein are the low cost and fibrous texture. Future study are required on protein-extraction yield and purification which could be predicted well using another mechanistic model developed as well as on flavor and texture meat analog products.

Table 7. Time-trends for development of alternative protein ingredients.

Protein ingredients	Approx. year introduced	References
Nuts	Increased imports post 1945 Soy	(Sadler, 2004)
Quorn™ (mycoprotein)	1984	
WheatPro™ (wheat protein)	1992	
Arrum™ (wheat and pea protein)	1995	
Fibrous vegetable protein	1997	

Acknowledgement

This work was supported by the China Agriculture Research System (CARS-04) and the Knowledge Innovation Program Funding of the Institute of Food Science and Technology, Chinese Academy of Agricultural Sciences (125161015000150013), "the Science and Technology Innovation Project" of the Chinese Academy of Agricultural Sciences (CAAS-ASTIP-2020-IFST-04). The first author gratefully thanks the Chinese Scholarship Council for providing a full scholarship to study PhD at the Graduate School of Chinese Academy of Agricultural Sciences, Beijing, China.

Conflicts of interest

There is no conflict of interest exit to the submission of this manuscript. This manuscript is approved by all authors for publication.

References

Aijie L., Shouwei Y. and Li L. 2014. Structure, trypsin inhibitor activity and functional properties of germinated soybean protein isolate. Int J Food Sci Technol. 49(3): 911–919. https://doi.org/10.1111/ijfs.12386

Aiking H. 2011. Future protein supply. Trends Food Sci Technol. 22(2–3): 112–120. https://doi.org/10.1016/j.tifs.2010.04.005

Aiking H., de Boer J. and Vereijken J. 2006. Sustainable protein production and consumption: pigs or peas? Vol. 45. Springer Science & Business Media, Springer, Dordrecht, The Netherlands.

Akdogan H. 1999. High moisture food extrusion. Int J Food Sci Technol. 34(3): 195–207. https://doi.org/10.1046/j.1365-2621.1999.00256.x

Alexandratos N. and Bruinsma, J. 2012. World agriculture towards 2030/2050: the 2012 revision, Position Paper. AgEcon Search. St. Paul, MN, USA. https://doi.org/10.22004/ag.econ.288998

Aschemann-Witzel J., Gantriis R.F., Fraga P. and Perez-Cueto F.J. 2021. Plant-based food and protein trend from a business perspective: markets, consumers, and the challenges and opportunities in the future. Crit Rev Food Sci Nutr. 61(18): 3119–3128. https://doi.org/10.1080/10408398.2020.1793730

Asgar M., Fazilah A., Huda N., Bhat R. and Karim, A. 2010. Nonmeat protein alternatives as meat extenders and meat analogs. Comprehen Rev Food Sci Food Saf. 9(5): 513–529. https://doi.org/10.1111/j.1541-4337.2010.00124.x

Barzegar F., Kamankesh M. and Mohammadi A. 2019. Heterocyclic aromatic amines in cooked food: a review on formation, health risk-toxicology and their analytical techniques. Food Chem. 280: 240–254. https://doi.org/10.1016/j.foodchem.2018

Beardslee T.A. 2000. IgE epitope mapping of soybean glycinin G1 acidic chain. The University of Nebraska, Lincoln. 9976975.

Beck S.M., Knoerzer K., Foerster M., Mayo S., Philipp C. and Arcot J. 2018. Low moisture extrusion of pea protein and pea fibre fortified rice starch blends. J Food Eng. 231: 61–71. https://doi.org/10.1016/j.jfoodeng.2018.03.004

Berghout J., Pelgrom P., Schutyser M., Boom R. and Van Der Goot A. 2015. Sustainability assessment of oilseed fractionation processes: a case study on lupin seeds. J Food Eng. 150: 117–124. https://doi.org/10.1016/j.jfoodeng.2014.11.005

Bryant C. and Barnett, J. 2018. Consumer acceptance of cultured meat: a systematic review. Meat Sci. 143: 8–17. https://doi.org/10.1016/j.meatsci.2018.04.008

Caillard R., Remondetto G. and Subirade M. 2010. Rheological investigation of soy protein hydrogels induced by Maillard-type reaction. Food Hydrocolloids. 24(1): 81–87. https://doi.org/10.1016/j.foodhyd.2009.08.009

Cheftel J., Kitagawa M. and Queguiner C. 1992. New protein texturization processes by extrusion cooking at high moisture levels. Food Rev Int. 8(2): 235–275. https://doi.org/10.1080/87559129209540940

Chen F.L., Wei Y.M. and Zhang B. 2011. Chemical cross-linking and molecular aggregation of soybean protein during extrusion cooking at low and high moisture content. LWT Food Sci Technol. 44(4): 957–962. https://doi.org/10.1016/j.lwt.2010.12.008

Chen F.L., Wei Y.M., Zhang B. and Ojokoh, A.O. 2010. System parameters and product properties response of soybean protein extruded at wide moisture range. J Food Eng. 96(2): 208–213. https://doi.org/10.1016/j.jfoodeng.2009.07.014

Choct M. 1997. Feed non-starch polysaccharides: chemical structures and nutritional significance. Feed Milling Int. 191(June issue): 13–26.

Day L. and Swanson B.G. 2013. Functionality of protein-fortified extrudates. Comprehen Rev Food Sci Food Saf. 12(5): 546–564. https://doi.org/10.1111/1541-4337.12023

Debruyne I. 2006. Soy base extract: soymilk and dairy alternatives. In: Riaz, M.N., editor. Soy applications in food. CRC Press Inc, Boca Raton, USA, pp. 111–133. https://doi.org/10.1201/9781420037951.ch7

Dekkers B.L., Boom R.M. and van der Goot, A.J. 2018. Structuring processes for meat analogues. Trends Food Sci Technol. 81: 25–36. https://doi.org/10.1016/j.tifs.2018.08.011

Dixit A.K., Antony J., Sharma N.K. and Tiwari R.K. 2011. Opportunity, Challenge and Scope of Natural Products in Medicinal Chemistry, 367–383.

Echeverria-Jaramillo E., Kim Y.-H., Nam Y.-R., Zheng Y.-F., Cho J.Y., Hong W. S., et al. 2021. Revalorization of the cooking water (Aquafaba) from soybean varieties generated as a by-product of food manufacturing in Korea. Foods. 10(10): 2287. https://doi.org/10.3390/foods10102287

Elzerman J.E., Van Boekel M.A. and Luning P.A. 2013. Exploring meat substitutes: consumer experiences and contextual factors. Br Food J. 115(5): 700–710. https://doi.org/10.1108/00070701311331490

Fang Y., Zhang B. and Wei Y. 2014. Effects of the specific mechanical energy on the physicochemical properties of texturized soy protein during high-moisture extrusion cooking. J Food Eng. 121: 32–38. https://doi.org/10.1016/j.jfoodeng.2013.08.002

Fiala N. 2008. Meeting the demand: an estimation of potential future greenhouse gas emissions from meat production. Ecol Econ. 67(3): 412–419. https://doi.org/10.1016/j.ecolecon.2007.12.021

Finnigan T.J., Wall B.T., Wilde P.J., Stephens F.B., Taylor S.L. and Freedman M.R. 2019. Mycoprotein: the future of nutritious nonmeat protein, a symposium review. Curr Dev Nutr. 3(6): nzz021. https://doi.org/10.1093/cdn/nzz021

Fiorentini M., Kinchla A.J. and Nolden A.A. 2020. Role of sensory evaluation in consumer acceptance of plant-based eat analogs and meat extenders: a scoping review. Foods. 9(9): 1334. https://doi.org/10.3390/foods9091334

Francis G., Makkar H.P. and Becker K. 2001. Antinutritional factors present in plant-derived alternate fish feed ingredients and their effects in fish. Aquaculture. 199(3–4): 197–227. https://doi.org/10.1016/S0044-8486(01)00526-9

Gagnon C., Poysa V., Cober E.R. and Gleddie S. 2010. Soybean allergens affecting North American patients identified by 2D gels and mass spectrometry. Food Anal Methods. 3(4): 363–374. https://doi.org/10.1007/s12161-009-9090-3

Golbitz P. and Jordan J. 2006. Soyfoods: market and products. In: Riaz, M.N., editor. Soy applications in food. CRC Press Inc, Boca Raton, USA, pp. 1–21.

Gu B.Y. and Ryu G.-H. 2017. Effects of moisture content and screw speed on physical properties of extruded soy protein isolate. J Korean Soc Food Sci Nutr. 46(6): 751–758. https://doi.org/10.3746/jkfn.2017.46.6.751

Guo J., Yang X.-Q., He X.-T., Wu N.-N., Wang J.-M., Gu W., et al. 2012. Limited aggregation behavior of β-conglycinin and its terminating effect on glycinin aggregation during heating at pH 7.0. J Agr Food Chem. 60(14): 3782–3791. https://doi.org/10.1021/jf300409y

Guo X., Sun X., Zhang Y., Wang R. and Yan X. 2018. Interactions between soy protein hydrolyzates and wheat proteins in noodle making dough. Food Chem. 245: 500–507. https://doi.org/10.1016/j.foodchem.2017.10.126

He L.-D., Guo X.-N. and Zhu K.-X. 2019. Effect of soybean milk addition on the quality of frozen-cooked noodles. Food Hydrocolloids. 87: 187–193. https://doi.org/10.1016/j.foodhyd.2018.07.048

John K.M., Khan F., Luthria D.L., Garrett W. and Natarajan S. 2017. Proteomic analysis of anti-nutritional factors (ANF's) in soybean seeds as affected by environmental and genetic factors. Food Chem. 218: 321–329. https://doi.org/10.1016/j.foodchem.2016.09.072

Jooyandeh H. 2011. Soy products as healthy and functional foods. Middle-East J Sci Res. 7(1): 71–80.

Joshi V. and Kumar S. 2015. Meat analogues: plant based alternatives to meat products – a review. Int J Food Ferment Technol. 5(2): 107–119. https://doi.org/10.5958/2277-9396.2016.00001.5

Kader M.A., Senge M, Mojid M.A. and Nakamura K. 2017. Mulching type-induced soil moisture and temperature regimes and water use efficiency of soybean under rain-fed condition in central Japan. Int Soil Water Conserv Res. 5(4): 302–308. https://doi.org/10.1016/j.iswcr.2017.08.001

Kumar P., Chatli M., Mehta N., Singh P., Malav O. and Verma A.K. 2017. Meat analogues: health promising sustainable meat substitutes. Crit Rev Food Sci Nutr. 57(5): 923–932. https://doi.org/10.1080/10408398.2014.939739

Kyriakopoulou K., Dekkers B. and van der Goot A.J. 2019. Plant-based meat analogues. In: Sustainable meat production and processing. Wageningen University & Research. Wageningen, The Netherlands, pp. 103–126. https://doi.org/10.1016/B978-0-12-814874-7.00006-7

Lakemond C.M., de Jongh H.H., Hessing M., Gruppen H. and Voragen A.G. 2000. Heat denaturation of soy glycinin: influence of pH and ionic strength on molecular structure. J Agr Food Chem. 48(6): 1991–1995. https://doi.org/10.1021/jf9908704

Lin S., Huff H. and Hsieh F. 2000. Texture and chemical characteristics of soy protein meat analog extruded at high moisture. J Food Sci. 65(2): 264–269. https://doi.org/10.1111/j.1365-2621.2000.tb15991.x

MacDonald R.S., Pryzbyszewski J. and Hsieh F.-H. 2009. Soy protein isolate extruded with high moisture retains high nutritional quality. J Agr Food Chem. 57(9): 3550–3555. https://doi.org/10.1021/jf803435x

Malav O., Talukder S., Gokulakrishnan P. and Chand S. 2015. Meat analog: a review. Crit Rev Food Sci Nutr. 55(9): 1241–1245. https://doi.org/10.1080/10408398.2012.689381

Ma M., Zhang H., Xie Y., Yang M., Tang J., Wang P., et al. 2020. Response of nutritional and functional composition, antinutritional factors and antioxidant activity in germinated soybean under UV-B radiation. LWT. 118: 108709. https://doi.org/10.1016/j.lwt.2019.108709

Mittermeier-Kleßinger V.K., Hofmann T. and Dawid C. 2021. Mitigating off-flavors of plant-based proteins. J Agr Food Chem. 69(32): 9202–9207. https://doi.org/10.1021/acs.jafc.1c03398

Olaofe O., Adeyemi F. and Adediran G.O. 1994. Amino acid and mineral compositions and functional properties of some oilseeds. J Agr Food Chem. 42(4): 878–881. https://doi.org/10.1021/jf00040a007

Orcutt M., Mcmindes M., Chu H., Mueller I., Bater B. and Orcutt A. 2006. Textured soy protein utilization in meat and meat analog products. In: Riaz, M.N., editor. Soy applications in food. CRC Press Inc, Boca Raton, USA, pp. 155–184.

Osen R., Toelstede S., Wild F., Eisner P. and Schweiggert-Weisz U. 2014. High moisture extrusion cooking of pea protein isolates: raw material characteristics, extruder responses, and texture properties. J Food Eng. 127: 67–74. https://doi.org/10.1016/j.jfoodeng.2013.11.023

Palanisamy M., Franke K., Berger R.G., Heinz V. and Töpfl S. 2019. High moisture extrusion of lupin protein: influence of extrusion parameters on extruder responses and product properties. J Sci Food Agr. 99(5): 2175–2185. https://doi.org/10.1002/jsfa.9410

Palanisamy M., Töpfl S., Aganovic K. and Berger R.G. 2018. Influence of iota carrageenan addition on the properties of soy protein meat analogues. LWT. 87: 546–552. https://doi.org/10.1016/j.lwt.2017.09.029

Paul A.A., Kumar S., Kumar V. and Sharma R. 2019. Milk analog: plant based alternatives to conventional milk, production, potential and health concerns. Crit Rev Food Sci Nutr. 60(18): 3005–3023. https://doi.org/10.1080/10408398.2019.1674243

Peluso I., Romanelli L. and Palmery M. 2014. Interactions between prebiotics, probiotics, polyunsaturated fatty acids and polyphenols: diet or supplementation for metabolic syndrome prevention? Int J Food Sci Nutr. 65(3): 259–267. https://doi.org/10.3109/09637486.2014.880670

Peng X., Ren C. and Guo S. 2016. Particle formation and gelation of soymilk: effect of heat. Trends Food Sci Technol. 54: 138–147. https://doi.org/10.1016/j.tifs.2016.06.005

Pietsch V.L., Emin M.A. and Schuchmann H.P. 2017. Process conditions influencing wheat gluten polymerization during high moisture extrusion of meat analog products. J Food Eng. 198: 28–35. https://doi.org/10.1016/j.jfoodeng.2016.10.027

Post M.J. 2012. Cultured meat from stem cells: challenges and prospects. Meat Sci. 92(3): 297–301. https://doi.org/10.1016/j.meatsci.2012.04.008

Preece K.E., Hooshyar N., Krijgsman A., Fryer P.J. and Zuidam N.J. 2017. Intensified soy protein extraction by ultrasound. Chem Eng Process Process Inten. 113: 94–101. https://doi.org/10.1016/j.cep.2016.09.003

Riascos J.J., Weissinger A.K., Weissinger S.M. and Burks A.W. 2010. Hypoallergenic legume crops and food allergy: factors affecting feasibility and risk. J Agr Food Chem. 58(1): 20–27. https://doi.org/10.1021/jf902526y

Riaz M. 2004. Texturized soy protein as an ingredient. In: Riaz, M.N., editor. Proteins in food processing. pp. 517–558.

Ritala A., Häkkinen S.T., Toivari M. and Wiebe M.G. 2017. Single cell protein—state-of-the-art, industrial landscape and patents 2001–2016. Front Microbiol. 82009. https://doi.org/10.3389/fmicb.2017.02009

Sadler M.J. 2004. Meat alternatives—market developments and health benefits. Trends Food Sci Technol. 15(5): 250–260. https://doi.org/10.1016/j.tifs.2003.09.003

Salgado J.M. and Donado-Pestana C.M. 2011. Soy as a functional food. In: El-Shemy H., editor. Soybean and nutrition. IntechOpen. London, UK, pp. 21–44.

Samard S., Gu B.Y. and Ryu G.H. 2019. Effects of extrusion types, screw speed and addition of wheat gluten on physicochemical characteristics and cooking stability of meat analogues. J Sci Food Agric. 99(11): 4922–4931. https://doi.org/10.1002/jsfa.9722

Scheiber M.D., Liu J.H., Subbiah M., Rebar R.W. and Setchell K.D. 2001. Dietary inclusion of whole soy foods results in significant reductions in clinical risk factors for osteoporosis and cardiovascular disease in normal postmenopausal women. Menopause. 8(5): 384–392. https://doi.org/10.1097/00042192-200109000-00015

Sha L. and Xiong Y.L. 2020. Plant protein-based alternatives of reconstructed meat: science, technology, and challenges. Trends Food Sci Technol. 102: 51–61. https://doi.org/10.1016/j.tifs.2020.05.022

Shahiri Tabarestani H. and Mazaheri Tehrani M. 2014. Optimization of physicochemical properties of low-fat hamburger formulation using blend of soy flour, split-pea flour and wheat starch as part of fat replacer system. J Food Process Preserv. 38(1): 278–288. https://doi.org/10.1111/j.1745-4549.2012.00774.x

Sharma S., Thind S.S. and Kaur A. 2015. In vitro meat production system: why and how? J Food Sci Technol. 52(12): 7599–7607. https://doi.org/10.1007/s13197-015-1972-3

Shen S.H., Shi X.D. and Yuan Y.C. 2012. Optimal design of conjugate cam-linkage combined mechanism for pressure device in die-cutting. Paper presented at the Applied Mechanics and Materials. 120: 178–181. https://doi.org/10.4028/www.scientific.net/AMM.120.178

Shih M.-C., Hwang T.-S. and Chou, H.-Y. 2016. Physicochemical and functional property changes in soy protein isolates stored under high relative humidity and temperature. J Food Sci Technol. 53(1): 902–908. https://doi.org/10.1007/s13197-015-2057-z

Simmons A.L., Smith K.B. and Vodovotz Y. 2012. Soy ingredients stabilize bread dough during frozen storage. J Cereal Sci. 56(2): 232–238. https://doi.org/10.1016/j.jcs.2012.05.007

Singh, G. 2010. The soybean: botany, production and uses. CABI. Cambridge, MA, USA.

Singh P., Kumar R., Sabapathy S. and Bawa A. 2008. Functional and edible uses of soy protein products. Comprehen Rev Food Sci Food Saf. 7(1): 14–28. https://doi.org/10.1111/j.1541-4337.2007.00025.x

Singha, P. and Muthukumarappan K. 2017. Effects of processing conditions on the system parameters during single screw extrusion of blend containing apple pomace. J Food Process Eng. 40(4): e12513. https://doi.org/10.1111/jfpe.12513

Smetana S., Mathys A., Knoch A. and Heinz, V. 2015. Meat alternatives: life cycle assessment of most known meat substitutes. Int J Life Cycle Assess. 20(9): 1254–1267. https://doi.org/10.1007/s11367-015-0931-6

Smith G., Marshall W., Carpenter Z., Branson R. and Mnnke, W. 1976. Textured soy proteins for use in blended ground beef patties. J Food Sci. 41(5): 1148–1152. https://doi.org/10.1111/j.1365-2621.1976.tb14405.x

Thadavathi Y.L., Wassén S. and Kádár R. 2019. In-line rheological and microstroctural characterization of high moisture content protein vegetable mixtures in single screw extrusion. J Food Eng. 245: 112–123. https://doi.org/10.1016/j.jfoodeng.2018.10.006

Uguz A., Lack G., Pumphrey R., Ewan P., Warner J., Dick J., et al.. 2005. Allergic reactions in the community: a questionnaire survey of members of the anaphylaxis campaign. Clin Exp Allergy. 35(6): 746–750. https://doi.org/10.1111/j.1365-2222.2005.02257.x

van der Weele C., Feindt P., van der Goot A.J., van Mierlo B. and van Boekel, M. 2019. Meat alternatives: an integrative comparison. Trends Food Sci Technol. 88: 505–512. https://doi.org/10.1016/j.tifs.2019.04.018

Wang F., Meng J., Sun L., Weng Z., Fang Y., Tang X., et al. 2020. Study on the tofu quality evaluation method and the establishment of a model for suitable soybean varieties for Chinese traditional tofu processing. LWT. 117: 108441. https://doi.org/10.1016/j.lwt.2019.108441

Wang T., Qin G.-X., Sun Z.-W. and Zhao Y. 2014. Advances of research on glycinin and β-conglycinin: a review of two major soybean allergenic proteins. Crit Rev Food Sci Nutr. 54(7): 850–862. https://doi.org/10.1080/10408398.2011.613534

Wolz M., Kastenhuber S. and Kulozik U. 2016. High moisture extrusion for microparticulation of whey proteins – influence of process parameters. J Food Eng. 185: 56–61. https://doi.org/10.1016/j.jfoodeng.2016.04.002

Wu M., Huang X., Gao F., Sun Y., Duan H. and Li, D. 2019. Dynamic mechanical properties and fractal analysis of texturized soybean protein/wheat gluten composite produced by high moisture extrusion. Int J Food Sci Technol. 54(2): 499–508. https://doi.org/10.1111/ijfs.13963

Zahari I., Ferawati F., Helstad A., Ahlström C., Östbring K., Rayner M., et al. 2020. Development of high-moisture meat analogues with hemp and soy protein using extrusion cooking. Foods. 9(6): 772. https://doi.org/10.3390/foods9060772

Zhang J., Liu L., Jiang Y., Faisal S. and Wang Q. 2020. A new insight into the high-moisture extrusion process of peanut protein: from the aspect of the orders and amount of energy input. J Food Eng. 264: 109668. https://doi.org/10.1016/j.jfoodeng.2019.07.015

Zhang J., Liu L., Jiang Y., Shah F., Xu Y. and Wang Q. 2020. High-moisture extrusion of peanut protein-/carrageenan/sodium alginate/wheat starch mixtures: effect of different exogenous polysaccharides on the process forming a fibrous structure. Food Hydrocolloids. 99: 105311. https://doi.org/10.1016/j.foodhyd.2019.105311

Zhang J., Liu L., Liu H., Yoon A., Rizvi S.S. and Wang Q. 2019. Changes in conformation and quality of vegetable protein during texturization process by extrusion. Crit Rev Food Sci Nutr. 59(20): 3267–3280. https://doi.org/10.1080/10408398.2018.1487383

Italian Journal of Food Science, 2022; 34 (2): 21–27

Marker-assisted selection of dairy cows for β-casein gene A2 variant

Carla Sebastiani[1†], Chiara Arcangeli[1†], Martina Torricelli[1*], Marcella Ciullo[1], Nicoletta D'avino[1], Giulia Cinti[2], Stefano Fisichella[1], Massimo Biagetti[1]

[1]Istituto Zooprofilattico Sperimentale dell'Umbria e delle Marche-Togo Rosati (IZSUM), Perugia, Italy; [2]R&D Cooperlat, Società Cooperativa Agricola, Jesi, Ancona, Italy

[†]These authors contributed equally.

*****Corresponding Author:** Martina Torricelli, Istituto Zooprofilattico Sperimentale dell'Umbria e delle Marche-Togo Rosati (IZSUM), Via Salvemini 1, 06126 Perugia, Italy. Email: m.torricelli@izsum.it; Giulia Cinti, R&D Cooperlat, Società Cooperativa Agricola, via Piandelmedico 74, 60035 Jesi (Ancona), Italy. Email: g.cinti@trevalli.cooperlat.it

Received: 25 January 2022; Accepted: 25 February 2022; Published: 2 April 2022
© 2022 Codon Publications

OPEN ACCESS CC BY NC SA

PAPER

Abstract

Many studies highlighted potential associations of β-casein A1 with specific human diseases and a minor digestibility of milk, due to the bioactive peptide β-casomorphin 7 (BCM-7) release during digestion. Conversely, the ancestral β-casein A2 variant seems to be a favorable trait because it is not associated with BMC-7 release. The aim of this work was to evaluate frequencies of β-casein variants in offspring of previously genotyped cows inseminated with A2 homozygous semen. The frequency of the A2/A2 animals has almost doubled from 37 to 69%. These are encouraging results with the perspective of reaching the goal of producing A2 milk.

Keywords: β-casein; bovine; marker-assisted selection (MAS); milk; polymorphisms; variants

Introduction

Marker-Assisted Selection (MAS) is a methodology that allows for the selection of important genetic animal traits in the population of interest by exploiting the genetic information at specific markers. Advancement in genomics made easier the identification of markers which could be ultimately utilized in MAS. In particular, the Genome Wide Association Study (GWAS) approach, initially used in human genetics research to associate genetic variations with particular diseases, is of special interest (Raina *et al.*, 2020). The method is based on scanning the genome of many different individuals for genetic markers that can be used to predict the presence of a disease in the population under study. More recently, GWAS has been applied to the field of domestic animal breeding and genetics, and many genetic markers affecting important economical traits have been described (Du *et al.*, 2021; Sharma *et al.*, 2015).

Cattle breeding programs, consisting of marker-assisted selection (MAS), has been applied to the selection of dairy cows for the presence of β-casein A2 variant, known to confer better digestibility to milk (Duarte-Vazquez *et al.*, 2017; Kaminski *et al.*, 2007; Park *et al.*, 2021).

Milk and dairy products are among the main components of the food tradition of many countries and they play a fundamental role in human health due to their valuable nutritional properties. In spite of various sources of milk being available on the market, bovine milk represents the most consumed variety of milk worldwide (Faye and Konuspayeva, 2012). It contains essential nutrients such as proteins with high biological value, lipids, carbohydrates (mainly lactose), minerals (calcium, phosphorus, zinc, and magnesium), and vitamins (i.e., B2, B12, D, and A) (Jenness *et al.*, 1979; Muehlhoff *et al.*, 2013). Regarding milk protein fraction, it is composed by soluble proteins, also known as whey proteins, and by insoluble proteins, that are caseins, which represent about 80% of the total bovine milk proteins. These are subdivided into four groups, αs1, αs2, β, and k, encoded respectively by the *CSN1S1*, *CSN1S2*, *CSN2*, and *CSN3* genes, all located on chromosome 6 (Rijnkels, 2002). In spite of high milk consumption all over the world, some people experience digestive disorders following the intake of milk and dairy products, because of lactose malabsorption or digestive difficulties due to other dairy components such as β-casein, which represents about 36% of milk protein content (Milan *et al.*, 2020). Specifically, some studies have shown a correlation between human health and some β-casein variants (Kay *et al.*, 2021; Thiruvengadam *et al.*, 2021). Indeed, *Bos taurus CSN2* gene harbors many nucleotide substitutions leading to the formation of 12 protein variants (A1, A2, A3, B, C, D, E, F, G, H1, H2, and I), seven of which (A1, A2, A3, B, C, I, and E) have been identified mainly in European cattle breeds (Barroso *et al.*, 1999; Daniloski *et al.*, 2021; Hohmann *et al.*, 2021; Massella *et al.*, 2017) (Table 1).

Among the dairy cattle breeds, A1 and the ancestral A2 variants are the most common while B and I variants are generally less frequent with some variability depending on the breed (Farrel *et al.*, 2004). Other variants, such as A3 and C, are rarely found (Farrel *et al.*, 2004; Massella *et al.*, 2017) and others are related to specific breeds or geographic areas, as it happens for the E and F variants that have been found with a very low frequency, only in the Italian Piedmontese breed and in animals reared in the Emilia-Romagna region (northern Italy), respectively (Massella *et al.*, 2017; Voglino *et al.*, 1972).

In the last two decades, much attention has been paid to the A1 and A2 β-casein content of milk, due to their suggested role in human health. A1 and A2 variants differ from each other at the gene level for a point mutation, which causes an amino acid change. Particularly, at position 67 of the protein chain, a histidine in the A1 variant is replaced by a proline in the A2 variant. Because of this difference in the protein sequence, the β-casein variants A1 and A2 are differently processed during digestion. Actually, digestive enzymes perform a proteolytic cleavage at position 67 of the β-casein chain only when a histidine is present generating a seven amino acids peptide named β-casomorphin 7 (BCM-7), while cleavage is prevented by the presence of a proline at the same position. Other variants are characterized by a proline at position 67 (A3, E, D, I, and H) and could exhibit the same behavior of the A2 variant as well as other variants, with a histidine at the same position (B, C, F, and G), and could behave as the A1 variant resulting in the formation of the β-casomorphin 7 (BCM-7) (Bodnar *et al.*, 2018).

BMC-7 is a bioactive peptide with strong opioid activity and an oxidant effect (EFSA Scientific Report 2009; Kay *et al.*, 2021) and its release has been related to the alteration of the physiology of different organ systems. In particular, several studies demonstrated the correlation with the onset of various human pathological conditions, such as heart disease, sudden infant death syndrome, milk intolerance, and also with the aggravation of symptoms associated with schizophrenia, autism, and type 1 diabetes (Caroli *et al.*, 2009; Cieslinska *et al.*, 2015; Kaminski *et al.*, 2007; Kay *et al.*, 2021; McLachlan, 2001; Pal *et al.*, 2015; Reichelt *et al.*, 2012). In more detail, it

Table 1. Differences in the amino acid sequence of β-casein variants.

β-casein Variant	Amino Acid Position								
	36	37	67	72	88	93	106	122	138
A2*	Glu (E)	Glu (E)	Pro (P)	Gln (Q)	Leu (L)	Met (M)	His (H)	Ser (S)	Pro (P)
A1*			**His (H)**						
A3*							**Gln (Q)**		
B*			**His (H)**					**Arg (R)**	
C*		**Lys (K)**	**His (H)**						
E*	**Lys (K)**								
I*						**Leu (L)**			
D									
F			**His (H)**						**Leu (L)**
G			**His (H)**					**Leu (L)**	
H1					**Ile (I)**				
H2				**Glu (E)**		**Leu (L)**			**Glu (E)**

In bold: amino acid variations with respect to the A2 ancestral variant.
Arg: arginine; Gln: glutamine; Glu: glutamic acid; His: histidine; Ile: isoleucine; Leu: leucine; Lys: lysine; Met: methionine; Pro: proline; Ser: serine;
*Allele variants detected in European cattle breeds.

has been reported in the literature that BMC-7, binding to μ receptor in the gastrointestinal (GI) tract, may alter gut microbiota, can increase inflammatory response, and may induce mucin production, thus triggering lactose intolerance-like symptoms. Moreover, BMC-7 may promote oxidative stress, may deregulate insulin metabolism, and can modulate DNA methylation reactions affecting neurodevelopment (Kay *et al.*, 2021). However, the European Food Safety Authority (EFSA) in 2009 carried out a meta-analysis of data present in the literature, releasing a scientific report that supports the absence of a cause–effect relationship between the consumption of milk containing the A1 variant and the etiology of the aforementioned diseases, so further studies are necessary in this field (EFSA Scientific Report, 2009). Therefore, the discussion on the adverse human health effects of the β-casein variant A1 remains still open also because other studies demonstrated that milk obtained from A2 homozygous cows seems to be more digestible than milk containing β-casein A1 (Deth *et al.*, 2016; He *et al.*, 2017; Ramakrishnan *et al.*, 2020). This effect could be traced back to the increase in the rate of gastrointestinal transit of A2 milk and to the lack of the pro-inflammatory effect instead associated with A1 milk consumption (Brooke-Taylor *et al.*, 2017; Kay *et al.*, 2021). In addition, A2 milk consumption increases the natural production of glutathione (GSH), which is reported to be a key antioxidant, widely recognized for its association with many health benefits. The consumption of A2 milk induces a twofold increase of blood GSH levels compared to the levels derived from conventional milk intake (Deth *et al.*, 2016). Interestingly, human breast milk, which is recommended by the World Health Organization (WHO) as the exclusive food for newborn feeding, is characterized by the presence of a β-casein protein carrying a proline residue in position 67 which is therefore very similar to the bovine A2 variant (Kay *et al.*, 2021).

As a consequence, in many countries, including Australia, the United Kingdom, the United States, New Zealand, the Netherlands, China and more recently also Italy, A2 cow's milk has been made commercially available, and it is widely recommended for people who suffer from milk-intolerance and for newborns who need formulas more soft to their digestive system (Brooke-Taylor *et al.*, 2017).

Considering this scenario, this study focused on the planning and execution of a breeding program based on the MAS selection of the β-casein A2 variant, in farms located in central Italy providing milk for an important drinking milk producing plant. A2 heterozygous and homozygous cows, previously genotyped (Sebastiani *et al.*, 2020), were artificially inseminated with semen from bulls homozygous for the A2 variant, and their offspring have been likewise analyzed in order to identify A2/A2 animals for A2 milk production.

Materials and methods

Sampling

A total of 1452 Italian Holstein Friesian cows, reared in farms located in central Italy and previously genotyped (Sebastiani *et al.*, 2020), were subjected to artificial insemination with semen from A2/A2 selected bulls (Co.S.A.P.A.M. Soc. Coop., Lodi, Italy; ABS Italia Srl, Cremona, Italy; INSEME Spa, Modena, Italy). Among these, 640 were A2 homozygous and 812 were A2 carriers (A1/A2, A2/B, A2/I) animals.

From the pregnant cows, 534 heifers were born. From these animals, whole blood samples were collected in tubes containing ethylenediaminetetra-acetic acid (EDTA) as an anticoagulant and stored at −20 °C until genetic analysis. Samples were taken in a single withdrawal, simultaneously with the mandatory periodic tests required by Italian National Health Programs and during breeders' voluntary health controls.

DNA extraction and sequencing

Genomic DNA was extracted using High Pure PCR Template Preparation Kit (Roche Life Science, Mannheim, Germany) according to the manufacturer's instructions. PCR reactions of both exons 6 and 7 were performed as previously described (Sebastiani *et al.*, 2020). Amplicons were analyzed through 2% agarose gel electrophoresis containing Midori Green Advanced DNA Stain (Nippon Genetics Europe GmbH, Düren, Germany). PCR products were purified with QIAquick® PCR Purification Kit (Qiagen, Hilden, Germany) and sequenced in both directions using BrilliantDye™ Terminator Cycle Sequencing Kit v3.1 (NimaGen BV, Nijmegen, Netherlands) according to the manufacturer's instructions.

Sequencing reactions were analyzed in a 3500 Genetic Analyzer (Applied Biosystems; Thermo Fisher Scientific Inc.). The obtained nucleotide sequences were aligned to the bovine β-casein gene (Accession number X14711.1) using the ClustalW tool of the BioEdit v7.2.5 software (Hall, 1999). Electropherograms were analyzed at each investigated mutation point to identify peaks in heterozygosity. In particular, polymorphisms at positions 36 and 37 of exon 6 and at positions 67, 72, 88, 93, 106, 122, and 138 of exon 7 were analyzed to discriminate the different β-casein variants.

Statistical analysis

Allele and genotype frequencies were directly calculated dividing the number of copies of each allele and genotype by the total alleles and by the total individuals, respectively. Furthermore, the Hardy–Weinberg (HW) equilibrium was verified using Chi-square test ($P < 0.05$) by the R Studio software (R Core Team, 2020).

Results

In this study, 1452 already genotyped dams (Sebastiani *et al.*, 2020), at least carrier of the A2 allele (A2 heterozygous and homozygous animals), were artificially inseminated using commercial semen from A2 homozygous bulls in order to increase A2 variant and A2/A2 genotype frequencies in the female progeny.

From inseminated cows that got pregnant, 534 heifers were born. Among these, 238 derived from A2 homozygous parents were analyzed to confirm the A2/A2 genotype as they have to be used for the production of A2 certified milk. The remaining 296 heifers, born from A2 heterozygous dams, were analyzed in order to define their genotype and separate the A2 homozygous ones in the herds with the same purpose.

Here, we report the results of the analysis carried out on this offspring in terms of allele and genotype frequencies of the different CSN2 gene variants. No deviation of HW equilibrium was observed at the considered polymorphic sites.

In the female offspring population obtained by the artificial insemination of A2 heterozygous and homozygous cows, sequencing analysis of the CSN2 gene PCR products highlighted the presence of four β-casein variants (A1, A2, B, and I) and four genotypes, (A2/A2, A1/A2, A2/B, A2/I) as shown in Table 2. After the application of the MAS on the herds participating in the project, the frequencies of A2 and I alleles, both characterized by a proline in position 67, increased from 60.65 to 84.46% and from 3.10 to 3.28%, respectively, in the progeny compared to dams. At the same time, the frequencies of the unfavorable A1 and B alleles decreased from 30.39 to 10.86% and from 5.68 to 1.40%, respectively. A3 and C alleles and their related genotypes, that were present with low frequencies in the population of dams, were not further found in the offspring. Regarding genotypes, the most interesting result concerned the about twofold increase of A2/A2 frequency from 36.96 to 68.91%. A similarly intriguing result, derived from the MAS application, was the consistent reduction of the frequency of A1/A2 animals, from 35.79 to 21.72%. The frequencies of the other A2 heterozygous genotypes found in the progeny, that is A2/I and A2/B, varied from 7.55 to 2.81% and from 3.83 to 6.55% (Table 2, Figure 1). Interestingly, since the I variant should behave in the same manner as A2

Table 2. Allele and genotype frequencies (%) in the examined animals, before (dams) and after (heifers) MAS selection.

Allele	Allele frequency (%)		Genotype	Genotype frequency (%)	
	Dams	Heifers		Dams	Heifers
A2	60.65	84.46	A2/A2	36.96	68.91
A1	30.39	10.86	A1/A2	35.79	21.72
B	5.68	1.40	A1/A1	9.88	/
I	3.10	3.28	A2/B	7.55	2.81
A3	0.15	/	A2/I	3.83	6.55
C	0.03	/	A1/B	3.07	/
			A1/I	2.03	/
			B/I	0.25	/
			B/B	0.18	/
			A2/A3	0.12	/
			A3/B	0.12	/
			A1/A3	0.06	/
			A1/C	0.06	/

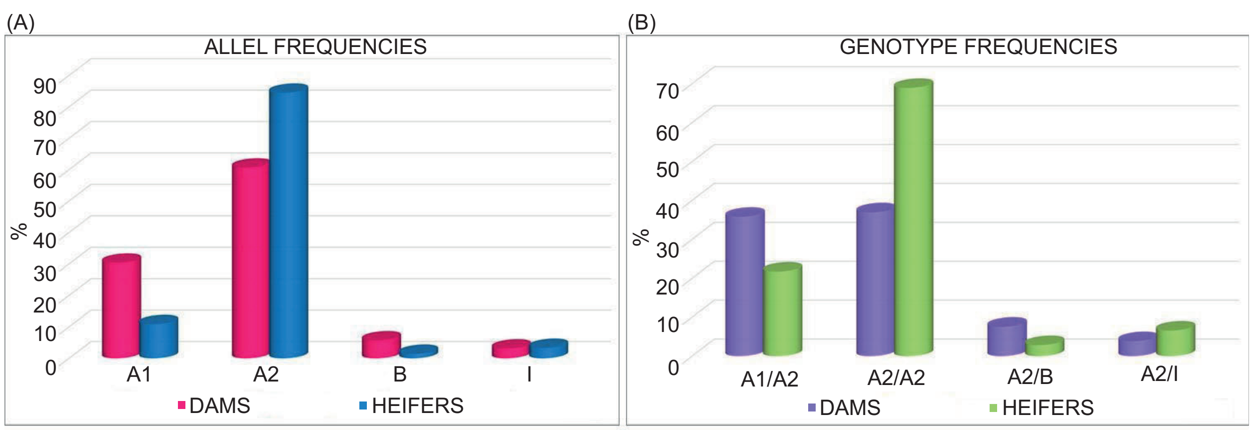

Figure 1. Graphics of the allele (A) and genotype (B) frequencies variation (%) in the examined dams and heifers after MAS selection.

variant in term of BMC-7 formation, A2/I animals could at least be used for the production of a more digestible milk, even though they could not contribute to the marketing of a certified A2 milk.

In conclusion, the first generation from the genotyped dams produced an extra number of 368 A2/A2 cows in addition to the A2 homozygous cows in reproductive age still present in the herds. So, both groups of animals may be used for reproduction and for the related A2 drinking milk production.

Discussion

The data presented here were derived from a larger research project whose purpose was primarily to evaluate the frequencies of the β-casein *CSN2* gene alleles in Italian Holstein Friesian dairy cattle reared in farms supplying milk to an important milk plant in central Italy.

In this study, we wanted to evaluate the increase of the A2 allele and A2/A2 genotype frequencies, in the female progeny of dams, previously genotyped and fertilized with A2/A2 semen in a selection program based on MAS. The final goal was the production of A2 cow's milk, due to its supposed association with health benefits for humans.

In fact, the presence in milk of the A2 isoform of β-casein is increasingly considered a desirable characteristic, because it confers greater digestibility to milk. This could allow milk intake even by people who suffer from lactose intolerance-like symptoms despite not being really lactose intolerant (Park *et al*., 2021).

The Italian Holstein Friesian breed is not among those breeds characterized by the highest frequency of the A2/A2 genotype, but it has a sufficiently high frequency to allow an effective genetic selection of this trait (Canavesi, 2016).

Production of A2 milk can be accomplished following a MAS scheme, which is based on selecting animal carriers of specific polymorphisms that characterize the A2 variant.

During the course of a MAS-based selection plan, aimed at obtaining a consistent number of A2 homozygous cows in the herd, milk coming from A2/A2 animals can be collected separately and directed to A2 milk commercialization. This approach requires organizing, logistical, and management efforts of cow sheds and milking barns, which however is rewarded by an economic gain in the sale of a type of milk with beneficial properties for human health.

In the last years, the commercialization of A2 milk has conquered large market portions in many non-European countries, while in Europe and in Italy it still remains a niche product (Brooke-Taylor *et al*., 2017). Actually, few medium/large Italian dairy industries have taken this route commercializing certified A2 milk, whose distribution is slowly spreading, starting to generate the interest of consumers.

The data reported here are very encouraging because they confirm the expected genetic improvement in the farms analyzed in this survey. The use in the future of certified A2/A2 sexed semen could help to accelerate the increase in the number of female animals to be used for A2 milk production.

Conclusions

In recent decades, advances in assisted reproductive technologies, animal molecular genetics, and statistical analysis applied to animal genetic improvement helped to maximize the genetic gain in livestock breeding worldwide.

In the past, cows produced milk whose β-casein protein was represented only by A2 isoform, considered to be ancestral, but over time changes in the genetic heritage led to the occurrence of other variants (Farrel *et al*., 2004). Cows have thus acquired the ability to produce milk with different β-casein isoforms, in particular A1 and A2.

Nowadays, β-casein A2 milk can be considered "a return to the origins" because it comes from selected cows that produce only the ancestral β-casein A2 protein. It has to be noted that in addition to the indexes evaluated for the selection of the best breeding bulls regarding traits related to morphology, health, and productivity, information about milk quality, such as β-casein genotype, has also been included.

In conclusion, the valorization of this genetic trait and production of A2 milk could be advantageous for the whole drinking milk chain, from producers to consumers.

Author Contributions

S.F., G.C., and M.B. conceptualized the study; C.S. and M.B. formulated the study; C.A. and C.S. did the formal analysis; C.A., M.T., M.C., and C.S. were in charge of investigation; G.C., S.F., and N.D. arranged the resources; C.A. and C.S. prepared the original draft; M.B., C.S., M.T., C.A, and G.C. reviewed and edited the manuscript; M.B. and C.S. supervised the study; M.B., G.C., and S.F.

were in charge of project administration; and S.F. and G.C acquired funding.

Disclosure Statement

All authors report no conflicts of interest. The funders had no role in the design of the study; in the collection, analyses, or interpretation of data; in the writing of the manuscript; or in the decision to publish the results.

Funding

This research was funded by Progetto Stalla 20.20—ID Progetto n. 21999—Misura 16.2-PSR Marche 2014-2020–Filiera Agro-Alimentare n. 497—Coordinator: Cooperlat Soc. Coop. Agr.

References

Barroso, A., Dunner, S. and Cañón, J., 1999. Technical note: use of PCR-single-strand conformation polymorphism analysis for detection of bovine β- casein variants A1, A2, A3, B. J. Anim. Sci. 77(10): 2629–2632. https://doi.org/10.2527/1999.77102629x

Bodnár, Á., Hajzser, A., Egerszegi, I., Póti, P., Kuchtík, J. and Pajor, F., 2018. A2 milk and its importance in dairy production and global market. Anim. Welf. 14(1): 1–7. https://doi.org/10.17205/SZIE.AWETH.2018.1.001

Brooke-Taylor, S., Dwyer, K., Woodford, K. and Kost, N., 2017. Systematic review of the gastrointestinal effects of A1 compared with A2 β-Casein. Adv. Nutr. 15(5): 739–748. https://doi.org/10.3945/an.116.013953

Canavesi, F., 2016. Selezionare per produrre latte A2. Professione allevatore. 16: 52–54.

Caroli, A.M., Chessa, S. and Erhardt, G.J., 2009. Invited review: milk protein polymorphism in cattle: effect on animal breeding and human nutrition. J. Dairy Sci. 92(11): 5335–5352. https://doi:10.3168/jds.2009-2461

Cieslinska, A., Sienkiewicz-Szłapka, E., Wasilewska, J., Fiedorowicz, E., Chwała, B., Moszy'nska-Dumara, M. and Kostyra, E., 2015. Influence of candidate polymorphisms on the dipeptidyl peptidase IV and μ -opioid receptor genes expression in aspect of the β-casomorphin-7 modulation functions in autism. Peptides 65: 6–11. https://doi.org/10.1016/j.peptides.2014.11.012

Daniloski, D., Cunha, N.M.D., McCarthy, N.A., O'Callaghan, T.F., McParland, S. and Vasiljevic, T., 2021. Health-related outcomes of genetic polymorphism of bovine β-casein variants: a systematic review of randomized controlled trials. Trends Food Sci. Technol. 111: 233–248. https://doi.org/10.1016/j.tifs.2021.02.073

Deth, R., Andrew Clarke, A., Jiayi, N.J. and Trivedi, M., 2016. Clinical evaluation of glutathione concentrations after consumption of milk containing different subtypes of β-casein: results from a randomized, cross-over clinical trial. Nutr. J. 15(1): 82–87. https://doi:10.1186/s12937-016-0201-x

Du, L., Duan, X., An, B., Chang, T., Liang, M., Xu, L., Zhang, L., Li, J., Guangxin, E. and Gao, H., 2021. Genome-wide association study based on random regression model reveals candidate genes associated with longitudinal data in Chinese Simmental Beef Cattle. Animals. 11(9): 2524. https://doi.org/10.3390/ani11092524

Duarte-Vázquez, M.Á., García-Ugalde, C., Villegas-Gutiérrez, L.M., García-Almendárez, B.E. and Rosado, J.L., 2017. Production of cow's milk free from beta-casein A1 and its application in the manufacturing of specialized foods for early infant nutrition. Foods. 6(7): 50. https://doi:10.3390/foods6070050

Farrel, H.M., Jimenez-Flores, R., Bleck, G.T., Brown, E.M., Butler, J.E., Creamer, L.K. and Swaisgood, H.E., 2004. Nomenclature of the proteins of cows' milk—sixth revision. J. Dairy Sci. 87(6): 1641–1674. https://doi.org/10.3168/jds.S0022-0302(04)73319-6

Faye, B. and Konuspayeva, G., 2012. The sustainability challenge to the dairy sector – the growing importance of non-cattle milk production worldwide. Int Dairy J. 24(2): 50–56. https://doi.org/10.1016/j.idairyj.2011.12.011

Hall, T.A., 1999. BioEdit: a user-friendly biological sequence alignment editor and analysis program for Windows 95/98/NT. Nucleic Acids Symp. Ser. 41: 95–98.

He, M., Sun, J., Jiang, Z.Q. and Yang, Y.X., 2017. Effects of cow's milk beta-casein variants on symptoms of milk intolerance in Chinese adults: a multicenter, randomized controlled study. Nutr. J. 16(1): 72. https://doi.org/10.1186/s12937-017-0275-0

Hohmann, L.G., Weimann, C., Scheper, C., Erhardt, G. and König, S., 2021. Genetic diversity and population structure in divergent German cattle selection lines on the basis of milk protein polymorphisms. Arch. Anim. Breed. 64(1): 91–102. https://doi.org/10.5194/aab-64-91-2021

Jenness, R., 1979. Comparative aspects of milk protein. J. Dairy Res. 46(2): 197–210. https://doi.org/10.1017/s0022029900017040

Kamiński, S., Cieślińska, A. and Kostyra, E., 2007. Polymorphism of bovine β-casein and its potential effect on human health. J. Appl. Genet. 48(3): 189–198. https://doi.org/10.1007/BF03195213

Kay, S.-I.S, Delgado, S., Mittal, J., Eshraghi, R.S., Mittal, R. and Eshraghi, A.A., 2021. Beneficial effects of milk having A2 β-casein protein: myth or reality? J. Nutr. 151(5): 1062–1072. https://doi.org/10.1093/jn/nxaa454

Massella, E., Piva, S., Giacometti, F., Liuzzo, G., Zambrini, A.V. and Serraino, A., 2017. Evaluations of bovine β-casein polymorphism in two dairy farms located in northern Italy. Ital. J. Food Safety. 6(3): 6904. https://doi.org/10.4081/ijfs.2017.6904

McLachlan, C.N., 2001. β-casein A1, ischaemic heart disease mortality and other illnesses. Med. Hypotheses 56(2): 262–272. https://doi.org/10.1054/mehy.2000.1265

Milan, A.M., Shrestha, A., Karlström, H.J., Martinsson, J.A., Nilsson, N.J., Perry, J.K., Day, L. and Barnett, M.P.G. and Cameron-Smith, D., 2020. Comparison of the impact of bovine milk β-casein variants on digestive comfort in females self-reporting dairy intolerance: a randomized controlled trial. Am. J. Clin. Nutr. 111(1): 149–160. https://doi.org/10.1093/ajcn/nqz279

Muehlhoff, E., Bennett, A. and McMahon, D., 2013. Milk and dairy product in human nutrition. FAO, Rome.

Pal, S., Woodford, K., Kukuljan, S. and Ho, S., 2015. Milk intolerance, β- casein and lactose. Nutrients 7(9): 285–297. https://doi.org/10.3390/nu7095339

Park, Y.W. and Haenlein, G.F.W., 2021. A2 bovine milk and caprine milk as a means of remedy for milk protein allergy. Dairy. 2(2): 191–201. https://doi.org/10.3390/dairy2020017

R Core Team, 2020. R: a language and environment for statistical computing. R Foundation for Statistical Computing, R Core Team, Vienna, Austria.

Raina, V.S., Kour, A., Chakravarty, A.K. and Vohra, V., 2020. Markerassisted selection visàvis bull fertility: coming full circle—a review. Mol. Biol. Rep. 47(11): 9123–9133. https://doi.org/10.1007/s11033-020-05919-0

Ramakrishnan, M., Eaton, T.K., Sermet, O.M. and Savaiano, D.A., 2020. Milk containing A2-casein only, as a single meal, causes fewer symptoms of lactose intolerance than milk containing A1 and A2-caseins in subjects with lactose maldigestion and intolerance: a randomized, double-blind, crossover trial. Nutrients. 12(12): 3855. https://doi.org/10.3390/nu12123855

Reichelt, K.L., Tveiten, D., Knivsberg, A.M. and Brønstad, G., 2012. Peptides' role in autism with emphasis on exorphins. Microb. Ecol. Health Dis. 23: 18958. https://doi.org/10.3402/mehd.v23i0.18958

Rijnkels, M., 2002. Multispecies comparison of the casein gene loci and evolution of casein gene family. J Mammary Gland Biol. Neoplasia. 7(3): 327–345. https://doi.org/10.1023/A:1022808918013

Scientific Report of EFSA prepared by a DATEX Working Group on the potential health impact of β-casomorphins and related peptides. 2009. EFSA Scientific Report. 231: 1–107. https://doi.org/10.2903/j.efsa.2009.231r

Sebastiani, C., Arcangeli, C., Ciullo, M., Torricelli, M., Cinti, G., Fisichella, S. and Biagetti, M., 2020. Frequencies evaluation of β-casein gene polymorphisms in dairy cows reared in central Italy. Animals. 10(2): 252. https://doi.org/10.3390/ani10020252

Sharma, A., Lee, J.S., Dang, C.G., Sudrajad, P., Kim, H.C., Yeon, S.H., Kang, H.S. and Lee, S.H., 2015. Stories and challenges of genome wide association studies in livestock—a review. Asian Australas. J. Anim. Sci. 28(10): 1371–1379. https://doi.org/10.5713/ajas.14.0715

Thiruvengadam, M., Venkidasamy, B., Thirupathi, P., Chung, I.M. and Subramanian, U., 2021. β-Casomorphin: a complete health perspective. Food Chem. 337: 127765. https://doi.org/10.1016/j.foodchem.2020.127765

Voglino, G.F., 1972. A new β- casein variant in piedmont cattle. Anim. Genet. 3(1): 61–62. https://doi.org/10.1111/j.1365-2052.1972.tb01233.x

Italian Journal of Food Science, 2022; 34 (2): 28–33

Study on the role of nutrients in food to improve the motion state of athletes

Hongkai Zhou[1,2]

[1]Pingdingshan University, Pingdingshan, Henan, China; [2]Sports College, Graduate University of Mongolia, Ulaanbaatar, Mongolia

Corresponding Author: Hongkai Zhou, Pingdingshan University, South Section of Future Road, Xincheng District, Pingdingshan City, Henan Province, China. Email: k6k262@163.com

Received: 22 September 2021; Accepted: 28 March 2022; Published: 20 April 2022
© 2022 Codon Publications

OPEN ACCESS

PAPER

Abstract

This study aims to analyze the role of nutrients in food in improving athletic performance and to understand the feasibility of food supplementation in sports training. Twenty athletes were randomly divided into two groups, A and B. The athletes in the two groups had the same diet and the same training content and differed only in the supplemented food. Group A was supplemented with *Siraitia grosvenorii* water, and Group B was supplemented with pure water. After 3 months of training, the body composition, exercise status, and blood indexes of the athletes in the two groups were compared. Compared with the athletes in group A before the experiment as well as in group B after the experiment, the athletes in group A showed a significant increase in fat-free weight, improved athletic performance, increased levels of hemoglobin (Hb) and red blood cell (RBC), and decreased levels of blood lactic acid (BLA) and blood urea nitrogen (BUN) ($P < 0.05$). Nutrients in food can effectively improve the body composition and exercise status of athletes and inhibit the decrease of Hb and RBC as well as the increase of BLA and BUN, which have good usability in sports training.

Keywords: athletes; food; motion state; nutrient

Introduction

In the process of improving sports performance, athletes need to carry out a lot of training and fierce competition; in such a case, the body state of athletes declines (Chuckravanen *et al*., 2019), free radicals accumulate, fatigue appears, and immune function declines, which may cause sports injury and directly affect the training effect and the results of competition. Therefore, the question of how to reduce the impact of a rigorous training on athletes and improve motion state has been widely concerned by researchers. In nature, many foods are rich in nutrients, which can be used as nutritional supplements for athletes. Guo (2015) studied jujube polysaccharides and carried out the weight-bearing swimming experiment on rats. They found that rats had significantly longer swimming time, larger body weight, and higher glycogen content after taking jujube polysaccharides. Liu *et al*. (2015) studied the polysaccharide components of *Hericium erinaceus*, analyzed its anti-fatigue activity, compared various indexes of mice under different doses of *Hericium erinaceus* polysaccharide, and found that it could reduce the content of blood lactic acid (BLA) and malondialdehyde (MDA). Zhang *et al*. (2015) simulated the plateau environment and analyzed the anti-fatigue effect of *Astragalus membranaceus* on mice. It was found that the swimming time of mice was prolonged, the lactic acid decreased, and the glycogen increased under the influence of *Astragalus membranaceus*, which indicated that *Astragalus membranaceus* could reduce the fatigue of mice in a plateau environment. Ren *et al*. (2017) studied the effect of soy whey protein supplementation on sports performance after long-term training. It was found that the average fatigue time of rats was longer, the activity of lactate dehydrogenase was higher, and the level of MDA was lower after supplementation of soybean whey protein. In this study, the nutrients in *Siraitia grosvenorii* were studied, and a comparative experiment was carried out. The indicators of the athletes, such as body composition and motion status, were analyzed to understand the application prospect of *Siraitia grosvenorii* in sports training.

Nutrients in *Siraitia grosvenorii* and Their Functions

Siraitia grosvenorii is a kind of medicinal and edible material unique to China (Tu *et al.*, 2015). It is mainly produced in provinces such as Guangxi and Guangdong in southern China. The fruits of *Siraitia grosvenorii* are spherical or oblong (Figure 1, left). The mature fruits have dark green pericarp, yellowing petioles, and high water content. After being processed and dried (Figure 1, middle), the surface is brown or yellowish-green with dark patches; it is light, brittle, and easy to crack, and the seeds are oblate (Figure 1, right), light red to reddish-brown, with a sweet taste.

Siraitia grosvenorii contains many cucurbitane triterpenoids (Niu *et al.*, 2017; Qiao *et al.*, 2019), which are sweet or slightly sweet substances (Shi *et al.*, 2019). The sweet or slightly sweet substances have high sweetness and low heat, which can substitute for sucrose (Abdel-Hamid *et al.*, 2020). It also contains flavonoids, but the content is not high. Moreover, there is a lot of protein and amino acids in *Siraitia grosvenorii*, including eight kinds of essential amino acids for the human body. The sugar content in *Siraitia grosvenorii* is very high, and the content of fructose is 14%. It contains 24 kinds of inorganic elements. The content of oil or fat is also very high, and the main component is squalene. It also contains rich vitamin C and vitamin E, suggesting high nutritional values.

The most important medicinal value of *Siraitia grosvenorii* is clearing away heat and moistening the lung (Gong *et al.*, 2019). According to traditional Chinese medicine, *Siraitia grosvenorii* is sweet and cool; therefore, it has a good therapeutic effect on lung heat and dry cough. The medicinal value of *Siraitia grosvenorii* also includes:

(1) Resistance to diabetes (Xu *et al.*, 2020). *Siraitia grosvenorii* has high sweetness and low calorie. It can be used as an ideal sugar substitute for diabetes mellitus patients. Also, some components in *Siraitia grosvenorii* can reduce blood glucose and blood lipid and improve renal function.

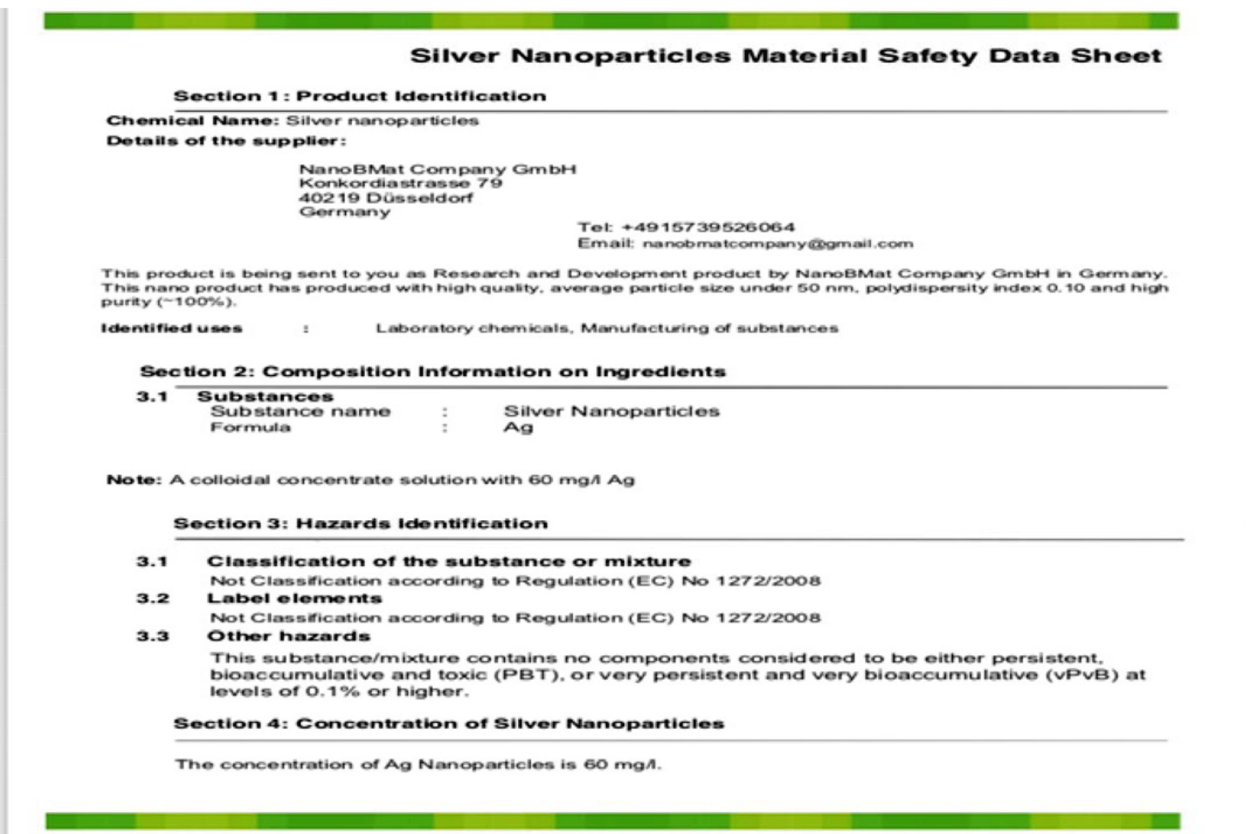

Silver Nanoparticles Material Safety Data Sheet

Section 1 : Product Identification

Chemical Name: Silver nanoparticles
Details of the supplier:

NanoBMat Company GmbH
Konkordiastrasse 79
40219 Düsseldorf
Germany

Tel: +4915739526064
Email: nanobmatcompany@gmail.com

This product is being sent to you as Research and Development product by NanoBMat Company GmbH in Germany. This nano product has produced with high quality, average particle size under 50 nm, polydispersity index 0.10 and high purity (~100%).

Identified uses : Laboratory chemicals, Manufacturing of substances

Section 2: Composition Information on Ingredients

3.1 Substances
Substance name : Silver Nanoparticles
Formula : Ag

Note: A colloidal concentrate solution with 60 mg/l Ag

Section 3: Hazards Identification

3.1 Classification of the substance or mixture
Not Classification according to Regulation (EC) No 1272/2008
3.2 Label elements
Not Classification according to Regulation (EC) No 1272/2008
3.3 Other hazards
This substance/mixture contains no components considered to be either persistent, bioaccumulative and toxic (PBT), or very persistent and very bioaccumulative (vPvB) at levels of 0.1% or higher.

Section 4: Concentration of Silver Nanoparticles

The concentration of Ag Nanoparticles is 60 mg/l.

Figure 1. ***Siraitia grosvenorii.***

(2) Protect the cardiovascular system. *Siraitia grosvenorii* is rich in unsaturated fatty acids, which can resist fatty liver; inorganic salts, such as selenium and magnesium, can protect myocardial cells and are also effective in expanding blood vessels and preventing thrombosis.
(3) Improve immunity. *Siraitia grosvenorii* has antibacterial and anti-inflammatory effects (Li *et al*., 2018), which can enhance the cellular and humoral immune functions of the body and coordinate the immune system.

Table 2. Measurement indexes of motion state.

Number	Content
X1	Standing long jump
X2	One minute push-ups
X3	One minute sit-ups
X4	50-m running
X5	Sit and reach

Measurement index

Experimental Methods

Research subjects

Twenty athletes were randomly selected from the Ministry of Public Sports of Zhejiang Shuren University. They were informed of the intention and process of the experiment. All the participants were randomly divided into group A and group B. Group A drank water soaked with *Siraitia grosvenorii*, while group B drank pure water. The athletes in both groups were in good health and had no physical injury within half a year. They took no strenuous exercise and did not take any caffeine or tea 24 h before the experiment. They were in a good mental state. There was no significant difference in general data, as shown in Table 1.

Research methods

The two groups of athletes were trained for 3 months, including sprinting, long-distance running, standing long jump, etc. They were trained twice a day, 2 h each session. The athletes took three meals in the school canteen every day, without any additional nutrition. The athletes in group A drank the water soaked with *Siraitia grosvenorii* at 8:00, 12:00, 16:00, and 20:00 every day, while the athletes of group B drank pure water. The dosage of *Siraitia grosvenorii* soaking water was 1/4 *Siraitia grosvenorii* and 1 L water, for four times, 250 ml each time. Before and after the experiment, blood samples and motion state tests were carried out on the athletes. The indexes are shown in Table 2.

Measurement index

Body composition: body weight and fat-free weight.

Movement state: as shown in Table 2.

Table 1. Comparison of general information.

	Group A (n = 10)	Group B (n = 10)
Age/years	22.78 ± 2.31	23.08 ± 1.56
Height/cm	178.64 ± 2.78	177.59 ± 3.08
Weight/kg	76.21 ± 5.29	75.94 ± 6.12

Blood indicators: including hemoglobin (Hb), red blood cell (RBC) count, BLA, and blood urea nitrogen (BUN).

Blood samples were sent to Hangzhou Second People's Hospital for testing.

Statistical analysis

The data were statistically processed by SPSS17.0 and expressed as $\bar{x} \pm SD$. The comparison between groups was conducted using the t-test. If the value of P was smaller than 0.05, then it suggested that there was a statistical difference.

Experimental Results

Comparison of body composition

Before and after the experiment, the changes in body composition of athletes in the two groups are shown in Table 3.

As shown in Table 3, before the experiment, there was no significant difference in body weight and fat-free weight between group A and group B ($P > 0.05$); after the experiment, the fat-free weight and body weight of athletes in the two groups increased slightly, and the fat-free weight of group A was 59.33 ± 3.25 kg, significantly higher than that before the experiment ($P < 0.05$) and group B, indicating that drinking *Siraitia grosvenorii* water was effective in improving athletes' fat-free weight.

Comparison of motion state

Before and after the experiment, the comparison of the motion state between the two groups of athletes is shown in Table 4.

As shown in Table 4, before the experiment, there was no significant difference in different motion states between the two groups; after the experiment, the standing long jump of group A was 2.62 ± 0.71 m, which showed a significant improvement compared with that before the experiment and group B; the number of push-ups in group A was 38.71 ± 3.59, and $P < 0.05$ compared to

Table 3. Changes in body composition.

	Group A		Group B	
	Before the experiment	After the experiment	Before the experiment	After the experiment
Weight/kg	76.21 ± 5.29	77.33 ± 4.62	75.94 ± 6.12	76.89 ± 5.78
Fat-free weight/kg	53.64 ± 0.86	59.33 ± 3.25*#	54.68 ± 1.12	56.48 ± 2.86

*Compared with that before the experiment, P < 0.05.
#Compared with group B, P < 0.05.

Table 4. Comparison of motion state.

	Group A		Group B	
	Before the experiment	After the experiment	Before the experiment	After the experiment
X1/m	2.43 ± 0.83	2.62 ± 0.71*#	2.51 ± 0.76	2.53 ± 0.48
X2/n	33.68 ± 4.86	38.71 ± 3.59*#	34.12 ± 4.77	35.62 ± 4.63
X3/n	37.12 ± 3.08	41.29 ± 5.57*#	37.25 ± 3.12	39.68 ± 4.51
X4/s	6.32 ± 0.33	5.88 ± 0.41*#	6.41 ± 0.27	6.03 ± 0.39*
X5/cm	15.33 ± 0.71	16.21 ± 0.33	16.12 ± 0.78	16.23 ± 0.56

*Compared with that before the experiment, P < 0.05.
#Compared with group B, P < 0.05.

Table 5. Comparison of Hb and RBC.

	Group A		Group B	
	Before the experiment	After the experiment	Before the experiment	After the experiment
Hb (g/L)	136.77 ± 1.87	141.34 ± 0.64*#	137.64 ± 0.92	131.66 ± 1.91*
RBC (1012/L)	4.63 ± 0.12	5.09 ± 0.26*#	4.57 ± 0.19	4.77 ± 0.21

*Compared with that before the experiment, P < 0.05.
#Compared with group B, P < 0.05.

before the experiment and group B; the number of sit-ups in group A was 41.29 ± 5.57, which was significantly different from that before the experiment and group B; the performance of the 50 m running of group A was 5.88 ± 0.41 s (P < 0.05 compared to before the experiment and group B), and the performance of group B also significantly improved after the experiment; finally, there was no significant difference in sit and reach before and after the experiment and between the two groups (P > 0.05). It was found that drinking *Siraitia grosvenorii* water was effective in improving athletes' performance and motion state.

Comparison of blood indexes

Before and after the experiment, the comparison of Hb and RBC count between the two groups is shown in Table 5.

It was seen from Table 5 that there was no significant difference in the comparison of Hb and RBC between the two groups before the experiment; after the experiment, the Hb of group A increased, while that of group B decreased, suggesting significant differences compared with that before the experiment, and the Hb value of group A was significantly higher than that of group B (P < 0.05); after the experiment, the RBC value of group A significantly increased, and P < 0.05 compared to that before experiment and group B. It was found that drinking *Siraitia grosvenorii* water could increase the RBC count and inhibit the decrease of Hb value.

The comparison of BLA and BUN between the two groups is shown in Figure 2.

As shown in Figure 2, before the experiment, the BLA values of the two groups were 3.27 ± 0.21 mmol/L and 3.26 ± 0.33 mmol/L, respectively, suggesting no significant difference; after the experiment, the BLA of group A increased to 8.16 ± 0.78 mmol/L, while that of group B increased to 11.27 ± 0.56 mmol/L, which were significantly different from those before the experiment, and the BLA value of group A was significantly smaller

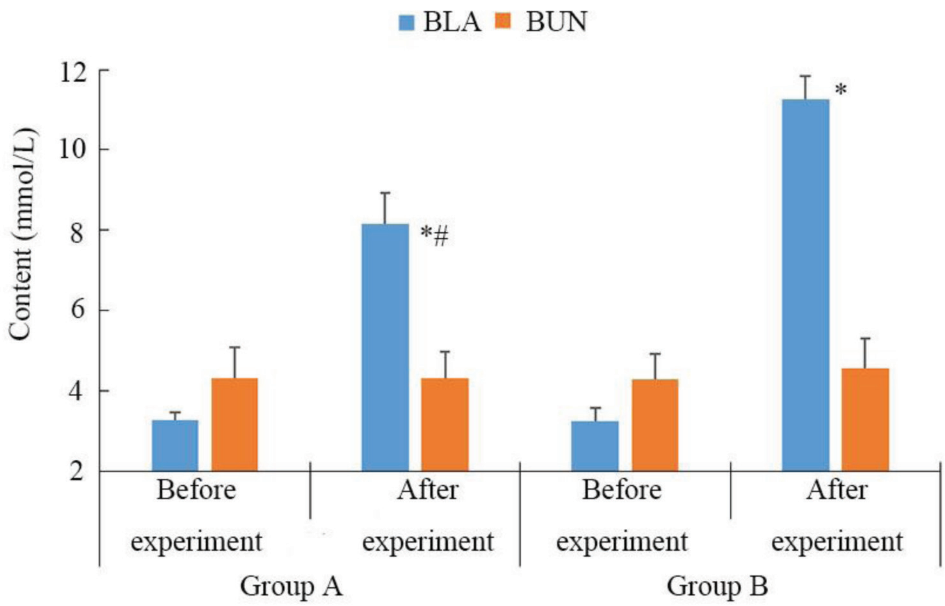

Figure 2. Comparison of BLA and BUN.
*P < 0.05 compared to before experiment. #P < 0.05 compared to group B.

than that of group B (P < 0.05); before the experiment, the BUN value of two groups were 4.31 ± 0.78 mmol/L and 4.29 ± 0.64 mmol/L, respectively; after the experiment, the BLA values of the two groups were 4.33 ± 0.64 mmol/L and 4.56 ± 0.74 mmol/L, respectively, which showed a slight increase, but the difference was not obvious. It was found that drinking *Siraitia grosvenorii* water could inhibit the growth of BLA.

Discussion

In exercise, the nutrients in the body are consumed rapidly, and the demand for protein and sugar increases. To improve the sport's ability of the human body, the supplement of nutrients is very important. By supplementing some foods with rich nutrients, the metabolic needs of athletes can be ensured to have good health state. Many foods contain a lot of nutrients, which can be widely used to improve the state of human movement. In this study, the nutrients in *Siraitia grosvenorii* were studied.

Based on the data shown in Tables 3 and 4, it was found that after the experiment, the fat-free weight of athletes who drank *Siraitia grosvenorii* water increased, and their standing long jump and push-up performance also improved. It shows that the motion state of athletes in group A significantly improved, and their sports performance was better after the experiment.

Hb is the carrier of O_2 and CO_2. In the process of long exercise sessions, a lot of free radicals appear in the human body and destroy RBC. Therefore, after a lot of exercise, the content of Hb in the human body decreases. As shown in Table 5, the Hb of athletes in group B decreased from 137.64 ± 0.92 g/L to 131.66 ± 1.91 g/L, while group A drank *Siraitia grosvenorii* water and had increased Hb value rather than decreased Hb value. The results showed that the nutrients in *Siraitia grosvenorii* could protect RBC, maintain the function of RBC, inhibit the decline of Hb, and improve the human body's movement state.

When the body exercises, lactic acid generated by the skeletal muscles enters the blood and is later eliminated by the process of metabolism. In the case of a large amount of exercise, the BLA in the human body increases rapidly, resulting in the accumulation of lactic acid (Romadhona *et al.*, 2019), and the metabolic level decreases, which leads to the decline of exercise ability. The results showed that the BLA value of group A and group B increased significantly after the experiment, but the BLA value of group A was smaller than that of group B (P < 0.05), which showed that nutrients in *Siraitia grosvenorii*, such as flavonoids, protected the cardiovascular system, and enhanced the metabolic capacity of the body, thus reducing the accumulation of lactic acid, maintaining the balance of the internal environment, relieving fatigue, and improving the exercise state of the human body.

BUN can reflect the body's protein metabolism. With the progress of exercise, the protein metabolism in the body increases, and the urea content becomes higher, which is not conducive to maintaining physical fitness. The results showed that the BUN values of the two groups increased slightly after the experiment, and the value of group A was slightly smaller than that of group B, but the difference was not obvious. It indicated that *Siraitia grosvenorii* water could stabilize the protein level, and inhibit the increase of BUN, thus improving the movement state of the human body.

Conclusion

This paper mainly studied nutrients in food with *Siraitia grosvenorii* as an example and its role in improving the athletic performance of athletes. Through the experiment and the analysis of the results, it was found that drinking *Siraitia grosvenorii* water could improve the athletes' fat-free weight, enhance the exercise state, inhibit the decrease of Hb, maintain the stability of RBC, reduce the production of BLA, restrain the increase of BUN, which had a positive role in improving the motion state of athletes. *Siraitia grosvenorii* water can be promoted and applied in practice.

References

Abdel-Hamid, M., Romeih, E., Huang, Z., Enomoto, T., Huang, L. and Li, L., 2020. Bioactive properties of probiotic set-yogurt supplemented with Siraitia grosvenorii fruit extract. Food Chemistry, 303: 125400.1–125400.7. https://doi.org/10.1016/j.foodchem.2019.125400

Chuckravanen, D., Bulut, S., Kürklü, G.B. and Yapali, G., 2019. Review of exercise-induced physiological control models to explain the development of fatigue to improve sports performance and future trend. Science & Sports, 34(3): 131–140. https://doi.org/10.1016/j.scispo.2018.10.017

Gong, X., Chen, N., Ren, K. and Jia, J., 2019. The fruits of Siraitia grosvenorii: a review of a Chinese food-medicine. Frontiers in Pharmacology, 10: 1400. https://doi.org/10.3389/fphar.2019.01400

Guo, X., 2015. Effect of Jujube date polysaccharide in resisting sports fatigue. Advance Journal of Food Science & Technology, 9(12): 939–943. https://doi.org/10.19026/ajfst.9.1778

Li, X., Xu, L.Y., Cui, Y.Q. and Pang, M.X., 2018. Anti-bacteria effect of active ingredients of Siraitia grosvenorii on the spoilage bacteria isolated from sauced pork head meat. Iop Conference, 292: 012012. https://doi.org/10.1088/1757-899X/292/1/012012

Liu, J., Du, C., Wang, Y. and Yu, Z., 2015. Anti-fatigue activities of polysaccharides extracted from Hericium erinaceus. Experimental & Therapeutic Medicine, 9(2): 483–487. https://doi.org/10.3892/etm.2014.2139

Niu, B., Ke, C.Q., Li, B.H., Li, Y.Y., Yi, Y.J., Luo, Y.W., Shuai, L., Yao, S., Lin, L.G., Li, J. and Ye, Y., 2017. Cucurbitane glucosides from the crude extract of Siraitia grosvenorii with moderate effects on PGC-1α promoter activity. Journal of Natural Products, 80: 1428–1435. https://doi.org/10.1021/acs.jnatprod.6b01086

Qiao, J., Luo, Z., Gu, Z. and Zhang, Y., 2019. Identification of a novel specific cucurbitadienol synthase allele in Siraitia grosvenorii correlates with high catalytic efficiency. Molecules, 24(3): 627. https://doi.org/10.3390/molecules24030627

Ren, G.X., Yi, S.Q., Zhang, H.R. and Wang, J., 2017. Ingestion of soy–whey blended protein augments sports performance and ameliorates exercise-induced fatigue in a rat exercise model. Food & Function, 8(2): 670. https://doi.org/10.1039/C6FO01692H

Romadhona, N.F., Sari, G.M. and Utomo, D.N. 2019. Comparison of sport massage and combination of cold water immersion with sport massage on decrease of blood lactic acid level. Journal of Physics Conference Series, 1146: 012012. https://doi.org/10.1088/1742-6596/1146/1/012012

Shi, H., Liao, J., Cui, S. and Luo, Z., 2019. Effects of Forchlorfenuron on the morphology, metabolite accumulation, and transcriptional responses of Siraitia grosvenorii fruit, Molecules, 24(22): 4076. https://doi.org/10.3390/molecules24224076

Tu, D.P., Mo, C.M., Ma, X.J., Zhao, H., Tang, Q., Huang, J., Pan, L.M. and Wei, R.C., 2015. [Selection of reference genes of Siraitia grosvenorii by real-time PCR]. Journal of Chinese Materia Medica, 40(2): 204–209.

Xu, X., Lu, F., Yang, Z. and Yan, X., 2020. Comparative study on the antidiabetic efficacy of unripe and ripe fruit extracts of Siraitia grosvenorii and the possible mechanism of action. European Journal of Medicinal Plants, 31(9): 10-18. https://doi.org/10.9734/ejmp/2020/v31i930266

Zhang, G., Zhou, S.M., Zheng, S.J., Liu, F.Y. and Gao, Y.Q., 2015. Astragalus on the anti-fatigue effect in hypoxic mice. International Journal of Clinical & Experimental Medicine, 8(8): 14030.

Italian Journal of Food Science, 2022; 34 (2): 34–42

Antimicrobial synergistic effects of dietary flavonoids rutin and quercetin in combination with antibiotics gentamicin and ceftriaxone against *E. coli* (MDR) and *P. mirabilis* (XDR) strains isolated from human infections: Implications for food–medicine interactions

Tarig M.S. Alnour[1,2,3], Eltayib H. Ahmed-Abakur[1,2], Elmutuz H. Elssaig[1,2], Faisel M. Abuduhier[1,2], Mohammad Fahad Ullah[1,2,*]

[1]Department of Medical Laboratory Technology (FAMS), University of Tabuk, Tabuk, Saudi Arabia; [2]Prince Fahad Research Chair, University of Tabuk, Tabuk, Saudi Arabia; [3]Faculty of Medical Laboratory Science, Department of Microbiology and Immunology, Alzaiem Alazhari University, Khartoum North, Sudan

***Corresponding Author:** Mohammad Fahad Ullah, Department of Medical Laboratory Technology (FAMS), University of Tabuk, Tabuk, Saudi Arabia. Email: m.ullah@ut.edu.sa

Received: 12 March 2022; Accepted: 1 April 2022; Published: 21 April 2022
© 2022 Codon Publications

OPEN ACCESS CC BY NC SA

PAPER

Abstract

Antimicrobial resistance has emerged as a major global concern for public health in the last two decades, which tends to compromise the existing drug regimens in treating common or severe infections. According to WHO, three million laboratory-confirmed bacterial infections have been reported from 70 countries in 2019, caused by pathogens of concern. The drug-resistant bacterial strains are characterized as multidrug-resistant (MDR), extensively drug-resistant (XDR), and pan drug-resistant (PDR) based on the different patterns of resistance. It is believed that novel strategies are essentially required to counter and eliminate drug resistance in a cost-effective manner to benefit the world population. Natural compounds and certain dietary agents show potential antimicrobial properties and these have been used since ancient times to treat human infections. In this study, we have investigated the synergistic effects of dietary flavonoids rutin and quercetin with antibiotics gentamicin (an aminoglycoside) and ceftriaxone (a third-generation cephalosporin) against the drug-resistant superbugs; clinical isolates including *Escherichia coli* (MDR), *Proteus mirabilis* (XDR), and *Klebsiella pneumoniae* (PDR). Conventional MIC assay and checkerboard test were used as standard protocols. Our results show that rutin and quercetin restore the antimicrobial activity of the antibiotics against MDR and XDR strains, while no such effect was observed in the case of the PDR strain. Quercetin, which is a aglycone of flavonoid rutin, demonstrates higher synergistic effects with ceftriaxone compared to rutin. Since rutin and quercetin are essentially present in human diets as constituents of fruits and vegetables, their use as nutraceuticals in adjuvant therapies in combination with antibiotics against drug resistance is a promising therapeutic strategy against superbug infections.

Keywords: nutraceuticals, rutin, quercetin, synergism, MDR, XDR, PDR, Superbugs, infections

Introduction

Antimicrobial resistance (AMR) develops when the microorganisms begin to display least or no susceptibility towards a previously effective antimicrobial drug or an antibiotic. AMR, including antibacterial resistance, has emerged as a major global concern for public health in the last two decades, which tends to compromise the existing drug regimens in treating common or severe infections (Oldenkamp *et al.*, 2021). A recent report of

ISSN 1120-1770 online, DOI 10.15586/ijfs.v34i2.2196

WHO's fourth Global Antimicrobial Resistance and Use Surveillance System has shown 3 million laboratory-confirmed bacterial infections reported from 70 countries in 2019, caused by pathogens of concern (GLASS, 2021). In particular, the data demonstrate discouraging trends for low- and middle-income countries where antibacterial resistance is steadily increasing, which adds to the existing burden of poor public healthcare in these countries. In United States alone, which has a robust healthcare system, at least 2.8 million antibiotic-resistant infections are reported each year, with more than 35,000 people dying due to ineffective treatment (CDC, 2019). The drug-resistant bacterial strains are characterized as multidrug-resistant (MDR), extensively drug-resistant (XDR), and pan drug-resistant (PDR) based on the different patterns of resistance. An acquired nonsusceptibility to at least one antimicrobial in three or more antimicrobial classes defines MDR; a nonsusceptibility to at least one agent in all except one or two antimicrobial classes defines XDR; and a nonsusceptibility to all agents in all antimicrobial classes defines PDR (Magiorakos *et al*., 2012).

Multidrug-resistant *Escherichia coli* strains have been reported to be significantly associated with a high incidence of morbidity and mortality (de Been *et al*., 2014). *Proteus mirabilis* displays an extensive drug-resistant phenotype with intrinsic resistance to antibiotics due to the presence of *Salmonella* genomic island (Qin *et al*., 2015). *Klebsiella pneumoniae* is an example of PDR bacterial strain which shows resistance to all available classes of antibiotics and results in high mortality among patients with bloodstream infections (Papadimitriou-Olivgeris *et al*., 2021).

It is believed that novel strategies are essentially required to counter and eliminate drug resistance in a cost-effective manner to benefit the world population, particularly the undeveloped and developing nations which are facing an imminent threat according to the current statistics. Natural compounds and certain dietary agents show potential antimicrobial properties and these have been used since ancient times to treat human infections (Gonelimali *et al*., 2018; Udeh *et al*., 2020; Xu *et al*., 2017). Flavonoids rutin (quercetin-3-O-rutinose) and its aglycone (quercetin) display important pharmacological properties including anti-inflammatory, anti-carcinogenic, and neuroprotective activities (Batiha *et al*., 2020; Yong *et al*., 2020). The chemical structures of the two phytochemicals, rutin and quercetin, are similar, with a rutino-side being absent in quercetin at C3 (Yang *et al*., 2019). Numerous studies have shown that the use of certain flavonoids diminishes the resistance to antibiotics and demonstrates susceptibility in a synergistic manner, which offers a consequential therapeutic strategy against drug-resistant bacteria (Miklasińska-Majdanik *et al*., 2018). The presence of glycosidic structures in flavonoids is known to alter their biological activities, as aglycones are likely to have more potent biological activities compared to glycosides (Williamson *et al*., 1996; Xiao, 2017). Furthermore, flavonoid showed low cytotoxicity, highlighting its higher safety index (Nizer *et al*., 2020). Since these flavonoids are dietary and are essential constituents of human diets, their utilization in repurposing pharmacological strategies have an advantage of no or least associated adverse effects.

In the current study, we examine the synergistic effects of dietary flavonoids rutin and quercetin with antibiotics gentamicin (an aminoglycoside) and ceftriaxone (a third-generation cephalosporin) (Figures 1 and 2) against the drug-resistant superbugs; clinical isolates including *E. coli* (MDR), *P. mirabilis* (XDR) and *K. pneumoniae* (PDR).

Materials and methods

This study is an analytical cross-sectional study conducted in the Prince Fahd Research Chair, University of Tabuk. As the study used an *in vitro* protocol that

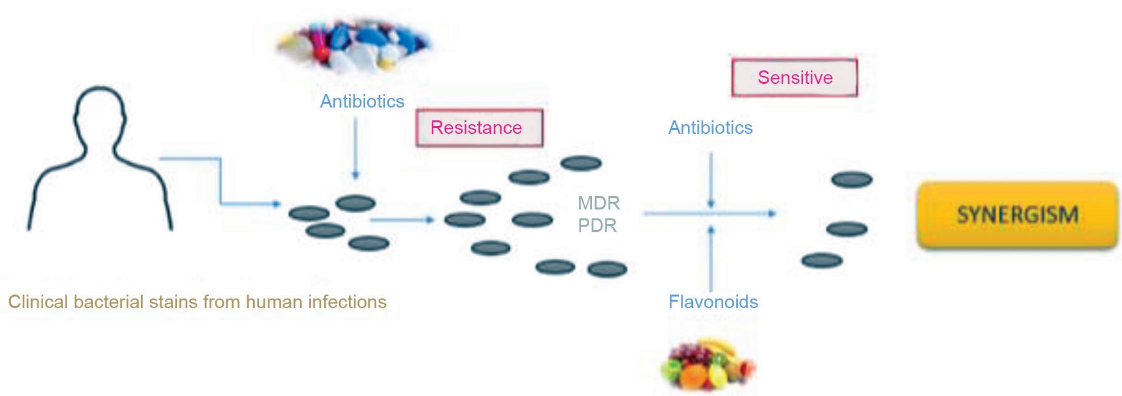

Figure 1. Schematic representation of the research theme.

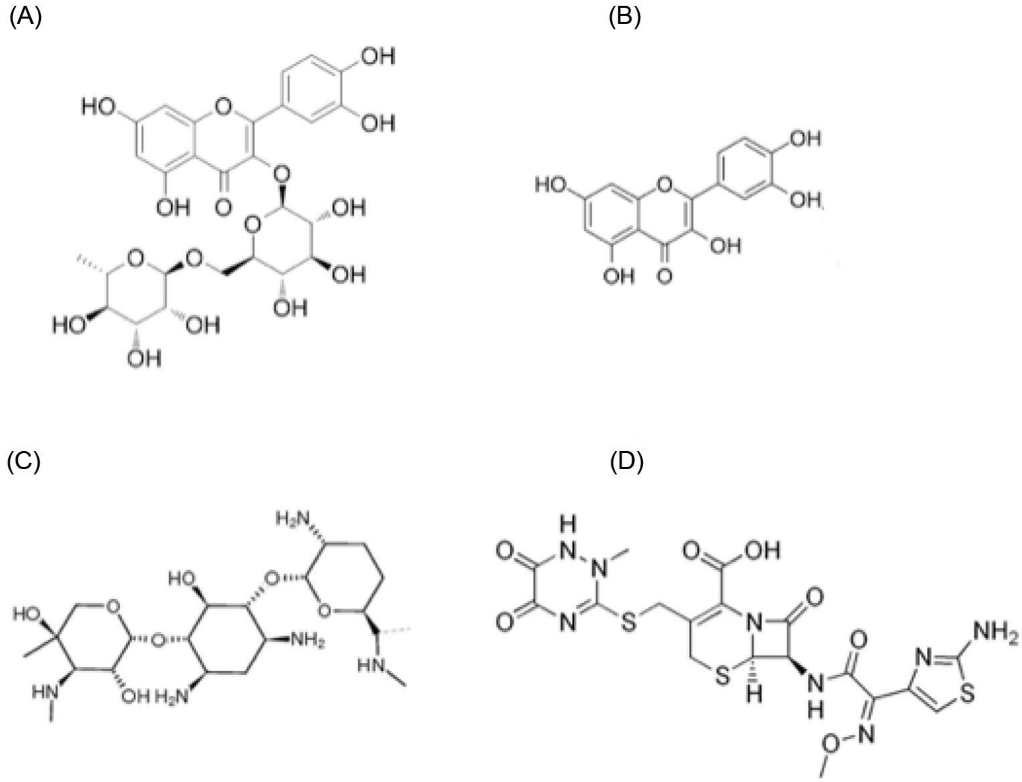

Figure 2. Chemical structures of flavonoids, rutin (A) and quercetin (B), and antibiotics, gentamicin (C) and ceftriaxone (D).

involved clinical isolates without patient's data, there was no need for patient's consent or ethical approval.

Bacterial isolates

Three clinical bacterial isolates that showed different antibiotic resistance patterns were identified in Prince Fahd Research Chair for biological studies, University of Tabuk (Alnour *et al*., 2021) and used in this study to demonstrate the antimicrobial effect of flavonoids, rutin and quercetin, in combination with antibiotics gentamicin and ceftriaxone. The drug-resistant isolates were *E. coli, P. mirabilis,* and *K. pneumoniae,* which showed MDR, XDR, and PDR, respectively. These isolates did not respond to the standard MIC level of gentamicin and ceftriaxone. The standard MIC level of gentamicin and ceftriaxone is 16 μg/mL and 64 μg/mL, respectively (Terbtothakun *et al*., 2021).

Preparation of stock solutions

Rutin and quercetin (Sigma) were dissolved in 10% dimethyl sulfoxide (DMSO) to prepare a stock solution of 1 mg/mL. Nitro-blue tetrazolium (NBT) (Sigma) was prepared to reach the final concentration of 50 μg/mL whereas gentamicin and ceftriaxone (Sigma) stock solutions were prepared to reach the concentrations of 16 to 64 and 64 to 512 μg/mL, respectively.

Minimum inhibitory concentration broth microdilution assay

Conventional MIC assay was performed using the NBT microplate dilution method. In brief, a two-fold serial dilution to the target flavonoid and antimicrobial agents was prepared; overnight broth cultures were adjusted to Mcfarland standard, 100 μL of standardized culture was added to each well in 96-well plate to obtain final bacterial suspension of 10^5CFU/mL, 50 μL of NBT was then added in all wells; antibiotics, gentamicin and ceftriaxone, and flavonoids, quercetin and rutin, were added to the wells to reach the required concentrations for each of these individually and in combination. The combination was as follows: rutin-gentamicin, rutin-ceftriaxone, quercetin-gentamicin, and quercetin-ceftriaxone. Positive control (resistance strain), negative control (well free of bacteria) were included. The plate was incubated at 37°C for 18–24 h, reduction of NBT (colorless) to formazan (blue) indicated the bacterial growth (resistance). The experiments were done in triplicate for three independent repeats.

Checkerboard test

Checkerboard assay, as described by Siriwong *et al.*, 2016 was performed to determine the synergistic activity of rutin and quercetin with gentamicin and ceftriaxone against MDR *E. coli*, XDR *P. mirabilis*, and PDR K. *pneumonia*. In brief, 50 µL of 10^5 CFU/mL bacterial suspension was treated with varying concentrations in combination: rutin with gentamicin, rutin with ceftriaxone, quercetin with gentamicin, and quercetin with ceftriaxone. Growth positive control was included containing bacterial suspension in Muller and Hinton broth and 10% DMSO, while growth negative control contains reaction mixture without addition of bacterial suspension. 50 µL of 50 µg/mL NBT was added to each well and the microtiter plate was incubated at 37°C for 18 h. The interaction between the two agents was calculated by the fractional inhibitory concentration (FIC) index of the combination as the following (Terbtothakun *et al.*, 2021):

FIC = MIC of component A in combination/MIC of component A alone + MIC of component B in combination/MIC of component B alone

Results were reported as synergism when the combination index is 0.5 or less.

Results

In order to study the interaction of flavonoids (rutin and quercetin) with antibiotics on resistant clinical isolates, combinations of the candidate compounds with gentamicin or ceftriaxone were evaluated by MIC and checkerboard assay.

The NBT microdilution results showed that the three isolates, *E. coli* (MDR), *P. mirabilis* (XDR), and *K. pneumoniae* (PDR), did not show any response when tested against the individual agents; rutin (MIC 1,000 µg/mL), quercetin (MIC 2,000 µg/mL), ceftriaxone (MIC 64 µg/mL), and gentamicin (MIC 16µg/mL) (Figure 3). It was found that the minimum inhibitory response for gentamicin was observed at 64 µg/mL while for ceftriaxone it was 512 µg/mL, which were significantly higher than the standard MIC for gentamicin and ceftriaxone (Figure 3).

Interestingly, growth inhibition of MDR and XDR isolates was observed when the quercetin at a concentration of 700 µg/mL was added to 64 µg/mL and 128 µg/mL of gentamicin, respectively. However, the combination of rutin (serially diluted up to 1,000 µg/mL) with gentamicin (16 µg/mL) did not affect the resistance patterns of XDR and PDR isolates and inhibited the growth of MDR isolate only.

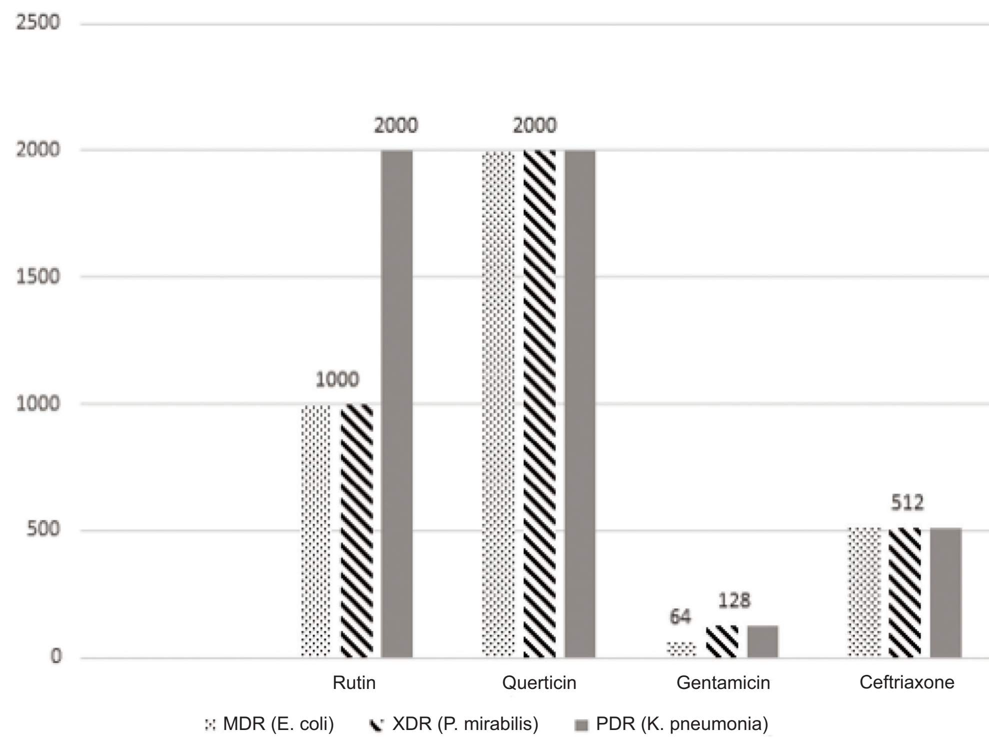

Figure 3. Minimum inhibitory concentrations of flavonoids and antimicrobials against the antibiotic-resistant clinical isolates, MDR, XDR, and PDR.

The results of the checkerboard assay showed a promising synergism effect between quercetin and ceftriaxone against both MDR isolate and XDR isolate; this synergism occurred at a concentration ranging between 100 and 800 µg/mL and 40 and 180 µg/mL for quercetin and ceftriaxone, respectively. The synergism is observed to increase with increasing the concentration of the antibiotic and reducing the concentration of quercetin (Figure 4a). This combination does not show effects against PDR *Klebsiella* pneumonia. While the combination between the quercetin and gentamicin displayed a weak effect against the MDR isolate and significant synergism against the XDR isolate, the synergism effect occurred at a concentration ranging between 200 and 700 µg/mL and 15 and 40µg/mL for quercetin and gentamicin, respectively. Similarly, no effect against PDR *Klebsiella* pneumonia was observed (Figure 4b). Surprisingly, this synergism occurred within the standard MIC level of gentamicin and ceftriaxone.

The combination between rutin and ceftriaxone displayed a significant effect against the MDR isolate and an insignificant effect against the XDR isolate (Figure 5a); the synergism effect was reported at concentrations of 100 and 180 µg/mL for rutin and ceftriaxone, respectively; other concentrations exhibited a weak effect. The combination between rutin and gentamicin showed only a weak effect on the MDR isolate and does not affect both XDR and PDR isolates (Figure 5b).

Discussion

The development of new antibiotic agents is costly, time-consuming, and needs various stages of toxicological assessments to ensure safety. A combination of existing antimicrobial agents and dietary flavonoids that display pharmacological properties has become an effective therapeutic strategy against numerous kinds of infections caused by MDR bacteria (Terbtothakun *et al.*, 2021).

The present study aimed to determine the antimicrobial potential of two flavonoids (rutin and quercetin) in

(A)

Isolates	Q 1mg/ml C 0mg/ml	Q 900 µg/ml C 20 µg/ml	Q 800 µg/ml C 40 µg/ml	Q 700 µg/ml C60 µg/ml	Q 600 µg/ml C 80 µg/ml	Q 500 µg/ml C100 µg/ml	Q 400 µg/ml C120 µg/ml	Q 300 µg/ml C 140 µg/ml	Q 200 µg/ml C 160 µg/ml	Q 100 µg/ml C 180 µg/ml	Q 0 µg/ml C 200 µg/ml
Escherichia coli (MDR)			0.48*	0.47*	0.46*	0.45*	0.43*	0.42*	0.41*	0.40*	
Proteus mirabilis (XDR)			0.48*	0.47*	0.46*	0.45*	0.43*	0.42*	0.41*		
Klebsiella pneumoniae (PDR)											

(B)

Isolates	Q 1mg/ml G 0mg/ml	Q 900 µg/ml G 5 µg/ml	Q 800 µg/ml G 10 µg/ml	Q 700 µg/ml G 15 µg/ml	Q 600 µg/ml G 20 µg/ml	Q 500 µg/ml G 25 µg/ml	Q 400 µg/ml G 30 µg/ml	Q 300 µg/ml G 35 µg/ml	Q 200 µg/ml G 40 µg/ml	Q 100 µg/ml G 45 µg/ml	Q 0 µg/ml G 50 µg/ml
Escherichia coli (MDR)				0.58*	0.61*	0.64*	0.67*	0.70*	0.73*		
Proteus mirabilis (XDR)				0.47*	0.46*	0.45*	0.43*	0.42*	0.41*		
Klebsiella pneumoniae (PDR)											

Figure 4. (A) Checkerboard test showed the combined effect of quercetin (Q) and ceftriaxone (C). (B) Checkerboard test showed the combined effect of quercetin (Q) and gentamicin (G). Grey shade indicates microbial growth (resistant isolate); white shade indicates growth inhibition.

*Checkerboard result: Synergism is considered when the FMIC is equal to or less than 0.5.

(A)

Isolates	R 1mg/ml C 0 mg/ml	R 900 µg/ml C 20 µg/ml	R 800 µg/ml C 40 µg/ml	R 700 µg/ml C 60 g/ml	R 600 µg/ml C 80 g/ml	R 500 µg/ml C 100 µg/ml	R 400 µg/ml C 120 µg/ml	R 300 µg/ml C 140 µg/ml	R 200 µg/ml C 160 µg/ml	R 100 µg/ml C 180 µg/ml	R 0 µg/ml C 200 µg/ml
Escherichia coli (MDR)		0.94*	0.88*	0.82*	0.76*	0.70*	0.63*	0.57*	0.51*	0.45*	
Proteus mirabilis (XDR)		0.94*	0.88*	0.82*	0.76*	0.70*	0.63*	0.57*	0.51*		
Klebsiella pneumoniae (PDR)											

(B)

Isolates	R 1 mg/ml G 0 µg/ml	R 900 µg/ml G 5 µg/ml	R 800 µg/ml G 10 µg/ml	R 700 µg/ml G 15 µg/ml	R 600 µg/ml G 20 µg/ml	R 500 µg/ml G 25 µg/ml	R 400 µg/ml G 30 µg/ml	R 300 µg/ml G 35 µg/ml	R 200 µg/ml G 40 µg/ml	R 100 µg/ml G 45 µg/ml	R 0 µg/ml G 50 µg/ml
Escherichiacoli (MDR)		0.98*	0.96*	0.93*	0.91*	0.89*	0.87*	0.85*	0.83*		
Proteus mirabilis (XDR)											
Klebsiella pneumoniae (PDR)											

Figure 5. Figure 5. (A) Checkerboard test showed the combined effect of rutin (R) and ceftriaxone (C). (B) Checkerboard test showed the combined effect of rutin (R) and gentamicin (G). Grey shade indicates microbial growth (resistant isolate); white shade indicates growth inhibition.

*Checkerboard result: Synergism is considered when the FMIC is equal to or less than 0.5.

combination with gentamicin and ceftriaxone against superbug bacterial isolates which showed a different pattern of resistance (MDR, XDR, and PDR). These isolates were selected to trace the antimicrobial efficiency of flavonoids with the standard drugs, as these have been reported as highly resistant and difficult to be treated, and the emergence of such superbugs poses a consistent threat to human lives world over (Adegoke *et al*., 2017; Alnour *et al*., 2021). The selected antimicrobial agents to be combined with flavonoids were gentamicin (aminoglycosides), which is an important class of antibiotics that are commonly used for the treatment of severe infections (Terbtothakun *et al*., 2021), and ceftriaxone, which is a beta-lactam antibiotic and a third-generation cephalosporin, that is marked by relatively high stability towards the beta-lactamases of gram-negative bacilli and is shown to be effective against a broad range of organisms (Maina *et al*., 2012).

Our results showed that gentamicin, ceftriaxone, and flavonoids alone failed to inhibit the growth of MDR *E. coli*, XDR *P. mirabilis*, and PDR *K. pneumoniae.* A similar result was obtained by Arima *et al*., 2002 and Nizer *et al*., 2020 who conducted a study to evaluate the antibacterial activity of rutin isolated from *Tontelea micrantha* leaves and concluded that rutin is not a promising antimicrobial agent. Contradictory to these findings, several other reports showed antimicrobial effects of flavonoids against several bacterial isolates. As such, Araruna *et al*., 2012 conducted a similar study that evaluated the antibiotic modifying activity of pilocarpine and rutin, and they demonstrated the inhibitory effects of rutin against *E. coli*. A comparable result for rutin was reported by Pimentel *et al*., 2013 against *P. mirabilis*, *P. aeruginosa,* and *Klebsiella* species. Moreover, Wang *et al*., 2018, demonstrated the bacteriostatic effect of quercetin and further reported an inhibitory effect on the growth of *P. aeruginosa*, *S. aureus*, *S. Typhimurium*, and *E. coli*. These variations could be attributed to the pattern of resistance shown by isolates under the study and the time of the study. In our study, we utilized *E. coli* (MDR), *P. mirabilis* (XDR), and *K. pneumoniae* (PDR) clinical isolates, which were bacterial strains of the enterobacteriaceae family, that are known to be naturally competent and can uptake naked DNA from the environment in appropriate conditions (Patil *et al*., 2019).

Interestingly, our results showed promising antibacterial activity of flavonoids when they were combined with gentamicin and ceftriaxone; the synergistic effects of gentamicin and ceftriaxone against the MDR isolate and the XDR isolate were observed in the presence of rutin or quercetin. The resistance pattern against gentamicin and ceftriaxone was converted to a susceptible pattern even at a low concentration of 15 μg/mL and 40 μg/mL for gentamicin and ceftriaxone, respectively. Numerous studies have evaluated the antimicrobial activities of flavonoids against various clinical isolates, but only a few reports showed inhibitory effects of rutin and quercetin against MDR and none describe their effect against XDR or PDR. It is believed that the restoring of the antimicrobial activities of the antibiotics in the presence of the flavonoids might be due to the ability of flavonoids to enhance the antibiotic drug efficacy (Vipin *et al*., 2020) or due to the simultaneous activities of the agents on two different cellular targets (Banik and Shamsuzzaman, 2021). Thus, the combination of quercetin or rutin with ceftriaxone or gentamicin generates multiple effects against the bacteria and displays strong growth inhibitory effects. However, rutin has been reported to possess an efficient mechanism against bacterial growth by inhibiting DNA gyrase and topoisomerase (Alajmi *et al*., 2018), and the combination of these molecules with a cell wall inhibitor, such as ceftriaxone, or protein synthesis inhibitor, such as gentamicin, can interfere with peptidoglycan synthesis (Fair and Tor 2014). The flavonoid quercetin acts as a cell wall and cell membrane inhibitor (Wang *et al*., 2018; Yang *et al*., 2020). Recently, Vipin *et al*., 2020 examined the effectiveness of several antibiotics, including ceftriaxone and gentamicin, in combination with quercetin, and reported synergistic activity of quercetin against drug-resistant *Pseudomonas aeruginosa* and stated that the ability of quercetin to empower the aminoglycoside activity was due to the quorum sensing inhibitory properties of flavonoids. In a related study, Terbtothakun *et al*., 2021 reported synergistic effects of aminoglycosides when combined with meropenem and stated that the penetration of aminoglycosides into the cytosol of bacteria is improved by other antimicrobial agents, which could also explain the synergism with flavonoids as reported in our study. The study showed that the addition of aminoglycosides as adjunctive therapy to meropenem can regain meropenem activity against carbapenem-resistant *Enterobacteriaceae* isolates harboring blaNDM (Terbtothakun *et al*., 2021).

The combination of flavonoids and antibiotics in our study had no effect on the PDR isolates; this may be due to the cumulative effects of multi-resistance mechanisms which are expressed by PAR isolates, such as overexpression of the efflux pump and porin with the β-lactamases, that lead to a high level of resistance.

Conclusion

Our findings showed a potential synergistic pattern of rutin and quercetin in combination with gentamicin and ceftriaxone. This finding suggests that rutin and quercetin can shift the resistance mechanisms of antimicrobial agents into susceptible ones, thereby restoring the drug efficacy. Since rutin and quercetin are essentially present in human diets as constituents of fruits and vegetables, their use as nutraceuticals in adjuvant therapies in combination with antibiotics against drug resistance is a promising repurposing therapeutic strategy against superbug infections.

Acknowledgment

The authors declare that this research was not funded partially or completely by any external support. The authors acknowledge the research facility at Prince Fahd Research Chair, University of Tabuk.

Conflict of Interest

The authors agreed that there are no conflict of interest for this research.

Data Availability

The data associated with the current study have been incorporated in this manuscript. Further queries can be forwarded to the corresponding author.

Research involving Human Participants and/or Animals

Not applicable.

Informed Consent

Not applicable

References

Adegoke, A., Faleye, A., Singh, G. and Stenström, T., 2017. Antibiotic resistant superbugs: assessment of the interrelationship of occurrence in clinical settings and environmental niches. Molecules 22: 29. https://doi.org/10.3390/molecules22010029

Alajmi, M.F., Alam, P., Rehman, M.T., Husain, F.M., Khan, A.A., Siddiqui, N.A., et al., 2018. Interspecies anticancer and antimicrobial activities of genus solanum and estimation of rutin by validated UPLC-PDA method. Evidence-Based Complementary and Alternative Medicine 2018: Article ID 6040815. https://doi.org/10.1155/2018/6040815

Alnour, T.M.S., Elssaig, E.H., Abuduhier, F.M., Alfifi, K.A.S., Abusuliman, M.S., Albalawi, T. and Ahmed-Abakur, E.H., 2021. Phenotypic and genotypic characterization of antibiotic resistant gram negative bacteria isolated in Tabuk City, Saudi Arabia. African Journal of Microbiology Research15(8): 433–439. https://doi.org/10.1101/2021.02.01.429288

Araruna, M.K.A., Brito, S.A., Morais-Braga, M.F.B., Santos, K.K.A., Souza, T.M., Leite, T.R., Costa, J.G.M. and Coutinho, H.D.M., 2012. Evaluation of antibiotic & antibiotic modifying activity of pilocarpine & rutin. Indian Journal of Medical Research 135(2): 252–254.

Arima, H., Ashida, H. and Danno, G. Rutin-enhanced antibacterial activities of flavonoids against *Bacillus cereus* and *Salmonella enteritidis*. Bioscience, Biotechnology, and Biochemistry 66(5): 1009–1014. https://doi.org/10.1271/bbb.66.1009

Banik, N. and Shamsuzzaman, S.M., 2021. Evaluation of effectiveness of antibiotic combination therapy in multi drug resistant *Escherichia Coli in vitro* and *in vivo*. Fortune Journal of Health Sciences 4: 470–478. https://doi.org/10.26502/fjhs.036

Batiha, G.E., Beshbishy, A.M., Ikram, M., et al., 2020. The pharmacological activity, biochemical properties, and pharmacokinetics of the major natural polyphenolic flavonoid: quercetin. Foods 9(3): 374. https://doi.org/10.3390/foods9030374

CDC 2019: Centers for Disease Control and Prevention. Drug resistance report 2019. Available at: https://www.cdc.gov/drugresistance/pdf/threats-report/2019-ar-threats-report-508.pdf.

De Been, M. et al., 2014. Dissemination of cephalosporin resistance genes between *Escherichia coli* strains from farm animals and humans by specific plasmid lineages. PLoS Genetics 10(12): e1004776. https://doi.org/10.1371/journal.pgen.1004776

Fair, R.J. and Tor, Y., 2014. Antibiotics and bacterial resistance in the 21st century. Perspectives in Medicinal Chemistry 6: 25–64. https://doi.org/10.4137/PMC.S14459

GLASS 2021: Global antimicrobial resistance and use surveillance system (GLASS) report: 2021. Available at: https://www.who.int/publications/i/item/9789240027336.

Gonelimalim F.D., Lin, J. and Miao, W., et al., 2018. Antimicrobial properties and mechanism of action of some plant extracts against food pathogens and spoilage microorganisms. Frontiers in Microbiology 9: 1639. https://doi.org/10.3389/fmicb.2018.01639

Magiorakos, A.P., Srinivasan, A., Carey, R.B., et al. Multidrug-resistant, extensively drug-resistant and pandrug-resistant bacteria: an international expert proposal for interim standard definitions for acquired resistance. Clinical Microbiology And Infection 18(3): 268–281. https://doi.org/10.1111/j.1469-0691.2011.03570.x

Maina, D., Revathi, G., Kariuki, S., Ozwara, H., 2012. Genotypes and cephalosporin susceptibility in extended-spectrum beta-lactamase producing enterobacteriaceae in the community. Journal of Infection in Developing Countries. 6(6): 470–477. https://doi.org/10.3855/jidc.1456

Miklasińska-Majdanik, M., Kępa, M., Wojtyczka, R.D., Idzik, D. and Wąsik, T.J., 2018. Phenolic compounds diminish antibiotic resistance of *Staphylococcus aureus* clinical strains. International Journal of Environmental Research and Public Health 15(10): 2321. https://doi.org/10.3390/ijerph15102321

Nizer, W.S., Ferraz, A.C., Moraes, T.F., Ferreira, F., Magalhães, C., Vieira-Filho, S.A., et al., 2020. Antimicrobial activity of rutin isolated from *T. micrantha* leaves. Journal of Pharmaceutical Negative Results 11(1): 9–14. https://doi.org/10.4103/jpnr.JPNR_12_19

Oldenkamp, R., Schultsz, C., Mancini, E. and Cappuccio, A., 2021. Filling the gaps in the global prevalence map of clinical antimicrobial resistance. Proceedings of the National Academy of Sciences of the United States of America. 118(1): e2013515118. https://doi.org/10.3390/antibiotics10010076

Papadimitriou-Olivgeris, M., Bartzavali, C., Georgakopoulou, A., et al. Mortality of pandrug-resistant *Klebsiella pneumoniae* bloodstream infections in critically ill patients: a retrospective cohort of 115 episodes. Antibiotics (Basel) 10(1): 76. https://doi.org/10.3390/antibiotics10010076

Patil, S., Chen, H., Zhang, X., Lian, M., Ren, P. and Wen, F., 2019. Antimicrobial resistance and resistance determinant insights into multi-drug resistant gram-negative bacteria isolates from paediatric patients in China. Infection and Drug Resistance 22(12): 3625–3634. https://doi.org/10.2147/IDR.S223736

Pimentel, R.B.D.Q., da Costa, C.A,, Albuquerque, P.M. and Junior, S.D., 2013. Antimicrobial activity and rutin identification of honey produced by the stingless bee Melipona compressipes manaosensis and commercial honey. BMC Complementary Medicine 1(13): 151. https://doi.org/10.1186/1472-6882-13-151

Qin, S., Qi, H., Zhang, Q., et al., 2015. Emergence of extensively drug-resistant *Proteus mirabilis* harboring a conjugative NDM-1 plasmid and a novel Salmonella genomic Island 1 variant, SGI1-Z. Antimicrobial Agents and Chemotherapy;59(10): 6601–6604. https://doi.org/10.1128/AAC.00292-15

Siriwong, S., Teethaisong, Y., Thumanu, K., Dunkhunthod B. and Eumkeb, G., 2016. The synergy and mode of action of quercetin plus amoxicillin against amoxicillin-resistant *Staphylococcus epidermidis*. BMC Pharmacology and Toxicology 17: 39. https://doi.org/10.1186/s40360-016-0083-8

Terbtothakun, P., Nwabor, O.F., Siriyong, T., Voravuthikunchai, S.P. and Chusri, S., 2021. Synergistic antibacterial effects of meropenem in combination with aminoglycosides against carbapenem-resistant *Escherichia coli* Harboring blaNDM-1 and blaNDM-5. Antibiotics 10: 1023. https://doi.org/10.3390/antibiotics10081023

Udeh, E.L., Nyila, M.A. and Kanu, S.A., 2020. Nutraceutical and antimicrobial potentials of Bambara groundnut (*Vigna subterranean*): a review. Heliyon 6(10): e05205. https://doi.org/10.1016/j.heliyon.2020.e05205

Vipin, C., Saptami, K., Fida, F., Mujeeburahiman, M., Rao, S., Athmika, A.B.A., et al., 2020. Potential synergistic activity of quercetin with antibiotics against multidrug-resistant clinical strains of Pseudomonas aeruginosa. PLoS One 15(11): e0241304. https://doi.org/10.1371/journal.pone.0241304

Wang, S., Yao, J., Zhou, B., Yang, J., Chaudry, M.T., Wang, M., et al., 2018. Bacteriostatic effect of quercetin as an antibiotic alternative *in vivo* and its antibacterial mechanism *in vitro*. Journal of Food Protection 81(1): 68–78. https://doi.org/10.4315/0362-028X.JFP-17-214

Williamson, G., Plumb, G.W., Uda, Y., Price, K.R. and Rhodes, M.J., 1996. Dietary quercetin glycosides: antioxidant activity and induction of the anticarcinogenic phase II marker enzyme quinone reductase in Hepalclc7 cells. Carcinogenesis 17(11): 2385–2387. https://doi.org/10.1093/carcin/17.11.2385

Xiao, J., 2017. Dietary flavonoid aglycones and their glycosides: which show better biological significance? Critical Reviews in Food Science and Nutrition 57(9): 1874–905.

Xu, C., Yagiz, Y., Zhao, L., Simonne, A., Lu, J. and Marshall, M.R., 2017. Fruit quality, nutraceutical and antimicrobial properties of 58 muscadine grape varieties (Vitis rotundifolia Michx.) grown in United States. Food Chemistry 215: 149–156. https://doi.org/10.1016/j.foodchem.2016.07.163

Yang, D., Wang, T., Long, M. and Li, P., 2020. Quercetin: Its main pharmacological activity and potential application in clinical medicine. Oxidative Medicine and Cellular Longevity 2020: Article ID 8825387. https://doi.org/10.1155/2020/8825387

Yang, J., Lee, H., Sung, J., Kim, Y., Jeong, H.S. and Lee, J., 2019. Conversion of rutin to quercetin by acid treatment in relation to biological activities. Preventive Nutrition and Food Science 24(3): 313–320. https://doi.org/10.3746/pnf.2019.24.3.313

Yong, D.O.C., Saker, S.R., Chellappan, D.K., et al., 2020. Molecular and immunological mechanisms underlying the various pharmacological properties of the potent bioflavonoid, rutin. Endocrine, Metabolic & Immune Disorders – Drug Targets 20(10): 1590–1596. https://doi.org/10.2174/1871530320666200503053846

Italian Journal of Food Science, 2022; 34 (2): 43–49

The role of whey protein in myogenic differentiation

Rui Xu[1]*, Yuejuan Xiao[2], Ying Zhang[2], Xiyan Zhao[1]

[1]College of Food Science and Technology, Hebei Normal University of Science and Technology, Changli, Qinhuangdao, China; [2]College of Marine Resources and Environment, Hebei Normal University of Science and Technology, Changli, Qinhuangdao, China

***Corresponding Author:** Rui Xu, College of Food Science and Technology, Hebei Normal University of Science and Technology, Changli, Qinhuangdao, 066600, China. Email: robust100@163.com

Received: 25 July 2021; Accepted: 28 March 2022; Published: 26 April 2022
© 2022 Codon Publications

OPEN ACCESS BY NC SA

PAPER

Abstract

Whey protein has been shown to prevent exercise-induced protein degradation and muscle damage. We hypothesized that whey protein would regulate muscle cell differentiation. Adding various concentrations of whey protein to C2C12 myoblasts induced cell differentiation and MyoD (myogenic differentiation protein) expression as well as the phosphorylation of AKT (protein kinase B). Whey protein-induced differentiation-specific markers increased the enzymatic activities of creatine kinase and citrate synthase and the expression of muscle-specific microRNA. Whey protein elevated AKT phosphorylation on Thr308 and Ser473, which was inhibited by LY294002 (a non-selective phosphoinositide 3-kinases inhibitor), suggesting that whey protein acts via PI3K (phosphatidylinositol 3-kinase). Blocking of the PI3K/AKT pathway with specific inhibitors revealed its requirement in mediating the promotive effects of whey protein on C2C12 cell differentiation. These effects of whey protein on myoblast differentiation suggest its positive influence in preventing muscle atrophy.

Keywords: C2C12, myoblast differentiation, whey protein

Introduction

Whey protein, including essential branched-chain amino acid, is one of the latest dietary supplements for promoting/aiding the increase in strength and improving the lean body mass. The branched-chain amino acid has been shown to increase muscle hypertrophy by inhibiting muscle degradation (Aoyama *et al*., 2019). A change in lean muscle mass is often attributed to a changed balance between protein synthesis and degradation rates in tissues. However, the direct effect of whey protein on myogenic mechanisms has never been studied. Here we examined the effects of whey protein on the differentiation of C2C12 myoblasts.

Skeletal muscle formation or myogenesis is a complex and highly regulated process that involves the proliferation of myoblasts, exit of these myoblasts from the cell cycle, and their differentiation into muscle fibers (Hernández-Hernández *et al*., 2017). The sequential expression of myogenic regulatory factors (MRFs), a group of basic helix-loop-helix (bHLH) transcription factors that include MyoD, Myf-5 (myogenic factor 5), myogenin, and MRF4 is required (Seale and Rudnicki, 2000). MyoD and Myf-5 are the primary MRFs required for the formation, proliferation, and survival of myoblasts whereas myogenin and MRF-4 act later to control myoblast differentiation and induce the expression of important muscle-specific genes, such as myosin heavy chain and creatine kinase.

MicroRNAs (miRNAs) are a class of highly conserved, non-coding RNAs molecules that play key roles in posttranscriptional gene regulation. A small number of muscle-specific miRNAs have been shown to have a crucial role in myoblast proliferation and differentiation (Wang *et al.*, 2018). Numerous miRNA expression profiling studies have consistently shown that miRNA-1 (miR-1), miR-133a, and miR-206 have to be muscle-specific (Motaei *et al.*, 2019). Analysis of the presumptive miR-1 promoter has shown that miR-1 expression is regulated by SRF (serum response factor), MyoD, MEF2 (myocyte enhancer factor-2), and Dorsal- and Twist-binding sites, all factors known to be important in conferring muscle-specific gene expression (Zhang *et al.*, 2021). miR-1 promotes the differentiation and exit of cardiac and skeletal progenitors from the cell cycle in mammals.

The phosphoinositide 3′-kinase (PI3K) plays a crucial role in effecting alterations in a broad range of cellular functions in response to extracellular signals. Akt phosphorylates a variety of substrates involved in the regulation of key cellular functions including cell growth and survival and protein translation. The PI3K/AKT pathway has been reported to play a major role in inducing cell differentiation and hypertrophy (Rommel *et al.*, 2001).

Given the importance of the muscle-specific miRNAs and PI3K/AKT signaling in muscle development, we must have the interest to determine what role they may have in skeletal muscle plasticity. To gain insight into the roles of whey protein in muscular hypertrophy, we analyzed the profiles of miR-1, miR-133a, and miR-206 expression as well as PI3K/AKT pathway in C2C12 cells.

Materials and Methods

Materials

C2C12 myoblast was purchased from China Center for Type Culture Collection. Dulbecco's modified Eagle's medium (DMEM) and fetal bovine serum (FBS) were purchased from Gibco (Grand Island, USA). Whey protein concentration contained 80.05% protein, which was measured using the Kjeldahl method. LY294002 is LY 294002 HYDROCHLORIDE, purchased from Beyotime Institute of Biotechnology (Jiangsu, China).

Cell culture

The cells were grown in DMEM containing 10% FBS. Once cells had reached 80% confluency, the medium was changed to DMEM supplemented with 2% horse serum. C2C12 myoblasts were differentiated into myotubes by incubation in the differentiation medium (2% horse serum in DMEM). Myotubes were maintained in the differentiation medium, and the medium was changed every 48 h. The inhibitors LY294002 (20 μM) was added before whey protein, which was used at 0.1 mg/mL or 0.4 mg/mL for C2C12 myoblasts.

Enzyme assays

The activities of two marker enzymes of differentiation, creatine kinase (CK) and citrate synthetase (CS), were assayed in cellular extracts using a spectrophotometric-based kit from Nanjing Jiancheng Bioengineering Institute (Nanjing, China) and Shanghai Genmed Pharmaceutical Co., Ltd (Shanghai, China), respectively.

Detection of mature miRNAs

To detect miRNA in all RNA samples, the All-in-one miRNA Q-PCR detection kit and PCR primer sets for miR-1, -133a, and -206 were used according to the manufacturer's directions (GeneCopoeia, Guangzhou, China). Further, the expression of all samples was normalized to Rnu6 (U6 small nuclear RNA) levels to account for possible differences in the amount of initial RNA.

Quantitative real-time PCR

Isolation of all RNA and RT-PCR was done as described by Dogra *et al.* (2006), but with a minor modification. Briefly, an RNAiso Plus Kit (TaKaRa, Dalian, China) was used to extract RNA from cells. All RNA samples were reverse-transcribed using gene-specific primer and Fermentas's reverse transcription kit according to the manufacturers' instructions. The sequences of primers used were as follows: MyoD, 5′-TGCGGTGCACCCAGGCCCAG-3′ (forward) and 5′-CCGCCTCACTGTAGTAGGCG-3′ (reverse); Myf5, 5′-CAAGAGTAGCAGCCTTCGGA-3′ (forward) and 5′-GGAGCTTTTATCTGCAGCAC-3′ (reverse); Myogenin, 5′-GCTATGAGCGGACTGAGCTC-3′ (forward) and 5′-GGAGTGCAGATTGTGGGCGT-3′ (reverse); GAPDH, 5′-CCTTCATTGACCTCAACTAC-3′ (forward) and 5′-AGCCCCACGGCCATCACGCC-3′ (reverse).

Quantitative real-time PCR was conducted using the same primers as described above and following a method as detailed by Dogra *et al.* (2006). Data normalization was accomplished using the endogenous control (GAPDH) and the normalized values were subjected to a $2^{-\Delta\Delta Ct}$ threshold cycle formula to calculate the fold change between the control and experiment groups.

Western blot analysis

Cells were extracted with (Radio Immunoprecipitation Assay) (RIPA) buffer and lysates were cleared by centrifugation. Equal amounts of protein were loaded and resolved by 12% (w/v) SDS-PAGE, then transferred to nitrocellulose membranes (Whatman). The membranes were blocked with 5% nonfat dry milk in Trisbuffered saline-0.1% Tween (TBST) and probed overnight with primary antibodies in TBST supplemented with 5% bovine serum albumin. After reaction in TBST with horseradish peroxidase-conjugated secondary antibodies (Boisynthesis, Beijing, China), bands were visualized using enhanced HRP-DAB reagents (Tiangen, Beijing).

After blocking, the membranes were incubated with the following primary antibodies: polyclonal anti-AKT (Cell Signaling), anti-phospho-AKT (Thr308), anti-phospho-AKT (Ser473), and monoclonal anti-myosin heavy chain (Santa Cruz), and polyclonal anti-β-Actin antibody (Boisynthesis).

Statistical analysis

Results are expressed as mean ± SE. A value of P < 0.05 was considered statistically significant unless otherwise specified and statistical analyses were performed using Origin 8.0.

Results

Assay of marker enzyme

The addition of various concentrations of whey protein to serum-starved C2C12 myoblasts for 24 h enhanced the enzymatic activity of the muscle differentiation-specific markers creatine kinase and citrate synthase in a dose-responsive manner, with the highest levels being observed at 0.4 mg/ml whey protein. The enzyme activities of CS and CK are shown in Table 1. There was no significant change in CS activities for the concentration of 0.1 mg/ml. Comparisons of the activities of markers of differentiated skeletal muscle CS and CK revealed increases from 2.61 to 5.87 U/mg·prot and from 41.7 to 68.4 μmol/mg·min, respectively.

Myogenic gene expression

Since the activation of MRFs is a prerequisite for myogenesis, we investigated the effect of whey protein on the expression of MyoD, myogenin, and Myf-5. C2C12 myoblasts were incubated in DM alone or with 0.1 and 0.4 mg/ml whey protein. The expression of MyoD, myogenin, and Myf-5 mRNA was measured using QRT-PCR. As shown in Figure 1, whey protein increased the expression of MyoD, Myf5, and Myogenin in C2C12 myoblasts. The mRNA levels of these genes were significantly higher in the experimental group as compared with the control group. These data suggest that whey protein regulates myogenic differentiation by influencing the MRF transcript levels.

Table 1. Enzymatic activity of two marker enzymes of differentiation.

Activity	Control	0.1 mg/ml whey	0.4 mg/ml whey
CK(U/mg·prot)	2.61 ± 0.12	3.94 ± 0.25*	5.87 ± 0.39+
CS(μmol/mg·min)	41.7 ± 3.09	53.2 ± 3.22	68.4 ± 4.41*

Data are expressed as means ± SE.
* Statistically significant difference from Control (P < 0.05).
+ Significantly different from Control (P < 0.01).

miRNA expression

There was no difference in the level of expression for miRNA-206, which was 2.6-fold higher in the low-dose group relative to the control group. As shown in Figure 2, expression of miRNA-1 and miRNA-206 increased by ~2.5-fold in response to whey protein, whereas miRNA-133a expression increased by ~1.7-fold. In contrast to the other miRNA, miRNA-206 and miR-133a expression did not change significantly after the low-dose treatment. The observed change in miRNA expression suggested there would be a similar change in the expression of the mature muscle-specific miRNAs, miR-1, miR-133a, and miR-206.

PI3K/AKT signaling pathways

Given our results, we sought to determine whether whey protein induces signaling pathways such as that of PI3K/AKT. In serum-starved C2C12 cells, AKT phosphorylation on amino acid Ser473 was upregulated after incubation with whey protein in an elevated manner. AKT phosphorylation was induced in C2C12 cells in a dose-dependent manner (Figure 3). Whey protein induced the phosphorylation of AKT phosphorylation sites, Ser473 and Thr308, both are required for full kinase activity. This phosphorylation was completely abolished in the presence of the specific PI3K inhibitor LY294002. LY294002 treatment completely abolished the whey-induced AKT phosphorylation, implying the requirement of PI3K activation for this response. Increases in protein synthesis require activation of the translational machinery and in addition may consist of indirect effects after stimulation of gene transcription. To test whether AKT phosphorylation is required for whey protein's stimulatory effect on myoblast protein synthesis, C2C12 myoblasts were treated with 0.1 and 0.4 mg/ml whey protein for 24 h with or without Ly294002, a stable PI3K inhibitor, which was added 30 min before the whey protein addition. A western blot analysis for MHC (myosin heavy chain) revealed that Ly294002 addition prevented the whey-induced MHC levels in C2C12 cells (Figure 3).

In the absence of LY294002, treatment with 0.4 mg/ml whey protein increased baseline protein synthesis compared to untreated controls for Serine and Threonine phosphorylation, respectively. These results indicate a strong impact of PI3K on baseline protein synthesis. The whey-induced increase in protein synthesis was reduced by LY294002 above the corresponding control conditions, indicating that PI3K contributes to whey protein-induced protein synthesis.

The whey-induced PI3K-dependent AKT phosphorylation is required for whey's promotive effect on the

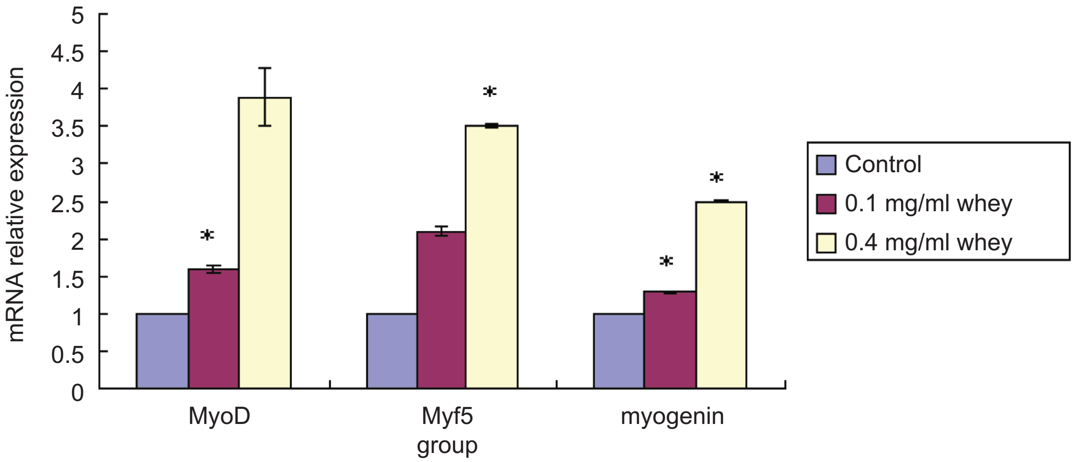

Figure 1. Whey protein increases markers of myogenic differentiation. C2C12 myoblasts were incubated in the absence or presence of whey protein at various concentrations for 24 h, and mRNA expression levels of myogenin, MyoD, and Myf5 were analyzed by quantitative real-time PCR using GAPDH as an internal control. *Statistically significant difference from Control (P < 0.05).

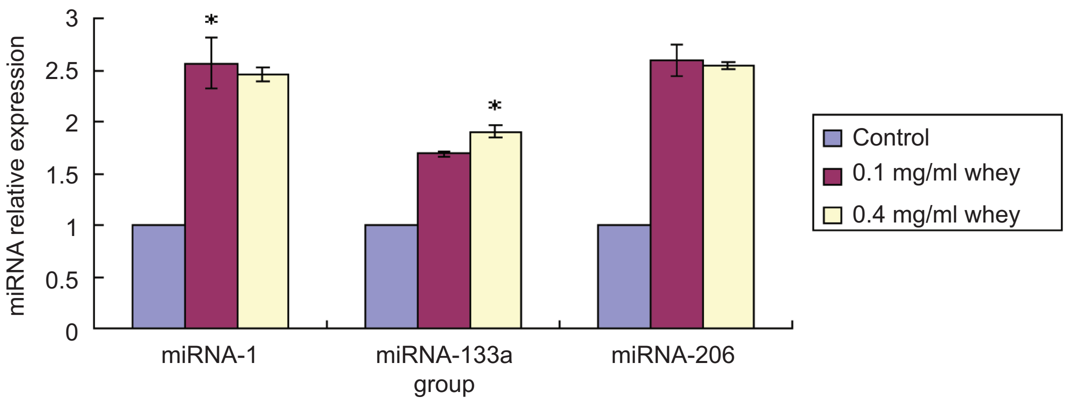

Figure 2. Whey protein increases the expression of muscle-specific miRNA. C2C12 myoblasts were incubated in the absence or presence of whey protein at various concentrations for 24 h, and miRNA expression levels were analyzed by fluorescence quantitative real-time PCR using U6 as an internal control. *Statistically significant difference from Control (P < 0.05).

differentiation of myoblasts. Taken together, these data suggest that whey protein has a beneficial effect on adult skeletal muscle, both during normal growth and under stress conditions.

Discussion

Our study demonstrates that whey protein promotes general protein accretion, muscle-specific gene expression, and myoblast fusion during myogenic differentiation. Moreover, our data suggest that stimulation of these processes by whey protein relies on positive regulation of AKT because increased AKT phosphorylation and a subsequent increase in MHC protein were observed in response to whey protein. In the enzymatic assay of CK and CS, the well-known and accepted markers of differentiation, cultures treated with a differentiation medium showed a higher activity, evidencing a higher degree of differentiation. As expected, a dose-dependent promotion in both CK and CS activity was seen in the presence of whey protein in C2C12 cultures. Many literatures (Griffen *et al.*, 2022; Thalacker-Mercer *et al.*, 2020) have shown that whey protein can promote muscle hypertrophy because it contains branched-chain amino acids. In the pre-experiment, we found that when whey protein concentration was 0.1 mg/ml, it showed an effect compared with the control group, so we chose these two doses (0.1 and 0.4 mg/ml).

Skeletal muscle differentiation can be regulated by at least three possible mechanisms, which include alteration in

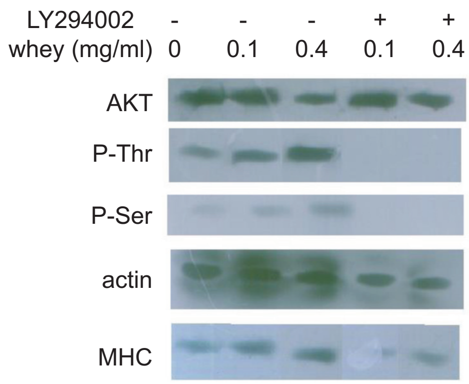

Figure 3. The PI3K/Akt pathway is induced by whey protein. Akt phosphorylation of serum-starved C2C12 myoblasts in response to various concentrations of whey protein. Akt phosphorylation was analyzed by western blot with the anti-phospho-Akt antibody followed by densitometric analysis normalized to levels of β-actin. The western blot analysis for MHC in C2C12 cells treated for 24 h with different concentrations of whey protein without or with LY294002 (25 μM).

protein degradation, mRNA stabilization, and gene transcription. Although evidence exists to support the first two mechanisms (Lee *et al.*, 2019; Vaisid and Kosower, 2013), modulation in gene expression appears to be most important during differentiation. This occurs via the activation of various phosphatases and kinases, which in turn alter the activity of downstream regulatory factors such as MEF2, Myf-5, myogenin, MyoD, serum response factor, and nuclear factor of activated T cells. Since the presence of whey protein increased the transcripts of MyoD, myf-5, and myogenin (Figure 1) and also promoted the protein synthesis of MHC in myoblasts (Figure 3), our data suggest that the increased myogenesis is the result of increased transcription of MRFs.

The current investigation was undertaken as an initial survey of muscle-specific miRNA expression in response to whey-induced differentiation to determine if these novel *trans*-factors have a potential role in adult skeletal muscle hypertrophy. The results of this study comprehensively provide the first evidence of miRNAs functions during whey-induced muscle hypertrophy and the foundation for future studies directed at elucidating the role of specific miRNAs during muscle growth. The possibility that miR-206 may have a role in the regulation of skeletal muscle hypertrophy is supported by a recent study demonstrating that miR-206 contributes to the hypertrophic phenotype of Texel sheep (Qin *et al.*, 2017). Quantitative trait loci mapping revealed Texel sheep have a single nucleotide polymorphism (SNP) within the 3′-UTR of the myostatin gene that results in the formation of a functional miR-1/miR-206 target site.

miR-1, miR-133a, and miR-206 are transcribed during myogenesis and seem to be regulated by MyoD and myogenin (Rosenberg *et al.*, 2006). miR-206 is transcribed independently of miR-1 and miR-133a, which are transcribed as a common pri-miRNA precursor from the miR-1/miR-133a locus, followed by alternative splicing to generate different primary transcripts (Taylor and Hughes, 2017). This is consistent with the present finding that miR-1 and miR-133a expression showed similar patterns in their induction and increase during differentiation. These observations suggested that miR-206 might be induced by MyoD whereas miR-1 and miR-133a might be induced by myogenin, as the onset and temporal sequence of miR-206 and miR-1/miR-133a expression seem to coincide with those of MyoD and myogenin expression during myogenesis. After their induction by MyoD and myogenin, however, other factors must be involved in the expression of these miRNAs at later stages.

The challenge for future studies will be to identify relevant target genes of each muscle-specific miRNA and how they contribute to the regulation of skeletal muscle growth and phenotype. Further studies are needed to address these complex regulatory roles of miRNAs, and the identification of bona fide, biologically relevant targets for miRNAs will be an important goal for miRNA researchers in the future.

Whey protein has been observed to influence muscle strength via various mechanisms, such as decreasing protein degradation and attenuating the proteosome–ubiquitin degradation pathway on the one hand, and increasing protein synthesis on the other. Taken together, our findings suggest that, at least in culture, whey protein can drive C2C12 myoblasts into the cell cycle, thus acting as a mitogen in these cells. The differential response of C2C12 cells to whey protein suggests this mitogen's species-specific effect. Many investigators have reported the stimulatory effect of essential amino acids on mRNA translation (Sans *et al.*, 2021), which generally relies on the enhanced activity of the ribosomal protein S6 kinase (S6K1) resulting from signaling through the PI3K/Akt/mTOR pathway.

Whey protein increased the protein levels of MHC in a dose-dependent manner. The signaling pathways through which whey protein exerts its effects are not fully understood. In this study, we demonstrate for the first time the promotive effect of whey protein on AKT phosphorylation and the requirement of this pathway to mediate its effects, as demonstrated by employing specific inhibitors. By blocking the PI3K/AKT pathway with specific inhibitors, we demonstrate that this pathway is required in mediating the promotive effect of whey protein on muscle cell differentiation. The crucial role of AKT in myogenic differentiation and hypertrophy induced by whey protein has been well demonstrated in this study.

Recent studies have reported that a class III PI3K mediates the amino acid activation of the mammalian target of rapamycin (mTOR) and its downstream molecules, which is distinct from the effect of insulin (Kwak *et al.*, 2016). Our findings indicate that whey protein fully activates AKT by inducing phosphorylation on both Thr308 and Ser473, while the latter phosphorylation is inhibited by LY294002, a specific PI3K inhibitor. However, we cannot rule out the possibility that whey protein activates the mTOR/p70S6k pathway in a manner similar to other amino acids.

Therefore, we believe that the promotive effects, shown here, of whey protein on muscle cell differentiation, together with its previously demonstrated anti-catabolic effects, justify its supplement as a therapeutic strategy to prevent muscle loss in myopathies as well as in aging and trauma. However, together with mRNA content, it could be expressed by showing the differences in cell morphology and quantifying the level of index fusion of the number of nuclei by another measurement method. Moreover, the PI3K/AKT axis such as p38 MAPK could also be discussed and we would have a great interest in it in the future.

Acknowledgments

This project was sponsored by the research project of Hebei Education Department, China (ZC2021230).

Conflict of Interest

There are no conflicts of interest.

References

Aoyama, S., Hirooka, R., Shimoda, T. and Shibata, S., 2019. Effect of different sources of dietary protein on muscle hypertrophy in functionally overloaded mice. Biochemistry and Biophysics Reports. 20: 100686–100693.

Dogra, C., Changotra, H., Mohan, S. and Kumar, A., 2006. Tumor necrosis factor-like weak inducer of apoptosis inhibits skeletal myogenesis through sustained activation of nuclear factor-kappaB and degradation of MyoD protein. Journal of Biological Chemistry 281: 10327–10336. https://doi.org/10.1074/jbc.M511131200

Griffen, C., Duncan, M., Hattersley, J., Weickert, M.O., Dallaway, A. and Renshaw, D., 2022. Effects of resistance exercise and whey protein supplementation on skeletal muscle strength, mass, physical function, and hormonal and inflammatory biomarkers in healthy active older men: a randomised, double-blind, placebo-controlled trial. Experimental Gerontology 158: 111651–111657. https://doi.org/10.1016/j.exger.2021.111651

Hernández-Hernández, J.M., García-González, E.G., Brun, C.E. and Rudnicki, M.A., 2017. The myogenic regulatory factors, determinants of muscle development, cell identity and regeneration. Seminars in Cell & Developmental Biology 72: 10–18. https://doi.org/10.1016/j.semcdb.2017.11.010

Kwak, S.S., Kang, K.H., Kim, S., Lee, S., Lee, J.-H., Kim, J.W., Byun, B., Meadows, G.G. and Joe, C.O.et al, 2016. Amino acid-dependent NPRL2 interaction with Raptor determines mTOR Complex 1 activation. Cellular Signalling 28(2): 32–41. https://doi.org/10.1016/j.cellsig.2015.11.008

Lee, S.-J., Bae, J.H., Lee, H., Lee, H., Park, J., Kang, J.-S. and Bae, G.-U., 2019. Ginsenoside Rg3 upregulates myotube formation and mitochondrial function, thereby protecting myotube atrophy induced by tumor necrosis factor-alpha. Journal of Ethnopharmacology 242: 112054–112059. https://doi.org/10.1016/j.jep.2019.112054

Motaei, J., Yaghmaie, M., Ahmadvand, M., Pashaiefar, H. and Kerachian, M.A., 2019. MicroRNAs as potential diagnostic, prognostic, and predictive biomarkers for acute graft-versus-host disease. Biology of Blood and Marrow Transplantation 25(12): e375–e386. https://doi.org/10.1016/j.bbmt.2019.08.004

Qin, Y., Peng, Y., Zhao, W., Pan, J., Ksiezak-Reding, H., Cardozo, C., Wu, Y., Pajevic, P.D., Bonewald, L.F., Bauman, W.A. and Qin, W. et al, 2017. Myostatin inhibits osteoblastic differentiation by suppressing osteocyte-derived exosomal microRNA-218: a novel mechanism in muscle-bone communication. Journal of Biological Chemistry 292(26): 11021–11033. https://doi.org/10.1074/jbc.M116.770941

Rommel, C., Bodine, S.C., Clarke, B.A., Rossman, R., Nunez, L., Stitt, T.N., Yancopoulos, G.D. and Glass, D.J., 2001. Mediation of IGF-1-induced skeletal myotube hypertrophy by PI(3)K/Akt/mTOR and PI(3)K/Akt/GSK3 pathways. Nature Cell Biology 3: 1009–1013. https://doi.org/10.1038/ncb1101-1009

Rosenberg, M.I., Georges, S.A., Asawachaicharn, A., Analau, E. and Tapscott, S.J., 2006. MyoD inhibits Fstl1 and Utrn expression by inducing transcription of miR-206. Journal of Cell Biology 175: 77–85. https://doi.org/10.1083/jcb.200603039

Sans, M.D., Crozier, S.J., Vogel, N.L., D'Alecy, L.G. and Williams, J.A., 2021. Dietary protein and amino acid deficiency inhibit pancreatic digestive enzyme mRNA translation by multiple mechanisms. Cellular and Molecular Gastroenterology and Hepatology 11(1): 99–115. https://doi.org/10.1016/j.jcmgh.2020.07.008

Seale, P. and, Rudnicki, M.A., 2000. A new look at the origin, function, and "stem-cell" status of muscle satellite cells. Developmental Biology 218: 115–124. https://doi.org/10.1006/dbio.1999.9565

Taylor, M.V. and Hughes, S.M., 2017. Mef2 and the skeletal muscle differentiation program. Seminars in Cell & Developmental Biology 72: 33–44. https://doi.org/10.1016/j.semcdb.2017.11.020

Thalacker-Mercer, A., Riddle, E. and Barre, L., 2020. Chapter two – protein and amino acids for skeletal muscle health in aging. Advances in Food and Nutrition Research 91: 29–64. https://doi.org/10.1016/bs.afnr.2019.08.002

Vaisid, T. and Kosower, N.S., 2013. Calpastatin is upregulated in non-immune neuronal cells via toll-like receptor 2 (TLR2) pathways by lipid-containing agonists. Biochimica et Biophysica Acta (BBA) – Molecular Cell Research 1833(10): 2369–2377. https://doi.org/10.1016/j.bbamcr.2013.06.006

Wang, J., Yang, L.Z., Zhang, J.S., Gong, J.X., Wang, Y.H., Zhang, C.L., Chen, H. and Fang, X.T., 2018. Effects of microRNAs on skeletal muscle development. Gene 668: 107–113. https://doi.org/10.1016/j.gene.2018.05.039

Zhang, H., Wang, Y., Tang, X., Dou, S., Sun, Y., Zhang, Q. and Lu, J., 2021. Combinatorial regulation of gene expression by uORFs and microRNAs in Drosophila. Science Bulletin 66(3): 225–228. https://doi.org/10.1016/j.scib.2020.10.012

Italian Journal of Food Science, 2022; 34 (2): 50–66

Exploring the potential of bottle gourd (*Lagenaria siceraria*) flour as a fat mimetic in biscuits with improved physicochemical and nutritional characteristics and anti-diabetic properties

Syed Muhammad Ghufran Saeed[1], Syed Arsalan Ali[1*], Rashida Ali[1,2,3], Syed Asad Sayeed[2] and Lubna Mobin[1]

[1]Department of Food Science and Technology, University of Karachi, Karachi, Pakistan; [2]Department of Food Science and Technology, Jinnah Women University, Karachi, Pakistan; [3]English Biscuits Manufacturer (Pvt.) Limited, Korangi Industrial Area, Karachi, Pakistan

***Corresponding Author:** Syed Arsalan Ali, Department of Food Science and Technology, University of Karachi, Karachi, Pakistan. Email: 786syedarsalanali@gmail.com

Received: 20 October 2020; Accepted: 12 May 2021; Published: 28 April 2022
© 2022 Codon Publications

OPEN ACCESS CC BY NC SA

PAPER

Abstract

Bottle gourd (*Lagenaria siceraria*) is a naturally rich source of several phytochemicals that play a vital role in the prevention of diseases. In the present study, the effect of bottle gourd flour (BGF) as a fat mimetic in biscuits at different concentrations (10, 15, 20, 25, and 50% w/w) was explored. Rheological properties, the microstructure of dough, bioactive compounds, anti-diabetic potential, storage stability, and the nutritional, physical, and sensory properties of samples were investigated. The addition of BGF in wheat flour (WF) showed increased water absorption (58.70–72.43%) and reduced dough stability time (11.71–5.01 min). Trough (1165.11–1096.10 Torque) and set back viscosities (471.21–448.09 Torque) decreased significantly ($P \leq 0.05$) with the increased level of BGF in WF. Furthermore, gluten content was also reduced. The baking process decreased the IC_{50} values, although total phenol content and total flavonoid content decreased. Shelf life study of 2 months revealed no significant ($P \leq 0.05$) difference in bioactive compounds, and alpha-amylase inhibition activity of fat-replaced biscuits. Moreover, the anti-hyperglycemic activity of BGF-WF biscuits in human subjects also showed positive results. The percentage increase in both peroxide value (0.2–2.87 milliequivalent O_2/kg of fat) and free fatty acid (0.1–0.9%) during storage was significantly ($P \leq 0.05$) lower than control biscuits (0.9–5.53 mill-equivalent O_2/kg of fat and 0.2–1.1%), which correlates to the enhanced activity of bioactive compounds in BGF-WF biscuits, which in turn relates to decreasing the rate of oxidation. The crude fiber and protein contents of BGF-WF biscuits were improved from 0.21 to 17.30% and 11.20 to 18.70%, respectively. Sensory and textural performance exhibited that the biscuits were acceptable after fat replacement of up to 15% BGF. Based on this study, BGF may be suggested as an excellent natural fat replacer to be used in nutraceuticals and functional foods.

Keywords: anti-diabetic potential; antioxidant; bottle gourd flour; dough rheology; physical properties; sensory profile

Introduction

Obesity is one of the biggest challenges of the present world. People are becoming highly conscious of their body weight due to the increased risk of obesity-linked diseases like diabetes mellitus, hypertension, cardiovascular disease, and cancer. Possible ways to control obesity are reducing the intake of fat, sugar, salt, limiting kilocalories in the daily diet, and increasing the consumption of high fiber vegetables and fruits. That's why ingredients that could replace fats and sugars are being extensively explored for applications in food industries.

Lagenaria siceraria is the most popular fruit vegetable throughout the world. It belongs to the family Cucurbitaceae and is commonly called as Bottle gourd (BG) or Lauki. Among the different vegetables grown in India and Pakistan, BG is more commonly consumed because it is inexpensive and well-known for its medicinal properties (Attar and Ghane, 2019). Several studies have revealed that BG served as an antidiabetic and anticancer agent. Besides, BG is also used to treat various neurological disorders like Alzheimer's disease. Nutritional evaluation reveals that it is a rich source of various nutrients such as vitamin B, C, pectin, fibers, beta-carotene, amino acids, proteins, and glycosides (Attar and Ghane, 2019). Its pulp and seeds have been used to manufacture different food products; high fiber and protein-rich biscuits were prepared by incorporating BG seed powder in wheat flour (Patel and Pradhan, 2015). In another study, BG pulp was used for the preparation of BG sweet meat and was evaluated for sensorial and textural properties (Saini and Sharma, 2018). On the basis of its diverse functional properties, bottle gourd flour (BGF) can be considered as a great source of fat mimetic. For instance, the presence of the nonpolar compounds confers lipid-soluble flavor-carrying capacity while polar groups facilitate water-binding, which together help to generate creaminess and lubricity in foods similar to that found in full-fat products (Saeed *et al*., 2020a).

Numerous studies have been conducted based on the utilization of dietary fiber or inulin as a fat replacer in biscuits and analyzed for its chemical, physical, and sensory properties. Saeed *et al.* (2021) studied the effect of fat replacement by date pit flour on the rheological and other quality parameters of the biscuits. Furthermore, Saeed *et al.* (2020c) studied the utilization of lotus root flour as a fat replacer in biscuits, while Roman *et al.* (2015) proved that extruded wheat flour paste with the addition of emulsifier could be an active fat replacer in cakes formulation.

Although some studies have demonstrated favorable health effects of bakery products that contain fat replacer or fat mimetic components, no information is available on the use of BGF as a fat mimetic. Therefore, this study was proposed to evaluate the functional properties of BGF and the effect of its incorporation at different levels (10–50%) on the physicochemical properties, rheological properties, microstructure of dough, nutritional profile, physical parameters (dimensional, color, and textural), and sensorial attributes of biscuits. Furthermore, the dough and biscuits were evaluated for their antioxidant activity, bioactive compounds, antidiabetic properties, and storage stability, so that new type of functional biscuits with optimum sensory and nutritional benefits could be introduced at the industrial level.

Materials and Methods

Raw materials

Commercial wheat flour (WF) made from wheat *Triticum aestivum* sp. *vulgare* (hexaploid) was received from Graib Sons Private Limited, Karachi. Icing sugar, BG, whole fresh egg, and salt were purchased from the local market of Karachi. Semi-solid fat (partially unsaturated) was purchased from Paracha Mills Ghee Textile Unit, Karachi. Glucose, sodium bicarbonate, and soy lecithin were obtained from Sulop Chemicals located in Karachi. All chemicals used for the study were of analytical reagent grade procured from Dae-Jung Chemicals, South Korea and Sigma-Aldrich, Germany.

Preparation of BGF

The BGs were thoroughly washed in distilled water, peeled, and then deseeded. BG was manually cut into thin slices of thickness 0.002 cm and dried in a hot air oven (DSO-300 D, digisystem laboratory instruments, Taiwan) at 60°C for 8 h. Dried BG flakes were milled by a laboratory miller (3100, Perten Instruments) and then passed through a sieve of 60 μm. The fine bottle gourd flour (BGF) was stored in airtight glass bottles at 4°C. Varying concentrations of BGF [10, 15, 20, 25, and 50% (w/w)] were added to wheat flour as a fat mimetic to have sample flours of varying wheat to BGF ratios, represented as BGF-WF.

Proximate composition

Proximate profiles of BGF-WF blends were analyzed according to the method of Ali *et al.* (2018). Moisture was determined by moisture analyzer (Brabender 51–55, CW Brabender, Duisbury, NJ, USA). Protein and ash contents were estimated by Brabender Kernelyzer (Brains Instruments, Germany). Fat content was estimated by AACC Method 30-25 (AACC, 1999). Carbohydrate content was calculated by subtracting the contents of protein, fat, ash, and moisture from 100. Wet gluten (WG), dry gluten (DG), gluten index (GI), and total gluten contents (TGC) were estimated by Glutomatic (2200, Perten Instruments). Each sample was tested in triplicates for proximate analysis.

Dough rheological properties

The effect of the incorporation of BGF in wheat flour in various concentrations on rheological properties was studied by using Farinograph (mixer bowl 300g, Brabender OHG, Duisburg, Germany) by the AACC

Method 54-21(AACC, 2000). The parameters measured include water absorption (WA), dough development time (DDT), the degree of softening (DoS), dough stability time (DST), and farinograph quality number (FQN).

Pasting properties of flour

The pasting properties were studied by Microvisco-amylo-graph (Brabender, Duisburg, Germany) according to the AACC Method 22-10 (AACC, 2000). The parameters measured for each sample included the average values for peak viscosity (PV), final viscosity (FV), and breakdown and setback viscosities.

Functional properties

Water absorption capacity (WAC) and oil absorption capacity (OAC) of flour samples were determined by the method of Saeed *et al.* (2020a). Briefly, the WAC was determined by taking 1 g of the flour sample in a 20 mL centrifuge, and 10 mL of distilled water was added to it; the mixture was vortexed for 2 min. The tube was centrifuged at 2200×g for about 20 min and the supernatant was decanted while the residual pellets were weighed and analyzed for WAC. The same procedure was used to determine OAC using 10 mL soya bean oil.

Micromorphology of biscuits dough

The microstructure of biscuit dough was evaluated using Scanning Electron Microscope (JOEL, Analysis system, Model # JSM-6380, Japan), as described by Ali *et al.* (2018). Briefly, the samples were first frozen at −20°C, then transferred into a freeze dryer (Laboratory Freeze Dryer VaCo 2, Germany), which operated at −50°C and 0.1m Pa. Freeze-dried dough samples were cut transversally into slices with a sharp blade without damaging the structure. Samples were mounted on the sample holder and sputter-coated with gold (2 min, 2 mbar). Scanning electron microscopic (SEM) studies were carried out on an applied voltage of 15 KV at 500´ magnification.

Biscuit preparation

Formulations of biscuits samples are presented in Table 1. Control and BGF-WF biscuits were prepared by incorporating different levels of fat. For the preparation of biscuit samples, fat was replaced from the recipe by BGF at concentrations of 10, 15, 20, 25, and 50%. The standard biscuits recipe was followed, which consists of flour 100 g (VMF and wheat flour mixed according to different ratios of fat replacement), sugar 40 g, fat 40 g, salt 0.5 g, egg 13.4 g, glucose 0.5 g, sodium bicarbonate1 g, soya lecithin 0.25 g, and water 20±5 mL. Biscuit samples were prepared, as reported by Ali *et al.* (2018). Briefly describing, the dough was sheeted at a fixed thickness of 7.2 mm and was cut into circular shapes using a biscuit cutter having a fixed diameter of 36.3 mm. Biscuits were baked at 180°C for 15 min in an oven. About 25 biscuits were baked per batch, and each batch was prepared in triplicates.

Antioxidant activity and phytochemicals

Antioxidant activity of BGF-WF blends, BGF-WF biscuits, and control biscuits was determined by free radical scavenging activity and ferric reducing power. Extracts of BGF-WF blends, control, and BGF-WF biscuit samples were prepared by the method of Saeed *et al.* (2021). The blends of BGF-WF and biscuit powder (control and BGF-WF) were added to methanol at a concentration of 60 mg/mL, 125 mg/mL, 185 mg/mL and 250 mg/mL, and the mixtures were analyzed.

2,2-diphenyl-1-picrylhydrazyl-DPPH radical scavenging activity

The technique mentioned by Saeed *et al.* (2020c) with slight modification was utilized for determining the

Table 1. Composition of biscuits prepared from bottle gourd flour (BGF).

S.No.	Ingredients (g)	Control	BGF (10%)	BGF (15%)	BGF (20%)	BGF (25%)	BGF (50%)
1	Flour	100	100	100	100	100	100
2	Fat	40	36	34	32	30	20
3	Icing Sugar	40	40	40	40	40	40
4	Egg	13.4	13.4	13.4	13.4	13.4	13.4
5	Soya Lecithin	0.25	0.25	0.25	0.25	0.25	0.25
6	Baking Powder	1	1	1	1	1	1
7	Salt	0.5	0.5	0.5	0.5	0.5	0.5
8	Glucose	0.5	0.5	0.5	0.5	0.5	0.5
9	Water	20±5	20±5	20±5	20±5	20±5	20±5
10	BGF	–	4	6	8	10	20

antioxidant activity of extracts of BGF-WF blends, control, and BGF biscuits. 2, 2-diphenyl-1-picrylhydrazyl (DPPH) solution was prepared by dissolving 33.9 mg of DPPH in 100 mL of methanol. One milliliter of each of the prepared samples (having concentrations of 60 mg/mL, 125 mg/mL, 185 mg/mL, and 250 mg/mL) was mixed with 1 mL of DPPH solution in a test tube and was placed in the dark for about 30 min. Absorbance (Abs) values were estimated at the wavelength of 517 nm using a spectrophotometer (Perkin Elmer, Lambda 25, and UV-Vis Spectrophotometer). The percentage scavenging activity was determined as follows.

$$\text{Scavenging activity }\% = \frac{\text{Abs of control} - \text{Abs of sample}}{\text{Abs of control}} \times 100 \quad (1)$$

Ferric/Ferricyanide (Fe^{3+}) reducing antioxidant power

Ferric/Ferricyanide reducing antioxidant power (FRAP) values of the samples were analyzed according to the method of Gawlik-Dziki *et al.* (2014) with slight modification adapted by Saeed *et al.* (2021). Perl's Prussian color was measured at an absorbance of 700 nm, where the increase in Abs is an indication of increased antioxidant activity.

Total phenolic content

Total phenolic content (TPC) of samples were determined by using Folin–Ciocalteu reagent, as described by Salar and Purewal (2017). The Abs of the extracts was recorded at 765 nm against a blank, and the results were expressed as milligram Gallic acid equivalent/100 g (mg GAE/100g) of the extract on dry weight (dw) basis obtained from the standard calibration curve.

Total flavonoid content

TFC of BGF-WF and biscuit samples were determined by the method of Gbenga *et al.* (2018). The Abs of the extracts was measured at 510 nm using Catechin as standard, and results were expressed as milligram Catechin Equivalent (mg CAE)/100 g of the extract on dry dw basis.

In vitro alpha-amylase inhibition in BGF biscuits

Alpha-amylase inhibition test by Elshibani *et al.* (2020) based on the starch–iodine technique was used to determine the *In-Vitro* enzyme inhibition in BGF biscuits. Abs was estimated at a wavelength of 630 nm .The alpha-amylase inhibitory activity was determined as follows:

$$\text{Inhibition of alpha} - \text{Amylase } (\%) = \frac{\text{Abs sample} - \text{Abs control}}{\text{Abs sample}} \times 100 \quad (2)$$

where Abs control is the Abs of all reagents except the test sample, and Abs sample is the absorbance of the test sample. All the experiments were carried out in triplicates.

Anti-hyperglycemic of BGF biscuits In-vivo

The anti-hyperglycemic activity of biscuits was determined in human subjects using the oral glucose tolerance test (OGTT) according to the method of Fombang and Saa (2016). Incremental area under the blood glucose response curve (IUAC) was calculated according to the method recommended by the Food and Agricultural Organization (1998).

Glycemic Index value was calculated as follows:

$$\text{Glycemic index (GI)} = \frac{\text{IUAC for the test food}}{\text{IUAC for the standard food}} \times 100 \quad (3)$$

Evaluation of changes in biscuits during storage

BGF biscuits and control biscuits were stored at room temperature (27 ± 2) in an air tight container at relative humidity of 67%. After every 15 days, shelf life study was performed for 2 months. And, biscuits samples were analyzed for free fatty acid value (FFA), peroxide value (PV), antioxidant activities, total phenolic content (TPC), total flavonoid content (TFC), and water activity (a_w)

Determination of free fatty acid (FFA) and Peroxide value (PV)

The FFA content of biscuit samples were analyzed by AOAC Method Cc 5a-40 (AOAC, 2001). The FFA content was calculated as the percentage of oleic acid according to the following equation:

$$\text{FFA as }\%\text{Oleic acid} = \frac{\text{ml NaOH} \times \text{NaOH normality} \times 28.2}{\text{Weight of sample (g)}} \quad (4)$$

PV of biscuit samples was analyzed by the AOAC Method Cd 8-53, (AOAC, 2001)

Evaluating the effect of storage changes on antioxidants, alpha amylase inhibition, and phytochemicals

The impact of storage conditions on the antioxidant activity was determined by FRAP and DPPH tests, while alpha amylase inhibition, TPC, and TFC were determined as described earlier in the above sections (2.9 and 2.10).

Water activity to evaluate the possibility of microbial growth

Water activity (a_w) of biscuits samples was determined in two duplicates of each formulation, using a Decagon

Aqua Lab meter (Pullman, WA, USA) at room temperature (25 ± 2°C), calibrated with a saturated potassium acetate solution (a_w = 0.22) (Saeed *et al.*, 2020a). Sufficient amount of sample was taken in the sample holder, and precaution was taken so that the sample does not touch the sensor.

Evaluation of biscuits quality

Color analysis

Color was measured according to the method of Saeed *et al.* (2020b) by using NH3 Colorimeter (China). Color values L*, a*, and b* were recorded, each value being the average of four measurements at different points of the biscuits. L* value represents the lightness variable from 100 for perfect white to zero for black, while as a* and b* values are the chromaticity values that indicate (+) redness/(-) greenness and (+) yellowness/(-) blueness, respectively.

Textural analysis

Biscuits sample were studied for the effect of fat mimetic on its breaking strength (hardness) and fracturability using texture analyzer (UTM, Zwick/Roell, Germany) as per the method described by Kuchtová *et al.* (2018) utilizing three points bend rig technique (Load cell: 5 kg, pre-test speed: 1.0 mm/s, test speed: 5.0 mm/s, post-test speed: 10.0 mm/s, distance: 10 mm, trigger force: 50 g).

Dimensional analysis

The diameter or the width of biscuits was measured with the help of a venire caliper (twice by rotating the biscuit at 90°C). The thickness of biscuits was measured by stacking three biscuits on top of one another and the total height was divided by three to get the average value. The spread ratio of biscuits was calculated from the fraction of diameter and thickness (Kohajdová *et al*., 2014).

Nutritional analysis

Nutritional analysis of samples included the analysis of protein, fat, carbohydrate, ash, moisture, crude fiber, and kilocalories. Protein and ash contents were determined by the Kjeldahl apparatus (Thermo Fisher Scientific) and Muffle furnace (Thermo Fisher Scientific), respectively, according to AACC Methods 08-01 and 46-10, respectively (AACC, 2000). Fat content and crude fiber were determined by the Soxhlet apparatus (Thermo Fisher Scientific) and Fiber digester (Marconi, MA-444, Brazil), respectively, by using AACC Methods 30-25 and 32-10, respectively (AACC, 2000). Moisture content was determined by moisture analyzer (Brabender 51–55, CW Brabender, Duisbury, NJ, USA). The total carbohydrate was determined by difference: Carbohydrate = 100 − (% moisture + % protein + % fat + % ash + % crude fiber). Calories were measured by applying the Atwater general factor system: carbohydrate (4 Kcal/g), lipid (9 Kcal/g), and protein (4 Kcal/g).

Sensory evaluation

Sensory examination was carried out in the baking laboratory following the method of Ali *et al.* (2018). Biscuit samples were evaluated by 40 trained panelists, male and female (age 24–45), comprising mainly of students and staff members of the Department of Food Science and Technology, University of Karachi (Karachi, Pakistan). The panelists were trained by utilizing the sensory profiles method (Lawless and Heymann, 2010) with the commercial biscuits and prototypes prepared in the baking laboratory. By means of this training, a specific terminology for the sensory characteristics and ranges for each attribute was agreed upon. The trained sensory panel passed the basic taste test, the odor test, and the color vision test, and their evaluation capacity were routinely verified by way of individual control cards. Panelists used 9 points hedonic scale (1 = extremely dislike to 9 = extremely like) for analyzing the desirability of biscuit samples for taste, color, appearance, texture, and overall acceptability

Statistical analysis

All the analyses were performed in triplicate and the average value was calculated. The results were expressed as mean ± standard deviation. The data were analyzed by analysis of variance (ANOVA) using SPSS (Version 17.0. Inc, Chicago, USA) statistical program. Duncan's multiple range test (DMRT) was applied to identify any significant differences among the treatments at $P \leq 0.05$. Furthermore, DMRT involves the computation of numerical boundaries that allow for the classification of the difference between any two treatment means as significant or nonsignificant. This requires calculation of a series of values each corresponding to a specific set of pair comparisons.

Results and Discussion

Proximate composition

Table 2 illustrates proximate compositions of BGF-WF blends. The moisture content of the refined wheat flour (14.1%) was slightly higher compared to the BGF-WF blends which ranged from 11.9 to 12.9%, and the decrease in moisture was due to less moisture content of raw BGF (8.01%) (Table 12). The increased ash content (0.93 to 2.02%) was due to the presence of a high amount of minerals in BGF than in the wheat flour. Similar results were reported by Saeed *et al*. (2020b) when black gram flour was incorporated in wheat flour as fat replacer. Since

Table 2. Effect of bottle gourd flour (BGF) addition on proximate and chemical properties of wheat flour.

Samples	Moisture content %	Ash %	Protein %	Gluten		
				Dry gluten	Wet gluten	Gluten index
Wheat flour	14.10 ± 0.13[e]	0.43 ± 0.01[a]	9.81 ± 0.10[a]	9.20 ± 0.2[d]	25.83 ± 0.26[e]	95.00 ± 1.2[d]
BGF 10%	11.91 ± 0.11[a]	0.93 ± 0.03[b]	13.82 ± 0.15[b]	9.00 ± 0.18[d]	24.00 ± 0.22[d]	92.00 ± 1.42[f]
BGF 15%	12.10 ± 0.12[b]	0.98 ± 0.05[b]	14.10 ± 0.18[bc]	8.80 ± 0.16[c]	24.20 ± 0.25[d]	88.00 ± 1.21[e]
BGF 20%	12.21 ± 0.10[b]	1.05 ± 0.08[c]	14.42 ± 0.19[c]	8.40 ± 0.15[bc]	23.60 ± 0.21[c]	86.00 ± 1.08[c]
BGF 25%	12.50 ± 0.13[bc]	1.09 ± 0.09[c]	14.91 ± 0.19[d]	8.30 ± 0.13[b]	18.70 ± 0.19[b]	84.00 ± 1.06[b]
BGF 50%	12.90 ± 0.12[d]	2.02 ± 0.09[d]	18.52 ± 0.21[e]	7.70 ± 0.11[a]	11.30 ± 0.14[a]	78.00 ± 1.03[a]

Values expressed are the mean ± standard deviation (n = 3). Means in the column with different superscripts are significantly (P ≤ 0.05) different.

protein in BGF has remarkable water holding property, the percentage moisture, WAC (%), and farinograph WA increased correspondingly (Table 3–4); the same results were observed by Saeed *et al.* (2020b). The wheat flour contained less protein content (9.8%) than the BGF as increasing the amount of BGF in wheat flour significantly increased (P ≤ 0.05) the protein content (13.8 to 18.5%). Gluten content (dry and wet) and gluten index also decreased as the level of incorporation of BGF increased in wheat flour, which might be due to dilution of gluten network which was also confirmed by micrograph scanning images (Figure 1). All these findings were in agreement with the study conducted by Saeed *et al.* (2020b).

Table 3. Functional properties of wheat flour and different ratios of bottle gourd flour (BGF) incorporated in wheat flour.

Samples	WAC%	OAC%
Wheat flour	145.61 ± 2.08[a]	153.03 ± 2.05[g]
BGF	500.16 ± 3.52[g]	100.21 ± 1.1[a]
BGF 10%	150.26 ± 2.11[b]	152.36 ± 2.25[f]
BGF 15%	157.42 ± 2.15[c]	150.22 ± 2.1e
BGF 20%	164.26 ± 2.05[d]	148.36 ± 1.05[d]
BGF 25%	170.26 ± 2.11[e]	146.81 ± 1.17[c]
BGF 50%	199.32 ± 2.57[f]	137.34 ± 1.11[b]

Values expressed are the mean ± standard deviation (n = 3). Means in the column with different superscripts are significantly (P ≤ 0.05) different. WAC, water absorption capacity; OAC, oil absorption capacity.

Functional properties

Water absorption and oil absorption capacities

WAC and OAC are the critical functional properties of the food ingredients because they determine the texture, mouthfeel, and yield of the product (Ram and Singh, 2004). Table 2 represents the WACs of BGF-WF blends. The WAC ranged from 146 to 162%. The highest WAC was observed for BGF 50% (162%) followed by BGF 25% (155.43%) and lowest for BGF 10% (146%). The study revealed that more the amount of BGF incorporated, the more was the resultant WAC. In previous research, purple rice flour incorporated in wheat flour also showed similar behavior (Klunklin and Savage, 2018). Hence, result suggested that the addition of BGF to wheat flour affected the amount of water absorption, as BGF competes with wheat flour for water absorption, which may be due to the difference in chemical composition and structure of the BGF. Probably, carbohydrate structure and the polarity of amino acids are responsible for the WAC (Saeed *et al.*, 2021).

The OAC ranged from 100.2 to 137.3% in BGF-WF blends. OAC of the raw BGF was determined as 100%, whereas wheat flour showed maximum OAC, i.e., 153.03%. The data reported in Table 2 proved that OAC of BGF decreased with the increase in their concentration in wheat flour. Similar findings were reported by Klunklin and Savage (2018). Generally protein contains both hydrophobic and hydrophilic groups which are responsible for oil and water absorption (Saeed *et al.*, 2021), which is also proved by our results as the amount of BGF increased in wheat flour, degree of nonpolarity, and hydrophobicity decreased so did the OAC. Hence, BGF contains more water interactive proteins.

Dough rheological properties

Table 4 presents the dough mixing properties of BGF-WF blends. A continuous increase in WA (63.6 to 72.4%) and stability time was observed with increased amount of BG. Increased WA was probably due to the presence of dietary fiber in BGF. Similar findings of WA and stability were reported by Ahmad*et al.* (2015) when different ratios of green tea powder were incorporated in wheat flour. DDT and DoS also increased with the inclusion of BGF in wheat flour. The increase in DDT is due to the rise in WA of the dough. In general, high WA means excellent baking performance. On the other hand, wheat flour showed lower DDT, lower DoS, and higher DST (except BGF10%) than the BGF-WF blends. Inconsistency in the mixing properties of flour samples was attributed to an increase in fiber and protein content with the increased level of BGF (Bae *et al.*, 2014). Another reason could be the increased FQN, which gave a hardening effect to flour and strength to the dough and ultimately caused delay in DDT, DS, and DoS (Ali *et al.*, 2018).

Generally molecules of fat gives strength and elasticity to the dough matrix (Ali *et al.*, 2018). However, similar functions were performed by the protein moles of BGF in the absence of fat molecules.

Pasting properties of flour samples

The results of the pasting properties of wheat flour and BGF-WF blends are shown in Table 5. An increase in starch gelatinization was found with an increased amount of BGF in the wheat flour. It was due to the quick rupture of starch granules leading to lower pasting temperatures and higher paste consistency (Kuchtová *et al.,* 2018). Similar findings were reported when grape skin was added in the wheat flour (Kuchtová *et al.,* 2018). The highest peak viscosity was observed for BGF 10% and lowest for BGF 50% because of increment in nonstarch content (i.e., protein) upon addition of higher amount of BGF in wheat flour. The less breakdown viscosity was estimated for wheat flour which was related to the limited swelling of the starch granules. However, breakdown viscosity significantly (P ≤ 0.05) increased when the level of BGF increased in wheat flour. The final viscosity decreased with an increased amount of BGF which resulted in less potential for the formation of viscous paste (Kuchtová *et al.*, 2018). In addition, trough and set back viscosities decreased significantly (P ≤ 0.05) as the concentration of BGF increased in wheat flour. The decrease in trough and set back viscosities reflected the less retrogradation tendency and hence contributed to less staling rate of the biscuits (Saeed *et al.*, 2020b).

The microstructure of biscuits dough

The micrograph of the control biscuits dough showed (Figure 1A) a thin sheet representing protein matrix along with small and large starch granules embedded in it. SEM image of dough with BGF 10% (Figure 1B) was very similar to control biscuit dough; however, with the gradual increase in the concentration of BGF in dough

Table 4. Farinograph properties of wheat flour and different ratios of bottle gourd flour (BGF) incorporated.

Samples	WA (%)	DDT (min)	DST (min)	DoS (ICC)	FQN
Wheat flour	58.70 ± 0.2[a]	1.67 ± 0.01[a]	8.58 ± 0.18[d]	35.12 ± 0.90[a]	88.21 ± 1.12[e]
BGF 10%	63.61 ± 0.20[b]	2.21 ± 0.04[b]	11.71 ± 0.18[e]	78.11 ± 1.11[b]	136.31 ± 1.52[f]
BGF 15%	64.52 ± 0.33[c]	5.20 ± 0.08[c]	5.10 ± 0.15[a]	129.10 ± 0.81[c]	65.01 ± 1.10[b]
BGF 20%	64.90 ± 0.51[c]	5.71 ± 0.03[d]	5.01 ± 0.11[a]	143.09 ± 1.72[d]	62.72 ± 1.11[a]
BGF 25%	65.83 ± 0.58[d]	5.82 ± 0.01[e]	6.01 ± 0.13[b]	153.32 ± 4.50[e]	72.01 ± 1.12[c]
BGF 50%	72.43 ± 0.81[e]	5.80 ± 0.01[e]	8.22 ± 0.16[c]	168.11 ± 3.21[f]	86.41 ± 1.14[d]

Means with different letters in superscript within a column differ significantly, calculated by the Duncan method (P ≤ 0.05). Each value was expressed as mean ± SD (n = 3). WA; water absorption, DDT; dough development time, DST; dough stability time, FQN; farinograph quality number.

Table 5. Microvisco-Amylo-Graph properties of wheat flour and different ratios of bottle gourd flour (BGF) incorporated.Means with different letters in superscript within a column differ significantly and are calculated by Duncan method (P ≤ 0.05), each value is expressed as mean ± SD (n = 3).

Samples	Gelatinization (Torque)	Peak viscosity (Torque)	Trough (Torque)	Final viscosity (Torque)	Breakdown (Torque)	Setback viscosity (Torque)	Pasting temperature (°C)
Wheat flour	24.01 ± 0.11[a]	1037.04 ± 10[a]	717.08 ± 4.11[a]	1542.32 ± 18.11[f]	378.18 ± 4.11[a]	479.21 ± 6.11[e]	57.91 ± 0.23[a]
BGF 10%	29.21 ± 0.32[d]	1253.10 ± 14[d]	1165.11 ± 11.01[b]	1367.11 ± 16.21[e]	456.14 ± 8.30[f]	471.21 ± 7.42[f]	76.01 ± 0.3[d]
BGF 15%	30.01 ± 0.40[e]	1222.01 ± 15[e]	1116.15 ± 12.13[d]	1299.12 ± 16.13[d]	466.13 ± 7.50[e]	493.41 ± 5.32[d]	81.13 ± 0.34[e]
BGF 20%	32.12 ± 0.60[f]	1221.13 ± 18[f]	1112.18 ± 13.10[e]	1240.21 ± 13.01[c]	485.13 ± 7.20[d]	481.71 ± 5.10[b]	81.13 ± 0.15[e]
BGF 25%	33.31 ± 0.21[b]	1217.30 ± 12[c]	1099.11 ± 14.10[f]	1120.91 ± 12.61[b]	551.15 ± 6.42[c]	457.14 ± 3.23[c]	72.04 ± 0.17[c]
BGF 50%	36.10 ± 0.36[c]	1215.11 ± 12[b]	1096.10 ± 10.00[c]	1131.12 ± 11.21[a]	613.19±5.11[b]	448.09±2.21[a]	68.03 ± 0.21[b]

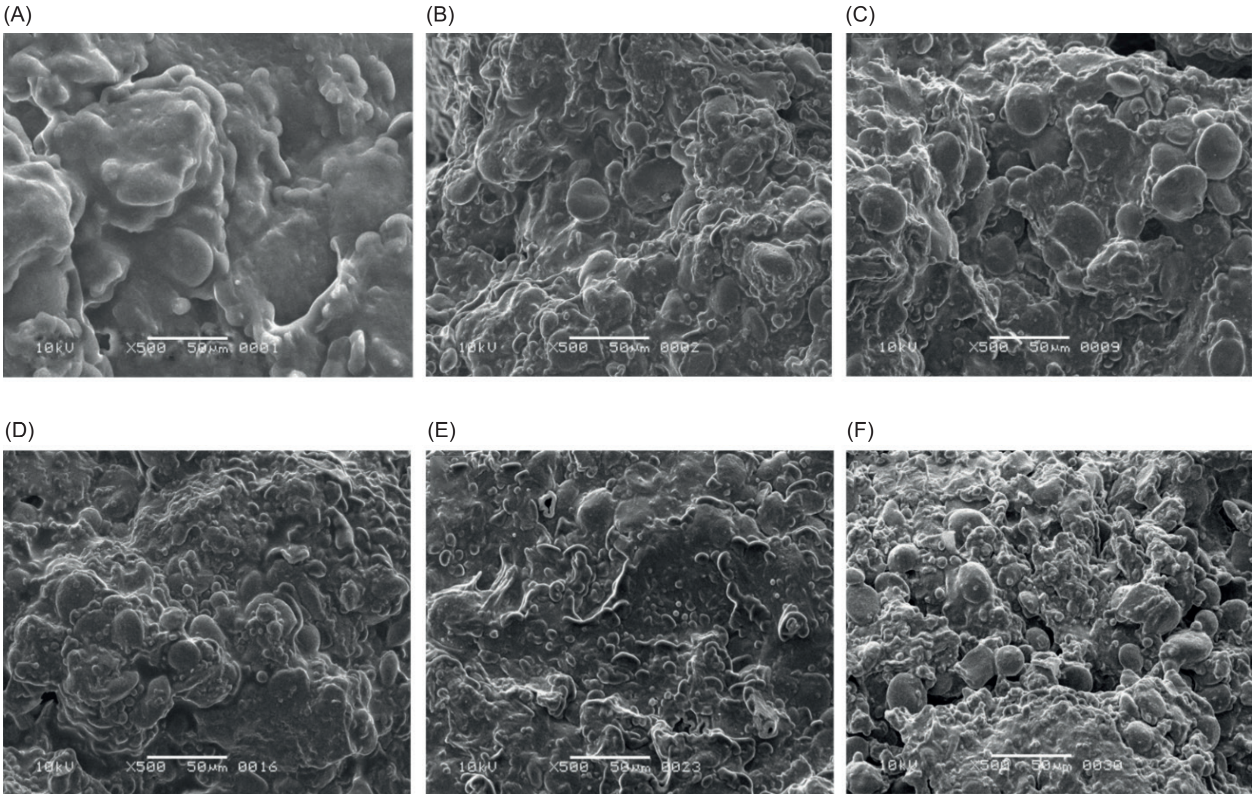

Figure 1. Scanning electron micrograph of biscuits dough (magnification, 500×): (A) control, (B) 10% bottle gourd flour, (C) 15% bottle gourd flour, (D) 20% bottle gourd flour, (E) 25% bottle gourd flour, and (F) 50% bottle gourd flour.

(Figure 1C), the BGF proteins were concentrated, and more and more large and small wheat starch granules were seen trapped in protein fibrils of BGF (Figure 1D and E). Similar observations were also depicted by Dachana *et al*. (2010) in their study on moringa leave powder which was used for the manufacturing of biscuits dough. Higher amount of fat substitution (Figure 1F) by higher level of fiber in BGF resulted in disrupted gluten matrix. Similarly, a reduction in gluten matrix was observed by Indrani *et al*. (2010) upon addition of 20% multi-grains. The literature revealed that even though microstructural properties of fat mimetics are quite different from fat when they are used to replace fat in food products, the end products show comparable qualities to the standard that is in agreement with our observations (Patel *et al*., 2020).

Free radical scavenging activity

The IC_{50} value of flour blends and biscuits samples are given in Tables 6 and 7, respectively. As predicted, the control biscuits demonstrated the lowest antioxidant activity and the IC_{50} value of BGF-WF biscuits reduced with the increment in the quantity of the BGF in biscuit samples. The increase in antioxidant activity of BGF-WF biscuits was probably due to the presence of bioactive compounds with hydrogen-donating ability such as vitamins, flavonoids, and phenols (Wojtunik-Kulesza *et al*., 2020). Results showed that storage time had no impact on antioxidant activity till the second week; however, it became obvious after the fourth week. Caleja *et al*. (2017) reported similar findings when fennel and chamomile extracts were used in biscuit samples; however, storage time did not influence antioxidant activity until the eighth week of storage. The development of antioxidative melanoidin pigments during baking further improved the free radical scavenging capacity (Sharma and Gujral, 2014). Similar observations were reported by Mabogo *et al.* (2021) when varying concentrations of unripe banana flour was incorporated in wheat-based biscuit samples.

Ferric/Ferricyanide (Fe^{3+}) reducing antioxidant power

The results of reducing the power of BGF-WF blends and biscuit samples are shown in Tables 6 and 7, respectively. FRAP value of biscuit samples increased with the incorporation of BGF. BGF-WF biscuits showed maximum reducing capacity, on the other hand, control biscuit samples demonstrated the highest IC_{50} value, hence the lowest reducing ability, which further became undetectable

Table 6. Antioxidant activity (DPPH and Ferric-reducing antioxidant power) and bioactive compounds (Total phenol content (TPC) and Total flavonoid content (TFC) of different levels of Bottle gourd flour (BGF)) incorporated in wheat flour.

Antioxidant activity			Bioactive compounds	
Samples	DPPH (IC_{50})	FRAP (IC_{50})	TPC (mg GAE/100 g DW)	TFC (mg CE/100 g DW)
Wheat flour	488.12 ± 3.15^{f}	327.21 ± 4.52f	16.73 ± 0.11^{a}	31.16 ± 1.01^{a}
BGF 10%	301.40 ± 1.29^{e}	127.35 ± 0.51^{e}	334.64 ± 1.18^{b}	174.82 ± 2.81^{b}
BGF 15%	245.62 ± 1.21^{d}	121.34 ± 0.21^{d}	437.81 ± 2.31^{c}	385.30 ± 2.14^{c}
BGF 20%	221.04 ± 1.01^{c}	89.32 ± 0.45^{c}	506.69 ± 3.42^{d}	456.83 ± 4.45^{d}
BGF 25%	200.60 ± 0.92^{b}	78.81 ± 0.13^{b}	543.37 ± 3.55^{e}	484.67 ± 4.61^{e}
BGF 50%	187.21 ± 0.43^{a}	57.62 ± 0.10^{a}	667.16 ± 3.81^{f}	583.65 ± 4.72^{f}

Means with different letters in the column differ significantly. They were calculated by the Duncan method ($P \leq 0.05$). Each value was expressed as mean ± standard deviation (n = 3), Nd, not detected.
Where, GAE, gallic acid equivalent. CE, catechin equivalent. dw, dry weight of the sample. Nd, not detected.

Table 7. DPPH radical scavenging activity, Ferric/Ferricyanide (Fe^{3+}) reducing antioxidant power (FRAP), and Alpha amylase inhibition about storage period at different levels of Bottle gourd flour (BGF) incorporated in biscuit samples.

Samples	Initial	Second week	Fourth week	Sixth week	Eighth week
DPPH-Scavenging activity- IC_{50} (mg/mL)					
Control	500.02 ± 3.15^{p}	Nd	Nd	Nd	Nd
BGF 10%	151.63 ± 1.29^{j}	152.12 ± 1.37^{jk}	166.44 ± 1.55^{l}	183.82 ± 1.82^{o}	185.02 ± 1.87^{o}
BGF 15%	139.91 ± 1.21^{i}	140.03 ± 1.23^{i}	154.24 ±1.28^{k}	178.87 ± 1.33^{m}	180.51 ± 1.41^{m}
BGF 20%	93.95 ± 1.01^{c}	93.98 ± 1.09^{c}	131.69 ±1.17^{gh}	167.87 ± 1.36^{l}	168.39 ± 1.21^{l}
BGF 25%	88.14 ± 0.92^{b}	88.94 ± 1.11^{b}	122.75 ±1.16^{f}	133.89 ± 1.25^{gh}	134.89 ± 1.28^{hg}
BGF 50%	68.36 ± 0.43^{a}	69.00 ± 0.81^{a}	96.56 ± 0.94^{d}	105.57 ± 1.11^{e}	108.55 ± 1.12^{e}
FRAP- IC_{50} (mg/mL)					
Control	350.14 ± 4.52^{o}	Nd	Nd	Nd	Nd
BGF 10%	52.44 ± 0.4^{i}	53.14 ± 0.42^{hij}	56.60 ± 0.44^{l}	59.74 ± 0.48^{m}	60.82 ± 0.52^{m}
BGF 15%	50.88 ± 0.3^{h}	52.88 ± 0.33^{h}	55.24 ± 0.36^{k}	57.45 ± 0.37^{l}	58.71 ± 0.44^{l}
BGF 20%	42.53 ± 0.15^{e}	43.24 ± 0.17^{e}	54.06 ± 0.25^{j}	55.40 ± 0.28^{k}	57.61 ± 0.31^{kl}
BGF 25%	33.87 ± 0.13^{d}	35.30 ± 0.1^{d}	45.08 ± 0.14^{f}	49.80 ± 0.17^{g}	50.13 ± 0.24^{g}
BGF 50%	12.69 ± 0.12^{a}	13.11 ± 0.11^{a}	22.51 ± 0.12^{b}	28.89 ± 0.14^{c}	29.14 ± 0.15^{c}
Alpha amylase inhibition -IC_{50} (mg/mL)					
Control	Nd	Nd	Nd	Nd	Nd
BGF 10%	105.78 ± 4.04^{i}	109.88 ± 4.21^{i}	121.56 ± 4.32^{l}	128.59 ± 4.41^{m}	132.02 ± 4.60^{n}
BGF 15%	96.50 ± 2.12^{g}	100.67 ± 3.11^{gh}	119.51 ± 3.20^{kl}	124.38 ± 3.28^{m}	128.51 ± 3.35^{m}
BGF 20%	62.42 ± 1.46^{c}	68.06 ± 1.52^{c}	92.22 ± 1.73^{f}	112.80 ± 3.00^{j}	120.62 ± 3.23^{l}
BGF 25%	50.04^{b} ± 1.57^{a}	54.94^{b} ± 1.40^{a}	89.15 ± 1.56^{e}	90.79 ± 2.12^{f}	100.50 ± 3.17^{h}
BGF 50%	47.94 ± 1.11^{a}	50.41 ± 1.70^{a}	80.81 ± 2.04^{d}	89.62 ± 2.09^{e}	93.02 ± 3.15^{fg}

Means with different letters in the row differ significantly. They are calculated by Duncan method ($P \leq 0.05$).
Each value expressed as mean ± SD (n = 3).
Nd, not detected.
Control represents biscuits without fat mimetic.

during storage. Results of storage stability also showed a similar pattern as that of DPPH for BGF-WF biscuits, there was no significant ($P \leq 0.05$) difference between the IC_{50} value of initial and second week of storage, although reducing power decreased from the fourth week of storage and further decreased to sixth week. However, there was no significant ($P \leq 0.05$) difference in IC_{50} values between sixth to eighth weeks of storage. Similar findings were reported by Caleja *et al.* (2017) when fennel and chamomile extracts were used in biscuit samples.

Like the DPPH test, baking further improves the FRAP as lower IC_{50} values were witnessed in biscuits (Table 7) when compared to flour samples (Table 6). An increase in reducing power upon baking has been reported by Mabogo *et al.* (2021) for biscuits prepared by incorporation of unripe banana flour in wheat flour.

Total phenolic content

Table 8 represents the TPC of BGF-WF biscuit samples during storage. Biscuits prepared with BGF 50% showed the highest TPC throughout the storage period of 8 weeks followed by BGF 25% and BGF 20%. It was observed that there is no significant ($P \leq 0.05$) difference between the first day and second week of storage. Although TPC reduced from the fourth week of storage, all BGF-WF biscuit samples have higher TPC as compared to control biscuit samples which exhibited the least TPC (18.56 mg GAE/100g dw). Despite greater decrease in TPC of BGF-WF biscuits during baking was found compared to BGF-WF blends (Table 6), the TPC value in BGF-WF biscuits was still higher than that of control biscuits. Jan *et al.* (2015) also found a decrease in TPC of buckwheat flour when heated to a temperature of 180°C. The decrease in TPC was may be due to alteration in the chemical structure of the phenolic compounds (Pintado *et al.*, 2021). In previous research, various natural sources of phenolic compounds were added to bakery products to increase the nutraceutical value (Pattnaik *et al.*, 2021).

Total flavonoid content

From Table 8, it can be observed that TFC in biscuit samples increased with the level of addition of BGF. Biscuits prepared with BGF 50% showed the highest TFC throughout the storage period of 8 weeks, followed by BGF 25% and BGF 20%. Natural flavonoid-containing ingredients were also added in bakery products to increase the bioactive compounds, as reported by many researchers; for instance, a study reported that biscuits prepared with water chestnut flour demonstrated enhanced TFC (Shafi *et al.*, 2016).

Inhibition of alpha-amylase activity In-vitro

The methanolic extract of BGF-WF biscuits samples showed significant ($P \leq 0.05$) inhibitory activity against alpha-amylase. From Table 7, it can be observed that IC_{50} values decreased with increasing ratio of BGF. The follow-up of storage changes in biscuits samples revealed that there was no significant ($P \leq 0.05$) change in enzyme inhibition up to 2 weeks of storage; however, IC_{50} of all BGF biscuits gradually increased after the second week of storage, and the inhibition activity was almost undetectable in control biscuits. Petrus *et al.* (2012) reported that antioxidant compounds such as catechin, phenolics, flavonoids, alkaloids, and triterpenoids possess anti-diabetic activity. Epicatechin, a flavonoid is known to possess insulin-like properties, while epigallocatechin gallate is

Table 8. Total phenol content (TPC) and total flavonoid content (TFC) concerning storage period at different levels of Bottle gourd flour incorporated in biscuit samples.

Samples	Initial	Second week	Fourth week	Sixth week	Eighth week
TPC-(mg GAE/100 g dw)					
Control	27.430^a ± 0.12	Nd	Nd	Nd	Nd
BGF 10%	326.66^f ± 2.18	323.33^f ± 1.31	255.5^c ± 1.14	230.00^b ± 1.12	225.50^b ± 1.1
BGF 15%	383.33^h ± 2.21	380.66^h ± 1.43	319.33^e ± 1.25	280.00^d ± 1.21	278.00^d ± 1.08
BGF 20%	413.83^j ± 3.12	410.88^j ± 1.97	391.66^i ± 1.45	371.66^g ± 1.32	368.50^g ± 1.11
BGF 25%	525.00^p ± 3.15	520.00^p ± 2.48	469.33^n ± 2.35	421.66^k ± 3.00	418.50^k ± 2.41
BGF 50%	638.33^q ± 3.21	634.00^q ± 3.11	486.00^o ± 3.07	460.00^m ± 3.17	454.16^l ± 3.04
TFC-(mg CE/100 g dw)					
Control	18.56^a ± 1.01	Nd	Nd	Nd	Nd
BGF 10%	104.32^e ± 2.21	100.84^e ± 1.44	90.24^c ± 1.25	76.16^b ± 1.23	74.24^b ± 1.22
BGF 15%	121.60^f ± 2.74	119.84^f ± 2.46	104.32^e ± 2.42	88.96^d ± 1.14	87.04^d ± 1.12
BGF 20%	380.51^i ± 3.45	376.66^i ± 3.21	338.83^h ± 3.19	330.5^g ± 3.14	326.66^g ± 3.11
BGF 25%	451.66^l ± 4.51	447.16^l ± 4.43	397.18^k ± 3.32	371.66^j ± 3.32	366.00^j ± 3.25
BGF 50%	558.33^n ± 4.82	552.00^n ± 4.89	460.00^m ± 4.61	397.16^k ± 3.41	394.00^k ± 3.33

Means followed by different letters in the raw differs significantly ($P \leq 0.05$). Calculations were made using the Duncan method. Each value is expressed as mean ± SD (n = 3), where GAE, gallic acid equivalent. CE, catechin equivalent. dw, dry weight of the sample. Nd, not detected.
*Control represents biscuits without fat replacement.

considered to be an effective hypoglycemic agent (Sun *et al*., 2020). Data reported in Table 8confirmed that BGF-WF biscuits have a significant ($P \leq 0.05$) amount of bioactive phenolics and flavonoids. Being inhibitors of alpha-amylase activity, these antioxidant compounds in the BGF biscuits could induce anti-diabetic potential in the biscuits and hence are helpful in controlling diabetes.

Anti-hyperglycemic of BGF biscuits In-vivo

Table 9 shows the mean blood glucose responses after the consumption of glucose and the test foods, that is, biscuits prepared with BGF 15% (selected due to good sensorial profile) and the control biscuits in healthy human subjects. The IAUC for glucose was found to be 143 mmol/L, and for BGF 15% and control were 31.05 mmol/L and 59.25 mmol/L, respectively. GI of control and BGF biscuits were 41.18 and 21.58, respectively. Although both Control and BGF biscuits contained an equal quantity of sugar, biscuits with BGF 15% significantly ($P \leq 0.05$) resulted in a lower glycemic response at the 120th minute of intake. Apart from phytochemicals, BG is a blend of soluble and insoluble fiber; however, impact on a glycemic level could be credited more for the presence of soluble fiber (Luan and Hong, 2016). The mechanism of action may be achieved through a reduction in both fasting blood glucose and insulin concentrations. This occurs because of water-soluble gel-forming fibers. These dietary fibers form a viscous solution in the small intestine, which reduces the contact and mixing of macronutrients with digestive enzymes, and this delays the absorption of glucose, which consequently reduces the postprandial plasma glucose and insulin levels (Mcrae, 2018). Another reason for decrease in blood glucose profile was credited to phenolics present in BGF-WF biscuits samples as these phenolic compounds are bioactive compounds with antioxidant potential, and hypoglycemic, hypolipidemic, and anti-tumor properties (Fombang and Saa, 2016). A similar trend of blood glucose modulation was observed in a study in which moringa tea was ingested by healthy human subjects for determination of glycemic response (Fombang and Saa, 2016). In previous research, various solvent extracts of BG have also been shown to exhibit antihyperglycemic activity in animal subjects, because of the presence of secondary metabolites; for instance, phenolic and flavonoids (Luan and Hong, 2016).

Peroxide value of biscuit samples

Figure 2A shows that PV was less than three mEq O_2/kg of fat for all the BGF biscuit samples during storage which is considered safe value according to Poilish Standard, PN-A-86908:1966. Less PVs of the BGF-WF biscuit samples were because of the two main reasons: first, the presence of antioxidants that contributed by controlling oxidation and hence peroxide formation. Second, fat replacement, the greater the amount of fat replaced by BGF, lesser the amount of fat that remained for the process of oxidation. In a previous study, addition of chokeberry polyphenols extract to butter cookies resulted in a higher PV than the recommended value after ninth week of storage (Bialek *et al*., 2016) which is contradictory to our findings. However, PV range after 6 weeks of preparing the biscuits with the addition of grape pomace extract was comparable to our findings (Zaky *et al*., 2020). There was a gradual increase of PV in all the BGF-WF biscuits samples during storage; on the other hand, control biscuits had the highest PV of 5.53 at the eight week of storage.

Free fatty acid in biscuit samples

Data reported in Tables 6, 7, and 8 demonstrated that BGF-WF blends and BGF-WF biscuits possessed significant ($P \leq 0.05$) antioxidant activity and hence were helpful for the inhibition of oxidation of fats in biscuits. During storage, increased FFA value was observed in all the biscuit samples. The increase was remarkably greater

Table 9. Blood glucose responses (mmol/L), incremental area under the curve (IUAC), and glycemic index (GI) in normal healthy volunteers following glucose, tested, and control biscuits.

Samples	Time Intervals (min)					IAUC	GI
	0	30	60	90	120		
Glucose	5.90 ± 0.13^b	7.83 ± 0.24^c	8.43 ± 0.25^c	5.74 ± 0.12^b	5.23 ± 0.1^b	143.00	–
BGF 15%	5.30 ± 0.11^a	5.45 ± 0.13^a	5.80 ± 0.16^a	5.63 ± 0.14^a	5.19 ± 0.1^a	31.05	21.58
Control*	5.96 ± 0.17^b	6.75 ± 0.22^b	6.83 ± 0.25^b	6.25 ± 0.18^c	5.91 ± 0.14^c	59.25	41.18

Means with different letters in the column differ significantly. They are calculated by the Duncan method ($P \leq 0.05$). Each value expressed as mean ± SD (n = 15 healthy female volunteers).
BGF, bottle gourd flour. IAUC, incremental area under the curve. GI, glycemic index.
*Control represents biscuits without fat mimetic.

in control (1.1%) as compared to BGF-WF biscuit samples. From Figure 2B, it was clear that initially the FFA was not detected in BGF-WF biscuit samples; however, a gradual increase (up to 0.9 %) was observed during storage indicating the capability of antioxidants present in BGF in reducing the formation of FFA. Therefore, the increment of FFA level in BGF biscuits was relatively slow. Similar observations were reported when a flavonoid-rich extract from green tea was incorporated in biscuit samples (Navaratne and Senaratne, 2014). Another study in which pomegranate peel was added in different ratios in biscuit samples was also in agreement with our findings (Ismail *et al.*, 2014). Hence, it can be concluded that BGF was capable of controlling the formation of FFA in biscuit samples when used as a fat mimetic.

Water activity to evaluate the possibility of microbial growth

Table 10 shows that an increase in the storage period increases the water activity of control and BGF-WF biscuits. The water requirement for the growth of microorganisms is expressed in terms of moisture available or water activity (Macedo *et al.*, 2020). In this study, even at 10% BGF, the water activity was found to be 0.58 at the eighth week of storage which assured the safety of product with respect to microbial profile (Morais *et al.*, 2018). Rodríguez *et al.* (2013) also reported a similar trend of decreased water activity when fat was replaced by inulin in biscuit samples. Lower water activity of BGF biscuits might be due to higher water-binding capacity of BGF, as less water evaporated during baking, and less free water remained in the biscuits, thus contributing to longer shelf life (Rodríguez *et al.*, 2013). No significant (P ≤ 0.05) change was observed in water activity of control and BGF biscuits from first day till the second week of storage. Although water activity increased after the fourth week of storage and this remained constant up to 8 weeks. Morais *et al.* (2018) also reported a similar trend of water activity in biscuit samples. The increased water activity can be attributed to the increased moisture of biscuits with respect to storage, but it remained limited under the value of 0.6 for 2 months to inhibit microbial growth

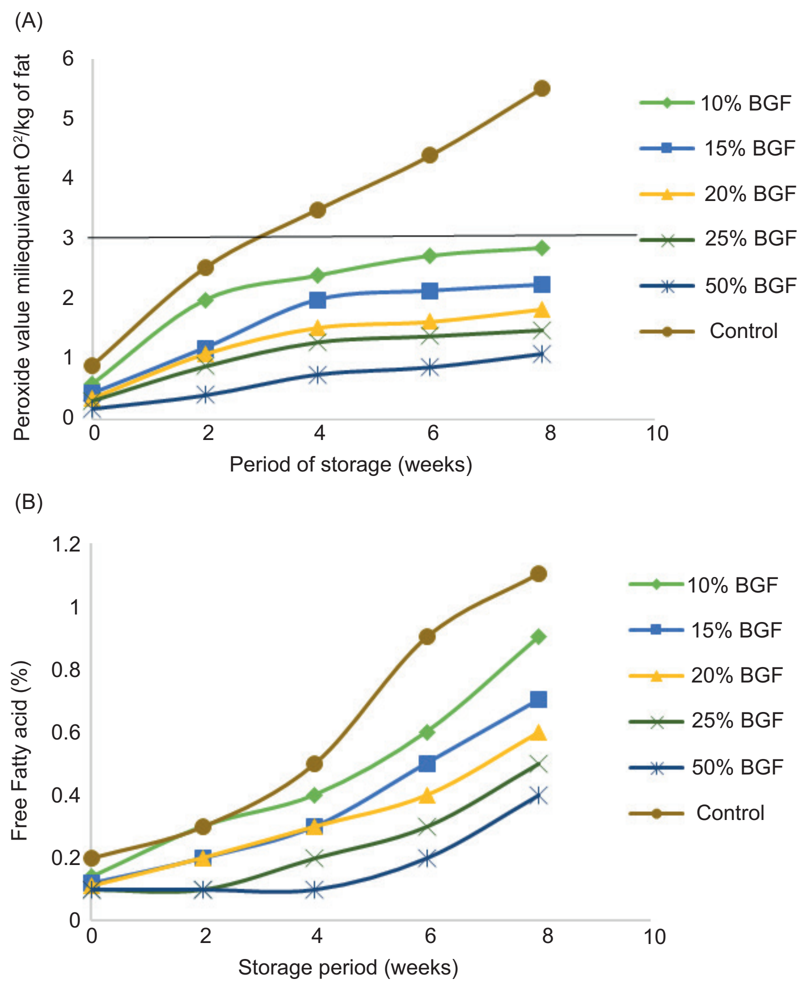

Figure 2. (A) Peroxide value levels in control and Bottle gourd flour incorporated biscuits stored for 2 months. (B) Free fatty acid (%) levels in control and bottle gourd flour incorporated biscuits stored for 2 months.

Table 10. Water activity concerning storage period at different levels of bottle gourd flour (BGF) incorporated in biscuit samples.

Samples	Initial	Second week	Fourth week	Sixth week	Eighth week
Control*	0.62 ± 0.02^{h}	0.61 ± 0.02^{h}	0.70 ± 0.02^{i}	0.71 ± 0.02^{i}	0.71 ± 0.02^{i}
BGF 10%	0.55 ± 0.08^{e}	0.55 ± 0.01^{e}	0.57 ± 0.04^{ef}	0.57 ± 0.02^{ef}	0.58 ± 0.01^{f}
BGF15%	0.52 ± 0.01^{d}	0.52 ± 0.03^{d}	0.56 ± 0.02^{ef}	0.56 ± 0.01^{ef}	0.56 ± 0.01^{ef}
BGF 20%	0.51 ± 0.02^{d}	0.52 ± 0.02^{d}	0.55 ± 0.05^{ef}	0.56 ± 0.02^{ef}	0.57 ± 0.01^{ef}
BGF 25%	0.47 ± 0.05^{c}	0.47 ± 0.08^{c}	0.50 ± 0.03^{d}	0.51 ± 0.02^{d}	0.51 ± 0.01^{d}
BGF 50%	0.35 ± 0.01^{a}	0.34 ± 0.01^{a}	0.38 ± 0.07^{b}	0.38 ±0.07^{b}	0.38 ± 0.01^{b}

Means with different letters in the row differ significantly (P ≤ 0.05). They are calculated by the Duncan method.
*Control represents biscuits without fat mimetic.

(Morais *et al*., 2018) and ensure product stability. On the other hand, water activity of control biscuits increased from 0.6 to 0.71 during 2 months of storage.

Physical properties of biscuit samples

Table 11 summarized the effects of the BGF as a fat mimetic on the physical properties of biscuits such as diameter, thickness, spread ratio, hardness, and fracturability. A standard decrease was observed in the diameter of fat mimetic biscuit samples, although biscuits prepared with BGF 10% and BGF 15% showed a maximum increase in diameter when compared with the control sample. In addition to this, biscuits containing BGF 10%, BGF 15%, and BGF 20% showed less thickness than control. BGF significantly (P ≤ 0.05) increased the spread ratio at the level of 10 and 15%, which was more than the control. Similarly, Kuchtová *et al*. (2018) and Mildner *et al*. (2013) reported an increase in the spread ratio of biscuit samples produced by incorporation of grape skin and white grape pomace, respectively. An increased amount of dietary fiber in BGF biscuits could be the reason for increased thickness, reduced diameter, and decreased spread ratio as a higher amount of fat was replaced with BGF. It has already been reported that the addition of dietary fiber from various sources and substitutes has a negative effect on the diameter, thickness, and spread ratio of biscuits/cookies (Saka *et al*., 2020). Another reason for the variation in these physical parameters could be the dilution of gluten network in biscuit dough (Kohajdová *et al*., 2014). Hardness and fracturability are textural properties that attract significant attention in the evaluation of baked goods; these parameters should be as low as possible (Saka *et al*., 2020). The increased amount of BGF from 10 to 15% resulted in considerable less hardness and fracturability; however, hardness increased when fat was replaced beyond 20%. This is possibly related to the high WAC of BGF, as it has been reported by Saeed *et al.* (2021) that components that enhance the water absorption of dough results in the development of the complex gluten network and ultimately hardens the texture of the biscuit samples.

Color characteristics of biscuits

Color plays an essential role in determining the quality of products in food processing industries and food engineering research (Palamthodi *et al*., 2019). Results of color measurements of biscuits made with different levels of BGF are given in Table 12. It was found that the lightness L* of the biscuits exhibited a decreasing trend with an increasing level of BGF. The reducing values of

Table 11. Effect of bottle gourd flour (BGF) on physical properties (dimension and texture) of biscuits.

Sample	Diameter (mm)	Thickness (mm)	Spread ratio (mm)	Breaking force (N)	Fracturability (mm)
Control*	42.67 ± 0.56^{d}	9.07 ± 0.52^{d}	4.71 ± 0.10^{d}	22.90 ± 0.39^{d}	2.10 ± 0.12^{b}
BGF 10%	42.74 ± 0.40^{e}	8.06 ± 0.2^{a}	5.30 ± 0.14^{f}	17.42 ± 0.2^{a}	0.87 ± 0.11^{a}
BGF 15%	42.84 ± 0.88^{f}	8.26 ± 0.20^{b}	5.18 ± 0.12^{e}	20.87 ± 0.23^{b}	0.90 ± 0.12^{a}
BGF 20%	41.74 ± 0.51^{c}	8.68 ± 0.21^{c}	4.67 ± 0.13^{c}	24.77 ± 0.30^{c}	2.45 ± 0.14^{c}
BGF 25%	41.59 ± 0.42^{b}	9.32 ± 0.24^{e}	4.37 ± 0.10^{b}	27.42 ± 0.41^{e}	2.74 ± 0.17^{d}
BGF 50%	40.78 ± 0.33^{a}	10.68 ± 1.02^{f}	3.81 ± 0.10^{a}	31.51 ± 0.44^{f}	2.81 ± 0.19^{e}

Values expressed are the mean ± standard deviation (n = 3). Means in the column with different superscripts are significantly (P ≤ 0.05) different.
*Control represents biscuits without fat mimetic.

Table 12. Effect of bottle gourd flour (BGF) on the color of biscuit samples.

Samples	L*	a*	b*
Control*	73.12 ± 0.82^{f}	6.13 ± 0.01^{a}	43.12 ± 0.21^{f}
BGF 10%	70.41 ± 0.67^{e}	6.91 ± 0.03^{b}	38.11 ± 0.15^{e}
BGF 15%	64.33 ± 0.34^{d}	7.30 ± 0.02^{c}	33.14 ± 0.13^{d}
BGF 20%	58.29 ± 0.13^{c}	7.81 ± 0.01^{d}	26.31 ± 0.10^{c}
BGF 25%	52.14 ± 0.11^{b}	8.11 ± 0.02^{e}	18.35 ± 0.10^{b}
BGF 50%	46.21 ± 0.10^{a}	10.32 ± 0.05^{f}	8.21 ± 0.06^{a}

Values expressed are the mean ± standard deviation (n = 4).
Means in the column with different superscripts are significantly (P ≤ 0.05) different.
*Control represents biscuits without fat mimetic.

L* indicated that the biscuits were darker at higher levels of BGF compared to the control sample. The effect might be due to the presence of natural pigments or the Maillard reaction products that were formed from amino acids and reducing sugars during baking (Mildner *et al.*, 2013). Furthermore, it was shown that the higher levels of BGF in biscuits increased redness (higher a* value) and decreased yellowness (lower b* value). This may be because BG contains a good amount of anthocyanin, a red-blue natural pigment (Palamthodi *et al.*, 2019). Kuchtová *et al.* (2018) and Sharma and Gujral (2014) reported a decrease in the color values of L*, an increase in redness a*, and decreased yellowness b* when grape seeds and buckwheat flour were incorporated in biscuits, respectively, and it is in agreement with our findings.

Nutritional analysis of biscuits

The nutrient composition of BGF, control, and fat mimetic biscuits are summarized in Table 13. BGF was found to be an excellent source of crude fiber (26.30%), protein (20.21%), and minerals (ash content 4.23%). All the fat mimetic biscuits showed higher protein, ash, and crude fiber contents than the control. As expected, fat content reduced with the level of addition of BGF than the control sample. As the concentration of BGF increased, the moisture content of biscuit samples reduced. According to Camelo-Méndez *et al.* (2018), moisture reduction was due to the decrease in the gluten network with the increase in the amount of BGF. The crude fiber, protein, and ash content increased with the increased amount of BGF in biscuit samples. The control sample showed a low value of crude fiber (6.0%) while the biscuits containing BGF 50% and BGF 25% possessed the highest crude fiber. The carbohydrate content and energy (Kcal) values were the highest in control (59.04% and 255.92 Kcal) and lowest in biscuits with BGF 50% (43.25% and 219.68 Kcal). Therefore, BGF biscuit samples showed less energy value and the reason was fat substitution.

Sensory characteristics of biscuits

Figure 3 presents the sensory scores of the biscuit samples (50% replacement of fat in biscuits excluded from the data reported because of the undesirable sensory profile). Biscuits with BGF10% demonstrated similar results as that of control sample in terms of taste, texture, color, and overall acceptability. On the other hand, at the level of BGF15%, score for color was higher than the control biscuits, although appearance, taste, texture, and overall acceptability were not significantly (P ≤ 0.05) different from control biscuits. As the level of BGF increased beyond 15%, taste which is one of the essential attributes, declined due to unpleasant mouthfeel, bitterness, and the texture also became harder. The bitterness was may be due to the interaction between a high amount of phenolic compounds in BGF and saliva present in the mouth (Kuchtová *et al.*, 2018) while the hard texture could be due to the low amount of fat in the biscuit recipe as fat

Table 13. Nutritional analysis of bottle gourd flour (BGF), control, and fat mimetic biscuits.

Samples	Moisture content %	Ash %	Protein %	Fat %	Dietary fiber %	Carbohydrate %	Kcal/100 g
Control*	5.02 ± 0.12^{a}	0.53 ± 0.01^{a}	11.20 ± 0.10^{a}	24.02 ± 0.20^{g}	0.21 ± 0.26^{a}	64.04 ± 0.80^{g}	517
BGF	8.01 ± 0.30^{d}	4.23 ± 0.10^{f}	20.21 ± 0.50^{f}	0.43 ± 0.01^{a}	26.30 ± 0.42^{f}	48.83 ± 0.30^{b}	280
BGF 10%	4.68 ± 0.14^{c}	2.73 ± 0.03^{b}	13.70 ± 0.12^{b}	20.21 ± 0.14^{f}	13.80 ± 0.20^{b}	49.56 ± 0.42^{c}	435
BGF 15%	4.68 ± 0.10^{c}	2.77 ± 0.01^{b}	13.90 ± 0.11^{bc}	19.11 ± 0.10^{e}	13.60 ± 0.11^{b}	50.62 ± 0.57^{d}	430
BGF 20%	4.65 ± 0.11^{b}	3.82 ± 0.02^{c}	13.60 ± 0.15^{b}	16.32 ± 0.21^{d}	14.00 ± 0.21^{c}	52.26 ± 0.64f	410
BGF 25%	4.64 ± 0.12^{b}	3.86 ± 0.06^{cd}	14.40 ± 0.20^{d}	15.01 ± 0.10^{c}	14.60 ± 0.13^{d}	52.13 ± 0.60e	401
BGF 50%	4.65 ± 0.13^{b}	3.87 ± 0.09^{ed}	18.70 ± 0.22^{e}	12.54 ± 0.11^{b}	17.30 ± 0.17^{e}	47.59 ± 0.54^{a}	378

Values expressed are the mean ± standard deviation (n = 3). Means in the column with different superscripts are significantly (P ≤ 0.05) different.
*Control represents biscuits without fat mimetic.

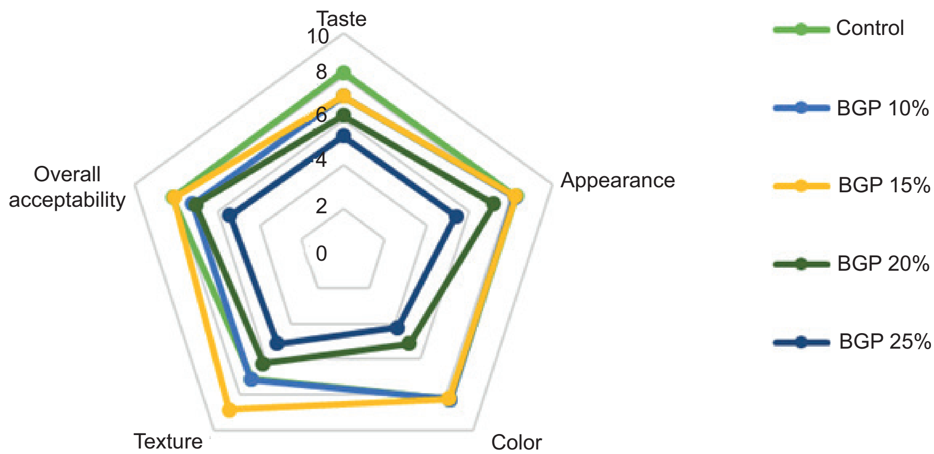

Figure 3. Effect of fat replacement by bottle gourd flour (BGF) on the sensorial quality of biscuits. Control represents biscuits without fat mimetic.

helps to lubricate and soften the structure of food and contributes desirable textural properties (Hasmadi *et al.*, 2014). Moreover, in the study conducted by Serin and Sayar (2017), maltodextrin and polydextrose were used as a fat replacer in biscuits which also resulted in increased hardness with the level of fat replacement.

Conclusion

The bakery industry is in constant innovation, and biscuits are products that are consumed worldwide by different classes of consumers. Therefore, the production of this type of product having nutraceutical effects may be attractive for consumers who are concerned about the choice of healthy foods. The result showed that the addition of BGF as a fat mimetic in the proportion of 10 to 15% produced desirable biscuits, and the functional properties of the wheat flour were not affected. BGF was observed to be an excellent source of phenolic and flavonoids, which makes it a valuable source of antioxidants. Incorporation of BGF raised the bioactive compounds in biscuits' enhanced antioxidant activity, and inhibited alpha-amylase. Biscuits with 15% BGF showed excellent physical properties and sensorial attributes. Therefore, administration of this formulation of biscuits in healthy volunteers for the determination of anti-hyperglycemic activity revealed a lower blood glucose response curve and glycemic index as compared to the control biscuits. Moreover, further studies are needed to improve the functional behavior and quality of biscuits.

Acknowledgment

The help of Ms. Uroosa Ejaz in proof reading of this manuscript is acknowledged. The authors are grateful to the University of Karachi for partial funding through a Dean Research Grant, and to English Biscuit Manufacturers management, particularly Dr. Zeelaf Munir and Madam Saadia Naveed, for their encouragement and support.

Ethics declarations

Conflict of interest

There is no conflict of interest.

Compliance with ethics requirements

This article contains *In-Vivo* studies with human participants (anti-hyperglycemic activity and sensory test).

References

AACC, 2000, Approved methods of the American Association Cereal Chemist, Chemist, edited, St. Pauls.

AACC,1999, Approved Methods of the American Association Cereal Chemist Chemist: St. Pauls.

Ahmad, M., Baba, W. N., A Wani, T., Gani, A., Gani, A. and Shah, U., 2015. Effect of green tea powder on thermal, rheological & functional properties of wheat flour and physical, nutraceutical & sensory analysis of cookies. Journal of Food Science and Technology. 52(9): 5799–5807. https://doi.org/10.1007/s13197-014-1701-3

Ali, R., Saeed, S.M.G., Ali, S.A., Sayed, S.A., Ahmed, R. and Mobin, L., 2018. Effect of black gram flour as egg replacer on microstructure of biscuit dough and its impact on edible qualities. Journal of Food Measurement and Characterization. 12(3): 1641–1647. https://doi.org/10.1007/s11694-018-9779-3

AOAC, 2001. Official methods of analysis of AOAC International, 16th ed., edited, The Association, Gaithersburg, MD.

Attar, U. and Ghane, S., 2019. In vitro antioxidant, antidiabetic, antiacetylcholine esterase, anticancer activities and RP-HPLC analysis of phenolics from the wild bottle gourd (Lagenaria siceraria (Molina) Standl.). South African Journal of Botonay. 125: 360–370. https://doi.org/10.1016/j.sajb.2019.08.004

Bae, W., Lee, B., Hou, G.G. and Lee, S., 2014. Physicochemical characterization of whole-grain wheat flour in a frozen dough system for bake off technology. Journal of Cereal Science. 60(3): 520–525. https://doi.org/10.1016/j.jcs.2014.08.006

Bialek, M., Rutkowska, J., Bialek, A. and Adamska, A., 2016. Oxidative stability of lipid fraction of cookies enriched with chokeberry polyphenols extract. Polish J Food and Nutrition Science. 66(2): 77–84. https://doi.org/10.1515/pjfns-2015-0027

Caleja, C., Barros, L., Antonio, A.L., Oliveira, M.B.P. and Ferreira, I.C., 2017. A comparative study between natural and synthetic antioxidants: evaluation of their performance after incorporation into biscuits. Food Chemistry. 216: 342–346. https://doi.org/10.1016/j.foodchem.2016.08.075

Camelo-Méndez, G.A., Agama-Acevedo, E., Rosell, C.M., Perea-Flores, M.D.J. and Bello-Pérez, L.A., 2018. Starch and antioxidant compound release during in vitro gastrointestinal digestion of gluten-free pasta. Food Chemistry. 263: 201–207. https://doi.org/10.1016/j.foodchem.2018.04.075

Dachana, K., Rajiv, J., Indrani, D. and Prakash, J., 2010. Effect of dried moringa (Moringa oleifera lam) leaves on rheological, microstructural, nutritional, textural and organoleptic characteristics of cookies. Journal of Food Quality. 33(5): 660–677. https://doi.org/10.1111/j.1745-4557.2010.00346.x

Elshibani, F., Alamami, A., Alshalmani, S., El Naili, E.A., Gehawe, H.A., Sharkasi, M.A. and Elremali, N., 2020. Estimation of phenolic content, flavonoid content, antioxidant properties and alpha-amylase inhibitory activities of Capparis spinosa L. Journal of Pharmacognocy and Photochemistry. 9: 24–28.

Fombang, E.N. and Saa, R.W., 2016. Antihyperglycemic activity of Moringa oleifera Lam leaf functional tea in rat models and human subjects. Food and Nutri Sci. 7(11): 1021. https://doi.org/10.4236/fns.2016.711099

Food and Agricultural Organization, 1998. Carbohydrates in human nutrition: report of a joint FAO. World Health Orginization. United States

Gawlik-Dziki, U., Świeca, M., Dziki, D., Sęczyk, Ł., Złotek, U., Różyło, R., Kaszuba, K., Ryszawy, D. and Czyż, J., 2014. Anticancer and antioxidant activity of bread enriched with broccoli sprouts. BioMed Research International. 2014: 608053. https://doi.org/10.1155/2014/608053

Gbenga-Fabusiwa, F. J., Oladele, E. P., Oboh, G., Adefegha, S. A. and Oshodi, A. A., 2018. Polyphenol contents and antioxidants activities of biscuits produced from ginger-enriched pigeon pea–wheat composite flour blends. Journal of Food Biochemistry. 42(4): e12526. https://doi.org/10.1111/jfbc.12526

Hasmadi, M., Matanjun, P., Salwa, I., Siti, F., Mansoor, A.H. and Ainnur, S.R., 2014. The effect of seaweed composite flour on the textural properties of dough and bread, J Applied Phycol. 26(2): 1057–1062. https://doi.org/10.1007/s10811-013-0082-8

Indrani, D., Soumya, C., Rajiv, J. and Venkateswara Rao, G., 2010. Multigrain bread–its dough rheology, microstructure, quality and nutritional characteristics. J of Texture Studies. 41(3): 302–319. https://doi.org/10.1111/j.1745-4603.2010.00230.x

Ismail, T., Akhtar, S., Riaz, M. and Ismail, A., 2014. Effect of pomegranate peel supplementation on nutritional, organoleptic and stability properties of cookies. International Journal of Food Sciences and Nutrition. 65(6): 661–666. https://doi.org/10.3109/09637486.2014.908170

Jan, U., Gani, A., Ahmad, M., Shah, U., Baba, W.N., Masoodi, F., Maqsood, S., Gani, A., Wani, I.A. and Wani, S., 2015. Characterization of cookies made from wheat flour blended with buckwheat flour and effect on antioxidant properties. Journal of Food Science and Technology. 52(10): 6334–6344. https://doi.org/10.1007/s13197-015-1773-8

Klunklin, W. and Savage, G., 2018. Physicochemical, antioxidant properties and in vitro digestibility of wheat–purple rice flour mixtures. International Journal of Food Science and Technology. 53(8): 1962–1971. https://doi.org/10.1111/ijfs.13785

Kohajdová, Z., Karovičová, J., Magala, M. and Kuchtová, V., 2014. Effect of apple pomace powder addition on farinographic properties of wheat dough and biscuits quality. Chemistry Papers. 68(8): 1059–1065. https://doi.org/10.2478/s11696-014-0567-1

Kuchtová, V., Kohajdová, Z., Karovičová, J. and Lauková, M., 2018. Physical, textural and sensory properties of cookies incorporated with grape skin and seed preparations. Polish Journal of Food and Nutrition Science. 68(4): 309–317. https://doi.org/10.2478/pjfns-2018-0004

Lawless, H.T. and Heymann, H., 2010. Sensory evaluation of food principles and practices, descriptive analysis, 2nd ed., Springer Science & Business Media, pp. 378–441. New York, USA.

Luan, N.K. and Hong, N.N., 2016. Antioxidant activity and anti-hyperglycemic effect of lagenaria siceraria fruit extract. Journal of Food Science and Engineering 6: 26–31. https://doi.org/10.17265/2159-5828/2016.01.004

Mabogo, F., Mashau, M. and Ramashia, S., 2021. Effect of partial replacement of wheat flour with unripe banana flour on the functional, thermal, and physicochemical characteristics of flour and biscuits. International Food Research Journal. 28: 138–147.

Macedo, L.L., Vimercati, W.C., da Silva Araújo, C., Saraiva, S.H. and Teixeira, L.J.Q., 2020. Effect of drying air temperature on drying kinetics and physicochemical characteristics of dried banana. Journal of Food Process Engineering 43: e13451. https://doi.org/10.1111/jfpe.13451

McRae, M. P., 2018. Dietary fiber intake and type 2 diabetes mellitus: an umbrella review of meta-analyses. Journal of Chiropractic Medicine. 17(1): 44-53. https://doi.org/10.1016/j.jcm.2017.11.002

Mildner-Szkudlarz, S., Bajerska, J., Zawirska-Wojtasiak, R. and Górecka, D., 2013. White grape pomace as a source of dietary fibre and polyphenols and its effect on physical and nutraceutical characteristics of wheat biscuits. Journal of the Science of Food and Agriculture 93(2): 389–395. https://doi.org/10.1002/jsfa.5774

Morais, M. P. d., Caliari, M., Nabeshima, E. H., BATISTA, J. E. R., CAMPOS, M. R. H. and Soares Junior, M., S. 2018. Storage stability of sweet biscuit elaborated with recovered potato starch from effluent of fries industry. Food Science and Technology. 38: 216–222. https://doi.org/10.1590/fst.32916

Navaratne, S. and Senaratne, C., 2014. Controlling of auto oxidation process of soft dough biscuits using flavonoids extracted from green tea (Camellia sinensis). International Journal of Science and Research. 3(4): 425–428.

Palamthodi, S., Kadam, D. and Lele, S., 2019. Physicochemical and functional properties of ash gourd/bottle gourd beverages blended with jamun. Journal of Food Science and Technology. 56(1): 473–482. https://doi.org/10.1007/s13197-018-3509-z

Patel, A.S. and Pradhan, R.C., 2015. Quality ranking of bottle gourd seed cake powder incorporated biscuits using fuzzy analysis of sensory attribute, BIOINFOLET-A Quarterly Journal of Life Sciences 12(4a): 901–908.

Patel, A. R., Nicholson, R. A. and Marangoni, A. G., 2020. Applications of fat mimetics for the replacement of saturated and hydrogenated fat in food products. Current Opinion in Food Science. 33: 61–68. https://doi.org/10.1016/j.cofs.2019.12.008

Pattnaik, M., Pandey, P., Martin, G.J., Mishra, H.N. and Ashokkumar, M., 2021. Innovative technologies for extraction and microencapsulation of bioactives from plant-based food waste and their applications in functional food development. Foods. 10: 279. https://doi.org/10.3390/foods10020279

Petrus, A., Hemalatha, S.S. and Suguna, G., 2012. Isolation and characterisation of the antioxidant phenolic metabolites of Boerhaavia erecta L. leaves. Jouranl of Pharmaceutical Science and Research. 4(7): 1856.

Pintado, T., Muñoz-González, I., Salvador, M., Ruiz-Capillas, C. and Herrero, A.M., 2021. Phenolic compounds in emulsion gel-based delivery systems applied as animal fat replacers in frankfurters: physico-chemical, structural and microbiological approach. Food Chemistry. 340: 128095. https://doi.org/10.1016/j.foodchem.2020.128095

Poilish Standard, P., 1966. Edible vegetable fats – refined vegetable oils. PN-A-86908.

Ram, S. and Singh, R., 2004. Solvent retention capacities of Indian wheats and their relationship with cookie-making quality. Cereal Chemistry. 81(1): 128–133. https://doi.org/10.1094/cchem.2004.81.1.128

Saeed, S.M.G., Ali, S.A., Ali, R., Naz, S., Sayeed, S.A., Mobin, L. and Ahmed, R., 2020a. Utilization of Vigna mungo flour as fat mimetic in biscuits: its impact on antioxidant profile, polyphenolic content, storage stability, and quality attributes. Legume Science 2: e58. https://doi.org/10.1002/leg3.58

Saeed, S.M.G., Ali, S.A., Ali, R., Sayeed, S.A., Mobin, L. and Ahmed, R., 2020b. Exploring the potential of black gram (Vigna mungo) flour as a fat replacer in biscuits with improved physicochemical, microstructure, phytochemicals, nutritional and sensory attributes. SN Applied Science. 2: 1–17. https://doi.org/10.1007/s42452-020-03797-6

Saeed, S.M.G., Tayyaba, S., Ali, S.A., Tayyab, S., Sayeed, S.A., Ali, R., Mobin, L. and Naz, S., 2020c. Evaluation of the potential of Lotus root (Nelumbo nucifera) flour as a fat mimetic in biscuits with improved functional and nutritional properties. CyTA-Journal of Food. 18: 624–634. https://doi.org/10.1080/19476337.2020.1812727

Saeed, S.M.G., Urooj, S., Ali, S.A., Ali, R., Mobin, L., Ahmed, R. and Sayeed, S.A., 2021. Impact of the incorporation of date pit flour an underutilized biowaste in dough and its functional role as a fat replacer in biscuits. Journal of Food Processing and Preservation. 45: e15218. https://doi.org/10.1111/jfpp.15218

Saini, C.S. and Sharma, H.K., 2018. Process development of bottle gourd sweetmeat by microwave heating: changes in rheological, textural, sensory and morphological parameters. Food Biosciences. 24: 95–102. https://doi.org/10.1016/j.fbio.2018.05.009

Saka, İ., Özkaya, H. and Özkaya, B., 2020. Potential utilization of bulgur bran as a source of dietary fiber in cookies. Cereal Chemistry. 97: 930–939. https://doi.org/10.1002/cche.10315

Salar, R. K. and Purewal, S. S., 2017. Phenolic content, antioxidant potential and DNA damage protection of pearl millet (Pennisetum glaucum) cultivars of North Indian region. Journal of Food Measurement and Characterization. 11(1): 126–133. https://doi.org/10.1007/s11694-016-9379-z

Serin, S. and Sayar, S., 2017. The effect of the replacement of fat with carbohydrate-based fat replacers on the dough properties and quality of the baked pogaca: a traditional high-fat bakery product. Food Science and Technollogy. 37: 25–32. https://doi.org/10.1590/1678-457x.05516

Shafi, M., Baba, W.N., Masoodi, F.A., Bazaz, R., 2016. Wheat-water chestnut flour blends: effect of baking on antioxidant properties of cookies. Journal of Food Science and Technology. 53(12): 4278–4288. https://doi.org/10.1007/s13197-016-2423-5

Sharma, P. and Gujral, H.S., 2014. Cookie making behavior of wheat–barley flour blends and effects on antioxidant properties. LWT-Food Science and Technology. 55(1): 301–307. https://doi.org/10.1016/j.lwt.2013.08.019

Sun, C., Zhao, C., Guven, E.C., Paoli, P., Simal-Gandara, J., Ramkumar, K.M., Wang, S., Buleu, F., Pah, A. and Turi, V., 2020. Dietary polyphenols as antidiabetic agents: advances and opportunities. Food Frontiers. 1: 18–44. https://doi.org/10.1002/fft2.15

Wojtunik-Kulesza, K., Oniszczuk, A., Oniszczuk, T., Combrzyński, M., Nowakowska, D. and Matwijczuk, A., 2020. Influence of in vitro digestion on composition, bioaccessibility and antioxidant activity of food polyphenols – a non-systematic review. Nutrients. 12: 1401. https://doi.org/10.3390/nu12051401

Zaky, A.A., Asiamah, E., El-Faham, S., Ashour, M. and Sharaf, A., 2020. Utilization of grape pomace extract as a source of natural antioxidant in biscuits. Eurpean Academic Research. 8: 108–126.

Italian Journal of Food Science, 2022; 34 (2): 67–73

Proximate analysis of lipid composition in Moroccan truffles and desert truffles

Fatima Henkrar[1]*, Lahsen Khabar[2]*

[1]Plant Biotechnology and Physiology Laboratory, Faculty of Sciences, University Mohammed V-Rabat, Morocco; [2]Botanical, Mycology and Environment Laboratory, Faculty of Sciences, University Mohammed V-Rabat, Morocco

***Corresponding Authors:** Fatima Henkrar, Plant Biotechnology and Physiology Laboratory, Faculty of Sciences, University Mohammed V-Rabat, Morocco. Email: f.henkrar@um5r.ac.ma; Lahsen Khabar, Botanical, Mycology and Environment Laboratory, Faculty of Sciences, University Mohammed V-Rabat, Morocco. Email: l.khabar@um5r.ac.ma

Received: 18 March 2022; Accepted: 17 May 2022; Published: 10 June 2022
© 2022 Codon Publications

OPEN ACCESS BY NC SA

PAPER

Abstract

Lipid composition in truffle is essential for nutraceutical and medicinal purposes. Currently, there is no data regarding the lipid content in Moroccan truffles. Therefore, we determined the fatty acid and sterol composition of six Moroccan truffles and desert truffles. The gas chromatography analysis revealed the predominance of fatty palmitic, oleic and linoleic acids. The prominent sterol components were brassicasterol and ergosterol. Besides, the sterol analysis discriminated between the *Tuber* and *Terfezia* truffles. These differences seem to be exploitable at a taxonomic level. This is a preliminary report disclosing the fatty acid and sterol composition of Moroccan truffles, indicating the potential use of lipids analysis, especially sterol analysis, as biomarker for truffles distinction.

Keywords: desert truffles, discrimination, fatty acid, gas chromatography, Moroccan truffle, sterol

Introduction

The truffles are edible ascocarp of hypogenous ascomycetes fungi that grow underground (Khabar *et al.*, 2001; Lee *et al.*, 2020). The term 'desert truffles' is used to describe truffles growing particularly in arid and semi-arid areas (Khabar *et al.*, 2001; Morte *et al.*, 2021), such as Morocco, Algeria, Tunisia, Egypt, South Africa, Saudi Arabia, Iraq, Syria and Kuwait (Khabar, 2014; Lee *et al.*, 2020). The genera found abundantly in those areas are *Terfezia* and *Tirmania*. Besides, other genera exist as well, namely *Delastria* and *Picoa* (Khabar, 2014). In Mediterranean countries, especially in North Africa, the truffles are harvested in abundance and known as 'Terfass,' also called 'Kame,' 'Kholassi,' 'Zoubaïdi,' 'Truffles of the deserts' and 'Truffles of the sands' because of their development in sandy soil (Khabar, 2014).

The determination of lipid composition in truffles is essential both for lipid analysis as well as for nutraceutical and medicinal purposes. The truffles contain only 4–9% by dry weight of total lipids (Tang *et al.*, 2011). Fatty acids and phytosterols are the main lipid compounds in truffle fruiting bodies, which are well known for their potential human benefits. Several studies through global chromatographic analysis demonstrated that desert truffles are rich in fatty acids, both saturated and unsaturated that have many positive effects on health (Akyüz, 2013; Al-Shabibi *et al.*, 1982; Bokhary *et al.*, 1989; Doğan and Aydın, 2013; Veeraraghavan *et al.*, 2021). For example, in *Terfezia boudieri* from Tunisia, Hamza *et al.* (2016) reported that essential fatty acids, like linoleic and oleic acids, account for 76% of the total fat content. Linoleic acid or omega-6 is an essential fatty acid and one of the most aromatic compounds in most truffle species (Lee *et al.*, 2020), which has protective and antioxidative effects beneficial for human health (Sokoła-Wysoczańska *et al.*, 2018). While, oleic acid, a bioactive compound, has the aptitude in reducing cholesterol levels (Lee *et al.*, 2020). Another example of *Terfezia claveryi* from Saudi Arabia, which is closely related to *T. boudieri* (Dahham *et al.*, 2018), was found to have arachidic, myristic, palmitic, behenic, pentadecanoic, stearic, heneicosanoic, nonadecanoic and margaric acids as saturated fatty acids along with unsaturated fatty acids (palmitoleic, oleic, erucic and linoleic) (Bokhary *et al.*, 1989). The lipid composition of desert truffles depends highly on the species as well as growing environments. For instance, *T. boudieri* from Saudi Arabia was rich in pentadecanoic, margaric, stearic and arachidic acids (Bokhary *et al.*, 1989). Whereas, the same species from Turkey contained mainly oleic, linoleic, linolenic, palmitic, palmitoleic, stearic and behenic acids (Akyüz, 2013). The most identified phytosterols in truffle reports were brassicasterol and ergosterol. Harki *et al.* (1996) reported that the prominent components identified in *Tuber melanosporum* were ergosterol and brassicasterol, accounting for about 90% of total sterols. As well, the major sterol components in the *Tuber* ascocarps were brassicasterol and ergosterol, accounting for about 17–64% and 25–67% of total sterols, respectively (Tang *et al.*, 2012). In *Terfezia* truffles, brassicasterol levels were 98% of the total sterols, while ergosterol was present in lower amounts (Tejedor-Calvo *et al.*, 2021). Other phytosterols such as beta-sitosterols, stigmasterol and campestanol were also present in low contents (Dahham *et al.*, 2018).

The six species included in this study were natives of Morocco. *Terfezia arenaria,* commonly called 'Pink Terfess of Mamora,' was harvested from acidic soil, in semi-arid climate under *Helianthemum guttatum*. It is an appreciated edible fungus, detected by the 'mark' method (Khabar, 2014) unlike *Delastria rosea*, known as 'Bitter Terfess of Taida' due to its bitter flavour. It was collected under *Pinus pinaster* var. atlantica and *Pinus halepensis* in Mamora forest between November and December (Khabar, 2014). Similarly, *Tuber oligospermum* was also collected under *P. pinaster* var. atlantica in Mamora forest, starting from December until April. The ascocarp of *T. boudieri* originated from Bouaarfa region, collected from limestone soil, under arid and sub-Saharan climate, and *Terfezia leptoderma* was obtained from Mamora forest from the acidic soil under *H. guttatum* at the beginning of February until May. *Tuber asa,* commonly called 'Terfass male of Terfass' because of its hard consistency, collected as well under *H. guttatum* on acidic soil of Mamora forest, towards the end of February at the same time as *T. leptoderma* (Khabar, 2014). The aims of this work were 1) to determine the lipid profile of the six Moroccan truffle species, 2) to determine the relation between the genus, species and lipid composition of truffles, and 3) to determine whether the lipid profile can be used as a tool for species or genus distinction.

Materials and methods

Fungus material

Six Moroccan truffle species were used in this experiment. The ascocarps of different species (Table 1) were collected directly from their natural environments and transported to the laboratory. Under the fume hood, the samples were surface sterilised with ethanol, peeled and then fragmented by hand. Several pieces were taken from the glebe and stored in pillboxes at −64°C. Alternatively, other samples were sun-dried for 2 months before being stored at −64°C.

Table 1. The name and location of six Moroccan truffle species used in this study.

Species name	Location
Terfezia leptoderma (1)	Mamora Forest under *Helianthemum*
T. leptoderma (2)	Mamora Forest under *Pinus pinaster*
Terfezia arenaria	Mamora Forest
Terfezia boudieri	Bouaarfa
Tuber asa	Mamora Forest
Tuber oligospermum	Mamora Forest under *P. pinaster*
Delastria rosea	Mamora Forest under *P. pinaster*

The different steps of extraction, separation and analysis of lipids were released at the Laboratory of Mycology, Phytopathology and Environment of the Littoral France University, following the method of Fontaine *et al.* (2001).

Extraction of total lipids

The extraction was performed with approximately 20–40 mg of freeze-dried material (pieces of truffle glebe). The solvent used for extraction was a mixture of dichloromethane and methanol (2:1 v/v) with 0.05% BHT (Butylated hydroxytoluene; Sigma) as antioxidant. The freeze-dried fungal material was first ground in 40 ml of the solvent using ultra-turrax homogenizer. The first extractions were performed in the dark to preserve the ergosterol, a photosensitive sterol. The extraction of total lipids was carried out under reflux (1 h at 70°C) with some pieces of pumice stone. After filtration, the lipid extract was recovered under nitrogen blowdown and rotary evaporator at 60°C. This step was repeated thrice.

Separation of fatty acids and total sterols by saponification

The crude lipid extract was used to separate fatty acids and total sterols by saponification. The crude extract was saponified under reflux (1 h at 90°C) in 2 ml of 6% (w/v) methanolic potash and some pieces of pumice. After cooling, two successive cold extractions with hexane were performed. The first extraction permitted the recovery of unsaponifiable fraction (sterols), while the second one enabled the retrieval of saponifiable fraction (fatty acid). To perform the first cold extraction, one volume of distilled water was added to the cooled saponified extract, followed by six volumes of hexane. This mixture was then vigorously stirred for 1 min with a vortex. After decantation, the organic phase (upper layer), which contains the unsaponifiable elements, was taken out and dehydrated with anhydrous sodium sulfate. This step was repeated three times, and the recovered extract was concentrated in a rotary evaporator at 50°C. For the fatty acid recuperation, the aqueous phase was acidified to pH 1 with 1 M HCl to liberate them from their saline combination. Afterwards, the acidified phase was extracted by performing three extractions with hexane. The concentration of these extracts was done under nitrogen.

Fatty acid analysis

The fatty acids were solubilise in 1 ml boron trifluoride–methanol (14% w/v). The methylation reaction was carried out for 2 min at 90°C in a water bath and then stopped by immersing the tubes in ice. After addition of 1 ml of distilled water and 2 ml of hexane, the tubes were vortexed for 30 s. The organic phase (upper phase) was taken out and dehydrated by adding anhydrous sodium sulfate. This step was repeated thrice. The methylated fatty acids were purified on silica gel of TLC (20 × 20 cm, type Silicagel F 254, Merck) with a solvent system composed of diethyl ether/hexane (10/90; v/v). The fatty acid spots were detected by primuline and eluted in about 1 ml of dichloromethane. Thereafter, the fatty acids were immediately taken up in 25–100 µl of hexane and injected into the gas chromatograph. Fatty acids were identified by comparing their relative retention times with internal standard such as methyl C 17:0 (methyl margarate) as well as other known standards (Alltech).

Sterol analysis

To obtain a better separation in gas chromatography, sterols were acetylated either for 12 h at room temperature or 2 h at 60°C by the mixture of toluene/acetic anhydride/pyridine (1/2/1; v/v/v). Sterol acetates were purified on silica gel thin layer with dichloromethane as migration solvent. Cholesterol acetate (1 mg/ml) was used as a control to localise acetylated products after spraying with 0.01% (w/v) primuline solution. The acetylated sterols were taken up in 25–100 µl of hexane and injected into the chromatograph. The sterol acetates were identified by comparing their relative retention times against an internal standard, cholesterol in alcohol form (non-acetylated) along with brassicasterol and other known acetylated standards.

Statistical analysis

The data were analysed using R studio software. The means and standard deviations were calculated. The pairwise comparisons among means were performed using two-way ANOVA and Tukey HSD test. To indicate significant differences, we used the multcompLetters4() function from the multcompView package.

Results and discussions

The objective of this work was to define the nature and proportion of fatty acids and sterols in six species of Moroccan truffles and to determine if this lipid profile could be used as a classification tool to discriminate between species or genus. This study was conducted for the first time on Moroccan truffles, disclosing distinctly the fatty acid and sterol components of truffles and desert truffles grown in Morocco.

Fatty acid composition

The fatty acid composition of Moroccan truffles has not been reported previously, and studies on fatty acid content of other truffles are scarce. The first and most reported studies on fatty acid composition were focused on *Tirmania pinoyi*, *Tirmania nivea*, *T. boudieri*, *T. claveryi* and *Picoa lefebvrei* from Saudi Arabia (Bokhary *et al.*, 1989; Bokhary and Parvez, 1995) and *T. claveryi* from Iraq (Al-Shabibi *et al.*, 1982). Recently, other studies appeared on fatty acid composition of *T. boudieri* from Iraq (Dahham *et al.*, 2018), *T. boudieri* from Turkey (Hamza *et al.*, 2016), *T. claveryi* and *Picoa juniperi* from Spain (Murcia *et al.*, 2003) as well as *T. nivea* from Libya (Shah *et al.*, 2020).

The chromatographic analysis results for the identification of fatty acids compositions are presented in (Table 2 and Figure 1). Seven fatty acids were detected in the six truffles species used in this experiment; four saturated fatty acids [palmitic (C16:0), stearic (C18:0), arachidic (C20:0) and behenic (C22:0)], and three unsaturated fatty acids [palmitoleic (C16:1), oleic (C18:1) and linoleic (C18:2)]. Bokhary *et al.* (1989) reported that palmitic, stearic, oleic and linoleic acids were predominant in *T. nivea* and *T. boudieri* which originated from Saudi Arabia. As well, the Turkish *T. boudieri* was also rich in behenic, palmitic, palmitoleic, stearic, oleic, linoleic and linolenic acids (Akyüz, 2013), which agree with our results and particularly with *T. boudieri*. Furthermore, a recent study on fatty acid composition in *Tuber maculatum*, *Tuber aestivum/uncinatum*, *Tuber borchii*, *T. melanosporum* and *T. nivea* revealed the dominance of palmitic, stearic, oleic and linoleic acids followed

Table 2. Fatty acid composition of the six Moroccan truffle species through gas–liquid chromatography analysis (percentage of dry weight of the lipid fraction).

Species	C 16:0	C 16:1	C 18:0	C 18:1	C 18:2	C 20:0	C 22:0
Terfezia leptoderma (1)	16.080 ± 0.936[a]	0.913 ± 0.372[a]	1.600 ± 0.185[a]	27.530 ± 0.598[a]	48.513 ± 1.179[a]	4.570 ± 0.589[a]	0.790 ± 0.147[a]
T. leptoderma (2)	17.456 ± 2.167[a]	1.733 ± 0.221[a]	1.026 ± 0.047[a]	26.106 ± 0.740[a]	48.633 ± 1.075[a]	5.753 ± 0.247[a]	0.803 ± 0.100[a]
Terfezia arenaria	21.470 ± 1.822[b]	1.066 ± 0.133[a]	3.253 ± 0.206[a]	27.020 ± 0.727[a]	38.803 ± 0.525[b]	8.563 ± 0.577[b]	0.900 ± 0.095[a]
Terfezia boudieri	20.823 ± 1.019[b]	0.830 ± 0.303[a]	2.433 ± 0.508[a]	28.333 ± 1.028[a]	42.770 ± 1.127[c]	4.580 ± 0.545[a]	0.710 ± 0.156[a]
Tuber asa	16.470 ± 1.483[a]	0.940 ± 0.096[a]	1.810 ± 0.259[a]	15.983 ± 0.879[b]	61.186 ± 0.315[d]	4.773 ± 0.396[a]	0.740 ± 0.070[a]
Tuber oligospermum	16.670 ± 0.138[a]	1.090 ± 0.389[a]	2.023 ± 0.200[a]	20.593 ± 0.450[c]	54.926 ± 1.601[e]	4.720 ± 0.500[a]	0.780 ± 0.105[a]
Delastria rosea	12.420 ± 1.574[c]	1.230 ± 0.166[a]	1.263 ± 0.112[a]	60.160 ± 0.916[d]	19.836 ± 1.237[f]	4.503 ± 0.678[a]	0.830 ± 0.052[a]

Data shown as mean ± standard deviation (n = 3). Different superscript letters in the same column indicate a statistically significant difference (P < 0.05).

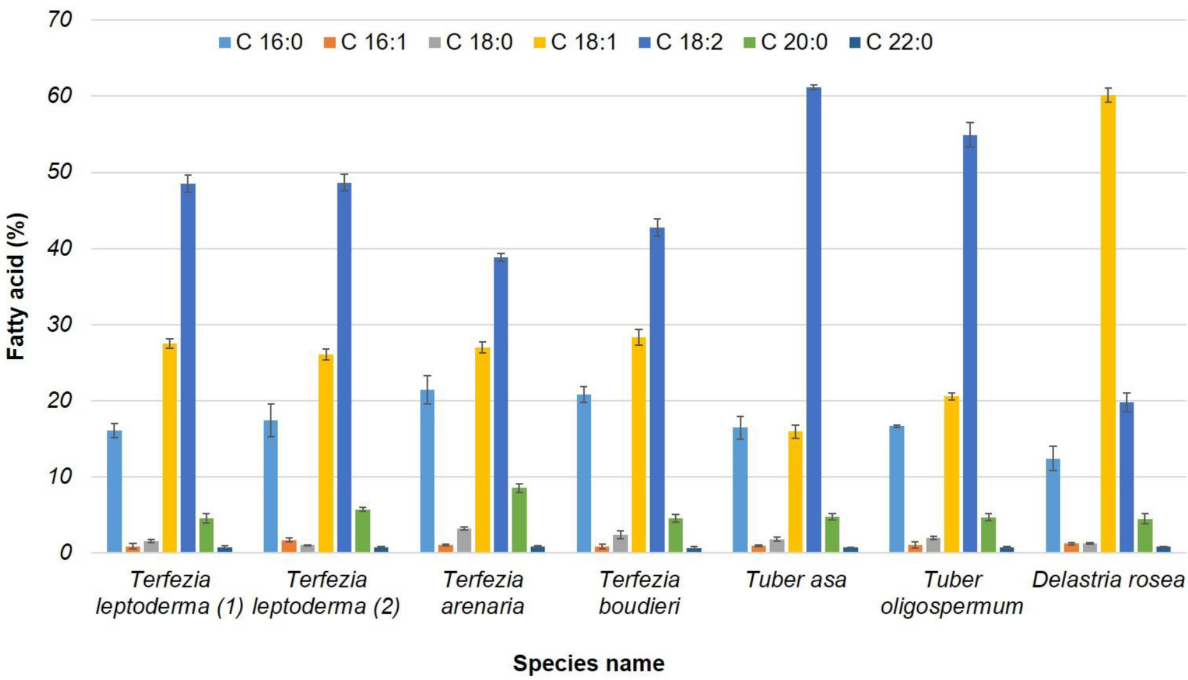

Figure 1. Fatty acid composition of the six Moroccan truffle species used in this study.

by traces of polyunsaturated fatty acids (Shah *et al.*, 2020).

The main fatty acids detected were palmitic, oleic and linoleic acids. The other fatty acids were also present but at lower levels. Similar findings were also reported in various species of *Terfezia* and *Tuber* (Hamza *et al.*, 2016; Tejedor-Calvo *et al.*, 2021). Our results demonstrated that the rate of palmitic acid (C16:0) is appreciably equal in all the species studied. We could also notice that the linoleic acid level was generally higher compared to the oleic acid (C18:1) level in all the species studied except for *D. rosea* where the opposite was true; the level of oleic acid was higher than linoleic acid. The same results were also reported by Hamza *et al.* (2016). The *T. boudieri* was characterised by its higher content of linoleic acid (54.10%) compared to oleic and palmitic acids that represented 22 and 20.40%, respectively (Hamza *et al.*, 2016). Linoleic acid level was considerably high in *Tuber* compared to *Terfezia* species. The rate of oleic acid was, on the other hand, slightly lower in *Tuber* genus compared to *Terfezia* genus. This remark goes with Tejedor-Calvo *et al.* (2021), who reported that linoleic acid content in *Tuber brumal* and *T. melanosporum* reached 78.3 and

61.12%, respectively, compared to *T. leptoderma* and *T. arenaria* which noticed only 51.3 and 30.9%, respectively. The fatty acid results of Moroccan truffles and desert truffles proved their richness in unsaturated and healthy fatty acids such as linoleic acid, suggesting their equivalent culinary value compared to European truffles.

Regarding fatty acid discrimination, it seems that these criteria could not differentiate clearly between the species of the two genera of *Tuber* and *Terfezia*. Indeed, the ratio of linoleic acid or oleic acid was approximately equal between the different species of the two genera. Nevertheless, the fatty acid composition could distinguish between *Delastria* and other two genera.

Sterol composition

The sterol composition of Moroccan truffles has never been reported before. The first report on sterol was that by Weete *et al.* (1985), which mentioned about both *Terfezia* and *Tuber* genera. Further, other studies principally on *Tuber* species including *T. melanosporum* (Harki *et al.*, 1996; Sancholle *et al.*, 1988), *Tuber magnatum*, *T. melanosporum*, *T. aestivum*, *Tuber albidum* and *Tuber indicum* were released (Sommer *et al.*, 2020).

Four sterols (brassicasterol, ergosterol and lanosterol) were identified in the ascocarps of the examined truffle species (Table 3 and Figure 2). Furthermore, the main

Table 3. Sterol composition of the six Moroccan truffle species through gel permeation chromatography analysis.

Sterols	Brassicasterols	Ergosterols	Lanosterol (1.31)	n.i. (1.42)
Terfezia leptoderma (1)	96.870 ± 1.260[a]	3.016 ± 0.621[a]	0 ± 0[a]	n.d.
T. leptoderma (2)	92.410 ± 2.606[a]	8.153 ± 0.143[a]	0 ± 0[a]	n.d.
Terfezia arenaria	96.833 ± 1.045[a]	0 ± 0[b]	2.003 ± 0.532[a]	n.d.
Terfezia boudieri	97.190 ± 2.416[a]	0 ± 0[b]	3.110 ± 0.298[a]	n.d.
Tuber asa	40.526 ± 2.377[b]	23.196 ± 0.718[c]	17.470 ± 0.856[b]	12.220 ± 2.186[b]
Tuber oligospermum	46.006 ± 2.001[c]	21.470 ± 1.990[c]	16.223 ± 4.441[b]	17.286 ± 1.997[b]
Delastria rosea	21.343 ± 1.770[d]	42.9633 ± 0.621[d]	22.826 ± 3.471[c]	12.886 ± 1.806[b]

Data shown as mean ± standard deviation (n = 3). Lanosterol and n.i. compounds are reported with their retention time (in minutes) between brackets. Different superscript letters in the same column indicate a statistically significant difference (P < 0.05). n.i., not identified; n.d., not detected.

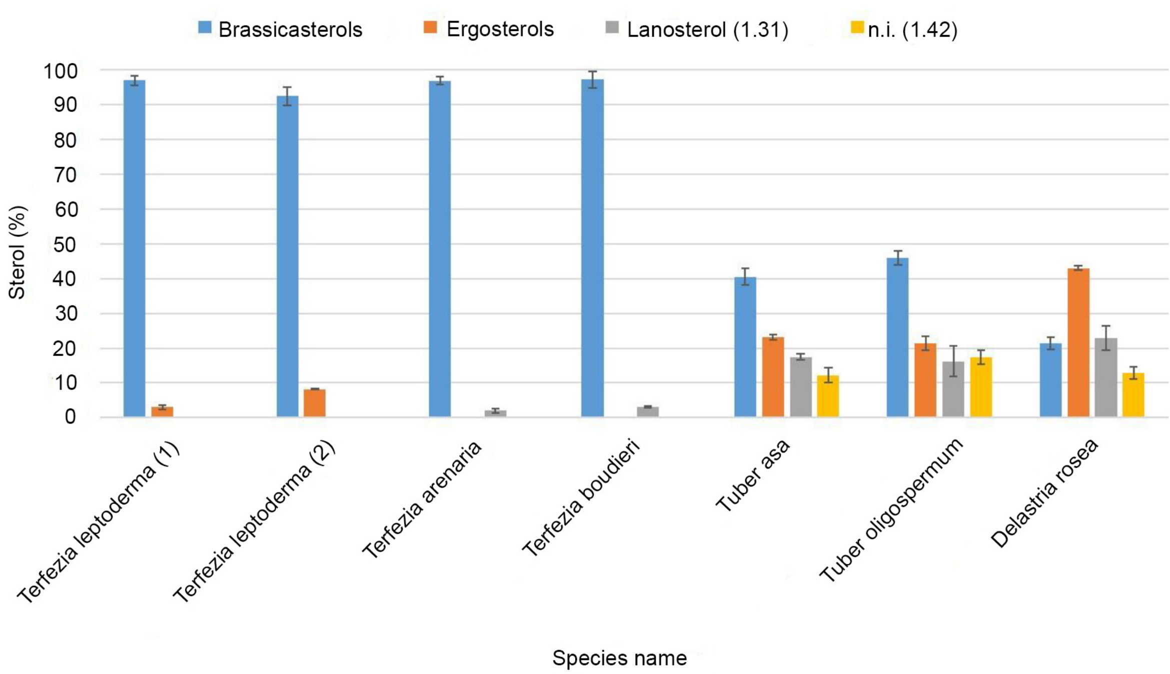

Figure 2. Sterol composition of the six Moroccan truffle species.

sterols were ergosterol and brassicasterol with the highest percentage in all the examined species. Similar results were disclosed in black truffle, where the sterol composition of *T. melanosporum* was analysed and ergosterol along with brassicasterol were identified as the major components (90%) (Harki *et al.*, 1996). As well, the examination of *Tuber sinense*, *T. aestivum*, *T. indicum*, *Tuber himalayense* and *T. borchii* revealed the predominance of brassicasterol and ergosterol, with 17–64% and 25–67% of total sterols, respectively (Tang *et al.*, 2012).

Besides, the ratio of ergosterol to brassicasterol changes according to the genera studied. In *Terfezia* species, brassicasterol was the main sterol identified, accounting for 92–97% of the total sterols, affirming the results of Weete *et al.* (1985), who reported that brassicasterol levels were 98% of total sterols in *Terfezia* truffles, while ergosterol was registered at very low amounts (0–8%). On the other hand, in *Tuber* species (*Tuber asa* and *Tuber oligospermum*) and *D. rosea*, the ergosterol represented a considerable amount compared to *Terfezia* species, accounting for 23, 21 and 43% of the sterols, respectively. These species also contained 40, 46 and 21% of brassicasterol, respectively. A recent study by Tejedor-Calvo *et al.* (2022) demonstrated that ergosterol and brassicasterol were the two main sterols in *T. claveryi* and *T. aestivum* ascocarps, with differences in ergosterol to brassicasterol ratio depending on the ascocarp genus. Lanosterol was also detected in *Tuber* species, as well as in *D. rosea*, in considerable quantities, accounting for 16 and 23% of the sterols, respectively. While in *Terfezia*, they were either totally absent or present in very small quantity (approximately 2–3%). The high amount of brassicasterol in *Terfezia* will increase the quality interest of the Moroccan genera, knowing that brassicasterol has several health benefits, such as antioxidative activity and anti-infective properties.

Finally, *Terfezia* genus was distinguished by the high brassicasterol content, while the *Tuber* genera and *Delastria* were characterised by the equivalent amount of ergosterol and brassicasterol. Hence, sterol analysis proved their importance to highlight differences between species and to separate the *Tuber* from *Terfezia* truffles collected in Morocco. These differences seem to be exploitable at the taxonomic level.

Conclusion

The lipid composition and concentration were highly influenced by truffle speciation and their growing area. This was the first report of lipid composition of Moroccan truffles, divulging the fatty acid and sterol compositions of six species of truffles and desert truffles and demonstrating the richness of Moroccan truffles in essential unsaturated fatty acid, such as linoleic acid. There was a slight difference between *Tuber* and *Terfezia* species in fatty acid component, which is not sufficient to differentiate between them. However, sterol analysis distinguished between these two genera. Hence, a comparison of their sterol composition with reported data seems to be plausible for *Tuber* and *Terfezia* distinction. Finally, a deeper study on other nutrient compounds and bioactive molecules of Moroccan truffles as well as their antioxidant evaluation is predetermined to improve their edible and culinary interest through their health benefits.

References

Akyüz, M., 2013. Nutritive value, flavonoid content and radical scavenging activity of the truffle (*Terfezia boudieri* Chatin). Journal of Soil Science and Plant Nutrition. 13:143–151.

Al-Shabibi, M.M.A., Toma, S.J. and Haddad, B.A., 1982. Studies on Iraqi truffles. I. Proximate analysis and characterization of lipids. Canadian Institute of Food Technology Journal. 15:200–202. https://doi.org/10.4067/S0718-95162013005000013

Bokhary, H.A. and Parvez, S., 1995. Studies on the chemical composition of the Ascomycete fungus *Phaeangium lefebvrei* Pat. Journal of King Saud University. 7:215–224.

Bokhary, H.A., Suleiman, A.A. and Basalah, M.O., 1989. The fatty acid components of the desert truffle 'Al Kamah' of Saudi Arabia. Journal of Food Protection. 52(9):668–669. https://doi.org/10.4315/0362-028X-52.9.668

Dahham, S.S., Al-Rawi, S.S., Ibrahim, A.H., Aman, S.A.M. and Amin, M.S.A.M., 2018. Antioxidant, anticancer, apoptosis properties and chemical composition of black truffle *Terfezia claveryi*. Saudi Journal of Biological Sciences. 25:1524–1534. https://doi.org/10.1016/j.sjbs.2016.01.031

Doğan, H.H. and Aydın, S., 2013. Determination of antimicrobial effect, antioxidant activity and phenolic contents of desert truffle in Turkey. African Journal of Traditional, Complementary and Alternative Medicines. 10:52–58.

Fontaine, J., Grandmougin-Ferjani, A., Hartmann, M.A. and Sancholle, M., 2001. Sterol biosynthesis by the arbuscular mycorrhizal fungus *Glomus intraradices*. Lipids. 36:1357–1363. https://doi.org/10.1007/s11745-001-0852-z

Hamza, A., Zouari, N., Zouari, S., Jdir, H., Zaidi, S., Gtari, M. and Neffati, M., 2016. Nutraceutical potential, antioxidant and antibacterial activities of *Terfezia boudieri* Chatin, a wild edible desert truffle from Tunisia arid zone. Arabian Journal of Chemistry. 9:383–389. https://doi.org/10.1016/j.arabjc.2013.06.015

Harki, E., Klaebe, A., Talou, T. and Dargent, R., 1996. Identification and quantification of *Tuber melanosporum* Vitt. sterols. Steroids. 61:609–612. https://doi.org/10.1016/s0039-128x(96)00121-3

Khabar, L., 2014. Mediterranean basin: North Africa. Ch.10. In: Kagan-Zur, V., Roth-Bejerano, N., Sitrit, Y. and Morte, A. (eds.) Desert truffles: phylogeny, physiology, distribution and domestication. Springer, Berlin, Heidelberg, pp. 143–158.

Khabar, L., Najim, L., Janex-Favre, M. and Paraguey-Leduc, A., 2001. Contribution à l'étude de la flore mycologique du Maroc. Les truffes marocaines. Bulletin de la Société mycologique de France. 117:213–229.

Lee, H., Nam, K., Zahra, Z. and Farooqi, M.Q.U., 2020. Potentials of truffles in nutritional and medicinal applications: a review. Fungal Biology Biotechnology. 7(9):1–17. https://doi.org/10.1186/s40694-020-00097-x

Morte, A., Kagan-Zur, V., Navarro-Ródenas, A. and Sitrit, Y., 2021. Cultivation of desert truffles—a crop suitable for arid and semi-arid zones. Agronomy. 11:1462. https://doi.org/10.3390/agronomy11081462

Murcia, M.A., Martínez-Tomé, M., Vera, A., Morte, A., Gutierrez, A., Honrubia, M. and Jiménez, A.M., 2003. Effect of industrial processing on desert truffles *Terfezia claveryi* Chatin and *Picoa juniperi* Vittadini): proximate composition and fatty acids. Journal of the Science of Food and Agriculture. 83:535–541. https://doi.org/10.1002/jsfa.1397

Sancholle, M., Weete, J.D., Kulifaj, M. and Montant, C., 1988. Changes in lipid composition during ascocarp development of the truffle, *Tuber melanosporum*. Mycologia. 80:900–903. https://doi.org/10.2307/3807580

Shah, N.N., Hokkanen, S., Pastinen O., Eljamil, A. and Shamekh, S., 2020. A study on the fatty acid composition of lipids in truffles selected from Europe and Africa. 3 Biotech. 10:415. https://doi.org/10.1007/s13205-020-02414-y

Sokoła-Wysoczańska, E., Wysoczański, T., Wagner, J, Czyż, K., Bodkowski, R., Lochyński, S. and Patkowska-Sokoła, B., 2018. Polyunsaturated fatty acids and their potential therapeutic role in cardiovascular system disorders—a review. Nutrients. 10(10): 1561. https://doi.org/10.3390/nu10101561

Sommer, K., Krauß, S. and Vetter, W., 2020. Differentiation of European and Chinese truffle (*Tuber* sp.) species by means of sterol fingerprints. Journal of Agricultural and Food Chemistry. 68(49):14393–14401. https://doi.org/10.1021/acs.jafc.0c06011

Tang, Y., Li, H.-M. and Tang, Y.-J., 2012. Comparison of sterol composition between *Tuber* fermentation mycelia and natural fruiting bodies. Food Chemistry. 132(3):1207–1213. https://doi.org/10.1016/j.foodchem.2011.11.077

Tang, Y., Li, Y.-Y., Li, H.-M., Wan, D.-J. and Tang, Y.-J., 2011. Comparison of lipid content and fatty acid composition between tuber fermentation mycelia and natural fruiting bodies. Journal of Agricultural and Food Chemistry. 59:4736–4742. https://doi.org/10.1021/jf200141s

Tejedor-Calvo, E., Amara, K., Reis, F.S., Barros, L., Martins, A., Calhelha, R.C., Venturini, M.E., Blanco, D., Redondo, D., Marco, P. and Ferreira, I.C.F.R., 2021. Chemical composition and evaluation of antioxidant, antimicrobial and antiproliferative activities of tuber and *Terfezia* truffles. Food Research International. 140:110071. https://doi.org/10.1016/j.foodres.2020.110071

Tejedor-Calvo, E., García-Barreda, S., Sánchez, S., Morte, A., Siles-Sánchez, M.D.N., Soler-Rivas, C., Santoyo, S. and Marco, P., 2022. Application of pressurized liquid extractions to obtain bioactive compounds from *Tuber aestivum* and *Terfezia claveryi*. Foods. 11(3):298. https://doi.org/10.3390/foods11030298

Veeraraghavan, V.P., Hussain, S., Balakrishna, J.P., Dhawale, L., Kullappan, M., Ambrose, J.M. and Mohan, S.K., 2021. A comprehensive and critical review on ethnopharmacological importance of desert truffles: *Terfezia claveryi*, *Terfezia boudieri*, and *Tirmania nivea*. Food Reviews International. 0:1–20. https://doi.org/10.1080/87559129.2021.1889581

Weete, J.D., Kulifaj, M., Montant, C., Nes, W.R. and Sancholle, M., 1985. Distribution of sterols in fungi. II. Brassicasterol in *Tuber* and *Terfezia* species. Canadian Journal of Microbiology. 31: 1127–1130. https://doi.org/10.1139/m85-212

Italian Journal of Food Science, 2022; 34 (2): 74–79

Policaptil Gel Retard® reduces body weight and improves insulin sensitivity in obese subjects

Giorgia Centorame[1], Maria Pompea Antonia Baldassarre[1]*, Giulia Di Dalmazi[1], Francesca Gambacorta[2], Fabrizio Febo[2], Agostino Consoli[1,2], Gloria Formoso[1,2]

[1]Department of Medicine and Aging Sciences, Center for Advanced Studies and Technology, University G. d'Annunzio of Chieti-Pescara, Chieti, Italy; [2]Endocrinology and Metabolic Disease Clinic of Pescara, Pescara, Italy

***Corresponding Author:** Maria Pompea Antonia Baldassarre, MD-PhD, Department of Medicine and Aging Sciences, Center for Advanced Studies and Technology, University G. d'Annunzio of Chieti-Pescara, Via Luigi Polacchi, 11 66100 Chieti (CH), Italy. Email: marbaldassarre@gmail.com

Received: 24 March 2022; Accepted: 18 May 2022; Published: 14 June 2022
© 2022 Codon Publications

OPEN ACCESS BY NC SA

PAPER

Abstract

Policaptil Gel Retard® (PGR), a natural fiber-based molecule, has been shown to prevent weight gain and ameliorate insulin-resistance indices in obese children and adolescents. The aim of this study was to compare the effects of 12 weeks of low calories and low glycemic index (LC-LGI) diet associated or not with the intake of PGR on anthropometric, bioimpedance, and metabolic parameters. Data from 20 obese adult subjects (10 per group) were analyzed. An LC-LGI diet with or without PGR intake reduced weight, BMI, and waist circumference. PGR intake elicited a reduction in fasting plasma insulin and insulin resistance index together with an improvement in insulin sensitivity.

Keywords: caloric intake; dietary fiber; glycemic index; Mediterranean diet; obesity

Introduction

The World Health Organization (WHO) declared obesity as the largest global chronic health disease in adults (Frühbeck *et al*., 2013). Obesity is a metabolic disease (ICD-10 code), with epidemic proportions, becoming one of the leading causes of cardiovascular disease, disability, and death worldwide (Blüher, 2019).

Obesity is the result of individual behaviors and environmental factors leading to excessive caloric intake and inadequate physical activity. It is characterized by a pro-inflammatory milieu leading to hyperinsulinemia, hyperglycemia, and hyperlipidemia, which can foster insulin resistance and metabolic abnormalities (Ceriello, 2003; Finer, 2015; WHO, 2015).

Appropriate goals of weight management involve achieving a realistic weight loss (at least 5% of baseline body weight) to promote a reduction in health risks and should include, besides weight loss, weight maintenance and prevention of weight regain (Frühbeck *et al*., 2013).

To date, conventional treatment for obesity is based on nutritional therapy, low-calories and low-glycemic index (LC-LGI) diets, combined with regular physical activity.

Nevertheless, results of several clinical studies indicate that is not often feasible to achieve and maintain weight loss (Dwyer *et al*., 2000).

An elevated consumption of fibers slows down the absorption of carbohydrates, thus reducing the extent and the velocity of post-prandial blood glucose increase (Weickert and Pfeiffer, 2008).

For this reason, integrating an LC-LGI diet with the intake of natural fiber-based molecules, such as the polysaccharide complex PGR, might improve the success rate of dietary intervention.

 ISSN 1120-1770 online, DOI 10.15586/ijfs.v34i2.2204

PGR is a patented complex of macromolecules produced by concentrating specific polysaccharide fractions obtained from: Cellulose, Opuntia Ficus indica, Amorphophallus Konjac, Althaea Officinalis, Linum Usitatissimum, Tilia Platyphyllos, and Cichorium Intybus.

PGR, with or without association with metformin, has been shown to prevent weight gain, and to ameliorate insulin-resistance indices, in obese children and adolescents (Stagi *et al.*, 2016, 2017). Recently, it has been observed that a single intake of PGR is associated with a significant reduction in appetite, ghrelin, and triglycerides in the postprandial period in obese children (Fornari *et al.*, 2020).

Guarino and coll. published results of a randomized controlled clinical trial showing that PGR supplementation and metformin have comparable effects in terms of glycemic control in obese adult subjects affected by metabolic syndrome (MS) or type 2 diabetes (T2D). Moreover PGR supplementation was associated with a greater serum lipid-lowering capacity and tolerability as compared to metformin (Guarino *et al.*, 2021).

The aim of this study was to compare the effects of an LC-LGI diet plus PGR assumption versus an LC-LGI diet alone on anthropometric, bioimpedance, and metabolic parameters in obese adults.

Materials and Methods

Study design and subjects

This was a retrospective pilot single center study conducted at the Endocrine and Metabolic Disease Unit, Pescara Town Hospital, Italy.

Data of obese adults (Body Mass Index, BMI ≥ 30 kg/m^2; age ≥18 years) treated for at least 12 weeks with an LC-LGI diet with or without PGR in the period between 01/01/2016 and 31/12/2020 were retrospectively collected.

We excluded from analysis subjects with T2D, thyroid dysfunction, treated with medications associated with weight gain or weight loss, affected by genetic syndromes associated with obesity or by autoimmune, chronic, or systemic diseases.

Patient's data were anonymously extracted from an electronic medical record system (MyStar Connect/Smart Digital Clinic, Meteda Srl, San Benedetto del Tronto, Italy) and divided into two groups according to whether or not PGR was part of patients' treatment (LC-LGI diet plus PGR group/LC-LGI diet alone group).

Data relative to body weight, BMI, waist circumference, bioimpedance data, fasting plasma glucose (FPG), plasma insulinemia levels and insulin resistance index (Homeostatic Model Assessment for Insulin Resistance, HOMA-IR), and sensitivity index (Quantitative Insulin Sensitivity Check Index, QUICKI) before and after 12 weeks of treatment were collected.

The study was conducted in compliance with the Declaration of Helsinki and European Guidelines on Good Clinical Practice. Ethical approval (ethical code PE 08) was obtained from the Chieti and Pescara Provinces Ethics Committee.

Bioimpedance analysis and insulin sensitivity

Bioimpedance analysis was performed using a BC-420 MA Class III body composition analyzer (Class III: compliant with the European Directive on medical devices) and the European NAWI standard relating to nonautomatic weighing instruments, Tanita, Tokyo, Japan. Body composition was evaluated by the instrument through a frequency of 50 kHz. The margin of error for the measurements performed corresponded to ±2%, which corresponds to a variation of approximately ±0.5% of the fat mass measurement in a standard figure (Esparza-Ros *et al.*, 2019).

Insulin resistance (HOMA-IR) and sensitivity (QUICKI) indexes were calculated according to the following formulas as previously reported:

- HOMA-IR: FPG (expressed in mg/100 mL) × fasting insulin (expressed in μU/mL)/405 (Matthews *et al.*, 1985);
- QUICKI: 1/(log (fasting insulin μU/mL) + log (FPG mg/dL.) (Katz *et al.*, 2000).

Dietary intervention

A personalized diet plan prescription was elaborated taking into consideration the subject's ideal body weight, lifestyle, eating habits, food preferences, and working shifts.

The energy intake was fixed by reducing by 25% the estimated caloric intake, which was calculated on the basis of food history and basal metabolism assessed by bioimpedance analysis.

The total amount of energy intake never fell below 1200 kcal per day.

The diet composition was formulated in compliance with the indications provided by the Italian Recommended Dietary Allowances (RADs) (SINU, 2019):

- carbohydrates 50–53 % kcal/day (<10% simple sugars);
- lipids 25–30 % kcal/day (<10% saturated fatty acids);
- protein 15–20 % kcal/day (about 0.9 g/kg/day);
- fibers at least 30 g/day.

The alimentary plan consisted of three main meals (breakfast, lunch, dinner) and one to three snacks (variable according to subject's habits) to avoid prolonged fasting between main meals (>5 h).

The low glycemic index was guaranteed by the presence of a balance among macronutrients and fibers. Moreover, dieticians strongly encouraged consumption of low glycemic index foods.

As per clinical practice, all subjects were encouraged to accumulate at least 30 min or more of moderate-intensity physical activity per day and underwent a follow-up visit every month to monitor weight changes, compliance with physical activity, diet and supplement prescribed for the entire duration of the treatment.

PGR supplementation

PGR® is a patented complex of macromolecules produced by Aboca Spa Company (Sansepolcro, Arezzo, Italy). This complex contains specific polysaccharide fractions obtained from: Cellulose, Opuntia Ficus indica, glucomannan (Amorphophallus konjac), Althaea officinalis, Linum usitatissimum, Tilia platyphyllos, and Cichorium intybus.

The PGR group patients consumed three PGR tablets with a large glass of water before their two main meals for a period of at least 12 weeks.

Statistical analysis

Variables distribution normality was checked using the Shapiro–Wilk test. Normally distributed data are shown as mean values ± standard deviation (SD), while data with nonnormal distribution are presented as median values and interquartile ranges.

Since the distributions of most of the quantitative variables were significantly different from the normal distribution (Shapiro-Wilk test), nonparametric tests were used. The Wilcoxon signed rank test was used to compare baseline and follow-up parameters within the study group. The Mann Whitney U test was used to compare differences between independent groups. Differences with $P < 0.05$ were considered statistically significant.

Statistical analysis was performed using the statistical software package Stata (version 16.1, StataCorp, 4905 Lakeway Drive, College Station, TX, USA).

Results

Baseline characteristics

The primary demographic, clinical, and biochemical characteristics of the two study groups are shown in Table 1. All baseline characteristics were similar in both groups.

Effects of 12-week intervention of an *LC-LGI diet versus* an *LC-LGI diet plus PGR*

Anthropometric measurements

After 12 weeks of intervention, there was a significant reduction in body weight, BMI, and waist circumference both in patients following an LC-LGI alone diet and in those on an LC-LGI diet plus PGR, as shown in Figure 1 and Table 2. The magnitude of the intervention effects on these parameters was not different between the two groups (Table 2).

Body composition variables

The effects of an LC-LGI diet and an LC-LGI diet plus PGR on body composition measurements are shown in

Table 1. Baseline demographic, clinical, and biochemical characteristics of the two study groups.

Parameters	LC-LGI diet (n = 10)	LC-LGI diet plus PGR (n = 10)	P value
Age (years)	54.5 ± 26	59.5 ± 11	ns
Gender (M/F)	2/10	4/6	ns
Height (cm)	160 ± 14	165 ± 5	ns
Weight (kg)	90.8 ± 12.5	97.1 ± 20.1	ns
BMI (kg/m2)	35.6 ± 8.9	36.7 ± 6.6	ns
WC (cm)	115.5 ± 29	111 ± 8.5	ns
FM (kg)	37.8 ± 10.4	45.3 ± 11.3	ns
FFM (kg)	50.9 ± 22.7	53.7 ± 10.1	ns
MM (kg)	48.3 ± 21.6	51 ± 9.9	ns
TBW (L)	36 ± 1.5	38.5 ± 7.7	ns
FPG (mg/dL)	95.5 ± 13	102.5 ± 10	ns
Fasting Insulin (μU/mL)	18.5 ± 8	14.7 ± 7.8	ns
HOMA-IR	4.5 ± 2.8	3.7.4 ± 1.9	ns
QUICKI	0.31 ± 0.03	0.31 ± 0.02	ns
PGR (weeks)	–	13 ± 1	–

Data shown as medians ± IQR. Abbreviations: IQR, interquartile range; LC-LGI, low-calorie and low-glycemic index; PGR, Policaptil Gel Retard; ns, not significant; BMI, body mass index; WC, waist circumference; FM, fat mass; FFM, fat free mass; MM, muscle mass; TBW, total body water; FPG, fasting plasma glucose; HOMA-IR, homeostatic model assessment for insulin resistance; QUICKI, quantitative insulin-sensitivity check index.

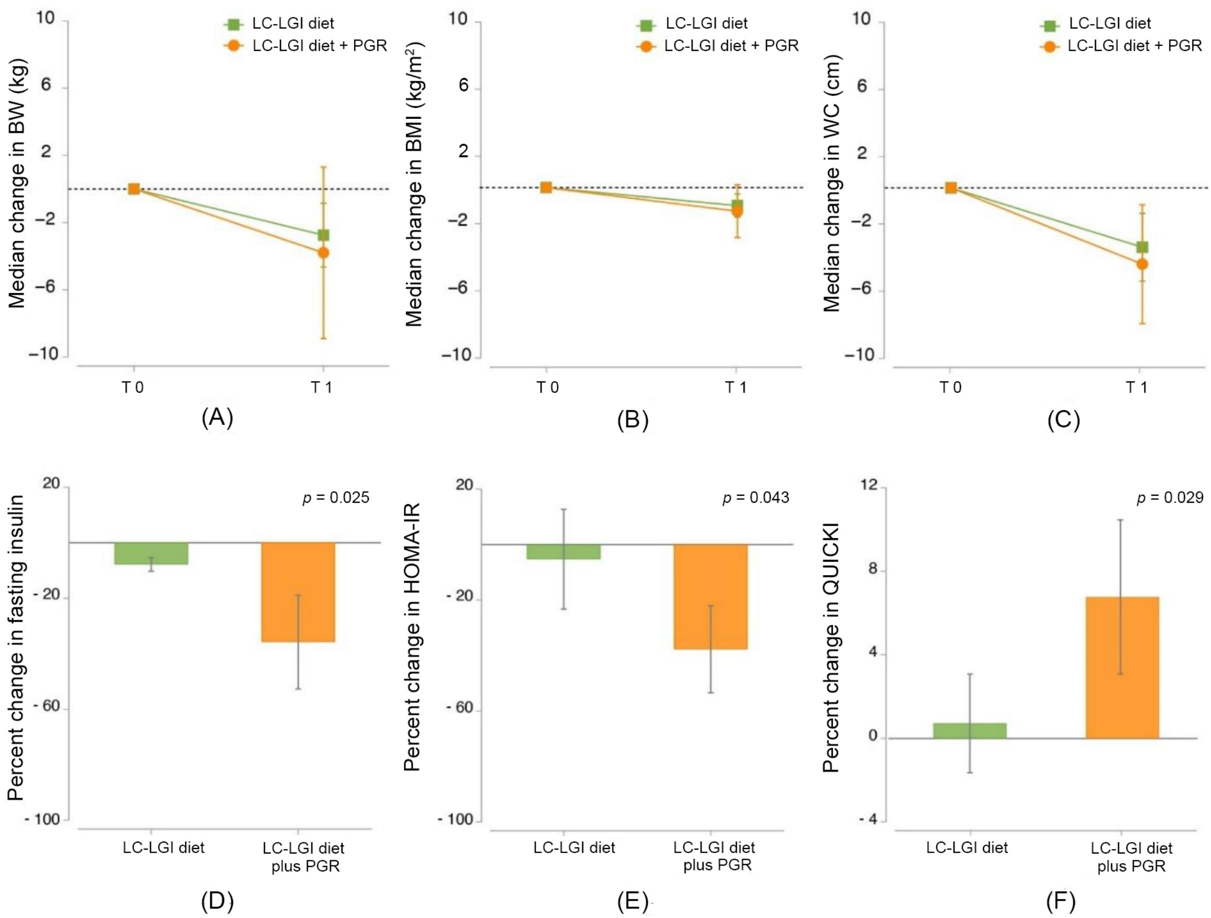

Figure 1. Median change from baseline (T0) in (A) body weight (BW), (B) body mass index (BMI), and (C) waist circumference (WC) to 12 weeks (T1) in obese subjects treated with an LC-LGI diet or an LC-LGI diet plus PGR. Change in (D) fasting insulin, (E) HOMA-IR, and (f) QUICKI after 12-week intervention of an LC-LGI diet versus an LC-LGI diet plus PGR.

Table 2. Fat mass (FM) and muscle mass (MM) slightly decreased after 12 weeks in the LC-LGI group. However, the difference between the two study groups with respect to FM, fat free mass (FFM), and MM loss was not statistically significant. There was no change in Total Body Water (TBW) in the study subjects (Table 2).

Metabolic profile

FPG did not change after 12 weeks of intervention in both study groups.

Compared to an LC-LGI diet, the LC-LGI diet plus PGR elicited a greater decrease in fasting insulin (–1.5 ± 1 vs –5.8 ± 4.3, P = 0.025, Table 2) and HOMA-IR index (–0.2 ± 0.9 vs –1.5 ± 1, P = 0.043, Table 2), with a percent change from baseline of –36 % and –37 %, respectively (Figure 1d and 1e).

QUICKI was significantly ameliorated in an LC-LGI plus PGR group (0.31 ± 0.02 vs 0.33 ± 0.02, P < 0.001, Table 2) with an increase of 7.1 % (Figure1f) but not in LGI group. The difference between the two study groups with respect to QUICKI was statistically significant (P = 0.029), as shown in Table 2.

Discussion

This retrospective pilot study shows that while an LC-LGI diet both with or without PGR intake reduce, as expected, weight, BMI, and waist circumference, as compared to the diet only intervention, 12 weeks of PGR intake induce a significant improvement in insulin circulating levels, in insulin resistance calculated by HOMA-IR index, as well as in insulin sensitivity calculated according to QUICKI.

These effects of PGR may be related to a reduction in the post meal glycemic and insulinemic peaks as suggested by Stagi and collaborators who demonstrated an amelioration of HOMA-IR in obese children and adolescents after 1 year of PGR intake (Stagi *et al.*, 2016, 2017). Moreover, Greco and colleagues recently observed an improvement

Table 2. Comparison of differences between baseline and 12 weeks in anthropometric, body composition, and metabolic parameters between the LC-LGI diet and LC-LGI plus PGR groups.

Parameters	LC-LGI diet			LC-LGI plus PGR			LC-LGI vs LC-LGI plus PGR
	Baseline (T0)	Follow-up (T1)	Change (ΔT0-T1)	Baseline (T0)	Follow-up (T1)	Change (ΔT0-T1)	P value
Weight (kg)	90.8 ± 12.5	88.3 ± 9.5	−2.8 ± 1.9*	97.1 ± 20.1	92.8 ± 22.6	−3.8 ± 5.1**	0.393
BMI (kg/m2)	35.6 ± 8.9	33.8 ± 9.5	−1.1 ± 0.7*	36.7 ± 6.6	36.1 ± 8.1	−1.4 ± 1.6**	0.413
WC (cm)	115.5 ± 29	111 ± 28	−3.5 ± 2*	111 ± 8.5	105.5 ± 9	−4.5 ± 3.5**	0.518
FM (kg)	37.8 ± 10.4	36.3 ± 9.4	−1.5 ± 1*	45.3 ± 11.3	45.4 ± 12.5	−1.6 ± 3.8	0.837
FFM (kg)	50.9 ± 22.7	50.7 ± 22.4	−1 ± 0.3	53.7 ± 10.1	49.5 ± 10.8	−1.5 ± 2.8	0.517
MM (kg)	48.3 ± 21.6	47.8 ± 21.5	−0.6 ± 0.1*	51 ± 9.9	49.3 ± 10.6	−1 ± 2.35	0.731
TBW (L)	36 ± 1.5	35.5 ± 2.5	−0.5 ± 0.3	38.5 ± 7.7	37.5 ± 9.3	−0.25 ± 1.9	0.865
FPG (mg/dL)	95.5 ± 13	91 ± 22	2.5 ± 10	102.5 ± 10	95.5 ± 11.5	−5 ± 12.5	0.402
Insulinemia (μU/mL)	18.5 ± 8	19 ± 11	−1.5 ± 1	14.7 ± 7.8	9.3 ± 3.3	−5.8 ± 4.3**	***0.025***
HOMA-IR	4.5 ± 2.8	4.5 ± 3.6	−0.2 ± 0.9	3.7.4 ± 1.9	2.3 ± 0.8	−1.5 ± 1**	***0.043***
QUICKI	0.31 ± 0.03	0.31 ± 0.04	0.00 ± 0.01	0.31 ± 0.02	0.33 ± 0.02	0.02 ± 0.01**	***0.029***

Data are shown as medians ± IQR. Wilcoxon signed rank test was used for intragroup comparisons (baseline vs follow-up). For intergroup analyses (LC-LGI diet vs LC-LGI plus PGR) the Mann Whitney U test for independent groups was applied. *P < 0.05; **P < 0.001. Abbreviations: IQR, interquartile range; LC-LGI, low-calorie and low-glycemic index; PGR, Policaptil Gel Retard; BMI, body mass index; WC, waist circumference; FM, fat mass; FFM, fat free mass; MM, muscle mass; TBW, total body water; FPG, fasting plasma glucose; HOMA-IR, homeostatic model assessment for insulin resistance; QUICKI, quantitative insulin-sensitivity check index.

of parameters defining metabolic syndrome in a mouse model fed with high-fat diet treated with PGR (Greco *et al*., 2020).

Similar results were obtained by Guarino and colleagues in adults in whom PGR supplementation induced a better effect on serum lipid and tolerability as compared to metformin (Guarino *et al*., 2021).

It is worth noting that in our study, similar observation has been made in a clinical setting, without the “trial effect,” thus confirming the potential effectiveness of PGR as a valid clinical tool in obesity management.

Insulin resistance and hyperglycemia are known risk factors of cardiovascular disease (Laakso and Kuusisto, 2014). Therefore, a treatment that improves insulin action leading to a considerable amelioration of metabolic profile in obese subjects could represent an efficacious strategy in the prevention of cardiovascular disease.

The small sample size is the main limitation of our study. Furthermore, even if our short observation period suggests an effect of PGR in improving the carbohydrate metabolism, we cannot exclude a concomitant effect given by the weight loss obtained through an LC-LGI diet. A randomized placebo-controlled study would be useful to better single out the effects of this macromolecular complex.

For all these reasons, further studies with suitable study design on larger samples with a longer follow-up period are needed to confirm our preliminary results.

Conclusions

PGR associated with a low calorie and low glycemic index diet may be useful to reduce body weight and improve insulin sensitivity in adult subjects affected by obesity.

References

Blüher, M., 2019. Obesity: global epidemiology and pathogenesis. Nature Reviews Endocrinology 15(5): 288–298. https://doi.org/10.1038/s41574-019-0176-8

Ceriello, A., 2003. New insights on oxidative stress and diabetic complications may lead to a “causal” antioxidant therapy. Diabetes Care 54(1), 1–7. https://doi.org/10.2337/diacare.26.5.1589

Dwyer, J.T., Melanson, K.J., Sriprachy-anunt, U., Cross, P. and Wilson, M., 2000. Dietary treatment of obesity. South Dartmouth (MA). Endotext. MDText.com, Inc.

Esparza-Ros, F., Vaquero-Cristóbal, R. and Marfell-Jones, M., 2019. International standards for anthropometric assessment (2019). p. 115. Available at: https://www.researchgate.net/publication/236891109_International_Standards_for_Anthropometric_Assessment

Finer, N., 2015. Medical consequences of obesity. Medicine (United Kingdom) 43(2): 88–93. https://doi.org/10.1016/j.mpmed.2014.11.003

Fornari, E., Morandi, A., Piona, C., Tommasi, M., Corradi, M. and Maffeis, C., (2020). Policaptil gel retard intake reduces post-prandial triglycerides, ghrelin and appetite in obese children: a clinical trial. Nutrients 12(1): 214. https://doi.org/10.3390/nu12010214

Frühbeck, G., Toplak, H., Woodward, E., Yumuk, V., Maislos, M. and Oppert, J.M., 2013. Obesity: the gateway to ill health – an EASO position statement on a rising public health, clinical and scientific challenge in Europe. Obesity Facts 6(2): 117–120. https://doi.org/10.1159/000350627

Greco, C.M., Garetto, S., Montellier, E., Liu, Y., Chen, S., Baldi, P., Sassone-Corsi, P. and Lucci, J., 2020. A non-pharmacological therapeutic approach in the gut triggers distal metabolic rewiring capable of ameliorating diet-induced dysfunctions encompassed by metabolic syndrome. Scientific Reports 10(1): 12915. https://doi.org/10.1038/s41598-020-69469-y

Guarino, G., Della Corte, T., Strollo, F. and Gentile, S., 2021. Policaptil gel retard in adult subjects with the metabolic syndrome: efficacy, safety, and tolerability compared to metformin. Diabetes & Metabolic Syndrome 15(3): 901–907. https://doi.org/10.1016/J.DSX.2021.03.032

Katz, A., Nambi, S.S., Mather, K., Baron, A.D., Follmann, D.A., Sullivan, G. and Quon, M.J., 2000. Quantitative insulin sensitivity check index: a simple, accurate method for assessing insulin sensitivity in humans. The Journal of Clinical Endocrinology & Metabolism 85(7): 2402–2410. https://doi.org/10.1210/jcem.85.7.6661

Laakso, M. and Kuusisto, J., 2014. Insulin resistance and hyperglycaemia in cardiovascular disease development. Nature Reviews Endocrinology 10(5): 293–302. https://doi.org/10.1038/nrendo.2014.29

Matthews, D.R., Hosker, Rudenski, Naylor, Treacher, and Turner, 1985. Homeostasis model assessment: insulin resistance and β-cell function from fasting plasma glucose and insulin concentrations in man. Diabetologia 28(7): 412–419. https://doi.org/10.1007/BF00280883SINU, 2019.

Livelli Di Assunzione Di Riferimento Di Nutrienti Ed Energia per La Popolazione Italiana (LARN). Available at: https://sinu.it/larn/

Stagi, S., Lapi, E., Seminara, S., Pelosi, P., Del Greco, P., Capirchio, L., Strano, M., Giglio, S., Chiarelli, F. and De Martino, M., 2016. Policaptil gel retard® significantly lowered body mass index and hyperinsulinemia, and reduced the risk of diabetes mellitus type 2 (DM2) in children and adolescents with obesity, family history and DM2. Pediatriya 56(2): 38–45. https://doi.org/10.1186/s13052-015-0109-7

Stagi, S., Ricci, F., Bianconi, M., Sammarco, M.A., Municchi, G., Toni, S., Lenzi, L., Verrotti, A. and de Martino, M., 2017. Retrospective evaluation of metformin and/or metformin plus a new polysaccharide complex in treating severe hyperinsulinism and insulin resistance in obese children and adolescents with metabolic syndrome. Nutrients 9(5): 1–17. https://doi.org/10.3390/nu9050524

Weickert, M.O. and Pfeiffer, A.F.H., 2008. Metabolic effects of dietary fiber consumption and prevention of diabetes. Journal of Nutrition 138(3) 439–442. https://doi.org/10.1093/jn/138.3.439

WHO, 2015. Obesity: preventing and managing the global epidemic. WHO.

Italian Journal of Food Science, 2022; 34 (2): 80–88

Molecular docking and *in vivo* studies of liquiritin against acute myocardial infarction via TLR4/MyD88/NF-κB signaling

Peng Zhou[1,2,3#], An-lu Shen[1#], Pei-pei Liu[1], Shu-shu Wang[1*], Liang Wang[1,2,3*]

[1]School of Integrated Chinese and Western Medicine, Anhui University of Chinese Medicine, Hefei, People's Republic of China; [2]Institute of Integrated Chinese and Western Medicine, Anhui Academy of Chinese Medicine, Hefei, People's Republic of China; [3]Anhui Province Key Laboratory of Chinese Medicinal Formula, Hefei, People's Republic of China

[#] These authors contributed equally to this work.

***Corresponding Author**: Shu-shu Wang, School of Integrated Chinese and Western Medicine, Anhui University of Chinese Medicine, Hefei, People's Republic of China. Email: wangss@ahtcm.edu.cn; Liang Wang, School of Integrated Chinese and Western Medicine, Anhui University of Chinese Medicine, Hefei, People's Republic of China. Email: wangliang_01@163.com

Received: 24 February 2022; Accepted: 13 May 2022; Published: 16 June 2022
© 2022 Codon Publications

OPEN ACCESS

SHORT COMMUNICATION

Abstract

Licorice (*Glycyrrhiza glabra L.*) is an essential herb in Chinese medicine, as well as a common ingredient in health foods and natural sweeteners. Liquiritin, the primary constituent of licorice, possesses a wide range of pharmacological and biological properties. This research aims to study the protective mechanism of liquiritin in the myocardium. The potential therapeutic efficacy of liquiritin against acute myocardial infarction (AMI) was tested using molecular docking and verified using an AMI rat model caused by the ligation of the LAD coronary artery. Molecular docking between liquiritin and toll-like receptor 4 (TLR4) and myeloid differentiation factor 88 (MyD88) was predicted using SystemsDock. Then, for experimental validation, *in vivo* studies were employed. Rats with the AMI model established by ligation of left anterior descending coronary artery were divided into four groups—sham group, model group, captopril group, and liquiritin group. LVSP, LVEDP, +dp/dtmax, and -dp/dtmax were detected and analyzed. HE and Masson staining were used to observe the pathological changes. The protein expressions of TLR4, MyD88, and nuclear factorκB p65 (NF-κB p65) were detected by Western blotting. Molecular docking showed that liquiritin may act on the TLR4 and MyD88, and, therefore, liquiritin was predicted to exert anti-inflammatory effects by regulating the TLR4/MyD88 signaling pathway. Liquiritin improved LVSP, +dp/dtmax, -dp/dtmax, and LVEDP levels, and alleviated pathological changes and cardiac fibrosis. Further study found that liquiritin could decrease the overexpression of TLR4, MyD88, and NF-κB, which validated the molecular docking study. Hence, liquiritin ameliorates AMI by reducing inflammation, and blocking TLR4/MyD88/NF-κB signaling. These results indicate that liquiritin as a potential compound could alleviate AMI and broaden its application.

Keywords: acute myocardial infarction; liquiritin; molecular docking; TLR4/MyD88/NF-κB signaling

Introduction

Acute myocardial infarction (AMI) is a major manifestation of ischemic heart disease (IHD), which is a leading cause of chronic heart failure (CHF) (Lin *et al.*, 2020). As a serious cardiovascular event, AMI has become the leading cause of death in the world, which is characterized by high morbidity and mortality. Therefore, it needs to be given enough attention, and it is particularly important to find an appropriate treatment (Yousufuddin *et al.*, 2019). The occurrence of AMI is related to many factors, such as arrhythmia, severe inflammatory response, and cardiac dysfunction (Sinnecker *et al.*, 2016). At present, the surgical treatment of AMI mainly includes reperfusion and revascularization therapy (Horikoshi *et al.*, 2021). Restoring coronary blood flow to the infracted myocardium can significantly reduce myocardial infarction; however, this process may further cause myocardial ischemia/reperfusion (I/R) injury, which causes secondary damage to AMI patients (Davidson *et al.*, 2019; Yang *et al.*, 2019). In spite of modern drugs for the prevention and treatment of AMI and improved public awareness, there is still a need for new and safe drugs to prevent AMI. Therefore, it is particularly important to find and develop new cardioprotective Traditional Chinese Medicine (TCM) for AMI patients.

Epidemiological evidence has suggested that diets rich in fruits and vegetables are associated with a lower incidence of cardiovascular diseases, as fruits and vegetables are rich in flavonoids and flavonoid glycosides (Krga *et al.*, 2016; Zhou *et al.*, 2020). Recent studies have found a positive correlation between higher intakes of flavonoids and reduced cardiovascular disease mortality (Yamagata, 2019). Licorice (*Glycyrrhiza glabra* L.) is an essential herb in Chinese medicine, which is also widely used in health foods and natural sweeteners (Jiang *et al.*, 2020; Kwon *et al.*, 2019). Licorice has anti-inflammatory, anti-obesity, anti-oxidant, anti-viral, and neuroprotective properties (Ahmed-Farid *et al.*, 2019; Ojha *et al.*, 2015; Sun *et al.*, 2019). Flavonoids and flavonoid glycosides are one of the main chemical components of licorice. Liquiritin, as a flavonoid glycoside, is also one of the main components of licorice, which possesses anti-myocardial fibrosis, anti-cancer, anti-oxidative and neuroprotective effects (Huang *et al.*, 2018; Sun *et al.*, 2010; Wei *et al.*, 2017). Previous studies have reported that liquiritin could suppress the levels of type I collagen, type II collagen, and alpha-smooth muscle-actin (α-SMA), reduce the release of inflammatory cytokines such as TNF-α, IL-6, and IL-17, and inhibit the protein expression of nuclear factorκB (NF-κB) phosphorylation via regulating IKKα/IκBα signaling pathway. It also has a protective effect against myocardial fibrosis (Zhang *et al.*, 2016). Our previous studies found that liquiritin could directly inhibit ATE1 overexpression and inhibit TAK1 and JNK1/2 phosphorylation in H9c2 transfected by pcDNA3.1/ATE1, which plays a role in reducing Ang II-induced cardiomyocyte hypertrophy due to its regulation of ATE1/ TAK1-JNk1/2 pathway (Mo *et al.*, 2022).

Toll-like receptor 4 (TLR4) can activate the expression of pro-inflammatory factors and chemokines by regulating the MyD88-dependent pathway, which affects many diseases, including cardiovascular diseases, allergic diseases, neuronal degeneration, and autoimmune diseases (He *et al.*, 2019; Mian *et al.*, 2019). Especially, in AMI, the pathogenesis is that the inflammatory response caused by activated TLR4 may be because of the TLR4-Myd88-dependent signaling pathway. Molecular docking can predict the potential target of the natural products, and then verify it through experiments, which can explain the mechanism of action of the natural products from Chinese Medicine.

Therefore, in this study, molecular docking technology was used to find whether liquiritin is a potential inhibitor of TLR4 and Myd88. The purpose of this study was to screen liquiritin for potential therapeutic targets for TLR4 and Myd88 through molecular docking, then determine possible pathological pathways, find the mechanism of interaction between liquiritin and receptors, and confirm results by an *in vivo* assay.

Materials and Methods

Animals

Sprague-Dawley (SD) rats (Male, weight 200±20 g, SCXK 2017-001) were purchased from the Experimental Animal Center of Anhui Medical University. All rats were housed under 23±2°C, 12/12 h light/dark cycles. All experimental procedures were followed by the Center of Scientific Research of Anhui University of Chinese Medicine.

Chemicals

Liquiritin was purchased from Shanghai Yuanye Biotechnology Company (Shanghai, China), and the purity was greater than 98%. TLR4 was from Affinity Bioreagents (Golden, CO). MyD88 and NF-κB p65 were from Abbkine (China).

Molecular docking

The liquiritin structure was obtained from the PubChem website. TLR4 (PDB ID: 3VQ2) (Ohto *et al.*, 2012) and MyD88 (PDB ID: 4DOM) (Snyder *et al.*, 2013) structures were obtained from RCSB (www.rcsb.org/pdb). SystemsDock was used for molecular docking (Hsin *et al.*, 2016). The method of molecular docking consisted of four major steps: (1) Upload docking protein receptors. (2) Prepare chemical molecules for docking. The structural file is uploaded in 2D SDF format. (3) Run docking simulation. The docking simulation is carried out with machine learning system. (4) Acquire molecular docking results including map information and pKd/pKi.

In vivo anti-acute myocardial infarction properties

Establishment of rat models

AMI model in rats with left anterior descending (LAD) coronary artery ligation as we have previously described (Raj *et al.*, 2017; Wang *et al.*, 2020). To reduce pain, all rats were anesthetized with isoflurane and ventilated artificially using a respirator. The AMI rat model was prepared by ligating a 6-0 silk suture with LAD 2 mm below the apex of the left atrial appendage. In the control group, rats were perforated but not ligated. After surgery, each rat was injected subcutaneously with 100,000 IU of penicillin to prevent infection and to increase the survival rate. The survival rate of both the sham group and the model group exceeded 90%.

Drug treatment

The control group received deionized water. Two weeks following the establishment of the AMI model, the AMI rats were randomized into three groups. The model group received deionized water, the captopril group received 3375 mg/kg of captopril, and the liquiritin group received 200 mg/kg of liquiritin. All rats were administered the intervention for four weeks. The captopril and liquiritin groups were gavaged once per day.

Measurement of hemodynamic indexes

Thirty minutes after the last treatment, all rats were sacrificed, and polystyrene was catheterized through the right carotid artery into the left ventricle of the heart. LVSP, LVEDP, +dp/dtmax, and -dp/dtmax were detected and analyzed by PowerLab (AD Instruments, Castle Hill, Australia).

Myocardial histopathology

Left ventricular myocardium containing myocardial infarction area was collected, and fixed with 4% paraformaldehyde. Thick tissue sections (4 μm) were prepared using paraffin-embedded tissues. Hematoxylin-eosin (HE) and Masson staining were used to observe the pathological changes.

Western Blotting

The concentration of myocardium-isolated total protein was determined using the BCA technique. Proteins were separated by SDS-PAGE, transferred to a nitrocellulose membrane, blocked in 5% nonfat dry milk for 2 h, and incubated overnight. The proportions of antibodies were TLR4 (1:1000), MyD88 (1:1000), and NF-κB p65 (1:1000). After incubating the membranes overnight at 4°C, the secondary antibodies were administered for 2 h at room temperature. After washing three times with TBST, electrogenerated chemiluminescence (ECL) was employed to develop and fix the gels, and a gel imager (FluorChem M, ProteinSimple, USA) was utilized for photographing the gels and performing a semiquantitative analysis. The experiment was repeated three times. β-actin was used as an internal control.

Statistical analysis

All data were analyzed using SPSS 23.0, with a significance level at $P < 0.05$. Multiple groups were compared by one-way analysis of variance and the LSD method. GraphPad Prism 5.0 was applied to all statistical analyses.

Results

Molecular docking of liquiritin with the biological targets

The docking score (pKd/pKi) between liquiritin and TLR4 was 6.28, which was slightly lower than the native ligand (7.35) (Table 1 and Figure 1). And, the docking score between liquiritin and MyD88 was 5.73, which was higher than the native ligand (4.18) (Table 2 and Figure 2). The binding affinity between liquiritin and TLR4 or MyD88 is mainly intermolecular hydrogen bond. The findings of the molecular docking prediction indicated that liquiritin may function on the TLR4/MyD88 signaling pathway; however, *in vivo* animal investigations are required to verify these results.

Liquiritin improves heart function

LVSP, $+dp/dt_{max}$, and $-dp/dt_{max}$ in the model group were decreased ($P < 0.01$), while LVEDP significantly increased compared with the sham group ($P < 0.01$). LVSP, +dp/dtmax, -dp/dtmax, and LVEDP in the liquiritin and captopril groups reversed the results compared to the model group ($P < 0.01$) (Figure 3). The results indicated that

Table 1. The docking scores (pKd/pKi) of liquiritin and TLR4.

Chemical constituents	Docking score	Binding of ligands to residues
Native ligand	7.35	Ile124, Glu122, Ser413, Phe151, Phe438, Phe126, Leu54, Val82, Leu87, Arg90, Phe121, Ile153
Liquiritin	6.28	Ile124, Ser413, Phe438, Leu54, Arg90, Phe121, **Ile52**

Bold means residue binding except for native ligand.

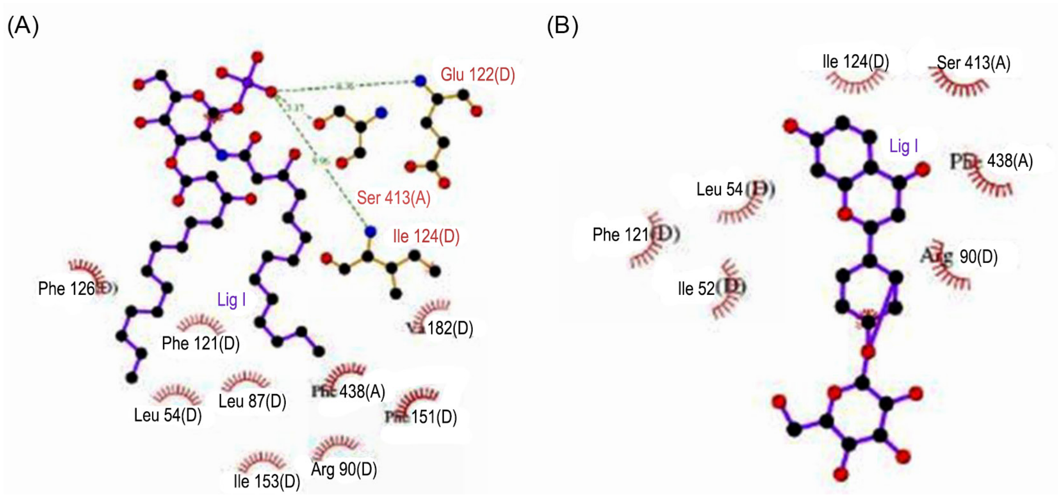

Figure 1. The pictures of native ligand and active site of TLR4. Native ligand (A, 2D), Liquiritin (B, 2D).

Table 2. The docking scores (pKd/pKi) of liquiritin and MyD88.

Chemical constituents	Docking score	Binding of ligands to residues
Native ligand	4.18	Tyr 257, Ala259, Thr277
Liquiritin	5.73	Tyr 257, Thr277, **Asp226**, **Ser224**, **Asp171**

Bold means residue binding except for native ligand.

liquiritin might enhance the cardiac function of rats with AMI.

Liquiritin improves the morphological changes via HE assay

As shown in Figure 4, the myocardium of rats in the sham group was evenly stained with normal morphology, clear texture, and orderly arrangement of myocardium cells, with a few cardiac fibroblasts. However, after ligation of LAD coronary artery induced AMI, pathological changes appeared in the myocardium, dyed unevenly, and were arranged in a disorderly manner. Myocardial cells in the model group were lytic, with fibroblasts proliferated and inflammatory cells infiltrated. Myocardial cells appeared with a regular cell arrangement and clear structure, and the pathological changes were attenuated in the liquiritin group and the captopril group.

Liquiritin improves the morphological changes via Masson staining

The myocardial fibers were red and collagen fibers were blue in each group. The texture of myocardial fibers was clear, arranged in an orderly manner, and the direction was consistent. A small amount of collagen fibers with uniform distribution could be observed in the sham group. Cardiac fibrosis was increased in the model group, while it was improved greatly in the captopril and liquiritin groups (Figure 5).

Effect of liquiritin on the expression of TLR4, MyD88, and NF-κB p65

Western blotting was used to measure the expression in the TLR4/MyD88/NF-κB signal pathway. As shown in Figure 6, the expression of TLR4, MyD88, and NF-κB p65 were significantly increased in the model group compared with the sham group ($P < 0.01$; $P < 0.05$). The expression of TLR4, MyD88, and NF-κB p65 were obviously decreased in the liquiritin group and the captopril group compared with the model group ($P < 0.01$; $P < 0.05$), but there were no significant differences between the liquiritin group and the captopril group.

Discussion

Myocardial inflammation plays a key role in the physiological and pathological mechanism of cardiac function and dysfunction. Myocardial inflammation is a general double-edged sword. Effective and appropriate inflammation is necessary and beneficial for host defense against injury. Excessive or chronic inflammation can cause severe myocardial damage to the myocardium, such as AMI (Liu *et al.*, 2019). AMI is a disease that causes damage and death to heart tissue due to the blockage of myocardial coronary arteries caused by atherosclerotic clots or arterial spasms, and now AMI has become one of the most common diseases that cause

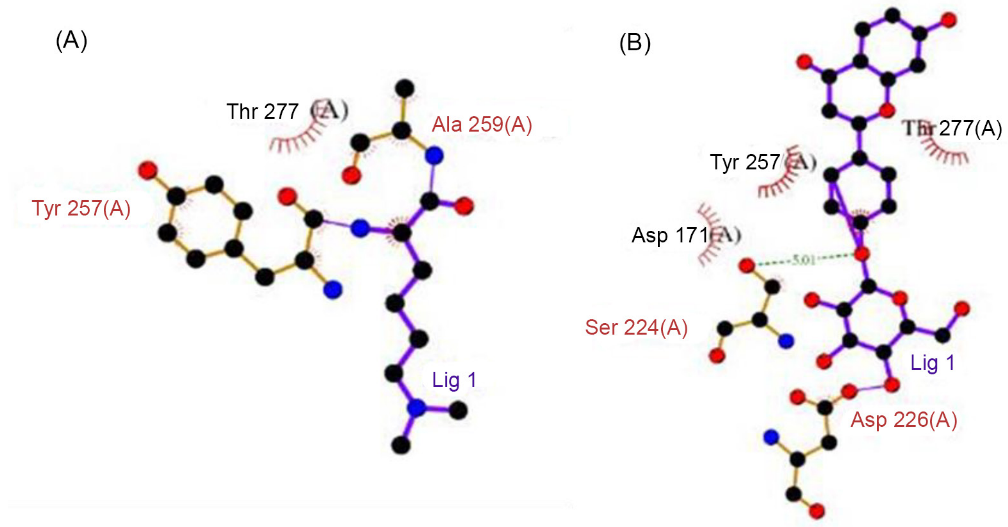

Figure 2. **The pictures of native ligand and active site of MyD88. Native ligand (A, 2D), Liquiritin (B, 2D).**

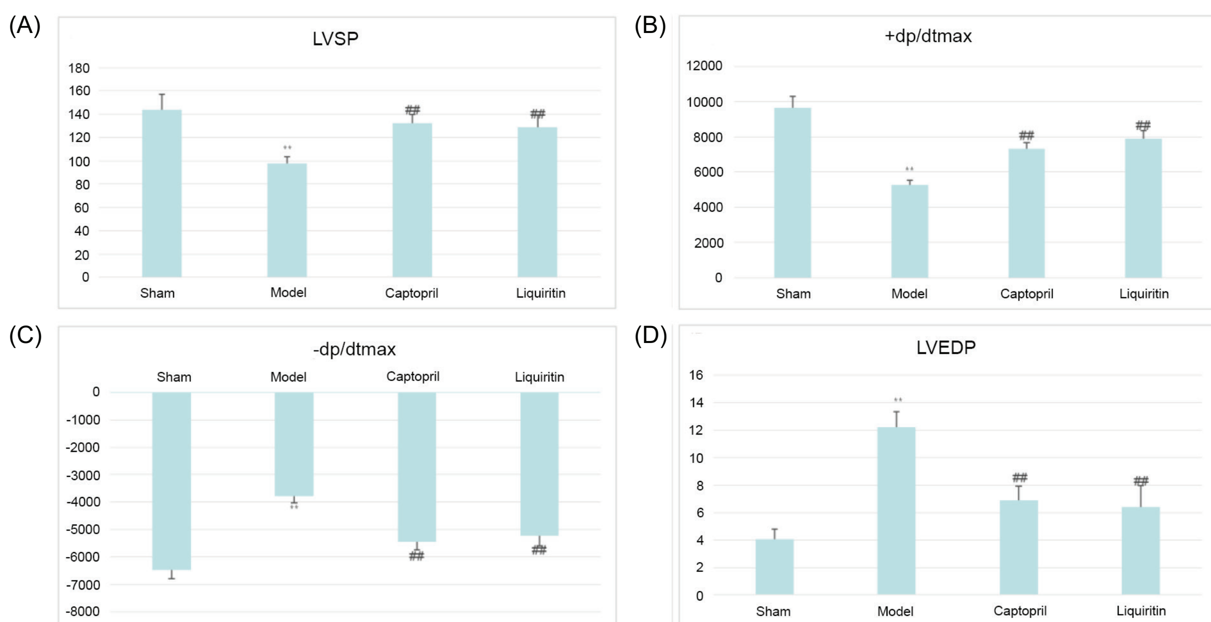

Figure 3. **Liquiritin improves hemodynamics dysfunction on (A) LVSP; (B) +dp/dtmax; (C) -dp/dtmax; (D) LVEDP. The values are expressed as mean ± SD (n = 10). **P < 0.01 versus Sham group, ##P < 0.01 versus Model group.**

morbidity and mortality worldwide. At present, the treatment of AMI mainly includes drug therapy, vascular reconstruction, and rehabilitation therapy, but these treatments have limited effect and find it difficult to prevent the progress of AMI (Amosse *et al.*, 2017). Although revascularization can effectively alleviate AMI, it is also accompanied by intractable complications, such as no-reflow after percutaneous coronary intervention (PCI), intrastent thrombosis, ischemia-reperfusion injury, etc. (Hernandez-Resendiz *et al.*, 2018). Therefore, it is of great significance for the development of new drugs to find effective therapeutic methods according to the pathogenesis of AMI. With the frequent and successful use of TCM in the prevention and treatment of AMI, the impact of Chinese medicine on AMI has drawn increasing attention.

As a "functional food," flavonoids can be widely used in the prevention and treatment of cardiovascular diseases. The anti-inflammatory effect of flavonoids can be used to prevent and treat CVDs found in fruits, vegetables, grains, bark, flowers, and tea (Choy *et al.*, 2019; Mozaffarian and Wu, 2018). Licorice contains multiple flavonoids, which possess a variety of biological activities.

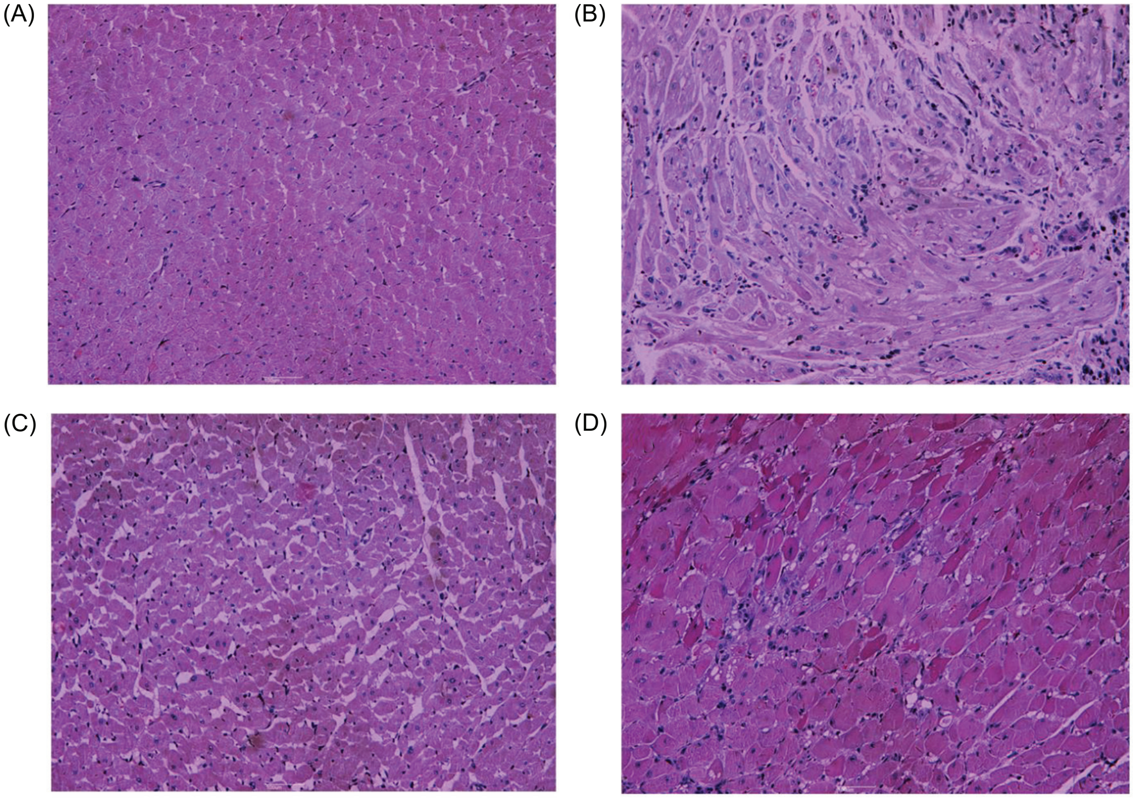

Figure 4. Morphological analysis of myocardial tissue stained with HE (×100). (A) Sham group. (B) Model group. (C) Captopril group. (D) Liquiritin group.

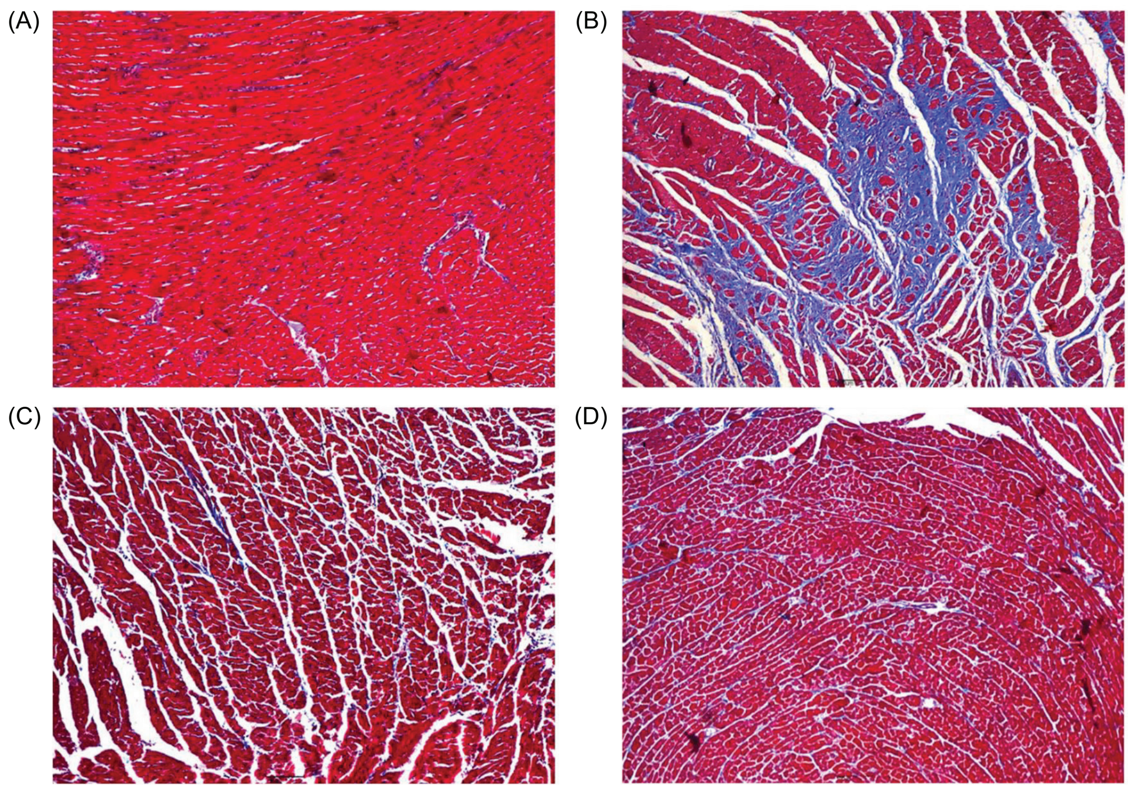

Figure 5. The Masson results of myocardium in different groups (×100). (A) Sham group. (B) Model group. (C) Captopril group. (D) Liquiritin group.

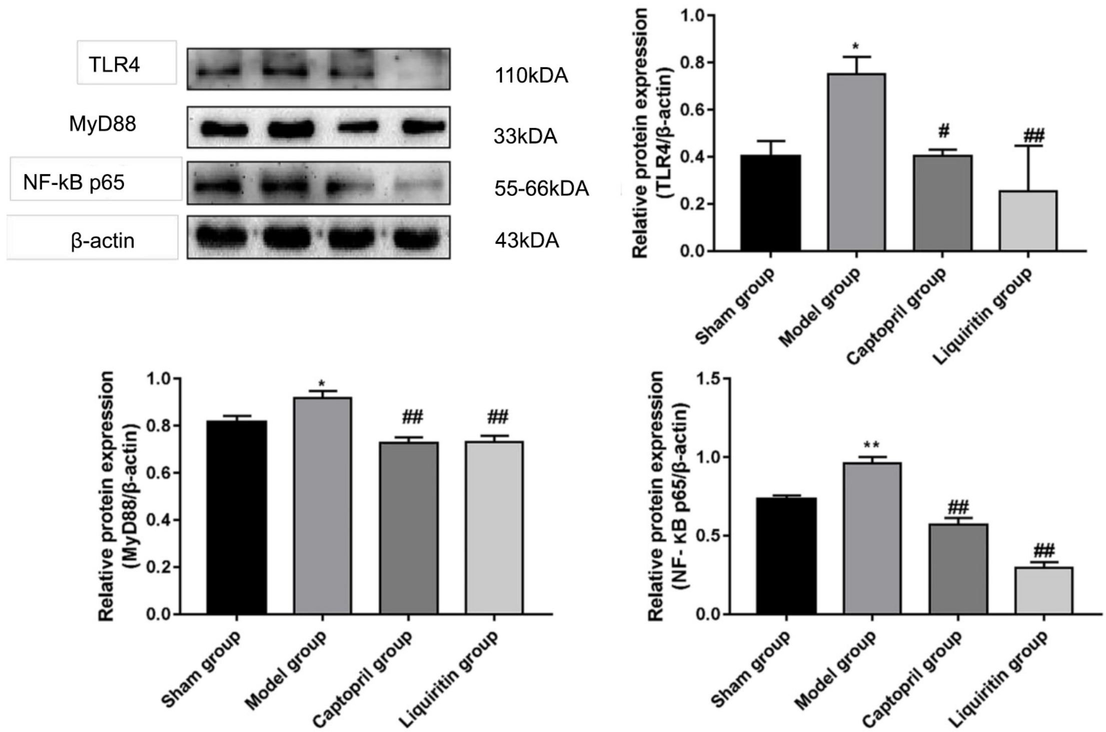

Figure 6. Effect of liquiritin on the expression of TLR4, MyD88, and NF-κB p65. The values were expressed as the mean±SD (n = 3), *P < 0.05, **P < 0.01, versus Sham group; #P < 0.01, ##P < 0.01, versus Model group.

Among them, liquiritin is a major constituent of Licorice, and it possesses anti-inflammatory activity. Liquiritin was effective in the inflammatory response to fructose stimulation *in vitro*, which can significantly reduce the release of inflammatory factors and NF-κB phosphorylation by inhibiting the IKKα/IκBα signaling pathway (Zhang *et al.*, 2016). Liquiritin can also significantly reduce the death rate of H9c2 cells after hypoxia/reoxygenation damage, increase the mitochondrial mass, and decrease the level of reactive oxygen species, and mitochondrial Ca^{2+} level (Thu *et al.*, 2021). The results of in vitro and in vivo experiments show that liquiritin can act as an agonist of AMP-activated protein kinase (AMPK), mainly because liquiritin can enhance the phosphorylation of AMPKα2 and decrease the phosphorylation of mTORC1, IκBα, and NFκB/p65 (Mou *et al.*, 2021).

In our study, liquiritin could increase the levels of LVSP, +dp/dtmax, and -dp/dtmax; reduce the level of LVEDP; and improve morphological changes through HE, and Masson staining, which showed that liquiritin has a good protective effect on AMI. Numerous studies have shown that TLR4 activates the expression of several pro-inflammatory cytokine genes that play a key role in myocardial inflammation, especially in myocarditis, myocardial infarction, ischemia-reperfusion injury, and heart failure (Hally *et al.*, 2017). Specifically, after TLR4 is stimulated by inflammatory signals, MyD88 binds to the cytoplasmic domain of TLR4 and activates IKK. Activated IKK kinase leads to phosphorylation and degradation of IκB in the proteasome, and NF-κB is then released from the NF-κB complex and transported to the nucleus, resulting in gene expression of pro-inflammatory cytokines (Yang *et al.*, 2016). Activation of TLR4/MyD88 signaling pathway leads to direct activation of NF-κB and promotes secretion of pro-inflammatory cytokines. In this study, liquiritin decreased the expression of TLR4, MyD88, and NF-κB p65 proteins, suggesting that liquiritin inhibited AMI through TLR4/MyD88/NF-κB signaling pathway.

However, the current study has several limitations. First of all, this study only adopted an *in vivo* experiment, without further verification by an *in vitro* cell experiment. Secondly, this study lacked the use of TLR4 inhibitor, so as to better explore the mechanism of action of liquiritin on AMI.

Conclusion

In conclusion, molecular docking combined with *in vivo* evaluation showed that liquiritin has a cardioprotective effect on AMI model rats by inhibiting the TLR4/MyD88/NF-κB signaling pathway. This pathway may be a new potential therapeutic target of liquiritin in the treatment of AMI, and these properties of liquiritin can be further explored to develop viable anti-AMI agents.

Declarations

Funding

Financial assistance was received with appreciation from the National Natural Science Foundation of China (No. 82004180), Key Project Foundation of Natural Science Research in Universities of Anhui Province in China (KJ2020A0411), and the Key Project Foundation of Natural Science Research of Anhui University of Chinese Medicine (2020zrzd06 and 2021zrzd22).

Conflict of Interest

The authors declare that they have no conflict of interest.

Data Availability Statement

The data that support the findings of this study are available from the corresponding author upon reasonable request.

References

Ahmed-Farid, O.A., Haredy, S.A., Niazy, R.M., Linhardt, R.J. and Warda, M., 2019. Dose-dependent neuroprotective effect of oriental phyto-derived glycyrrhizin on experimental neuroterminal norepinephrine depletion in a rat brain model. Chemico-Biological Interactions 308: 279–287. https://doi.org/10.1016/j.cbi.2019.05.045

Amosse, J., Martinez, M.C. and Le Lay, S., 2017. Extracellular vesicles and cardiovascular disease therapy. Stem Cell Investigation 4: 102. https://doi.org/10.21037/sci.2017.11.07

Choy, K.W., Murugan, D., Leong, X.F., Abas, R., Alias, A. and Mustafa, M.R., 2019. Flavonoids as natural anti-inflammatory agents targeting nuclear factor-kappa B (NF-κB) signaling in cardiovascular diseases: a mini review. Frontiers in Pharmacology 10: 1295. https://doi.org/10.3389/fphar.2019.01295

Davidson, S.M., Ferdinandy, P., Andreadou, I., Bøtker, H.E., Heusch, G., Ibáñez, B., Ovize, M., Schulz, R., Yellon, D.M., Hausenloy, D.J., Garcia-Dorado, D. and CARDIOPROTECTION COST Action (CA16225), 2019. Multitarget strategies to reduce myocardial ischemia/reperfusion injury: JACC review topic of the week. Journal of the American College of Cardiology 73(1): 89–99. https://doi.org/10.1016/j.jacc.2018.09.086

Hally, K.E., La Flamme, A.C., Larsen, P.D. and Harding, S.A., 2017. Platelet toll-like receptor (TLR) expression and TLR-mediated platelet activation in acute myocardial infarction. Thrombosis Research 158: 8–15. https://doi.org/10.1016/j.thromres.2017.07.031

He, J., Han, S., Li, X.X., Wang, Q.Q., Cui, Y. and Chen, Y., 2019. Diethyl blechnic exhibits anti-inflammatory and antioxidative activity via the TLR4/MyD88 signaling pathway in LPS-stimulated RAW264.7 cells. Molecules 24: 4502. https://doi.org/10.3390/molecules24244502

Hernandez-Resendiz, S., Chinda, K., Ong, S.B., Cabrera-Fuentes, H., Zazueta, C. and Hausenloy, D.J., 2018. The role of redox dysregulation in the inflammatory response to acute myocardial ischaemia-reperfusion injury-adding fuel to the fire. Current Medicinal Chemistry 25(11): 1275–1293. https://doi.org/10.2174/0929867324666170329100619

Horikoshi, T., Nakamura, T., Yoshizaki, T., Watanabe, Y., Uematsu, M., Kobayashi, T., Nakamura, K., Saito, Y., Obata, J.E. and Kugiyama, K., 2021. Impact of persistent endothelial dysfunction in an infarct-related coronary artery on future major adverse cardiovascular event occurrence in STEMI survivors. Heart and Vessels 36(4): 472–482. https://doi.org/10.1007/s00380-020-01723-9

Hsin, K.Y., Matsuoka, Y., Asai, Y., Kamiyoshi, K., Watanabe, T., Kawaoka, Y. and Kitano, H., 2016. systemsDock: a web server for network pharmacology-based prediction and analysis. Nucleic Acids Research 44(W1): W507–W513. https://doi.org/10.1093/nar/gkw335

Huang, Z., Sheng, Y., Chen, M., Hao, Z., Hu, F. and Ji, L., 2018. Liquiritigenin and liquiritin alleviated MCT-induced HSOS by activating Nrf2 antioxidative defense system. Toxicology and Applied Pharmacology 355: 18–27. https://doi.org/10.1016/j.taap.2018.06.014

Jiang, M., Zhao, S., Yang, S., Lin, X., He, X. and Wei, X., 2020. An "essential herbal medicine"-licorice: a review of phytochemicals and its effects in combination preparations. Journal of Ethnopharmacology 249: 112439. https://doi.org/10.1016/j.jep.2019.112439

Krga, I., Milenkovic, D., Morand, C. and Monfoulet, L.E., 2016. An update on the role of nutrigenomic modulations in mediating the cardiovascular protective effect of fruit polyphenols. Food Function 7: 3656–3676. https://doi.org/10.1039/C6FO00596A

Kwon, Y.J., Son, D.H., Chung, T.H. and Lee, Y.J., 2020. A review of the pharmacological efficacy and safety of Licorice root from corroborative clinical trial findings. Journal of Medicinal Food 23(1): 12–20. https://doi.org/10.1089/jmf.2019.4459

Lin, M., Liu, X., Zheng, H., Huang, X., Wu, Y., Huang, A., Zhu, H., Hu, Y., Mai, W. and Huang, Y., 2020. IGF-1 enhances BMSC viability, migration, and anti-apoptosis in myocardial infarction via secreted frizzled-related protein 2 pathway. Stem Cell Research & Therapy 11(1): 22. https://doi.org/10.1186/s13287-019-1544-y

Liu, L., Gan, S., Li, B., Ge, X., Yu, H. and Zhou, H., 2019. Fisetin alleviates atrial inflammation, remodeling, and vulnerability to atrial fibrillation after myocardial infarction. International Heart Journal 60: 1398–1406. https://doi.org/10.1536/ihj.19-131

Mian, M.O.R., He, Y., Bertagnolli, M., Mai-Vo, T.A., Fernandes, R.O. and Boudreau, F., 2019. TLR (Toll-Like Receptor) 4 antagonism prevents left ventricular hypertrophy and dysfunction caused by neonatal hyperoxia exposure in rats. Hypertension 74: 843–853. https://doi.org/10.1161/HYPERTENSIONAHA.119.13022

Mo, J., Zhou, P., Chu, Z., Zhao, Y. and Wang, X., 2022. Liquiritin attenuates angiotensin II-induced cardiomyocyte hypertrophy via ATE1/TAK1-JNK1/2 pathway. Evidence-Based Complementary and Alternative Medicine 2022: 7861338. https://doi.org/10.1155/2022/7861338

Mou, S.Q., Zhou, Z.Y., Feng, H., Zhang, N., Lin, Z., Aiyasiding, X., Li, W.J., Ding, W., Liao, H.H., Bian, Z.Y. and Tang, Q.Z., 2021. Liquiritin attenuates lipopolysaccharides-induced cardiomyocyte injury via an AMP-activated protein kinase-dependent signaling pathway. Frontiers in Pharmacology 12: 648688. https://doi.org/10.3389/fphar.2021.648688

Mozaffarian, D. and Wu, J.H.Y., 2018. Flavonoids, dairy foods, and cardiovascular and metabolic health: A review of emerging biologic pathways. Circulation Research 122(2): 369–384. https://doi.org/10.1161/CIRCRESAHA.117.309008

Ohto, U., Fukase, K., Miyake, K. and Shimizu, T., 2012. Structural basis of species-specific endotoxin sensing by innate immune receptor TLR4/MD-2. Proceedings of the National Academy of Sciences of the United States of America 109(19): 7421–7426. https://doi.org/10.1073/pnas.1201193109

Ojha, S.K., Sharma, C., Golechha, M.J., Bhatia, J., Kumari, S. and Arya, D.S., 2015. Licorice treatment prevents oxidative stress, restores cardiac function, and salvages myocardium in rat model of myocardial injury. Toxicology and Industrial Health 31(2): 140–152. https://doi.org/10.1177/0748233713491800

Raj, P., McCallum, J.L., Kirby, C., Grewal, G., Yu, L., Wigle, J.T. and Netticadan, T., 2017. Effects of cyanidin 3-O-glucoside on cardiac structure and function in an animal model of myocardial infarction. Food Function 8: 4089–4099. https://doi.org/10.1039/C7FO00709D

Sinnecker, D., Dommasch, M., Steger, A., Berkefeld, A., Hoppmann, P., Müller, A., Gebhardt, J., Barthel, P., Hnatkova, K., Huster, K.M., Laugwitz, K.L., Malik, M. and Schmidt, G., 2016. Expiration-triggered sinus arrhythmia predicts outcome in survivors of acute myocardial infarction. Journal of the American College of Cardiology 67(19): 2213–2220. https://doi.org/10.1016/j.jacc.2016.03.484

Snyder, G.A., Cirl, C., Jiang, J., Chen, K., Waldhuber, A., Smith, P., Römmler, F., Snyder, N., Fresquez, T., Dürr, S., Tjandra, N., Miethke, T. and Xiao, T.S., 2013. Molecular mechanisms for the subversion of MyD88 signaling by TcpC from virulent uropathogenic Escherichia coli. Proceedings of the National Academy of Sciences of the United States of America 110(17): 6985–6990. https://doi.org/10.1073/pnas.1215770110

Sun, Y.X., Tang, Y., Wu, A.L., Liu, T., Dai, X.L., Zheng, Q.S. and Wang, Z.B., 2010. Neuroprotective effect of liquiritin against focal cerebral ischemia/reperfusion in mice via its antioxidant and antiapoptosis properties. Journal of Asian Natural Products Research 12(12): 1051–1060. https://doi.org/10.1080/10286020.2010.535520

Sun, Z.G., Zhao, T.T., Lu, N., Yang, Y.A. and Zhu, H.L., 2019. Research progress of glycyrrhizic acid on antiviral activity. Mini Reviews in Medicinal Chemistry 19(10): 826–832. https://doi.org/10.2174/1389557519666190119111125

Thu, V.T., Yen, N.T.H. and Ly, N.T.H., 2021. Liquiritin from *Radix Glycyrrhizae* protects cardiac mitochondria from hypoxia/reoxygenation damage. Journal of Analytical Methods in Chemistry 2021: 1857464. https://doi.org/10.1155/2021/1857464

Wang, L., Shi, H., Huang, J.L., Xu, S. and Liu, P.P., 2020. Linggui Zhugan decoction inhibits ventricular remodeling after acute myocardial infarction in mice by suppressing TGF-β1/Smad signaling pathway. Chinese Journal of Integrative Medicine 26(5): 345–352. https://doi.org/10.1007/s11655-018-3024-0

Wei, F., Jiang, X., Gao, H.Y. and Gao, S.H., 2017. Liquiritin induces apoptosis and autophagy in cisplatin (DDP)-resistant gastric cancer cells in vitro and xenograft nude mice in vivo. International Journal of Oncology 51(5): 1383–1394. https://doi.org/10.3892/ijo.2017.4134

Yamagata, K., 2019. Polyphenols regulate endothelial functions and reduce the risk of cardiovascular disease. Current Pharmaceutical Design 25(22): 2443–2458. https://doi.org/10.2174/1381612825666190722100504

Yang, J., Zhang, F., Shi, H., Gao, Y., Dong, Z., Ma, L., Sun, X., Li, X., Chang, S., Wang, Z., Qu, Y., Li, H., Hu, K., Sun, A. and Ge, J., 2019. Neutrophil-derived advanced glycation end products-Nε-(carboxymethyl) lysine promotes RIP3-mediated myocardial necroptosis via RAGE and exacerbates myocardial ischemia/reperfusion injury. FASEB Journal 33(12): 14410–14422. https://doi.org/10.1096/fj.201900115RR

Yang, Y., Lv, J., Jiang, S., Ma, Z., Wang, D., Hu, W., Deng, C., Fan, C., Di, S., Sun, Y. and Yi, W., 2016. The emerging role of Toll-like receptor 4 in myocardial inflammation. Cell Death & Disease 7(5): e2234. https://doi.org/10.1038/cddis.2016.140

Yousufuddin, M., Takahashi, P.Y., Major, B., Ahmmad, E., Al-Zubi, H., Peters, J., Doyle, T., Jensen, K., Al Ward, R.Y., Sharma, U., Seshadri, A., Wang, Z., Simha, V. and Murad, M.H., 2019. Association between hyperlipidemia and mortality after incident acute myocardial infarction or acute decompensated heart failure: a propensity score matched cohort study and a meta-analysis. BMJ Open 9(12): e028638. https://doi.org/10.1136/bmjopen-2018-028638

Zhang, Y., Zhang, L., Zhang, Y., Xu, J.J., Sun, L.L. and Li, S.Z., 2016. The protective role of liquiritin in high fructose-induced myocardial fibrosis via inhibiting NF-κB and MAPK signaling pathway. Biomedicine & Pharmacotherapy 84: 1337–1349. https://doi.org/10.1016/j.biopha.2016.10.036

Zhou, P., Hua, F., Wang, X. and Huang, J.L., 2020. Therapeutic potential of IKK-β inhibitors from natural phenolics for inflammation in cardiovascular diseases. Inflammopharmacology 28: 19–37. https://doi.org/10.1007/s10787-019-00680-8

Italian Journal of Food Science, 2022; 34 (2): 89–97

Fatty Acid Profile of Functional Emulsion-Based Food Products Containing Conventional and Unconventional Ingredients

Almas Mukhametov[1]*, Laura Mamayeva[1], Moldir Yerbulekova[1], Gulsim Aitkhozhayeva[2]

[1]Department of Technology and Safety of Food Products, Kazakh National Agrarian Research University, 8 Abai Avenue, Almaty, Kazakhstan; [2]Department of Land Resources and Cadastre, Kazakh National Agrarian Research University, Almaty, Kazakhstan

***Corresponding Author:** Almas Mukhametov, Department of Technology and Safety of Food Products, Kazakh National Agrarian Research University, 8 Abai Avenue, Almaty A05D5F7, Kazakhstan. Email: almmukhametov@rambler.ru

Received: 9 February 2022; Accepted: 26 May 2022; Published: 16 June 2022
© 2022 Codon Publications

OPEN ACCESS BY NC SA

PAPER

Abstract

The creation of new emulsion-based food products has great potential for the food industry at the present stage of its development. The purpose of the paper is to explore the physical and chemical characteristics (content of fatty acids and tocopherols) of nine mixtures (blends) of conventional and unconventional vegetable oils with regard to the changes in the peroxide values of the oil blends stored under different temperatures for different periods. The study was conducted in 2020 in Almaty (Kazakhstan). Nine vegetable oil blends were prepared by mixing conventional and unconventional ingredients. Each of the resulting blends was tested in 30 replicates for the content of fatty acids (oleic, linoleic, and linolenic acids) and tocopherols. The blends were stored at 10°C and 20°C. Samples were taken to determine peroxide values. The results were compared to the control (refined sunflower oil). In all nine blends, the optimal ratio of the evaluated fatty acids and the optimal concentration of tocopherols were confirmed. After 6 months of storage, the peroxide values of blend No. 1 stored at 10°C and 20°C were 3 and 6, respectively. Blend No. 2 stored for the same period at the same temperatures demonstrated the respective peroxide values of 2.5 and 4.5. For blend No. 3, the respective values obtained were 2.5 and 5.5, and for blend No. 4, the respective values were 3.0 and 6.5. The most drastic changes were observed in blend No. 5, with respective peroxide values of 2.5 and 7.2. The respective peroxide values of blend No. 6 were 3.7 and 5.5, blend No. 7, 3.5 and 7.0, blend No. 8, 4.0 and 6.5, and blend No. 9, .5 and 5.5. All in all, the peroxide values of the nine tested blends were significantly lower than those of the control ($p \leq 0.05$–0.01). The proposed nine blends can be used as food additives exhibiting biological activities. After 6 months of storage, the minimal changes in the peroxide values were observed in blend Nos. 2 and 3, while the maximum changes were reported for blend Nos. 5, 7, and 8. In the future, an investigation of the therapeutic effects of the obtained blends should be undertaken, with a focus on possible adverse heating-induced changes in some components (flaxseed oil).

Keywords: blends; food additives; peroxide value; storage temperature conditions

Introduction

Functional foods make up a significant part of modern diet. These data are supported by the global trend toward consumption of functional foods. This trend is predominantly observed in the developed countries. For example, in the United States, the increase in the consumption of special-purpose fat products exceeds the overall food production growth. The use of functional food products is primarily promoted by the studies concerning the structure of modern diet. People want to benefit from the declared properties of functional foods, which include stabilization of metabolic processes in the body and maintaining the normal functions of the immune, nervous, and endocrine systems (Truzzi *et al*., 2021). Among modern functional fatty products, a focus of the food industry is on the development of mayonnaise, various fat pastes, and creams (Khudzaifi *et al*., 2019). Inevitably, manufacturers introduce into their products some additives that are typical for certain regions of the planet, taking into account the preferences of the local population. Plant and animal products are often combined. A variety of sources are available due to various flavors rather than spices, as the latter are added only in small quantities. Fat and water-soluble vitamins and dietary fibers contribute to the taste and texture of the finished fatty products (Marchetti *et al*., 2019). The mixtures obtained in this experiment can be used as an alternative to sunflower or olive oil, which are widely used globally. One important and urgent task to be undertaken in the nearest future is to reduce the calorie content of functional food products that are being developed. Of note, the average dietary intake of fat is 35% of total calories. Therefore, the fat content of food is often reduced so that it falls within the range of 5–25%. This determines the relevance of developing new formulations of functional food products containing fat emulsions. The ultimate goal of developing functional emulsion-based food products is to make them appropriate for consumption by people of different age groups.

In order to work properly, the human body needs fatty acids (in particular, linoleic, arachidonic, and linolenic acids). In most cases, this need is met in the diet by including various vegetable oils made from conventional forage crops (sunflower, corn, soybeans, and olive; Cerceau *et al*., 2020). However, in addition to the conventional vegetable oils, oils are also extracted from unconventional crops, which have not been widely used in the food industry. This refers to the oils obtained from the processing of cereals, fruits, seeds, and nuts. Wheat germ oil and oils extracted from other cereals are of special importance. These unconventional oils are rich in linolenic, hexaenoic, pentaenoic, and other fatty acids, which are vital for the human body (Vargas Jentzsch *et al*., 2018). The optimal ratio of ω-6 and ω-3 fatty acids that constitutes the oil is 10:1. The role of fatty acids (e.g., linoleic and linolenic acids) is crucial, since they form important components of cell membranes, participate in hormone synthesis, regulate cellular metabolic processes, maintain normal blood pressure, remove excess cholesterol from the body, and improve the elasticity of blood vessels. Since these acids are not produced in the human body (Bulat and Volkov, 2016), they are considered essential (Juliani *et al*., 2006). As for arachidonic acid, its synthesis involves linoleic acid and vitamin B_6. An insufficient intake of these acids from food sources triggers cardiovascular diseases and activates pathological processes in cell membranes. Linoleic acid and its derivatives inhibit platelet aggregation, reduce the levels of cholesterol, blood pressure, and the amount of low-density lipoproteins that are harmful to the body. Interestingly, the smallest quantities of linolenic acid are found in the body of infants and senior people.

Thus, fatty acids and phospholipids are one of the most important compounds required by the human body for forming cell membranes and maintaining the normal functioning of the immune system. In this regard, it is very important to look for new, unconventional ingredients that may be incorporated into emulsion-based food products (Safonov, 2022). Unfortunately, there are very few papers covering the topic, and this fact determines the relevance of this study. Most of the available papers have considered generally the effect produced by a single unconventional ingredient. This paper describes nine different blends containing unconventional ingredients. The authors assumed that the physical and chemical properties of the experimental blends would be at least non-inferior to those of conventional emulsion-based food products (with shelf life being equivalent or longer).

The purpose of the study was to explore the physical and chemical properties of new blends of refined vegetable oils that could be used in the production of functional emulsion-based food products, subject to the shelf life of obtained blends. The objectives of the study include the following: (a) to prepare the blends of refined vegetable oils for producing functional emulsion-based food products; (b) to explore their physical and chemical properties (fatty acid profile and tocopherols); and (c) to determine the shelf life of the obtained blends.

Materials and Methods

Methods

The study was conducted in 2020 in Almaty (Kazakhstan). The formulations presented in this paper used both vegetable oils obtained from conventional sources (sunflower, soybeans, and corn; refined oils were used) and unconventional vegetable oils. Unconventional oils were extracted by oil seed pressing and purified by separation of plant residues. Refined vegetable oils derived from conventional sources were mixed with different amounts of unconventional oils. Thus, the mixtures were obtained that could be suitable for the preparation of oil-in-water emulsions.

The blends intended for fat emulsions were prepared using the ingredients shown in Table 1.

The content of fatty acids in the blends and oils under investigation was determined according to the GOsudarstvennyy STandart (GOST) 30418-96 (*Vegetable*

Table 1. Composition of the vegetable oil blends under investigation.

Blend No.	Oils used for blend recipe	Blend ratio of oils	Amount of oils as related to the total volume of fat emulsion
1	Sunflower, soybean, and flaxseed oils	20:15:10	45
2	Sunflower and pumpkin seeds oils	35:15	50
3	Sunflower, corn, and sea buckthorn oils	30:15:10	55
4	Sunflower, wheat germ, barley, and sea buckthorn oils	5:10:5:10	30
5	Sunflower, millet seed, walnut, and apricot kernel oils	10:15:5:5	35
6	Sunflower, rapeseed, tomato seed, oat, and plum kernel oils	8:8:8:8:8	40
7	Sunflower, sesame, lupine, rye, and flaxseed oil	10:5:5:5:5	45
8	Sunflower, mustard, cherry, buckwheat, and rice oils	10:10:10:10:10	50
9	Olive, wheat germ, barley germ, rosehip, and chestnut oils	15:15:15:5:5	55

oils. Method for determination of fatty acid content). For this, the capillary column gas chromatography method was applied. The researchers used polar columns Zebron ZB-50 with the column length of 30 m and internal diameter of 0.32 mm. The peaks were identified by comparing the chromatograms obtained for the analyzed blends and a mixture of fatty acid methyl esters as standards. Graphs of the peaks observed were plotted separately for saturated and unsaturated fatty acids. To build all straight lines, the investigators proceeded from the fact that 2–3 points were required for saturated fatty acids and only 1–2 points for unsaturated ones. The volume of each sample was 1 mm^3 of hexane solution containing fatty acid methyl esters.

Study design

The study consisted of two parts. In the first part, the researchers assessed the fatty acid profiles of vegetable oils (i.e., measured the levels of oleic, linoleic, and linolenic acids) and quantified the content of tocopherol. The second part of the study highlighted the changes in the stability of the tested oil blends observed at different time points of the storage period (time interval from the beginning of the experiment to 6 months of the experiment). The peroxide value was chosen as the tested parameter. The storage temperatures were 10°C and 20°C. These temperature regimes were convenient for comparing the stability of the experimental blends at different time points of the storage period. The study followed international standards applicable to scientific research. It intended to develop effective blends of vegetable oils using conventional and nonconventional ingredients for their subsequent testing and use asemulsion-based food products.

Statistical analysis

In order to analyze statistical differences, the Statistica program (version 10) was used. Arithmetic mean values were calculated for each of the tested parameters (the content of fatty acids and other components). For each comparison, the sample size of 30 was used. Differences were identified using Student's t-test. The level of significance was set at $p \leq 0.05$.

Results

The studied blends were found to contain different amounts of fatty acids. In blend No. 1, soybean and flaxseed oils were 0.5 times inferior to sunflower oil in terms of oleic acid content ($p \leq 0.05$), and flaxseed oil was twice inferior to soybean and sunflower oils ($p \leq 0.01$), the content of linolenic acid in flaxseed oil was seven times higher than in soybean oil ($p \leq 0.001$) and more than 100 times higher than in sunflower oil ($p \leq 0.0001$). Soybean oil had a slightly higher content of tocopherols as compared to the other two oils (Table 2).

In blend No. 2, the content of oleic acid in sunflower oil was 0.5 times higher than in pumpkin seed oil ($p \leq 0.05$), with no significant differences in the content of linoleic acid ($p \geq 0.05$). Pumpkin seed oil had 16 times higher content of linolenic acid ($p \leq 0.001$). There were more tocopherols in sunflower oil ($p \leq 0.05$).

In blend No. 3, sea buckthorn oil had the highest content of oleic acid. The levels of oleic acid determined in sea buckthorn oil were 1.5–2.0 times higher than in sunflower and corn oils ($p \leq 0.05$). Corn and sunflower oils had the highest content of linoleic acid as compared to the other oils used in the blend ($p \leq 0.05$). Corn oil had the highest content of linolenic acid ($p \leq 0.01$). The content of tocopherols in sunflower oil was twice lower than in sea buckthorn and corn oils ($p \leq 0.05$).

In blend No. 4, oleic acid was found in abundance in sea buckthorn oil, with twice less of it found in sunflower oil ($p \leq 0.05$), and four times less of it found in wheat germ and barley oils ($p \leq 0.01$). In terms of the content of linoleic acid, wheat germ and barley oils were not inferior

Table 2. Content of fatty acids and tocopherols in oils used for the blends under investigation.

Blend no.	Oils used for the blend recipe	Oleic acid (%)	Linoleic acid (%)	Linolenic acid (%)	Tocopherols (mg)
1	Soybean oil	25	52	8	160
	Flaxseed oil	28	20	57	113
	Sunflower oil	36	56	0.5	116
2	Sunflower oil	36	56	0.5	116
	Pumpkin seed oil	26	55	8	86
3	Sea buckthorn oil	63	38	0.1	250
	Sunflower oil	36	56	0.5	116
	Corn oil	48	56	0.8	247
4	Sea buckthorn oil	63	38	0.1	250
	Sunflower oil	36	56	0.5	116
	Wheat germ oil	14	59	4.5	140
	Barley oil	16	56	5.6	100
5	Sunflower oil	36	55	0.5	116
	Millet seed oil	27	67	10	96
	Walnut oil	35	83	15	52
	Apricot kernel oil	79	32	1.5	78
6	Sunflower oil	36	55	0.5	116
	Rapeseed oil	44	42	11	55
	Tomato oil	30	62	2.5	127
	Oat oil	41	43	2	75
	Plum kernel oil	72	25	0.5	130
7	Sunflower oil	36	55	0.5	116
	Sesame oil	48	55	3	144
	Lupine oil	55	23	8	2
	Rye oil	17	68	12	91
	Flaxseed oil	28	20	57	113
8	Sunflower oil	36	55	0.5	116
	Mustard oil	31	24	18	110
	Cherry oil	50	42	10	10
	Buckwheat oil	40	39	4	50
	Rice oil	43	53	4	110
9	Olive oil	80	22	2.5	90
	Wheat germ oil	13	65	5.5	480
	Chestnut oil	72	30	2	78
	Rosehip oil	55	30	2	260
	Barley oil	16	58	7	98

to sunflower oil ($p \geq 0.05$), with the levels of linoleic acid in wheat germ and barley oils being twice higher than those in sea buckthorn oil ($p \leq 0.05$). Wheat and barley oils contained 8–10 times more linolenic acid than found in sunflower oil ($p \leq 0.01$) and 40–50 times more linolenic acid than in sea buckthorn oil ($p \leq 0.0001$). Sea buckthorn oil contained twice more tocopherols than found in the rest of oils making up the blend ($p \leq 0.05$).

In blend No. 5, apricot oil contained twice more oleic acid than in the other oils ($p \leq 0.05$). The content of linoleic acid in walnut oil was 83%. The levels of linoleic acid in walnut oil exceeded by 2.5 times that determined in apricot oil ($p \leq 0.05$) and by 1.5 times than that determined in millet seed and sunflower oils ($p \leq 0.05$). Maximum content of linolenic acid was observed in walnut oil, followed by millet seed oil ($p \leq 0.05$), but 7–20 times less linolenic acid was found in the rest of oils ($p \leq 0.001$). All oils exhibited lower content of tocopherols as compared to sunflower oil ($p \leq 0.05$).

In blend No. 6, oleic acid accounted for 72% of the fatty acid composition of plum oil. There was 1.5–2.0 times less oleic acid in rest of the oils added to the blend

($p \leq 0.05$). Linoleic acid was found in abundance in tomato oil, thrice less abundant in plum oil ($p \leq 0.01$), and 1.5 times less abundant in the rest of the analyzed oils. The maximum content of linolenic acid was reported in rapeseed oil (11%), with its content being 5–20 times lower in the other oils making up the blend ($p \leq 0.01$). The content of tocopherols in plum and tomato oils was slightly higher than in sunflower oil ($p \leq 0.05$). Oat and rapeseed oils contained twice less tocopherols than found in plum and tomato oils ($p \leq 0.05$).

In blend No. 7, the maximum amount of oleic acid was observed in lupine oil, 0.5–1.5 times less oleic acid was found in sesame, sunflower, and flaxseed oils ($p \leq 0.05$), and the minimum amount of oleic acid was observed in rye oil ($p \leq 0.01$). The content of linoleic acid was maximum in rye, sesame, and sunflower oils, with twice less of it detected in lupine and flaxseed oils ($p \leq 0.05$). Flaxseed oil was richest in linolenic acid. The content of linolenic acid was 5 times lower in rye oil ($p \leq 0.01$), 7 times lower in lupine oil (≤ 0.01), and 20 times lower in sesame oil ($p \leq 0.001$). The minimum content of linolenic acid was reported for sunflower oil ($p \leq 0.0001$) in comparison to its content in flaxseed oil. Tocopherols were found in abundance in sesame oil, with the minimum levels observed in lupine oil ($p \leq 0.00001$).

In blend No. 8, the highest content of oleic acid was the characteristic for cherry oil, while the other oils contained 0.3–0.5 times less oleic acid ($p \leq 0.05$). Linoleic acid was in abundance in sunflower and rice oils. The other oils making up the blend were 0.5 times (buckwheat and cherry oils) and twice (mustard oil) inferior to sunflower and rice oils in terms of the content of linoleic acid ($p \leq 0.05$). Levels of linolenic acid were maximum in mustard oil, twice lower in cherry oil ($p \leq 0.05$), and four times lower in buckwheat and rice oils ($p \leq 0.01$). The minimum content of linolenic acid was observed in sunflower oil ($p \leq 0.001$). The content of tocopherols was maximum in rice, sunflower, and mustard oils, twice lower in buckwheat oil ($p \leq 0.05$), and 10 times lower in cherry oil ($p \leq 0.01$).

In blend No. 9, the highest content of oleic acid was reported for olive oil. Slightly lower level of oleic acid was revealed in chestnut oil ($p \leq 0.05$), 1.5 times less oleic acid was detected in rosehip oil ($p \leq 0.05$), and seven times less in barley and wheat germ oils ($p \leq 0.01$). The maximum amount of linoleic acid was found in wheat germ and barley oils and the minimum amount was found in chestnut, rosehip, and olive oils ($p \leq 0.05$). Maximum linolenic acid was found in wheat germ and barley oils, with the other oils being twice inferior to wheat germ and barley oils regarding content of linolenic acid ($p \leq 0.05$). The maximum content of tocopherols was documented for wheat germ oil, twice less tocopherols were quantified in rosehip oil ($p \leq 0.05$), and four times less tocopherols were quantified in the rest of oils making up the blend ($p \leq 0.01$).

The qualitative parameters of oil mixtures are shown in Figures 1–5. In each of these figures, the curves corresponding to numbers 3 and 4 reflect the changes observed in the control sample (refined sunflower oil) stored at 20°C and 10°C. The analysis demonstrated that the peroxide values of all nine oil blends prepared by the researches increased insignificantly even after 3 months of storage. Following 6 months of storage, the maximum peroxide value obtained was 7.2 mmol of active oxygen (½ O) per kg of oil blend. This variable was identified for blend No. 5.

The results of statistical analysis of changes in peroxide values are presented in Table 3.

After 6 months of storage, the peroxide values of blend No. 1 stored at 10°C and 20°C were 3 and 6, respectively (Figure 1A). Blend No. 2 stored for the same period under the same temperature conditions demonstrated the peroxide values of 2.5 and 4.5, respectively (Figure 1B). For blend No. 3, the respective values obtained were 2.5 and 5.5 (Figure 2A), for blend No. 4, the respective values were 3.0 and 6.5 (Figure 2B). The changes were more drastic in blend No. 5, with respective peroxide values of 2.5 and 7.2 (Figure 3A). The respective peroxide values

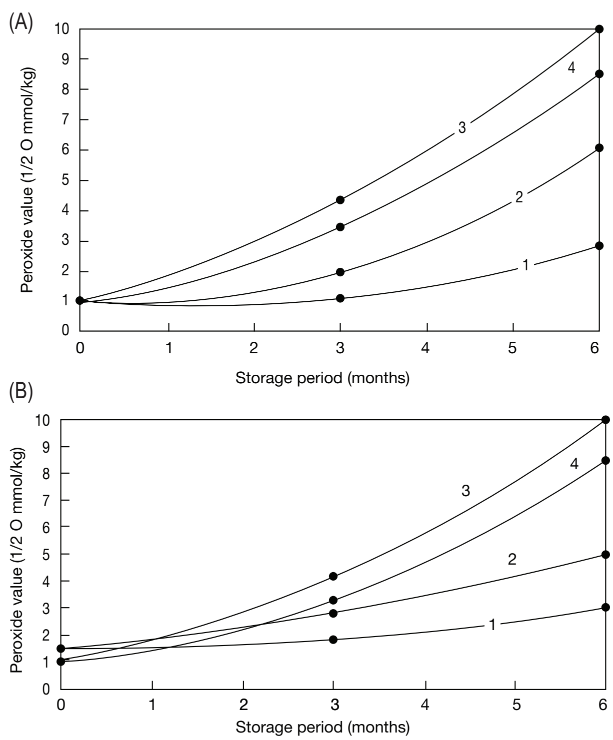

Figure 1. Peroxide values of (A) blend No. 1, and (B) blend No. 2. *Note:* Curves 3 and 4 reflect the values obtained for the control sample. Curves 1 and 2 correspond to the experimental blends stored at 10°C and 20°C, respectively.

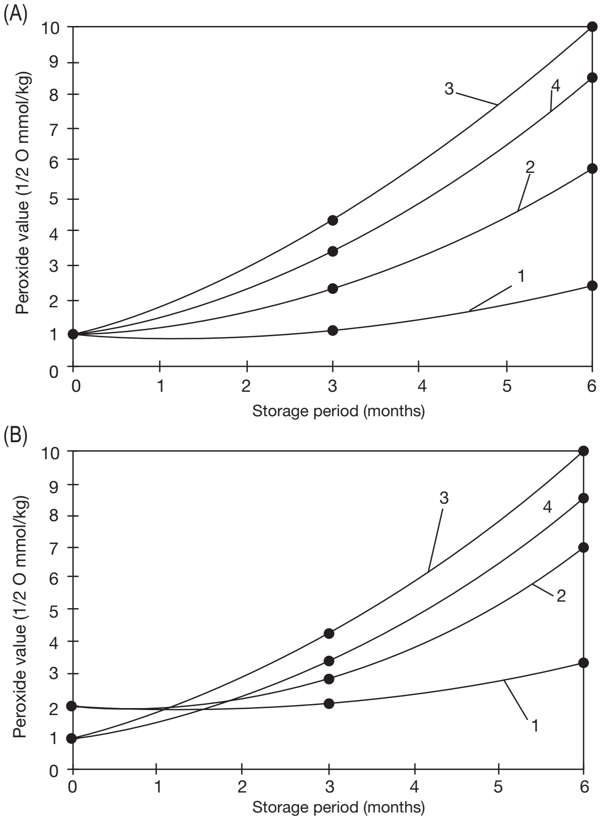

Figure 2. Peroxide values of (A) blend No. 3, and (B) blend No. 4. *Note:* Curves 3 and 4 reflect the values obtained for the control sample. Curves 1 and 2 correspond to the experimental blends stored at 10°C and 20°C, respectively.

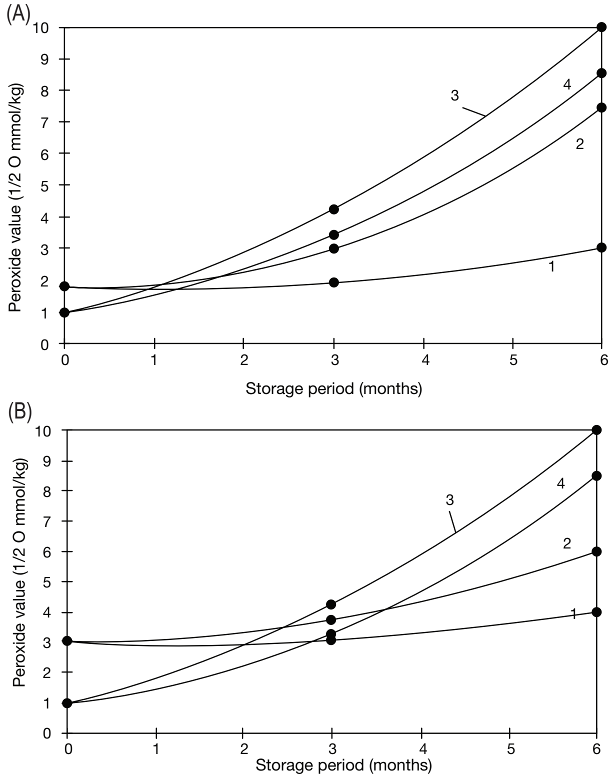

Figure 3. Peroxide values of (A) blend No. 5, and (B) blend No. 6. *Note:* Curves 3 and 4 reflect the values obtained for the control sample. Curves 1 and 2 correspond to the experimental blends stored at 10°C and 20°C, respectively.

of blend No. 6 were 3.7 and 5.5 (Figure 3B), for blend No. 7 3.5 and 7.0 (Figure 4A), for blend No. 8 4.0 and 6.5 (Figure 4B), and for blend No. 9 4.5 and 5.5 (Figure 5). In all cases, the peroxide values of analyzed blends were significantly lower than the peroxide values of control ($p \leq 0.05$).

Discussion

The results presented in this article indicate that the proposed blends of different vegetable oils have a much longer shelf life as compared to the control sample of sunflower oil. This is confirmed by the fact that peroxide values of the prepared oil blends kept under different storage conditions increased by 0.5–2.0 times slower than the peroxide value of the control sample. A range of theoretical and practical studies established that blending of conventional and unconventional vegetable oils not only increases their shelf life but also provides the optimal balance of the three main fatty acids required for functioning of the body: oleic, linoleic, and linolenic acids (Samburova *et al.*, 2022). Kinetic dependencies signaled that the proposed blends have a longer shelf life and are less susceptible to oxidative processes than the control sample.

Vegetable oils have been studied quite well. They are characterized by the basic ratio of fatty acids (Papotti *et al.*, 2015). However, most nutritionists favor the use olive and flaxseed oils. Corn, sunflower, and cottonseed oils are claimed to have benefits if used from time to time (Marchetti *et al.*, 2019; Popescu *et al.*, 2015). Ingredients that are typically present in oil mixtures (blends) are sunflower, soy, and flax (Vigli *et al.*, 2003). All of these were used in the proposed nine blends. It must be remembered that some reports support the use of flaxseed oil blends in a cold form, since flaxseed oil gives off a rather specific smell when exposed to heat (Ventsova and Safonov, 2021). Hence, the content of flaxseed oil in a blend should not exceed 5% (Marchetti *et al.*, 2019). The blends offered by different studies meet the above requirement and are recommended for consumption in a cold form. Some authors have observed that flaxseed oil is instable (Raveau *et al.*, 2020). They claim that additional protective measures must be taken to compensate for the rancidity of flaxseed oil. Nevertheless, stability of the oil blends used in this experiment has been demonstrated.

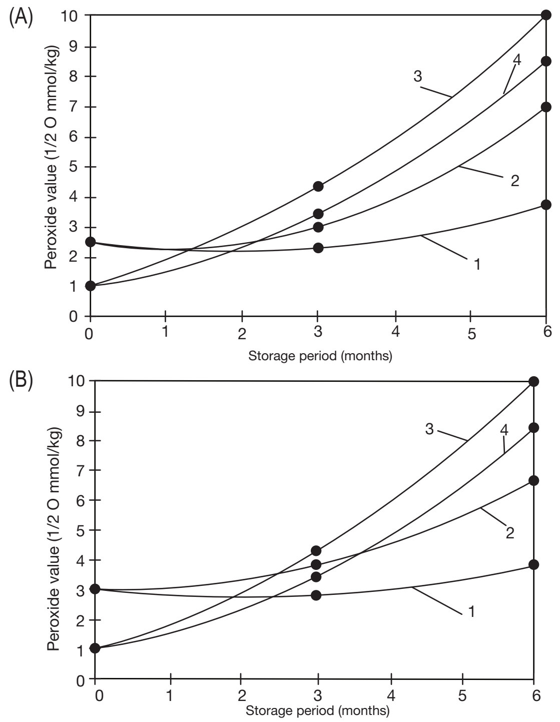

Figure 4. Peroxide values of (A) blend No. 7, and (B) blend No. 8. *Note:* Curves 3 and 4 reflect the values obtained for the control sample. Curves 1 and 2 correspond to the experimental blends stored at 10°C and 20°C, respectively.

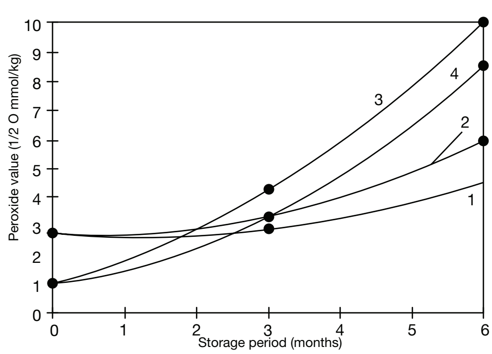

Figure 5. Peroxide value of blend No. 9. *Note:* Curves 3 and 4 reflect the values obtained for the control sample. Curves 1 and 2 correspond to the experimental blend stored at 10°C and 20°C, respectively.

In addition, oils extracted from unconventional sources, such as pumpkin, watermelon, amaranth, and wheat, are being used more extensively. These types of oils have not only high nutritional value but also an apparent therapeutic effect (Orsavova *et al.*, 2015). Moreover, there is a gradual increase in the production volumes of camelina and hemp oils, both rich in linolenic acid.

The blends described in the article organically combine three essential fatty acids. Quite often, blends are made

Table 3. Changes in peroxide values calculated for the nine blends and control sample stored for different periods under different temperatures.

		Control		Experiment			Control		Experiment		
Blend no.	**At the beginning of the experiment**	**After 3 months of storage at 10°C**	**After 3 months of storage at 20°C**	**After 3 months of storage at 10°C**	**After 3 months of storage at 20°C**	**Significance of differences for 3-month storage**	**After 6 months of storage at 10°C**	**After 6 months of storage at 20°C**	**After 6 months of storage at 10°C**	**After 6 months of storage at 20°C**	**Significance of differences for 6-month storage**
1	1	3	4	1.1	1.6	0.05	8	10	2	5.8	0.05
2	1.5	3	4	1.2	2	0.05	8	10	2.5	4.5	0.05
3	1	3	4	1.1	2.2	0.05	8	10	2.5	5.8	0.05
4	2	3	4	2.2	2.8	0.05	8	10	3	6.9	0.05
5	2	3	4	2.2	2.7	0.05	8	10	3	7	0.05
6	3	3	4	3.2	3.5	0.05	8	10	3.7	5.5	0.05
7	2.5	3	4	2.7	2.9	0.05	8	10	3.5	7	0.05
8	3	3	4	3.1	3.7	0.05	8	10	3.5	6.5	0.05
9	3	3	4	3.1	3.2	0.05	8	10	3.9	5.9	0.05

from sunflower and camelina oils. The grassy taste associated with camelina oil becomes milder if its content in the oil blend is limited to 15–30%.

Wheat germ oil is often used in blends because of having a high content of tocopherols (Rueda *et al*., 2014). To clarify, the content of tocopherols in different components of the blends is one of the aspects considered in this paper. It should be mentioned that wheat germ oil is added to blends only in small amounts ranging from 1% to 5%, as it is quite expensive. An effective marketing approach is labeling of therapeutic effects of wheat germ oil used as a blend component. Some blends contain pumpkin seed oil and other oils of unconventional origin (such as sea buckthorn, apricot, and hazelnut oils; Vigli *et al*., 2003). Most of the mentioned unconventional vegetable oils presented in this paper are components of the analyzed blends.

Limitations of this study are associated with the small-scale production of the proposed unconventional oils. This means that production of blends based on these types of oils cannot be started and boosted immediately. Further research is required focusing mainly on the development of methods of production increase and investigation of therapeutic effects of unconventional vegetable oils. At this stage, the proposed blends can be used as biologically active food additives.

Conclusions

Following an analysis of the obtained graphical models of dependencies, the researchers revealed that all nine oil blends demonstrated a slight increase in peroxide value after being stored for 3 months. Following 6 months of storage, the maximum peroxide value was confirmed for blend No. 5 (7.2 mmol of active oxygen/kg of oil blend). The obtained results established that the quality of experimental blends improved as compared to sunflower oil. These findings justify the use of these blends as a source of fats in the production of emulsion-based food products.

Owing to theoretical and experimental studies, scientific basis has been provided for obtaining the fatty phase of emulsion-based food products by using blends having optimal amounts of conventional and unconventional vegetable oils. This approach allows enriching the fatty acid composition of emulsion-based food products.

Appropriate criteria have been formulated to evaluate the effects of fatty acid profile on the biological and nutritional values of emulsion-based food products. Besides, respective dependences have been revealed that are valuable from the practical point of view.

Optimal storage conditions and shelf life were determined based on the kinetics of oxidative processes occurring in the developed blends of vegetable oils and emulsion-based food products.

Acknowledgments

This article is written in the framework of the scientific work on "*Development of the technology of fat products with a balanced fatty acid composition*" IRN AP08053397. The authors express their gratitude to the anonymous reviewer for the recommendations and comments that improved the quality of the article.

Conflict of Interest

The authors declared no potential conflict of interest with respect to the research, authorship, and/or publication of this article.

Funding

The authors received no financial support for the research, authorship, and/or publication of this article.

Data Availability

Data will be available on request.

References

Bulat P.V. and Volkov K.N. 2016. Detonation jet engine. Part II—construction features. Int J Environ Sci Educ. 11(12): 5020–5033.

Cerceau C.I., Barbosa L.C., Alvarenga E.S., Maltha C.R. and Ismail F.M. 2020. 1H-NMR and GC for detection of adulteration in commercial essential oils of Cymbopogon ssp. Phytochem Anal. 31(1): 88–97. https://doi.org/10.1002/pca.2869

Juliani H.R., Kapteyn J., Jones D., Koroch A.R., Wang M., Charles D. and Simon J.E. 2006. Application of near-infrared spectroscopy in quality control and determination of adulteration of African essential oils. Phytochem Anal. 17(2): 121–128. https://doi.org/10.1002/pca.895

Khudzaifi M., Retno S.S. and Rohman A. 2019. The employment of FTIR spectroscopy and chemometrics for authentication of essential oil of *Curcuma mangga* from candle nut oil. Food Res. 4(2): 515–521. https://doi.org/10.26656/fr.2017.4(2).313

Marchetti L., Pellati F., Benvenuti S. and Bertelli D. 2019. Use of 1H NMR to detect the percentage of pure fruit juices in blends. Molecules. 24(14): 2592. https://doi.org/10.3390/molecules24142592

Orsavova J., Misurcova L., Ambrozova J.V., Vicha R. and Mlcek J. 2015. Fatty acids composition of vegetable oils and its contribution to dietary energy intake and dependence of cardiovascular mortality on dietary intake of fatty acids. Int J Mol Sci. 16(6): 12871–12890. https://doi.org/10.3390/ijms160612871.

Papotti G., Bertelli D., Graziosi R., Maietti A., Tedeschi P., Marchetti A. and Plessi M. 2015. Traditional balsamic vinegar and balsamic vinegar of Modena analyzed by nuclear magnetic resonance spectroscopy coupled with multivariate data analysis. LWT—Food Sci Tech. 60(2): 1017–1024. https://doi.org/10.1016/j.lwt.2014.10.042

Popescu R., Costinel D., Dinca O.R., Marinescu A., Stefanescu I. and Ionete R.E. 2015. Discrimination of vegetable oils using NMR spectroscopy and chemometrics. Food Control. 48: 84–90. https://doi.org/10.1016/j.foodcont.2014.04.046

Raveau R., Fontaine J. and Lounès-Hadj Sahraoui A. 2020. Essential oils as potential alternative bio-control products against plant pathogens and weeds: a review. Foods. 9(3): 365. https://doi.org/10.3390/foods9030365

Rueda A., Seiquer I., Olalla M., Giménez R., Lara L. and Cabrera-Vique C. 2014. Characterization of fatty acid profile of argan oil and other edible vegetable oils by gas chromatography and discriminant analysis. J Chem. 2014: 843908. https://doi.org/10.1155/2014/843908

Safonov V. 2022. Comparison of LPO-AOS indices and biochemical composition of animal blood in biogeochemical provinces with different levels of selenium. Biol Trace Elem Res. 200: 2055–2061. https://doi.org/10.1007/s12011-021-02825-9.

Samburova M., Safonov V. and Avdushko S. 2022. Ecological and biological features of the primrose distribution in Transbaikalia as the model territory of Eastern Siberia. Bot Rev. 88: 50–62. https://doi.org/10.1007/s12229-021-09264-0

Truzzi E., Marchetti L., Benvenuti S., Ferroni A., Rossi M.C. and Bertelli D. 2021. Novel strategy for the recognition of adulterant vegetable oils in essential oils commonly used in food industries by applying 13C NMR spectroscopy. J Agric Food Chem. 69(29): 8276–8286. https://doi.org/10.1021/acs.jafc.1c02279.

Vargas Jentzsch P., Gualpa F., Ramos L.A. and Ciobotă V. 2018. Adulteration of clove essential oil: detection using a handheld Raman spectrometer. Flavour Fragr J. 33(2): 184–190. https://doi.org/10.1002/ffj.3438

Ventsova I. and Safonov V. 2021. Biochemical screening of lipid peroxidation and antioxidant protection in imported cows during adaptation. Adv Anim Vet Sci. 9(8): 1203–1210. http://doi.org/10.17582/journal.aavs/2021/9.8.1203.1210

Vigli G., Philippidis A., Spyros A. and Dais P. 2003. Classification of edible oils by employing 31P and 1H NMR spectroscopy in combination with multivariate statistical analysis. A proposal for the detection of seed oil adulteration in virgin olive oils. J Agric Food Chem. 51(19): 5715–5722. https://doi.org/10.1021/jf030100z.

Italian Journal of Food Science, 2022; 34 (2): 98–109

Wine recommendation algorithm based on partitioning and stacking integration strategy for Chinese wine consumers

Weisong Mu, Yumeng Feng, Haojie Shu, Bo Wang, Dong Tian*

College of Information and Electrical Engineering, China Agricultural University, Beijing 100083, P.R. China

***Corresponding Author**: Dong Tian, College of Information and Electrical Engineering, China Agricultural University, Beijing 100083, P.R. China. Email: td_tiandong@cau.edu.cn

Received: 6 April 2022; Accepted: 10 June 2022; Published: 28 June 2022
© 2022 Codon Publications

OPEN ACCESS

PAPER

Abstract

This study tries to propose a wine recommendation algorithm based on partitioning and Stacking Integration Strategy for Chinese wine consumers. The approaches follow the idea of partitioning, decomposing traditional recommendation task into several subtasks according to wine attributes, using neural network, support vector machine (SVM), decision tree, random forest, optimized random forest, Adaboost and XGBoost as recommendation models. Then, based on Stacking integration method, five models are screened out for each recommendation index as the base classifier, and the decision tree or logistic regression model is selected as the meta-learner to construct a two-layer Stacking integration framework. Finally, the optimal recommendation algorithm be built for recommendation subtasks according to the prediction accuracy. The result showed that the Stacking integrated recommendation model was suitable for the recommendation of eight attributes including colour, sweetness, foamability, mouthfeel, aroma type, year, packaging and brand, while SVM model was suitable to recommend aroma concentration and price, and the XGboost model was most appropriate for origin. This study would subserve consumers to choose the wine more easily and conveniently and provide support for wine companies to improve customer satisfaction with consumer services. The study expands the approach of concerning research and proposes a specific multi-model recommendation strategy based on artificial intelligence models to recommend multiattribute commodities.

Keywords: Chinese consumers; machine learning; preference for wine attributes; Recommendation algorithm; Stacking integration

Introduction

The development and application of big data analysis technology play an important role in reducing operating costs for businesses and accurately recommending products for customers. Due to the rich attributes and various categories of wine, and indifference of wine knowledge among Chinese consumers, there will be problems such as indecision, time consumption and high cost of trial and error when consumers purchase wine. Therefore, accurate identification of customers' wine drinking preferences and making personalised recommendations are of great significance to improving customer satisfaction and business performance.

Recommendation algorithm can help users quickly and accurately screen out the corresponding business information from massive data without knowing their own preferences (Liu *et al.*, 2017). Traditionally, similarity measurement and its variants are usually used to make recommendations. With the emergence of machine learning methods in the field of artificial intelligence,

 ISSN 1120-1770 online, DOI 10.15586/ijfs.v34i2.2209

scholars have introduced machine learning technology into recommendation algorithms (Zhang and Lei, 2021), which mainly focuses on using supervised learning algorithms to predict user preferences in different fields (Portugal *et al*., 2018). A study in 2018 proposed an innovative association classification method, which mined demand satisfaction rules according to the feedback behaviour of users on the recommended products by the system, with the aim of making recommendations based on consumer initiative decision. However, there is a problem of cold start of users, and this method is not applicable when there is no interactive data of users on wine purchase (Yin *et al*., 2018). Meng and Xiong (2021) used Latent Dirichlet Allocation topic model to divide all user–doctor history consultation text in online medical community into different themes. Then, relevant therapists for users were recommended by combining with the implied disease information in the consultation text and collaborative filtering framework. Compared with the traditional recommendation algorithm, the overall accuracy has improved, whereas the applicable data type is only unstructured text data. Most of the above-mentioned studies used a single machine learning model and optimized it to find out a better prediction result. Although the prediction method of single model is relatively mature, the generalisation ability still needs to be improved. In addition, random factors will affect the model effect and lead to low prediction accuracy (Xie *et al*., 2020).

In order to effectively reduce or offset the influence of random factors and improve the prediction accuracy and credibility of the prediction model in a single model, ensemble learning has become one of the hot topics in machine learning (Hu *et al*., 2021). Ensemble methods usually use multiple weak classifiers to form a strong classifier algorithm to improve the classification accuracy. Ensemble learning algorithms mainly include Bagging (He *et al*., 2019), Boosting and Stacking algorithms, among which Bagging and Boosting algorithms can only integrate single learners of the same type to reduce variance and deviation (Wang *et al*., 2019). Different from the previous ideas, Stacking can integrate many different types of learners, which can compensate the weakness of single algorithm, enhance the generalisation ability, reduce the risk of overfitting, and improve accuracy. Xie *et al*. (2020) put forward a Stacking framework, which can realize the automatic classification of six types of *Anoectochilus roxburghii* leaves. Considering that the research object is image data with poor interpretability, this method is not suitable for many mixed data sets. Li and Zhai (2019) used Adaboost and random forest as base classifiers of Stacking algorithm to predict and analyse the turnover factors of enterprise staff, aiming at strengthening the management and control of top managers on staffs. Tao *et al*. (2019) used the stacking algorithm to classify the continued spectral series of rape vegetation, and then embedded the algorithm into unmanned aerial vehicle to distinguish different growing rapes accurately. Based on the interactive behaviour data between users and retail products, Zhang and Lei (2021) established a Stacking algorithm which combines LightGBM, XGboost and random forest to predict the possibility of buying by users in the future and the specific purchase time. However, new users who have not generated behaviour are not considered, it could not solve the cold start problem of new users. Based on the above analysis, in most cases, the combined model has better prediction performance than the single model.

Numerous studies have been conducted on the issue of consumer preference on wine attributes in recent years, which focus on attribute preference influencing factors (Gustafson *et al*., 2016; Mehta and Bhanja, 2018; Szolnoki and Hauck, 2020) and the actual impact on consumers (Areta *et al*., 2017; Lee and Lee, 2008; Li *et al*., 2022). Most of these studies use simple statistical methods or single machine learning algorithms. For example, by using a simple best–worst method, Stanco *et al*. (2020) concluded that traditional attributes such as 'geographical indications' and 'grape variety,' influence consumer purchase behaviour more than untraditional attributes such as 'alcohol-free wine' and 'vegan wine.' Chu *et al*. (2020) built a predictive model for Chinese wine consumers' sensory preferences based on multivariate disorder logistic regression method. On the other hand, using simple logistic regression algorithm is one-sided in analysing the influence of consumers' personal characteristics on wine selection. Although there has been a great deal of research into consumer preferences on wine, recommendation algorithms and personalised recommendation strategies for wine are less researched and still need further development.

In summary, considering the rich attributes and factors on wine recommendation, and the immature research on personalised recommendation strategy, this study first decomposes the recommendation task of wine product into several recommendation subtasks according to wine attributes with the idea of divide and conquer. Based on the discrete and classified data on wine consumers' preferences, decision tree, random forest, optimized random forest, neural network, support vector machine (SVM), Adaboost and XGBoost algorithms are used to train the data of each recommendation subtask. The node partition of random forest has a significant effect on the classification performance of multi-classification attributes; therefore, the node partition of random forest algorithm is optimized by linear combination of information gain rate and Gini coefficient, which is used as a recommendation model. Further, the models with the top five accuracies are taken for Stacking integration, and the best recommendation models of each subtask were screened out according to precision. Finally, these models are used to determine which wine attributes can be recommended to consumers, to establish a specific strategy for wine recommendation.

Materials

Acquisition and preprocessing of data

Preliminary selection of wine recommendation subtasks and independent variables

According to the sensory system of Chinese wine and the research literature of wine field, this study used the inherent wine attributes as recommended index, including colour, sweetness, foamability, mouthfeel, price, concentration and type of aroma, year, origin, packaging and brand of wine. The data types were all discrete. For the convenience of subsequent calculation, the dependent variables were coded by natural numbers according to the specific labels in the recommended index. The inherent attributes of wine applied in this study can be concluded in Figure 1.

Scholars have shown that gender, age, education, occupation, nationality, region and other factors (Capitello *et al.*, 2019; Pagan *et al.*, 2021; Rodríguez-Donate *et al.*, 2021) affect consumers' purchasing behaviour of wine. The research by Cai *et al.* (2015) showed that people with different eating habits have different degrees of aroma recognition for wine, and this affect consumers' purchase to some extent. For wine, consumer's characteristics is a vital subdivision variable, and these variables interact with each other to influence consumers' purchase of wine (Cai *et al.*, 2015). Based on the synthesis of existing research literature, the factors influencing consumer's purchase behaviour, that is, independent variables proposed in this study, can be divided into the following: personal characteristics, geographical location, psychological and dietary. Among them, psychological factors which affect consumers' wine purchase include the degree of influence of others, advertising, purchase channels, magazines and promotions. The labels can be divided into three categories: high, medium and low influence. The data types of independent variables are all discrete. For the convenience of subsequent calculation, the labels of independent variables were coded by natural numbers, which have been summarised in Table 1.

The data involved in this study originate from the survey of National Grape Industry Technology System, based on a questionnaire survey for Chinese wine drinkers, with a total of 3421 samples collected from June to October 2020. The study was conducted by interviewing a convenient sample of general wine consumers over the age of 18 (regulations indicate that alcohol operators are not allowed to sell alcohol to minors, and 'minors' are defined as natural persons under the age of 18). The participants were invited through different information and social media platforms (web links, WeChat, QQ app). The

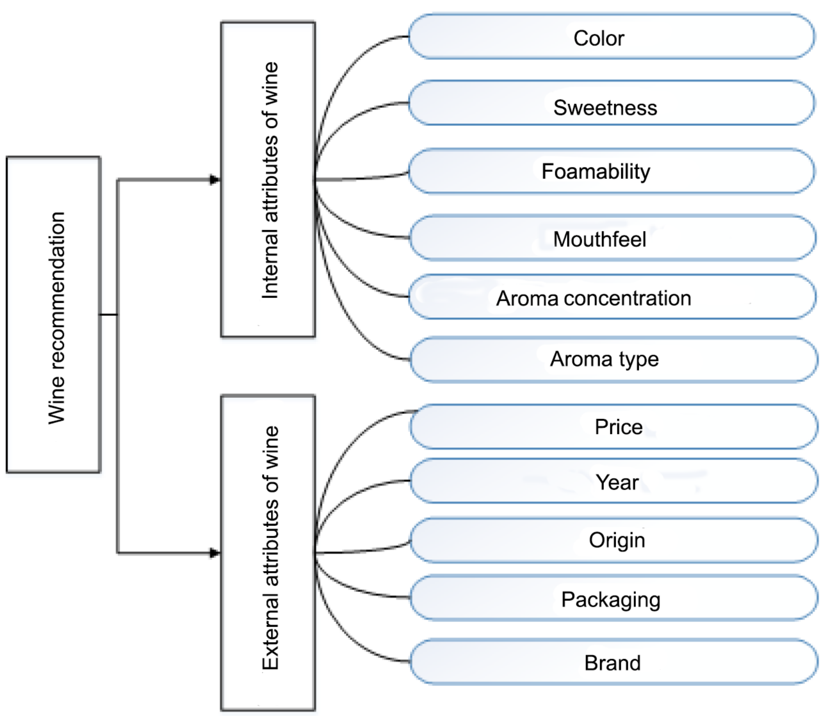

Figure 1. Recommended index of wine.

Table 1. Independent variables of wine recommendation.

Independent variables	Attribute value of independent variable	Attribute value after coding by natural number
Gender	Male, female	(1, 2)
Age	18–25, 26–35, 36–45, 46–55, above 55	(1, 2, 3, 4, 5)
Education level	Below senior high school, High school or technical secondary school, University or Junior college, Postgraduate or more	(1, 2, 3, 4)
Occupation	Students, farmers, freelancers, retirees, employees of state-owned enterprises, employees of private enterprises, party and government organs and institutions, education and scientific research personnel, others	(1, 2, 3, 4, 5, 6, 7, 8, 9)
Monthly disposable income	Under 5000, 5000–10,000, 10,000–15,000, above 15,000	(1, 2, 3, 4)
Marital status	Married, unmarried	(1, 2)
Number of families	3 or less, 4–7, more than 7	(1, 2, 3)
Nation	Han, ethnic minorities	(1, 2)
Address	East China, Northeast China, North China, Central China, South China, Northwest China, Southwest China	(1, 2, 3, 4, 5, 6, 7)
Cognitive level of wine	High, medium, low	(1, 2, 3)
Taste preference	Light taste, heavy taste	(1, 2)
Eating preferences	Sour, sweet, bitter, spicy	(1, 2,3,4)
Meat type	White meat, red meat	(1, 2)
Meat preference	Fat meet, lean meat	(1, 2)
Influence of others	High, medium, low	(1, 2, 3)
Influence of magazines	High, medium, low	(1, 2, 3)
Influence of advertisements	High, medium, low	(1, 2, 3)
Influence of promotions	High, medium, low	(1, 2, 3)
Influence of purchase channels	Supermarkets, stores, online stores and chateau	(1, 2, 3, 4)

Data collection

questionnaires were anonymous and distributed in proportion to the population of each province in China. The sample size obtained from the survey was able to cover the main provincial divisions of China, and at the same time, the sample size supported the operation of machine learning algorithms, and all information collected was used for the purpose of the study. Data preprocessing mainly included optimization of outlier and processing of missing values. Furthermore, after data cleaning, the number of valid questionnaires was 3398.

Independent variables of wine recommendation subtasks

Correlation analysis and significance analysis of variables

1. Mutual information method

Mutual information is mainly used to judge the information contributed by the appearance of one variable to the appearance of another variable (Pascoal *et al.*, 2017). The result of mutual information method is called mutual information value, abbreviated as MI. The value of MI can reflect whether discrete variables are related or not, and further, it can be used to realize data fusion. The formula is shown in Equation (1):

$$I(x,y) = \sum_{y\in Y}\sum_{x\in X} P(x,y)\log\left(\frac{P(x,y)}{p(x)p(y)}\right) \quad (1)$$

2. Gini coefficient method

Gini coefficient algorithm represents the interaction between the independent variables and wine attributes and judges the significance by the purity change after splitting the attributes (Hao *et al.*, 2021), and finally the value of the importance of each independent variable can be obtained. The formula is shown in Equation (2):

$$Gini(s) = I - \sum_{i=1}^{m} p_i^2 \quad (2)$$

Eventually independent variables used for recommendation subtasks

In this study, there are 19 independent variables and 11 recommended indicators involved in correlation analysis.

The threshold of MI is 0.01. If the absolute value of MI of two variables is greater than or equal to the threshold, it is considered that the two variables are related, and if the value is less than the threshold, it is judged that the two variables are not related. To further reduce the number of independent variables, Gini coefficient and information gain are used to analyse the importance of independent variables of each recommended index, and finally the top 10 crucial independent variables of each recommended index are obtained. The wine recommendation indicators and the corresponding top 10 independent variables are mentioned in Table 2.

Methodology

Prediction algorithms for wine consumers' sensory attribute preferences

The variables involved in wine recommendation index are all discrete data with obvious labels. Because supervised classification algorithm can effectively solve such problems, single hidden layer BP neural network algorithm, SVM algorithm, decision tree algorithm, random forest algorithm, Adaboost algorithm and Xgboost algorithm are used in the selection of machine algorithms as recommendation models. Table 3 introduces the pros and cons of the selected algorithms for this study.

Random forest is a widely used and powerful classification algorithm currently. Its construction process is roughly as follows: firstly, build multiple decision trees, secondly, use multiple decision trees to train samples, and finally, predict the category of samples in a way that the minority obeys the majority (Janitza *et al.*, 2016). Among them, the construction of decision tree is the vital factor that determines the category of tested samples, and so how to accurately split the nodes is a crucial factor to optimize the random forest. Each recommendation subtask of this data has diverse attributes when building a tree, and the number of classification categories is also varied, so the internal confusion of samples in each subtasks is different. The tree-based models in random forest algorithm involves an optimization problem as to how to split the internal node in chaotic samples and make the results accord with the actual situation. It is necessary to optimize the node-splitting mode in random forest algorithm because the traditional node-splitting standard may cause inaccurate feature division. The CART tree using the Gini coefficient is insufficient for the trend of node division in multi-classified datasets, yet it has higher accuracy of node division for purer datasets. ID3 tree using information gain is easier to distinguish the value of features compared with Gini coefficient when dealing with chaotic datasets, still information gain is partial to the attributes with more values, and as a result, multi-valued attributes are regarded as

Table 2. Recommended indicators of wine and corresponding independent variables.

Recommended subtasks	Eventually independent variables used for modeling (Importance from high to low)
Colour	Meat type, occupation, monthly disposable income, influence of others, age, influence of promotions, advertising influence, education level, influence of magazines, eating preferences
Sweetness	Meat type, monthly disposable income, occupation, influence of others, age, education level, advertising influence, influence of promotions, eating preferences, meat preferences
Foamability	Monthly disposable income, occupation, influence of others, advertising influence, promotion influence, magazine influence, age, education level, meat type, meat preferences
Mouthfeel	Occupation, monthly disposable income, influence of others, advertising influence, age, promotion influence, magazine influence, education level, meat type, eating preferences
Aroma concentration	Occupation, monthly disposable income, advertising influence, influence of others, age, promotion influence, education level, meat preferences, eating preferences, taste preference
Aroma type	Occupation, monthly disposable income, promotion influence, influence of others, advertising influence, age, meat type, eating preferences, education level, meat preferences
Price	Education level, meat type, gender, promotion influence, magazine influence, marital status, advertising influence, age, occupation, monthly disposable income
Year	Monthly disposable income, meat preferences, age, magazine influence, influence of others, advertising influence, eating preferences, gender, promotion influence, marital status
Origin	Influence of others, advertising influence, meat type, monthly disposable income, promotion influence, meat preferences, marital status, eating preferences, age, education level
Packaging	Gender, marital status, influence of others, occupation, advertising influence, education level, magazine influence, meat preferences, eating preferences, meat type
Brand	Magazine influence, monthly disposable income, meat type, meat preferences, eating preferences, education level, age, marital status, advertising influence, gender

Table 3. Strengths and weaknesses of different types of algorithms.

Algorithm	Merit	Defect
BP neural network algorithm	Strong learning ability, easy training, convenient and fast.	Unstable network structure, low reliability and slow convergence (Diez *et al.*, 2019)
Support vector machine	The effect of processing discrete data is better; The boundaries are more diverse; Solve the problem of non-linear separable classification.	Poor interpretability, slow calculation and easy overfitting.
Decision tree algorithm	Time complexity is small, efficiency is high, importance of each feature can be obtained (Yang and IEEE, 2019), suitable for small samples.	It is easier to make mistakes for tasks with many categories; The information gain is more inclined to the characteristics of multi-category attributes; Prone to overfitting; Poor generalisation ability.
Random forest algorithm	Fast processing speed; For unbalanced data sets, the error can be balanced; Reduce the possibility of overfitting.	Compared with decision tree, the calculation cost is high; When the number of noisy data is large, the results are easily affected by extreme values (Roy and Larocque, 2012) and easy to overfit. The feature weights are biased towards the features with many categories.
Adaboost	No overfitting phenomenon; The training error rate decreases with the increase of iteration times.	The training process is more inclined to the samples that are difficult to classify, which is easily disturbed by noise (Liao and Zhou, 2012); Relying on weak classifier; long training time.
Xgboost	Strong accuracy; Using regular terms to reduce overfitting; good interpretability.	The complexity of time and space is high.

the optimal partition nodes, and the nodes that really need to be partitioned are ignored. Ulteriorly, the information gain ratio further improves this problem by adding term weight to the information gain of each attribute. Therefore, this study structures the linear combination of information gain ratio and Gini coefficient as a new rule of node splitting, to improve the accuracy of random forest algorithm in classification of wine attributes. The formula of the new rule of node splitting is shown in Equation (3):

$$\Phi(\alpha) = \alpha_1 \mathrm{Gini}_{\mathrm{split}}(S,A) - \alpha_2\, \mathrm{GainRation}(A) \qquad (3)$$

Where, 0 ≤ 1, the and cannot assume the minimum or maximum value, which means that the weight coefficients cannot exist in such a pairing as (0,0) or (1,1), and the optimal values of the two weights are determined by the grid search method. When dividing the attributes, the node with the smallest difference value is selected for division.

Construction of Stacking integration algorithm

Stacking is a special and concrete combination strategy, which is a typical representative of ensemble learning algorithm (Montesinos-López *et al.*, 2019). The process of Stacking integration is to train the upper layer model first, and take the corresponding training results as the input of the next layer model, which is equivalent to constructing a two serial superposition classifier for the same data (Ahmadi *et al.*, 2019). The purpose is to improve the classification accuracy of the model.

In this study, decision tree, random forest, optimized random forest, neural network, SVM, Adaboost and Xgboost algorithms modeled each wine recommendation subtask, and the top five models with the highest recommended comprehensive accuracy of each recommendation index were selected as the base models. Further, to avoid the overfitting caused by complicated model, the second meta-model selected decision tree or logistic regression model. The construction process of Stacking integrated algorithm can be concluded in Figure 2.

Multimodel wine recommendation strategy

To establish the most appropriate recommendation strategy of each recommendation subtask, it is necessary to compare the recommended comprehensive accuracy of the models before and after Stacking integration. The final framework of wine recommendation in this study is shown in Figure 3.

The personalised wine recommendation method comprises the following steps:

Step 1: Collect user's preference data for wine, including 19 independent variables and 11 dependent variables.
Step 2: Clean the data, eliminate or optimize the wrong information, and encode the data by natural number after obtaining the effective information.
Step 3: Experiment with decision tree, random forest, optimized random forest, neural network, SVM, Adaboost, Xgboost and Stacking integration model for each recommendation subtask and select the model with

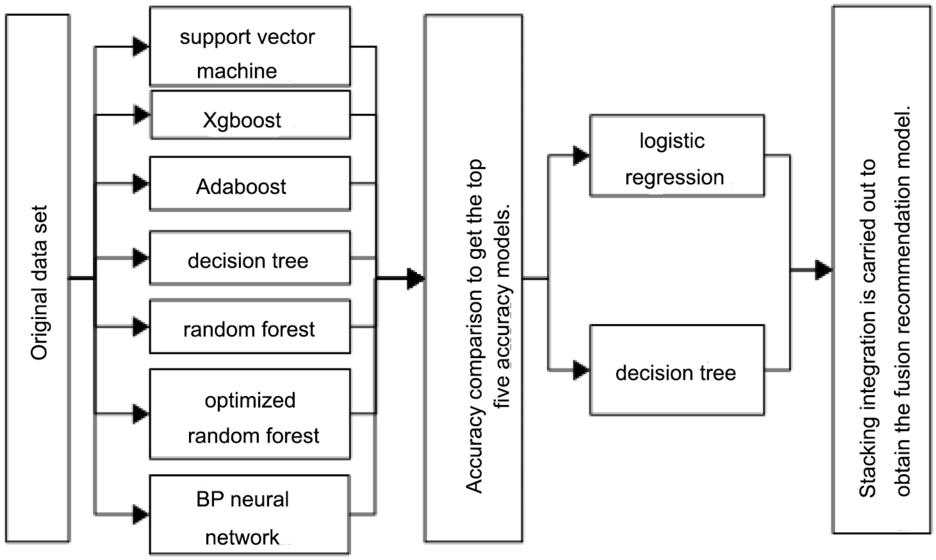

Figure 2. The construction process of Stacking integration model.

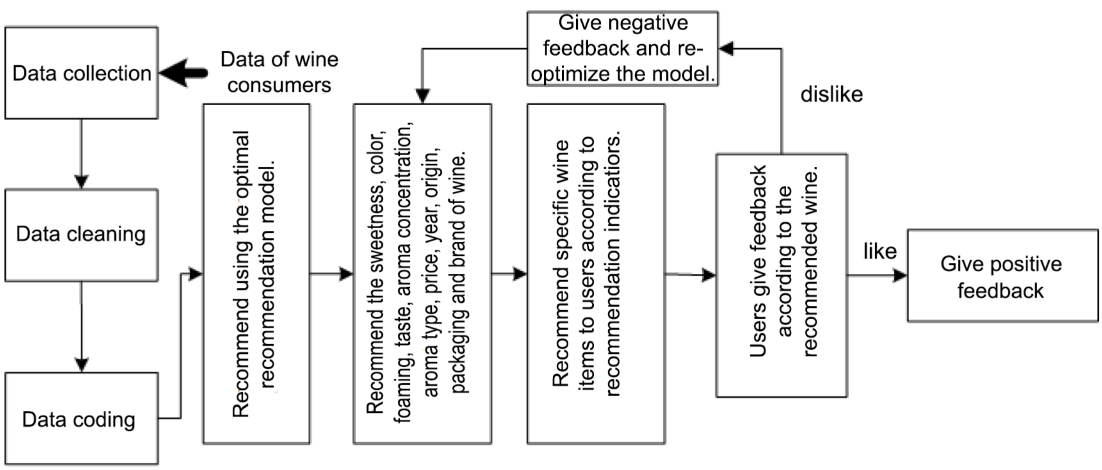

Figure 3. The process of personalised wine recommendation.

the highest accuracy as the optimal recommendation strategy to recommend wine.

Step 4: There is a user interaction module in the recommendation method. If the user likes the recommended wine, they give correct feedback to the recommendation model; if the user doesn't like it, they give negative feedback so that the strategy can continue to learn and further be optimized.

Evaluation index for recommendation algorithm

Accuracy

Accuracy refers to the proportion of the sum of correctly classified samples to the total samples in the prediction results. The formula is expressed in Equation (4):

$$acc = \frac{TP + TN}{total} \tag{4}$$

m-F1

The F1 score considers both the accuracy and recall of the classification model and can be regarded as a harmonic mean of the accuracy and recall. In this study, we put forward the concept of m-F1, which represents the arithmetic average of F1 scores of each category of the same model and the same recommended subtask.

Table 4. The recommended comprehensive accuracy of each single model.

	Colour	Sweetness	Foamability	Mouthfeel	Aroma type	Brand	Price	Year	Origin	Packaging	Aroma concentration
BP neural network	0.788	0.755	0.801	0.765	0.779	0.756	0.733	0.757	0.773	0.770	0.741
Support vector machine (SVM)	0.802	0.827	0.791	0.717	0.761	0.771	0.762	0.741	0.747	0.792	0.777
Decision tree	0.783	0.797	0.758	0.743	0.677	0.753	0.738	0.728	0.732	0.751	0.737
Random forest	0.817	0.829	0.763	0.756	0.689	0.774	0.748	0.742	0.745	0.763	0.762
Optimized random forest	0.833	0.845	0.792	0.786	0.716	0.798	0.761	0.629	0.745	0.738	0.466
Adaboost	0.825	0.842	0.761	0.752	0.686	0.787	0.742	0.736	0.781	0.780	0.774
XGboost	0.818	0.853	0.788	0.771	0.725	0.745	0.742	0.736	0.778	0.784	0.726

Table 5. The base model and meta-model of Stacking integration for each recommended subtask.

Recommended index	Base model 1	Base model 2	Base model 3	Base model 4	Base model 5	Meta-model
Foamability	BP neural network	Optimized random forest	Support vector machine (SVM)	XGboost	Random forest	Logical regression
Mouthfeel	Optimized random forest	XGboost	BP neural network	Random forest	Adaboost	Decision tree
Aroma concentration	SVM	Adaboost	Random forest	BP neural network	Decision tree	Logical regression
Colour	Optimized random forest	Adaboost	XGboost	Random forest	Support vector machine (SVM)	Decision tree
Sweetness	XGboost	Optimized random forest	Adaboost	Random forest	SVM	Logical regression
Aroma type	BP neural network	SVM	XGboost	Optimized random forest	Random forest	Logical regression
Year	BP neural network	Random forest	SVM	Adaboost	XGboost	Decision tree
Origin	XGboost	BP neural network	SVM	Random forest	Optimized random forest	Logical regression
Packaging	SVM	XGboost	Adaboost	BP neural network	Random forest	Logical regression
Brand	Optimized random forest	Adaboost	Random forest	SVM	BP neural network	Decision tree
Price	SVM	Optimized random forest	Random forest	XGboost	Adaboost	Logical regression

Recommended comprehensive accuracy

In this study, the concept of recommended comprehensive accuracy is proposed, which is expressed by the arithmetic average of m-F1 and accuracy.

Results and Discussion

Construction and verification of single recommendation model

This section needs to complete the training and evaluation of single recommendation model of each wine subtask. The independent variables and recommendation indicators used in building the recommendation model are shown in Section 2.2. The 10-fold cross-validation method is used to divide and train the sample. To better evaluate the effect of the model, this study randomly selected 300 questionnaires from the valid data to test the model. The recommended comprehensive accuracy proposed in this study blends the accuracy and m-F1 scores, so that it only presents the recommended comprehensive accuracy of each single model for each wine recommended subtask. The results are shown in Table 4.

The recommendation comprehensive accuracy shows that the optimized random forest is better than the random forest in colour, sweetness, foaming, taste, aroma type, price and brand of wine, and the precision has been improved. For the colour, brand and taste of wine, changing the splitting mode of nodes can improve the recommendation accuracy, and the optimized random forest algorithm model has the best recommendation effect. As for sweetness, there is some noise in the sample. Compared with other subtasks, sweetness of wine pays more attention to variance in modeling, while XGboost adopts regularisation constraint to simplify the model. Using XGboost makes the comprehensive accuracy up to 0.853. For foamability, aroma type, year and origin of wine, the distribution of these data is diverse, and this kind of data need a better fitting algorithm for recommendation. Among these machine learning algorithms, the advantage of neural network is to constantly fit data. So neural network performs best. For price, aroma concentration and packaging, there is almost no noise, and there are some key points similar to the support vector in the data, so SVM is more suitable for the recommendation of these wine attributes.

Screening of base model for Stacking integration algorithm

According to the above results, the top five recommendation models with the highest comprehensive accuracy of each subtask are selected as the base models. To avoid the overfitting caused by the complexity of the two-layer models, the decision tree or logistic regression model is selected as the meta-model to reduce the complexity. The established machine learning algorithm of the two-layer basic model for each wine recommendation subtask is shown in Table 5.

Implementation and verification of Stacking Integrated Algorithm

Firstly, train the single model and the integrated model on the training set. Secondly, randomly select 300 questionnaires from the valid data as the test set and make predictions. By comparing the recommendation comprehensive accuracy of each subtask before and after Stacking integration, the model with the highest value is selected as the optimal recommendation model, and finally an exclusively multimodel recommendation strategy for wine is established. The recommendation

Table 6. The comprehensive accuracy of the optimal model of each recommended index.

Recommended index	Optimal recommendation model	Comprehensive accuracy after Stacking integration	Optimal Comprehensive accuracy before Stacking integration
Sweetness		0.838	0.833
Colour		0.873	0.853
Foamability		0.820	0.801
Mouthfeel	Stacking integration model	0.803	0.786
Aroma type		0.803	0.779
Year		0.771	0.757
Packaging		0.815	0.792
Brand		0.804	0.798
Price	Support vector machine	0.731	0.762
Aroma concentration		0.760	0.777
Origin	XGboost	0.762	0.778

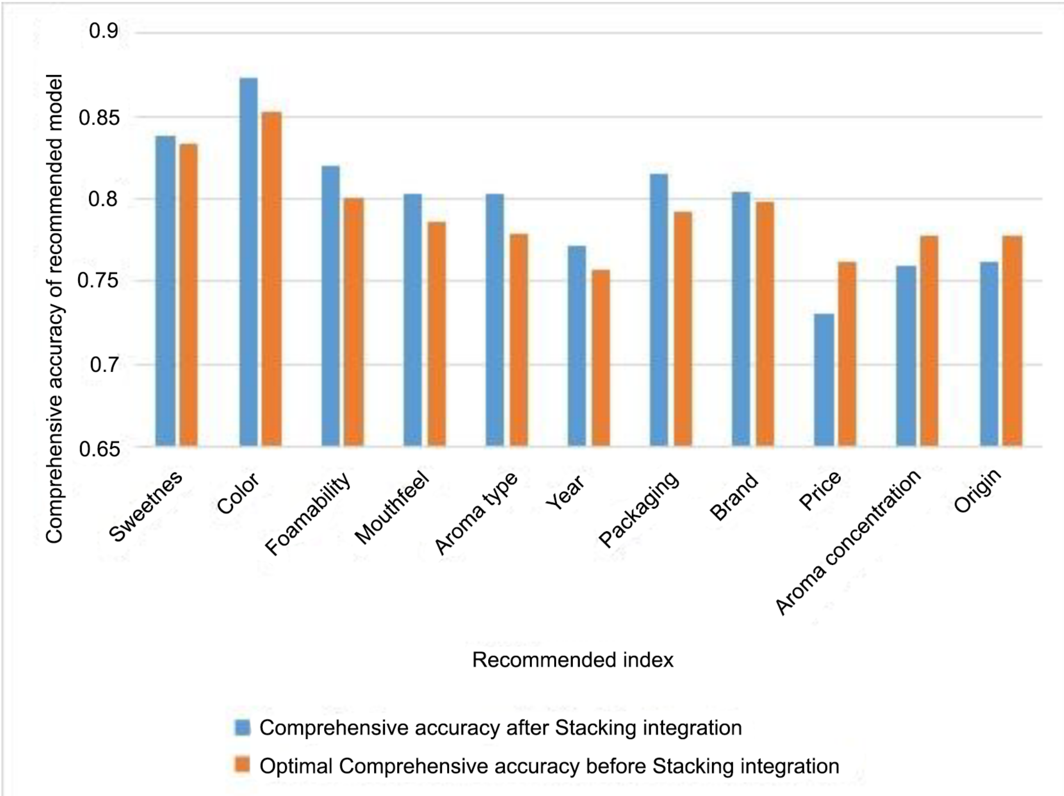

Figure 4. Comprehensive accuracy of recommended model.

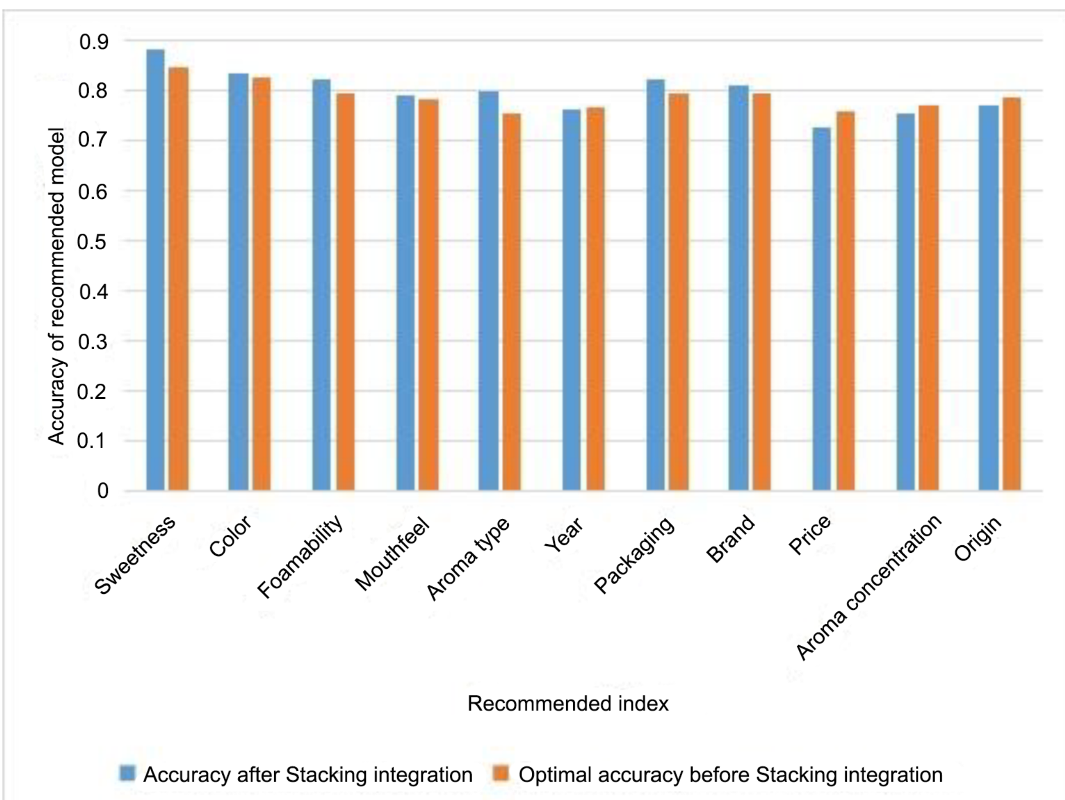

Figure 5. Accuracy of recommended model.

comprehensive accuracy after fusion and the highest value before fusion are summarised as follows.

To present the results more visually, Table 6 is transformed into Figure 4.

As can be seen from Table 6, for the eight indexes of colour, sweetness, foamability, mouthfeel, aroma type, year, packaging and brand, the optimal recommendation model is Stacking integrated algorithm, while the SVM model is most suitable for the recommendation of aroma concentration and price of wine, and XGboost model is the best algorithm for origin. The Stacking integration strategy has better performance than the single model and has significant effect on improving the accuracy of wine recommendation.

The accuracy after fusion and the highest value before fusion are shown in Figure 5.

The literature (Chu *et al*., 2020) uses a predicting method based on multivariate disorder logistic and shows that this method is only suitable for predicting colour, sweetness, aroma type and taste preference with an accuracy of between 70 and 75%, whereas the wine recommendation algorithm proposed in this study achieved an accuracy of over 79% for these attributes, which is better than the method proposed in the literature.

Conclusions and Future Work

In this study, a multimodel recommendation algorithm strategy is proposed to predict users' preferences about wine and realize personalised recommendation of wine. The independent variables of each wine recommendation subtask were screened by mutual information method and Gini coefficient method, and the top 10 factors with the highest correlation of each recommendation subtasks included personal characteristics of consumers such as age, education level, monthly disposable income and occupation, which indicated that personal characteristics of consumers had a crucial influence on wine purchase.

By combining the information gain rate and Gini coefficient to change the node splitting mode, the random forest algorithm was further optimized, which made the algorithm more accurate in recommending seven indicators such as colour, sweetness, foamability, mouthfeel, aroma type, price and brand of wine, and also showed that the optimized random forest algorithm is more suitable for classification tasks with numerous feature divisions.

To effectively reduce or offset the influence of random factors and improve the prediction accuracy and credibility in a single model, the Stacking integration was introduced into wine recommendation. The results showed that the integration algorithm could be used to improve the recommendation accuracy of eight indicators, including colour, sweetness, foamability, mouthfeel, aroma type, year, packaging and brand. The average recommendation accuracy is increased by 1.9%, and the highest is increased by 3%. However, it is not suitable for the attributes with large deviation such as aroma concentration. For this kind of tasks, Adaboost and other algorithms are more suitable for recommendation.

Based on the above research, the conclusion of this study is that colour, sweetness, foamability, mouthfeel, aroma type, year and packaging adopted Stacking integrated algorithm, aroma concentration finally adopted Adaboost algorithm, origin finally adopted XGboost algorithm, and wine price finally adopted SVM algorithm. Compared to the existing recommendation methods, the wine recommendation strategy proposed in this study can be more perfect, comprehensive and flexible in recommending wine for users.

Our approach might still be needed to improve, and the future attempts are as follows: Firstly, due to the limited amount of data in this study, the accuracy and the screening results of the optimal model may be varied for a large amount of data, so further exploration is still needed. Secondly, the future work can be expanded to conduct empirical analysis on other multiattribute drinks' recommendation. In addition, one of the typical examples in China's market, the wine multimodel recommendation strategy may also provide an effective method for dealing with preference prediction in other multi-feature goods.

References

Ahmadi, E., Garcia-Arce, A., Masel, D.T., Reich, E., Puckey, J. and Maff, R. 2019. A metaheuristic-based stacking model for predicting the risk of patient no-show and late cancellation for neurology appointments. IISE Transactions on Healthcare Systems Engineering. 9(3): 272–291. https://doi.org/10.1080/24725579.2019.1649764

Areta, A., Bardaji, I. and Iraizoz, B. 2017. Spanish wines in the US market: what attributes do US consumers look for in Spanish wines? Spanish Journal of Agricultural Research. 15(4): e0120. https://doi.org/10.5424/sjar/2017154-10006

Cai, J., Pang, J., Hu, K. and Tao, Y. 2015. Chinese familiarity with wine aromas characteristics. Journal of Food Science and Technology. 33(04):47–51.

Capitello, R., Bazzani, C. and Begalli, D. 2019. Consumer personality, attitudes and preferences in out-of-home contexts. International Journal of Wine Business Research. 31(1): 48–67. https://doi.org/10.1108/IJWBR-06-2018-0022

Chu, X., Li, Y., Xie, Y., Tian, D. and Mu, W. 2020. Regional difference analyzing and prediction model building for Chinese wine consumers' sensory preference. British Food Journal. 122(8): 2587–2602. https://doi.org/10.1108/BFJ-06-2019-0465

Diez, F.J., Navas-Gracia, L.M., Martinez-Rodriguez, A., Correa-Guimaraes, A. and Chico-Santamarta, L. 2019. Modelling of a flat-plate solar collector using artificial neural networks for different working fluid (water) flow rates. Solar Energy. 188: 1320–1331. https://doi.org/10.1016/j.solener.2019.07.022

Gustafson, C.R., Lybbert, T.J. and Sumner, D.A. 2016. Consumer sorting and hedonic valuation of wine attributes: exploiting data from a field experiment. Agricultural Economics. 47(1): 91–103. https://doi.org/10.1111/agec.12212

Hao, L., Fang, Y. and Zhang, Q. 2021. Rediscussion on statistical measure on Gini coefficient. Statistics & Decision. 37(7): 27–32.

He, Y., Zou, H. and Yu, H. 2019. Recommender system model based on dynamic-weighted bagging matrix factorization. Journal of Nanjing University (Natural Science). 55(04): 644–650.

Hu, Y., Qu, B., Liang, J., Wang, J. and Wang, Y. 2021. A survey on evolutionary ensemble learning algorithm. Chinese Journal of Intelligent Science and Technology. 3(1):18–33.

Janitza, S., Tutz, G. and Boulesteix, A. 2016. Random forest for ordinal responses: prediction and variable selection. Computational Statistics and Data Analysis. 96(C): 57–73.

Lee, S.J. and Lee, K.G. 2008. Understanding consumer preferences for rice wines using sensory data. Journal of the Science of Food and Agriculture. 88(4): 690–698. https://doi.org/10.1002/jsfa.3137

Li, Q. and Zhai, L. 2019. Analysis and research on employee turnover prediction based on stacking algorithm. Journal of Chongqing Technology and Business University (Natural Science Edition). 36(01): 117–123.

Li, Y., Jia, X., Wang, R., Qi, J., Jin, H., Chu, X. and Mu, W. 2022. A new oversampling method and improved radial basis function classifier for customer consumption behavior prediction. Expert Systems with Applications. 199: 116982. https://doi.org/10.1016/j.eswa.2022.116982

Liao, H. and Zhou, D. 2012. Review of AdaBoost and its improvement. Computer Systems & Applications. 21: 240–244.

Liu, H., Guo, M. and Pan, W. 2017. Overview of personalized recommendation systems. Journal of Changzhou University (Natural Science Edition). 29: 51–59.

Mehta, R. and Bhanja, N. 2018. Consumer preferences for wine attributes in an emerging market. International Journal of Retail & Distribution Management. 46(1): 34–48. https://doi.org/10.1108/IJRDM-04-2017-0073

Meng, Q. and Xiong, H. 2021. Doctor recommendation based on online consultation text information. Information Science. 39(06): 152–160.

Montesinos-López, O.A., Montesinos-López, A., Crossa, J., Cuevas J., Montesinos-López, J.C., Gutiérrez, Z.S., Lillemo, M., Philomin, J. and Singh, R. 2019. A Bayesian genomic multi-output regressor stacking model for predicting multi-trait multi-environment plant breeding data. G3 (Bethesda). 9(10): 3381–3393. https://doi.org/10.1534/g3.119.400336

Pagan, K.M., Giraldi, J.D.M.E., Maheshwari, V., de Paula, A.L.D. and de Oliveira, J.H.C. 2021. Evaluating cognitive processing and preferences through brain responses towards country of origin for wines: the role of gender and involvement. International Journal of Wine Business Research. 33(4): 481–501. https://doi.org/10.1108/IJWBR-08-2020-0043

Pascoal, C., Oliveira, M.R., Pacheco, A. and Valadas, R. 2017. Theoretical evaluation of feature selection methods based on mutual information. Neurocomputing. 226: 168–181.

Portugal, I., Alencar, P. and Cowan, D. 2018. The use of machine learning algorithms in recommender systems: A systematic review. Expert Systems with Application. 97: 205–227. https://doi.org/10.1016/j.eswa.2017.12.020

Rodríguez-Donate, M.C., Romero-Rodríguez, M.E. and Cano-Fernández, V.J. 2021. Wine consumption preferences among generations X and Y: an analysis of variability. British Food Journal. 123(11): 3557–3575. https://doi.org/10.1108/BFJ-12-2020-1156

Roy, M. and Larocque, D. 2012. Robustness of random forests for regression. Journal of Nonparametric Statistics. 24(4): 93–1006. https://doi.org/10.1080/10485252.2012.715161

Stanco, M., Lerro, M. and Marotta, G. 2020. Consumers' preferences for wine attributes: a best–worst scaling analysis. Sustainability. 12(7): 2819. https://doi.org/10.3390/su12072819

Szolnoki, G. and Hauck, K. 2020. Analysis of German wine consumers' preferences for organic and non-organic wines. British Food Journal. 122(7): 2077–2087. https://doi.org/10.1108/BFJ-10-2019-0752

Tao, Y., Peng, Y., Jiang, Q., Li, Y., Fang, S. and Gong, Y. 2019. Remote detection of critical growth stages in rapeseed using vegetation spectral and stacking combination method. Journal of Geomatics. 44(5): 20–23.

Wang, Y., Liao, X. and Li, S. B. 2019. Resealed boosting in classification. IEEE Transactions on Neural Networks and Learning Systems. 30(9): 2598–2610.

Xie, W., Chai, Q., Gan, Y., Chen, S., Zhang, X. and Wang, W. 2020. Strains classification of *Anoectochilus roxburghii* using multi-feature extraction and Stacking ensemble learning. Transactions of the Chinese Society of Agricultural Engineering. 36: 203–210.

Yang, F.J. & IEEE. 2019. An extended idea about decision trees. 2019 *6TH INTERNATIONAL CONFERENCE ON COMPUTATIONAL SCIENCE AND COMPUTATIONAL INTELLIGENCE (CSCI 2019)*. 6th Annual Conference on Computational Science and Computational Intelligence (CSCI 2019). 349–354.

Yin, C., Guo, Y., Yang, J. and Ren, X. 2018. A new recommendation system on the basis of consumer initiative decision based on an associative classification approach. Industrial Management & Data Systems. 118(1): 188–203. https://doi.org/10.1108/IMDS-02-2017-0057

Zhang, J. and Lei, J. 2021. Stacking Fusion Model for customer purchase behavior prediction. Shanghai Management Science. 43: 12–19.